RODRIGO CORRÊA BASSO

"EQUILÍBRIO LÍQUIDO-LÍQUIDO NAS ETAPAS DE PURIFICAÇÃO DE BIODIESEIS ETÍLICOS E ANÁLISE DE SUAS PROPRIEDADES FÍSICAS"

Campinas

2013

UNIVERSIDADE ESTADUAL DE CAMPINAS

FACULDADE DE ENGENHARIA DE ALIMENTOS

RODRIGO CORRÊA BASSO

"EQUILÍBRIO LÍQUIDO-LÍQUIDO NAS ETAPAS DE PURIFICAÇÃO DE BIODIESEIS ETÍLICOS E ANÁLISE DE SUAS PROPRIEDADES FÍSICAS"

Orientador: Prof. Dr. Eduardo Augusto Caldas Batista

Tese de Doutorado apresentada ao Programa de
Pós Graduação em Engenharia de Alimentos da Faculdade
de Engenharia de Alimentos da Universidade Estadual de Campinas
para a obtenção do título de Doutor em Engenharia de Alimentos.

ESTE EXEMPLAR CORRESPONDE À VERSÃO FINAL
DA TESE DEFENDIDA PELO ALUNO RODRIGO CORRÊA BASSO
E ORIENTADA PELO PROF. DR. EDUARDO AUGUSTO CALDAS BATISTA.

Assinatura do Orientador

_____

CAMPINAS

2013

Ficha Catalográfica
Universidade Estadual de Campinas
Biblioteca da Faculdade de Engenharia de Alimentos
Claudia Ap. Romano de Souza - CRB8/5816

Basso, Rodrigo Corrêa, 1978-
B295e Equilíbrio líquido-líquido nas etapas de purificação de biodieseis etílicos e análise de suas propriedades físicas / Rodrigo Corrêa Basso. -- Campinas, SP: [s.n.], 2013.

Orientador: Eduardo Augusto Caldas Batista.
Tese (doutorado) - Universidade Estadual de Campinas, Faculdade de Engenharia de Alimentos.

1. Equilíbrio líquido-líquido. 2. Biodiesel. 3. Termodinâmica. 4. Purificação. 5. Propriedades Físicas. I. Batista, Eduardo Augusto Caldas. II. Universidade Estadual de Campinas. Faculdade de Engenharia de Alimentos. III. Título.

Informações para Biblioteca Digital

Título em inglês: Liquid-liquid equilibrium in the ethyl biodiesel purification steps and analysis of their physical properties
Palavras-chave em inglês:
Liquid-liquid equilibrium.
Biodiesel
Thermodynamic
Purification
Physical properties
Área de concentração: Engenharia de Alimentos
Titulação: Doutor em Engenharia de Alimentos
Banca examinadora:
Eduardo Augusto Caldas Batista [Orientador]
Christianne Elisabete da Costa Rodrigues
Theo Guenter Kieckbusch
Rílvia Saraiva de Santiago Aguiar
Cintia Bernardo Gonçalves
Data da defesa: 26-08-2013
Programa de Pós-Graduação: Engenharia de Alimentos

Banca Examinadora

Professor Dr. Eduardo Augusto Caldas Batista
Orientador

Prof.ª Dr.ª Christianne Elisabete da Costa Rodrigues
Membro Titular
FZEA/ USP

Professor Dr. Theo Guenter Kieckbusch
Membro Titular
FEQ/ UNICAMP

Prof.ª Dr.ª Rílvia Saraiva de Santiago Aguiar
Membro Titular
DEQ/ UFC

Prof.ª Dr.ª Cintia Bernardo Gonçalves
Membro Titular
FZEA/ USP

Prof.ª Dr.ª Ana Paula Badan Ribeiro
Membro Suplente
FCA/ UNICAMP

Prof. Dr. Marcos Lúcio Corazza
Membro Suplente
DEQ/ UFPR

Prof.ª Dr.ª Vania Regina Nicoletti Telis
Membro Suplente
IBILCE/ UNESP

As duas Marias,

Maria Sebastiana, minha mãe,

e Maria Aparecida, minha avó,

pelo amor e dedicação,

pelos exemplos e ensinamentos,

e pela importância que tem, e sempre terão,

em minha vida.

"O significado das coisas não está nas coisas em si,

mas sim em nossa atitude com relação a elas."

Antoine de Saint-Exupéry

Agradeço...

A minha mãe e minha avó, por tudo que me ensinaram, me possibilitaram e me perdoaram.

Ao meu orientador, Professor Eduardo, por seus constantes ensinamentos, por sua confiança e acolhida, por sua simplicidade e companheirismo, e por sua disponibilidade em ajudar e contribuir sempre.

A Mirian, uma grande surpresa nesse período, por todo o apoio.

A Ana Paula, grande amiga e exemplo de competência, caráter e profissionalismo, por seu companheirismo, incentivo, confiança e pelas inúmeras oportunidades.

Àqueles dos quais fui mais próximo no ExTrAE, com os quais convivi, discuti idéias, colaborei, aprendi, conversei, compartilhei momentos e dei boas risadas.

Aos alunos de iniciação científica Camila e Fábio, que realizaram seus trabalhos com maturidade e independência.

Aos companheiros e amigos Chiu e André.

A Ana Carla, amiga querida sempre presente.

A Fabi, Lizielle, Daniel, Giovanni, Bruno, Leonardo, Caio, Alexandre, Julio, Gustavo, Eriksen, Monise, Glaziele e Valter, por sua presença em diferentes momentos nesses anos do doutorado.

Ao Professor Walter Esteves, ao Dr. Rodolfo Rohr e ao pessoal da Consultec pelas conversas, oportunidades e pelo aprendizado constante.

Ao Professor Theo que sempre me recebeu com muita consideração e respeito em seu laboratório e em suas pesquisas.

Ao Professor Tomzé, pela disponibilização da estrutura física para a realização de meus experimentos, e pelas conversas e discussões.

Ao CNPq pela concessão da bolsa de doutorado.

À Drª Renata Celeguini e às Professoras Christianne Elisabete e Roberta Ceriani pela atenção e orientação nos momentos em que precisei no decorrer de minha tese.

Aos Professores Cintia Bernardo, Rílvia Saraiva, Marcos Corazza e Vânia Nicoletti pelas atenciosas correções e valiosas sugestões a minha tese.

SUMÁRIO

Resumo Geral

Uma vez que a decantação é comumente usada na purificação do biodiesel, o conhecimento da distribuição dos componentes entre as duas fases líquidas formadas, dado pelo equilíbrio líquido-líquido (ELL), faz-se necessário. O comportamento deste biocombustível em motores e o dimensionamento de equipamentos para sua produção são dependentes de suas propriedades físicas. As informações referentes ao ELL e as propriedades físicas dos biodieseis etílicos são insuficientes na literatura científica, a despeito de sua importância como combustível completamente biorenovável. Deste modo, os objetivos do presente trabalho foram obter dados experimentais e modelar o ELL de sistemas contendo etanol + biodiesel etilíco + água ou glicerol; simular as etapas de decantação na purificação dos biodieseis; obter dados experimentais e estudar o comportamento da densidade, da viscosidade e do perfil térmico de biodieseis etílicos; desenvolver um modelo para o cálculo da viscosidade de ésteres etílicos e sistematizar uma metodologia preditiva para o cálculo das densidades de biodieseis. Os resultados mostraram que a temperatura teve pouco efeito no ELL de sistemas contendo glicerol + etanol + biodiesel etilíco de óleo de crambe. Os modelos NRTL e UNIQUAC descreveram o ELL dos sistemas com desvios globais menores que 1,22% e 1,07% para os sistemas contendo, respectivamente, água e glicerol. UNIFAC e UNIFAC-Dortmund apresentaram uma inadequada capacidade preditiva, com desvios globais maiores que 1,9% e 2,27% para os sistemas contendo, respectivamente, água e glicerol. A remoção parcial do etanol de sistemas contendo etanol + biodiesel etílico + glicerol reduziu o teor de glicerol na fase rica em biodiesel a concentrações inferiores ao mínimo requerido pelos padrões de qualidade do biodiesel. Usando um decantador para a separação do glicerol e dois conjuntos misturador/separador em contracorrente na lavagem do biodiesel, a quantidade de água requerida para a remoção de etanol e glicerol foi aproximadamente 1/4 da massa do biodiesel a ser purificado, e 1/8 da quantidade de água usada com um único conjunto misturador/separador. Os biodieseis de óleo de crambe e de óleo de coco tiveram, respectivamente, as maiores e as menores viscosidades, e o biodiesel de óleo de macauba teve o maior ponto de fusão entre os biodieseis analisados. A sistematização da metodologia predita para o cálculo de densidade resultou em desvios relativos menores que 0,89% e o modelo desenvolvido para o cálculo da viscosidade de ésteres etílicos resultou em desvios relativos médios menores que 14,73%.

Abstract

Since settling is commonly used in the biodiesel purification, the knowledge of the component distribution between both liquid phases, given by the liquid-liquid equilibrium (LLE), is required. The biodiesel behavior in engines and the equipment design for its synthesis process are dependent on physical properties of this biofuel. Despite its importance as a completely renewable biofuel, experimental data in the scientific literature about LLE and physical properties of biodiesel produced by ethanolysis are scarce. Because of this, the aims of the present work were to obtain and to model LLE experimental data of systems containing ethanol + ethyl biodiesel + water or glycerol; to simulate the settling in the biodiesel purification; to determine experimental data and to evaluate the behavior of density, viscosity and thermal profile of ethyl biodiesels; to develop a new model for calculation of ethyl ester viscosity and to present a systematized methodology for biodiesel density calculation. The results showed little temperature effect on the LLE of the systems containing glycerol + ethanol + ethyl biodiesel from crambe oil. NRTL and UNIQUAC models described the LLE of the systems with overall deviations lower than 1.22% and 1.07%, for the systems containing, respectively, water and glycerol. UNIFAC and UNIFAC-Dortmund showed poor predictive capacity, with overall deviations higher than 1.9% and 2.27% for the systems containing, respectively, water and glycerol. Partial removal of ethanol from the systems containing ethanol + ethyl biodiesel + glycerol decreases the glycerol content in the biodiesel-rich phase to lower content than that required by biodiesel standard. Using a settler for glycerol separation and two sets mixer/settler in countercurrent for biodiesel water washing, the water content required for ethanol and glycerol removal was about 1/4 of the mass of biodiesel previous to settling, and 1/8 of the water content required for the biodiesel purification using only a single set mixer/settler. The biodiesels from crambe and coconut oil showed, respectively, the highest and the lowest viscosities, and the biodiesel from macauba pulp oil showed the highest melting point among the studied biodiesels. The systematized methodology resulted in relative deviations lower than 0.89% for the densities, and the developed model for the viscosity calculation showed relative deviations lower than 14.73%.

Capítulo 1. Introdução e Objetivos

1.1. Introdução

Os óleos vegetais são compostos predominantemente (em média 95%) por diferentes moléculas de triacilgliceróis. Cada molécula de triacilglicerol é formada por três moléculas de ácidos graxos ligadas a uma molécula de glicerol através de ligações ésteres.

Os ésteres de ácidos graxos, constituintes majoritários do biodiesel, podem ser comumente obtidos a partir da reação de transesterificação entre uma matriz de triacilgliceróis e um álcool. Como resultado da alcoólise das moléculas de triacilgliceróis, tem-se também a formação de glicerol, um tri-álcool com grande importância tecnológica. Além do glicerol, o excesso de álcool, adicionado no início da reação como forma de favorecer a formação dos ésteres, o catalisador e os sabões formados durante a transesterificação devem ser removidos para a obtenção do biodiesel.

As sementes de crambe (*Crambe abyssinica*) possuem elevado teor de óleo rico em ácidos graxos monoinsaturados, sendo composto predominantemente por ácido erúcico. Esta espécie apresenta um curto ciclo entre a semeadura e a colheita, podendo ser cultivada entre dois plantios de soja (FALASCA et al., 2010; MANDAL et al., 2002). O óleo de polpa de macaúba (*Acrocomia aculeata*) contém majoritariamente ácidos graxos de cadeia média (16 – 18 átomos de carbono), com mais de 50 % de ácidos graxos monoinsaturados e aproximadamente 25% de ácido palmítico (COIMBRA; JORGE, 2012). O nabo forrageiro (*Raphanus sativus*) possui uma excelente capacidade de reciclar os micronutrientes do solo, crescimento rápido, reduzida necessidade de nutrientes agronômicos e baixo custo de plantio. Seu óleo possui cerca de cerca de 60% de ácidos graxos monoinsaturados, sendo composto predominantemente por ácido oléico, ácido linoléico, ácido linolênico, ácido gadoléico e ácido erúcico (CRUSCIOL et al., 2005; DOMINGOS et al., 2008).

O equilíbrio líquido-líquido (ELL) está diretamente relacionado a duas etapas de purificação do biodiesel. A primeira etapa consiste na decantação do glicerol formado durante a reação. Nesta etapa são formadas duas fases, uma rica em glicerol e uma rica em biodiesel, com etanol distribuído em ambas as fases. Como esta primeira etapa é insuficiente para atingir o teor de pureza em ésteres a níveis recomendados pelos padrões de qualidade, são realizadas etapas de lavagem com água da fase rica em ésteres seguida por decantação e evaporação.

O estudo do ELL é essencial em processos que se fundamentam na diferença de partição de componentes de uma solução entre duas diferentes fases no estado líquido, notadamente na extração líquido-líquido. A aplicação de modelos termodinâmicos voltados à representação do ELL tem como principal vantagem a possibilidade de se conhecer a distribuição dos componentes em duas fases imiscíveis, ou parcialmente miscíveis, em equilíbrio utilizando-se uma quantidade reduzida de dados experimentais. Deste modo, a avaliação da descrição do ELL de diferentes sistemas por diferentes modelos termodinâmicos, bem como a comparação entre eles, adquire significativa importância no estudo das etapas de purificação do biodiesel regidas pelo ELL.

Os ésteres de ácidos graxos têm suas propriedades físicas e químicas afetadas pelo comprimento de cadeia e grau de insaturação dos ácidos graxos. A viscosidade dos ésteres alquílicos normalmente aumenta com o comprimento da cadeia carbônica da molécula de ácido graxo presente e diminui com o número de duplas ligações (KNOTHE; STEIDLEY, 2005). A concentração de ésteres saturados e insaturados no biodiesel tem efeito significativo na termodinâmica da nucleação e da cristalização em baixas temperaturas (DUNN, 2008).

O conhecimento do comportamento da densidade e da viscosidade do biodiesel em função da temperatura é importante na determinação das condições operacionais e na optimização de seus processos de produção e em seu uso direto no motor. O dimensionamento de tubulações, reatores, misturadores, decantadores, e outros equipamentos envolvidos nas etapas de produção do biodiesel são dependentes do conhecimento de um conjunto de propriedades físicas, dentre elas a densidade e a viscosidade. Em relação ao funcionamento do motor, combustíveis com elevada viscosidade tendem a formar grandes gotas durante o processo de injeção, o que pode resultar em pobre atomização do combustível. Por outro lado, viscosidades muito baixas podem resultar em lubrificação insuficiente dos componentes de injeção. Por sua vez, a quantidade de combustível injetada no motor está diretamente relacionada à densidade (KNOTHE; STEIDLEY, 2005; REFAAT, 2009; BOUDY; SEERS, 2009). A formação de cristais e agregados cristalinos a baixas temperaturas podem provocar entupimento de filtros de combustíveis com consequente falha do motor (DUNN, 2005).

1.2. Objetivos

Os objetivos gerais desta tese de doutorado foram estudar o ELL de sistemas envolvidos nas etapas de purificação de biodieseis produzidos por etanólise; analisar, a partir de modelos termodinâmicos, as etapas de decantação e lavagem de biodieseis etílicos usando um *software* de simulação comercial e estudar o comportamento da densidade, da viscosidade e do perfil térmico durante a fusão desses biocumbustíveis.

Dentre os objetivos específicos podem ser destacados:

- obtenção de dados experimentais e a modelagem do ELL de sistemas constituídos por água + etanol + biodieseis etílicos de óleo de crambe, nabo forrageiro e polpa de macaúba a 298,2 K;
- obtenção de dados experimentais e a modelagem do ELL de sistemas constituídos por glicerol + etanol + biodiesel etílico de óleo de crambe a 298,2, 318,2 e 338,2 K;
- obtenção de dados experimentais e a modelagem do ELL de sistemas constituídos por glicerol + etanol + biodiesel etílico de óleo de polpa de macaúba a 298,2 K e análise de sensibilidade aplicada a etapa de decantação desse biocombustível;
- obtenção de dados experimentais e a modelagem do ELL de sistemas constituídos por glicerol + etanol + biodiesel etílico de óleo de nabo forrageiro a 298,2 K e estudo das etapas de decantação e de lavagem com água desse biocombustível;
- sistematizar uma metodologia preditiva para o cálculo da densidade de ésteres e biodieseis metílicos e etílicos e desenvolver uma metodologia para cálculo da viscosidade de ésteres etílicos com dependência da temperatura utilizando como dados de entrada apenas o número de carbonos e de insaturações destes componentes, bem como avaliar diferentes modelos no que se refere ao cálculo destas propriedades físicas a partir de dados experimentais de densidade e viscosidade de biodieseis etílicos de soja, canola e palma em temperaturas de até 363,2 K;
- apresentar dados experimentais de comportamento térmico, densidade e viscosidade de biodieseis etílicos de óleo de crambe, nabo forrageiro, coco e

polpa de macaúba a temperaturas de até 363,2 K, e avaliar a descrição do comportamento destas duas últimas propriedades físicas por modelos da literatura.

1.3. Apresentação do Trabalho

O presente trabalho encontra-se dividido em capítulos. O Capítulo 2 apresenta uma revisão bibliográfica sobre os temas abordados na tese. Cada capítulo, a partir do número 3 até o número 8, constitui-se de um artigo científico, publicado, submetido ou a ser submetido, originados dos resultados obtidos ao longo do cumprimento dos objetivos descritos para esta tese. A apresentação destes foi organizada de modo a propiciar o melhor encadeamento das etapas do trabalho, sem a preocupação com a ordem cronológica de obtenção dos resultados. O capítulo 9 é uma conclusão dos resultados apresentados nos capítulos precedentes. Na sequência deste capítulo, estão apresentadas algumas sugestões de projetos futuros que poderiam complementar os resultados e colcusões apresentadas na presente investigação. Ao final deste manuscrito, está presente um apêndice contendo o detalhamento da metodologia experimental utilizada nas diversas etapas desta tese.

Deste modo, a estrutura dessa tese de doutorado está ordenada do seguinte modo:

O Capítulo 1, “Introdução”, posiciona o leitor quanto à importância do trabalho em relação ao contexto científico no qual está inserido. Explicita os objetivos visados pelo presente estudo, bem como descreve detalhadamente, os objetivos específicos propostos e alcançados ao longo do delineamento do mesmo. Neste capítulo, cada objetivo específico é apresentado de maneira correlata a um capítulo, referente à apresentação dos resultados da presente pesquisa. Este último tópico descreve a estrutura da tese bem como justifica o modo como a mesma foi dividida.

O Capítulo 2, “Revisão Bibliográfica”, situa o leitor em relação aos trabalhos publicados na literatura científica sobre os temas abordados no presente estudo. Uma vez que os capítulos referentes à apresentação e discussão de resultados encontram-se na forma de artigos científicos, parte da literatura citada neste capítulo está presente também em alguns dos demais capítulos.

O Capítulo 3, “Liquid-Liquid Equilibrium Data and Thermodynamic Modeling, at T/K = 298.2, in the Washing Step of Ethyl Biodiesel Production from Crambe, Fodder

Radish and Macauba Pulp Oil", apresenta-se como um artigo submetido ao periódico "Fuel". O mesmo é composto por dados experimentais de ELL referentes a três sistemas contendo água + etanol + biodieseis etílicos de óleo de crambe, de nabo forrageiro e de polpa de macaúba, componentes estes envolvidos na etapa de lavagem dos citados biodieseis. Os modelos termodinâmicos NRTL e UNIQUAC têm seus parâmetros de interação binária ajustados aos dados experimentais desses sistemas. Os valores calculados pelos modelos moleculares são comparados aos valores preditos pelos modelos de contribuição de grupos UNIFAC-LLE e UNIFAC-Dortmund.

O Capitulo 4, "Liquid-Liquid Equilibrium of Pseudoternary Systems Containing Glycerol + Ethanol + Ethylic Biodiesel from Crambe Oil (*Crambe abyssinica*) at *T/K* = (298.2, 318.2 338.2) and Thermodynamic Modeling" refere-se a um artigo publicado em periódico (Basso, R. C.; Meirelles, J. A. A.; Batista, E. A. C. **Fluid Phase Equilibria**, v.333, p. 55-62, 2012). No presente capítulo estão apresentados dados experimentais do ELL de sistemas compostos por glicerol + etanol + biodiesel etílico de óleo de crambe, compostos envolvidos na etapa de decantação da produção de biodiesel, em três diferentes temperaturas. A quantificação individual dos ésteres etílicos desse biodiesel nas duas fases formadas na etapa de decantação, fase rica em glicerol e fase rica em biodiesel, é apresentada, validando-se, desse modo, a suposição de considerar o biodiesel, nesses sistemas, como um pseudo-componente. O modelo termodinâmico NRTL tem seus parâmetros de interação binária ajustados aos dados experimentais, e sua descrição do ELL é comparada aos valores preditos pelo modelo de contribuição de grupos UNIFAC, utilizando dois conjuntos distintos de parâmetros.

O Capitulo 5, "LLE Experimental Data, Thermodynamic Modeling and Sensitivity Analysis in the Ethyl Biodiesel from Macauba Pulp Oil Settling Step", constitui-se de um artigo publicado em periódico (Basso, R. C.; da Silva, C. A. S.; Sousa, C. O.; Meirelles, J. A. A.; Batista, E. A. C., **Bioresource Technology**, v. 131, p. 468-475, 2013). O capítulo apresenta dados experimentais do ELL, a 298,2 K, de um sistema contendo glicerol + etanol + biodiesel de óleo de polpa de macaúba, quantificando-se a distribuição individual de cada éster que compõem este biodiesel nas duas fases formadas durante a etapa de decantação. A partir dos dados de ELL os parâmetros dos modelos NRTL e UNIQUAC são ajustados, e sua capacidade descritiva é comparada com a capacidade preditiva dos modelos de contribuição de grupo UNIFAC-LLE e UNIFAC-Dortmund. Os quatro modelos são empregados em uma análise de sensibilidade, utilizando-se o programa comercial de

simulação ASPEN Plus (ASPEN Technology), na qual o teor de etanol é gradualmente alterado no sistema de modo a se analisar o efeito de diferentes concentrações desse componente sobre o processo de decantação do biodiesel. Os resultados desta análise, obtidos por meio de diferentes modelos, são comparados entre si de forma a se avaliar o impacto de cada um deles em na simulação desta etapa de purificação.

O Capítulo 6 “Liquid-Liquid Equilibrium, Experimental Data, NRTL Thermodynamic Modeling and Sensitivity Analysis in the Purification Steps of Ethyl Biodiesel from Fodder Radish Oil Production” refere-se a um artigo a ser submetido para o periódico Bioresource Technology. Neste capítulo são apresentados dados inéditos de equilíbrio líquido-líquido de um sistema constituído por glicerol + etanol + biodiesel de óleo de nabo forrageiro, com a apresentação da partição individualizada dos ésteres etílicos constituintes desse sistema. Os parâmetros do modelo NRTL são ajustados a partir dos dados experimentais apresentados neste capítulo, em associação com os dados apresentados no Capítulo 3. A partir dos parâmetros ajustados, as etapas de decantação e lavagem da produção deste biocombustível são estudadas avaliando-se diferentes arranjos de unidades de misturadores/separadores utilizando-se o simulador comercial ASPEN Plus (ASPEN Technology).

O Capítulo 7, “Densities and Viscosities of Fatty Acid Ethyl Esters and Biodiesels Produced by Ethanolysis from Palm, Canola and Soybean Oils: Experimental Data and Calculation Methodologies”, compõe-se de um artigo publicado em periódico (Basso, R. C.; Meirelles, J. A. A.; Batista, E. A. C. **Industrial & Engineering Chemistry Research**, v. 52, p. 2985-2994, 2013). O capítulo apresenta dados experimentais de densidade e de viscosidade dos biodieseis de óleo de palma, canola e soja a temperaturas de até 363,2 K; aborda a elaboração de um novo modelo para o cálculo da viscosidade de ésteres etílicos em função da temperatura e dos números de carbonos e de insaturações das moléculas desses componentes; descreve a sistematização de um modelo totalmente preditivo para o cálculo da densidade desses biodieseis; avalia e compara a diferentes modelos utilizados no cálculo destas propriedades físicas.

O Capítulo 8, “Biodiesels Produced by Ethanolysis: Melting Profile, Densities and Viscosities Correlated to Ester Composition and Calculations Methodologies” é constituído por um artigo submetido ao periódico Energy & Fuels. O capítulo apresenta dados experimentais originais de densidade e viscosidade, na faixa de temperatura de 283,2 até

363,2 K, e de comportamento térmico durante a fusão, obtidos por meio de calorimetria exploratória diferencial (DSC), dos biodieseis de óleo de crambe, de polpa de macaúba, de nabo forrageiro e de coco, produzidos por etanólise. O comportamento de cada propriedade descrita é correlacionado à composição em ésteres etílicos de cada biodiesel. Dois modelos desenvolvidos para o cálculo da viscosidade, com dependência de temperatura, e dois modelos para o cálculo das densidades são avaliados quanto a descrição dos dados experimentais.

O Capítulo 9, “Conclusões”, apresenta as principais conclusões provenientes da análise dos resultados dos capítulos em relação às propriedades físicas estudadas, equilíbrio líquido-líquido e ao estudo das etapas de decantação e lavagem na produção do biodiesel etílico.

Capítulo 2. Revisão Bibliográfica

2.1. Biodiesel

Biodiesel é uma mistura de ésteres monoalquílicos de ácidos graxos derivado de fontes renováveis como óleos vegetais e gorduras animais, para o uso em motores de ignição por compressão. A produção deste biocombustível normalmente é feita por meio da reação de transesterifcação, sendo a catálise alcalina o processo mais empregado industrialmente devido à elevada conversão, condições operacionais amenas e baixa ação corrosiva do catalisador em comparação com os ácidos fortes empregados na catálise ácida (MARCHETTI; MIGUEL; ERRAZU, 2007; MEHER; SAGAR; NAIK, 2006; KNOTHE; VAN GERPEN; KRAHL, 2005).

Dentre as vantagens desse biocombustível, em relação aos combustíveis fósseis, estão a sua origem parcial ou completamente renovável, a sua maior biodegradabilidade, maior ponto de fulgor, menor teor de enxofre e redução na emissão de gases poluentes durante a combustão (MOSER, 2009).

Conforme observado na **Figura 1**, a primeira etapa da transesterificação por catálise básica (etapa 1) é a reação de uma base com um álcool, produzindo um alcóxido e um catalisador protonado. O ataque nucleofílico do alcóxido ao grupo carbonila do triacilglicerol gera um intermediário tetraédrico (etapa 2), a partir do qual o éster alquílico e o correspondente ânion de diacilglicerol são formados (etapa 3). Este último desprotona o catalisador, regenerando-o (etapa 4) e tornando-o capaz de reagir com uma segunda molécula de álcool, iniciando outro ciclo catalítico. Diacigliceróis e monoacigliceróis são convertidos pelo mesmo mecanismo até a formação de uma mistura de ésteres alquílicos e glicerol (TAFT; NEWMAN; VERHOEK, 1950; GUTHRIE, 1991; SCHUCHARDT; SERCHELI; VARGAS,1998).

A razão estequiométrica na reação de transesterificação é de 1:3 de triacilglicerol: álcool, produzindo três moles de ésteres e um mol de glicerina. No entanto, álcool em excesso normalmente é usado para deslocar o equilíbrio da reação de modo a favorecer a formação de ésteres de ácidos graxos (MEHER; SAGAR; NAIK, 2006). Na transesterificação com etanol, quantidades inferiores a 3 mol de etanol em excesso foram consideradas insuficientes na otimização da formação de ésteres etílicos. Por outro lado, grande quantidade de etanol em excesso, além de consumir uma quantidade desnecessária de reagente, dificulta a etapa de decantação na produção de biodiesel uma vez que glicerol e ésteres etílicos são solúveis no álcool (ENCINAR et al., 2002).

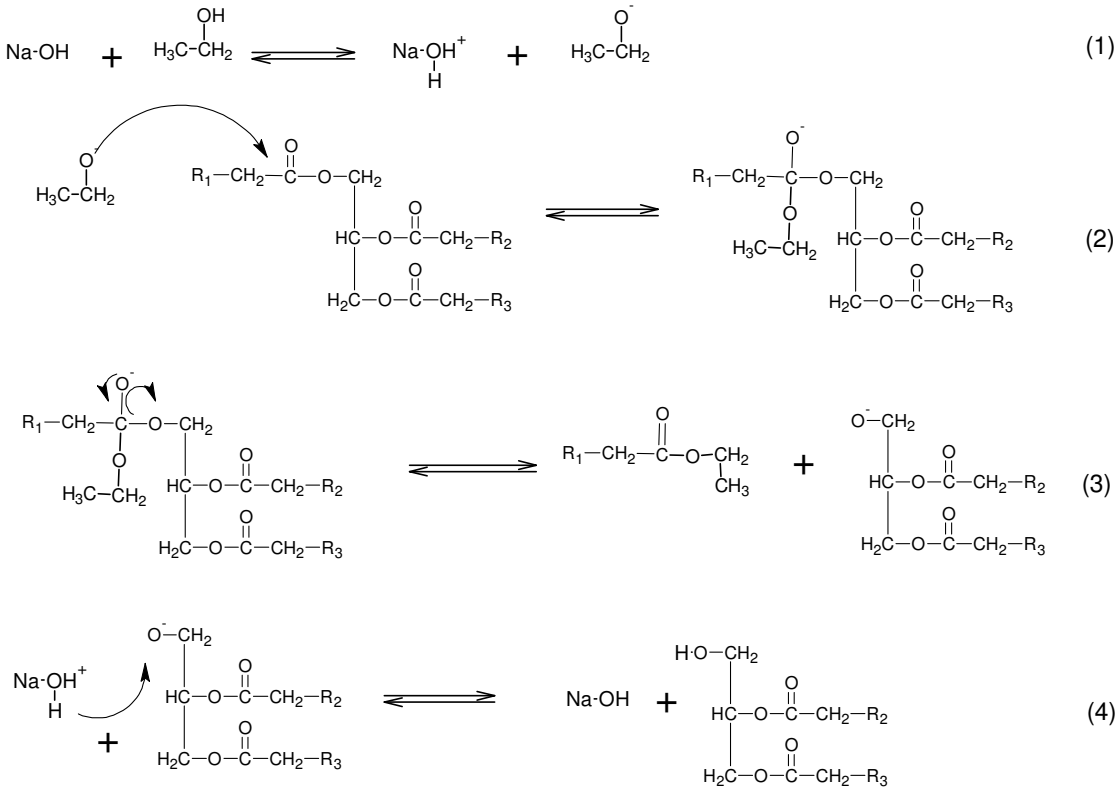

Figura 1. Mecanismo de transesterificação por catálise básica.

A etanólise se processa de maneira mais lenta do que a metanólise devido a maior reatividade do ânion metóxido em comparação ao ânion etóxido. O aumento da cadeia do ânion alcóxido corresponde a uma diminuição em sua nucleofilicidade, resultando na redução da reatividade do etóxido em comparação ao metóxido. Apesar de mais lenta, a conversão global em ésteres etílicos é maior do que a conversão em ésteres metílicos devido à menor miscibilidade entre os triacilgliceróis e o metanol em comparação com a miscibilidade entre o etanol e os triacilgliceróis (MOSER, 2009; SRIDHARAN; MATHAI, 1974).

A produção de ésteres etílicos é um processo mais complexo do que a produção de ésteres metílicos, especificamente na etapa de purificação, devido à maior possibilidade de formação de emulsões estáveis. A menor polaridade do etanol, em comparação ao metanol, associada à agitação pode levar à formação de emulsões mais estáveis do que na transesterifcação com metanol, o que dificulta o processo de separação e purificação (MOSER, 2009; KORUS et al., 1993; ZHOU; KONAR; BOOCOCK, 2003; ZHOU; BOOCOCK , 2006).

Apesar de algumas desvantagens técnicas e econômicas, como o elevado preço do etanol em comparação com metanol, a produção de ésteres de ácidos graxos a partir do etanol apresenta uma série de vantagens. A maior solubilidade dos triacilgliceróis neste álcool permite o contato mais íntimo entre os reagentes. O etanol, em oposição ao metanol, apresenta toxidez bastante reduzida. O uso do etanol é sustentavelmente vantajoso para a produção de biodiesel etílico uma vez que é produzido de fontes biorenováveis, podendo ser considerado um combustível proveniente exclusivamente de fontes agrícolas (ENCINAR et al., 2002; STAMENKOVIC; VELICKOVIC; VELJCKOVIC, 2011).

Após a reação de transesterificação, realizada a separação entre da fase rica em glicerol da fase rica em ésteres de ácidos graxos. Este processo é baseado na diferença de densidades entre o biodiesel, em média 880 kg/m^3, e o glicerol, em média 1050 kg/m^3, e na quase total imiscibilidade entre estes dois produtos. Deste modo, esta etapa pode ser feita for simples decantação ou centrifugação (ATADASHI et al., 2011).

A lavagem do biodiesel com água é um modo efetivo de remover um conjunto de contaminantes da mistura de ésteres. Devido à elevada solubilidade dos resíduos de sabões e glicerina na água, bem como a elevada miscibilidade desta com o excesso de álcool (metanol ou etanol) empregado no processo, a lavagem do biodiesel com água reduz o teor de impurezas aos requeridos pelos padrões de qualidade de biodiesel. Esse processo pode ser feito à temperatura ambiente sem perda significativa de sua eficiência como meio de purificação da mistura de ésteres. (ATADASHI et al., 2011; BERRIOS; SKELTON, 2008; RAHAYU; MINDARIANY, 2007).

Os ésteres provenientes de óleos vegetais além de servirem como combustíveis podem ser utilizados em diversas outras finalidades. Eles podem servir como intermediários na produção de álcoois graxos para uso em surfactantes e produtos de limpeza. Ésteres ramificados são usados como lubrificantes, sendo interessantes devido a questões ambientais por sua elevada biodegradabilidade. Eles também possuem propriedades desejáveis como solventes. Ésteres de óleo de colza (rico em ácido erúcico) são indicados na produção de plásticos e como absorventes de elevada temperatura de ebulição na descontaminação de gases industriais (KNOTHE; VAN GERPEN; KRAHL, 2005; PETERS, 1999; WILLING, 1999; WEHLMAN, 1999; BAY; WANKO; ULRICH, 2004).

As propriedades individuais dos vários ésteres graxos que compõem o biodiesel determinam as propriedades globais do biocombustível. Por sua vez, as propriedades dos ésteres de ácidos graxos são determinadas pela estrutura das moléculas dos ácidos graxos e dos alcoóis que compõem os ésteres. As principais características estruturais das moléculas de ésteres graxos que afetam algumas das principais propriedades físicas do biodiesel são o comprimento da cadeia carbônica, o número e posição das duplas ligações e a presença de radicais na cadeia carbônica (KNOTHE, 2005; KNOTHE; DUNN, 2009).

2.2. Viscosidades dos Ésteres de Ácidos Graxos e de Biodieseis

O efeito da influência do número de carbonos e de duplas ligações sobre a viscosidade dos ésteres metílicos foi avaliado por Ramirez-Verduzco (2013). Foi observado que o aumento progressivo do número de pares de carbonos, em até seis átomos, na molécula do ácido graxo constituinte dos ésteres metílicos saturados, levou a incrementos de 23,63%, 50,20% e 79,80% em suas viscosidades enquanto um aumento gradual de uma dupla ligação, em até três ligações, provocou decrementos de 13,33%, 24,88% e 34,91% nessa propriedade.

Segundo observado por Knothe (2005), a viscosidade é um importante parâmetro na escolha do óleo para produção de biodiesel, uma vez que afeta a atomização do combustível na injeção dentro do cilindro de combustão, bem como a formação de depósitos nos motores. Normalmente, o valor dessa propriedade aumenta com o aumento no comprimento da cadeia carbônica e diminui com o grau de insaturação dos ésteres alquílicos.

A viscosidade dinâmica dos ésteres metílicos dos ácidos palmitoléico (C16:1), gadoléico (C20:1) e erúcico (C22:1) foram estimadas por Yuan, Hansen e Zhang (2009) a partir das viscosidades dos ácidos palmítico (C16:0), araquídico (C20:0) e beênico (C22:0) com bases nas diferenças entre as viscosidades dos ésteres metílicos de ácido oléico e linoléico (equação 1). A hipótese considerada na abordagem aplicada foi a de que as diferenças entre as viscosidades devido à dupla ligação seriam proporcionais entre os ésteres metílicos com mesmo tamanho de cadeia carbônica. A estimativa não resultou em aumento dos desvios entre os valores calculados e experimentais das misturas de ésteres metílicos.

$$\eta_d = \frac{\eta_{18:1} - \eta_{18:0}}{\eta_{18:0}} \quad (1)$$

onde η_d é a diferença relativa entre as viscosidades dinâmicas; $\eta_{18:1}$ e $\eta_{18:0}$ são as viscosidades dinâmicas dos ésteres metílicos de ácido oléico e ácido esteárico, respectivamente.

As viscosidades dinâmicas dos ésteres puros, saturados e insaturados, metílicos e etílicos dos ácidos caprílico, capróico, láurico, mirístico, palmítico, esteárico, oléico, linoléico, linolênico, araquídico, e metílicos dos ácidos palmitoléico, gadoléico, beênico, erúcico e lignocérico foram determinadas experimentalmente por Pratas et al. (2010) e Pratas et al. (2011a) em temperaturas entre 278,15 K e 363,15 K. Foi observado que, tanto em relação aos ésteres etílicos quanto metílicos, a viscosidade aumentou com o aumento do tamanho da cadeia carbônica e diminuiu com o aumento do número de duplas ligações dos ácidos graxos presentes no grupo alquila dos ésteres.

Uma metodologia para o cálculo da viscosidade de biodieseis metílicos, baseada no princípio dos estados correspondentes, foi apresentada por do Carmo et al. (2012). Segundo esse princípio, se pressão, volume e temperatura são relacionados com as correspondentes propriedades críticas, a função que relaciona pressão reduzida a volume reduzido torna-se a mesma para todas as substâncias (REID; PRAUSNITZ; POLING, 1987). Os desvios relativos entre os valores calculados por meio dessa metodologia e os obtidos experimentalmente foram de 9,4% e 8,3% usando a densidade de um e de dois fluidos de referência, respectivamente.

Algumas modificações em um modelo de contribuição de grupos, originalmente desenvolvido por Sastri e Rao (1992) para o cálculo de viscosidade de líquidos orgânicos a partir da pressão de vapor dos mesmos, foram propostas por Anand, Ranjan e Mehta (2010a) para a predição da viscosidade de ésteres metílicos (equações 2 – 4). Quando aplicado ao cálculo da viscosidade de catorze diferentes biodieseis metílicos, o desvio relativo médio entre os valores experimentais e calculados foi de 4,2%, enquanto o desvio relativo máximo ficou abaixo de 10%.

$$\eta_i = \sum \Delta\eta_B p_{vp}^{-(0,25+\alpha)} \quad (2)$$

$$lnp_{vp} = (4{,}5398 + 1{,}0309 lnT_{nb})\left\{1 - \frac{[3 - 2(T/T_{nb})]^{\beta}}{T/T_{nb}} - 0{,}38\left[3 - 2\left(\frac{T}{T_{nb}}\right)\right]^{\beta} ln\left(\frac{T}{T_{nb}}\right)\right\} \quad (3)$$

$$\alpha = \sum \Delta N - 0{,}01 n_d - 0{,}005 \quad (4)$$

onde η_i é a viscosidade dinâmica; p_{vp} é a pressão de vapor do componente (atm); $\Delta\eta_B$ e ΔN são os parâmetros de contribuição de grupo; T_{nb} é a temperatura normal de ebulição (K); T é a temperatura de interesse (K); $\beta = 0{,}155$ (ajustado para ésteres metílicos); α é uma função do número de duplas ligações; n_d é o número de dupla ligações nos ésteres metílico insaturados.

Um modelo, constituído por dois conjuntos de equações, foi desenvolvido por Krisnangkura, Yimsuwan e Pairintra (2006) para cálculo da viscosidade cinemática de ésteres metílicos saturados (equações 5-6) e insaturados (equações 7-10). Essa metodologia utiliza dois conjuntos de parâmetros para o cálculo da viscosidade de ésteres metílicos saturados de cadeia curta, até 12 átomos de carbono (equação 5) e de cadeia média, até 18 átomos de carbono (equação 6) e quatro conjuntos de parâmetros para o cálculo da viscosidade de ésteres metílicos provenientes de quatro ácidos graxos insaturados, ácido oléico (equação 7), ácido linoléico (equação 8), ácido linolênico (equação 9) e ácido erúcico (equação 10). Segundo os autores, o modelo permite refinamentos adicionais e a possível extensão para o cálculo das viscosidades de outras séries funcionais homólogas. Os desvios mínimos e máximos, obtidos a partir desse modelo, para os biodieseis metílicos de óleo de coco e de óleo de algodão foram, respectivamente, de 5,53% até 9,20% e de 2,06% até 4,48%.

$$ln\mu = -2{,}915 - 0{,}158z + \frac{492{,}12}{T} + \frac{108{,}35z}{T} \quad (5)$$

$$ln\mu = -2{,}177 - 0{,}202z + \frac{403{,}66}{T} + \frac{109{,}77z}{T} \quad (6)$$

$$ln\mu = -5{,}03 + \frac{2051{,}5}{T} \quad (7)$$

$$ln\mu = -4{,}51 + \frac{1822{,}5}{T} \quad (8)$$

$$ln\mu = -4{,}18 + \frac{1685{,}5}{T} \quad (9)$$

$$ln\mu = -5{,}42 + \frac{2326{,}2}{T} \quad (10)$$

onde μ é a viscosidade cinemática ($mm^2 \cdot s$); z é o número de carbonos da série homóloga; e T é a temperatura absoluta.

O desenvolvimento de um modelo empírico para o cálculo da viscosidade dinâmica de ésteres metílicos foi elaborado por Ramirez-Verduzco (2013) a partir da observação do efeito da massa molecular, do número de duplas ligações e da temperatura sobre essa propriedade física. O uso desse modelo no cálculo da viscosidade de dezenove biodieseis metílicos e vinte e quatro de suas misturas pseudobinárias, resultou em um desvio absoluto global de 6,39%, e um desvio máximo de 17,04%.

A proposição de um modelo (equações 11-15) baseado no conceito de contribuição de grupos para a predição da viscosidade dinâmica de alcoóis graxos, ácidos graxos, acilgliceróis parciais, triacilgliceróis e ésteres de ácidos graxos, com dependência de temperatura, contendo seis termos de perturbação relacionados a cada grupo funcional da molécula do composto em estudo, calculados a partir da regressão de valores de viscosidade de um banco de dados, foi feita por Ceriani, Gonçalvez e Coutinho (2011). Os desvios relativos entre os valores calculados e os dados experimentais foram, de 0,02% a 15,17%, 0,0004% a 16,43%, 0,02% a 16,86%, 0,03% a 32,79% e 0,21% a 10,73% para ácidos graxos, ésteres de ácidos graxos, alcoóis graxos, triacilgliceróis e diacilgliceróis, respectivamente.

$$ln(\eta_i) = \left[\sum_k N_k \cdot A_{1k} + \frac{\sum_k N_k \cdot B_{1k}}{(T + \sum_k N_k \cdot C_{1k})}\right] + M_i \left[\sum_k N_k \cdot A_{2k} + \frac{\sum_k N_k \cdot B_{2k}}{(T + \sum_k N_k \cdot C_{2k})}\right] + Q \quad (11)$$

$$Q = \xi_1 q + \xi_2 \quad (12)$$

$$q = \alpha + \frac{\beta}{T + \gamma} \quad (13)$$

$$\xi_1 = f_0 + N_c f_1 \quad (14)$$

$$\xi_2 = s_0 + N_{cs} s_1 \quad (15)$$

onde η_i é a viscosidade dinâmica (mPas); k representa os diferentes grupos da molécula; $A_{1k}, B_{1k}, C_{1k}, A_{2k}, B_{2k}$ e C_{2k} são os termos de perturbação; M_i é a massa molar do componente; N_k é o número de grupos *na* molécula i; T é a temperatura absoluta; Q é o termo de correção, q é uma função da temperatura absoluta, α, β, e γ são parâmetros otimizados; N_c é o número de átomos de carbono na molécula; f_0 e f_1 são constantes otimizadas; ξ_1 é uma função de N_c; N_{cs} é o número de átomos de carbono no grupo alcoólico; s_0 e s_1 são constantes otimizadas; ξ_2 é o termo que descreve as diferenças entre as viscosidades dos isômeros ésteres na mesma temperatura.

Três metodologias propostas por Ceriani et al. (2007), por Krisnangkura, Yimsuwan e Pairintra (2006) e por Yuan, Hansen e Zhang (2009) e um grupo de parâmetros reajustados da metodologia proposta por estes últimos autores, para o cálculo das viscosidades de 24 biodieseis metílicos ou misturas desses, foram avaliados por Freitas et al. (2011), resultando em desvios relativos globais entre os valores calculados e experimentais, respectivamente, de 8,07%, 7,25%, 5,34% e 4,65%.

A não associatividade entre os ésteres de ácidos graxos nos biodieseis foi considerada por Allen et al. (1999), a partir da observação de que estes compostos possuem estruturas químicas similares e, devido a essa similaridade, provavelmente não interajam entre si nas misturas, apresentando comportamento similar a um componente individual. Deste modo, o cálculo da viscosidade dos biodieseis a partir da viscosidade

dos ésteres de ácidos graxos puros, pode ser feito a partir da consideração de nulidade do termo de interação da equação proposta por Grunberg e Nissan (1949) (equação 16).

$$l\,n(\eta_{mix}) = \sum_{i} x_i \cdot ln(\eta_i) + \frac{1}{2}\sum_{i=1}^{n}\sum_{j=1}^{n} x_i x_j G_{ij} \qquad (16)$$

onde η é a viscosidade; x é a fração molar; i e j denotam os componentes da mistura; G é o parâmetro de interação entre os componentes da mistura; mix denota a mistura de ésteres alquílicos.

2.3. Densidade dos Ésteres de Ácidos Graxos e de Biodieseis

A densidade dos ésteres puros, saturados e insaturados, metílicos e etílicos dos ácidos caprílico, capróico, láurico, mirístico, palmítico, esteárico, oléico, linoléico, linolênico, araquídico, e metílicos dos ácidos palmitoléico, gadoléico, beênico, erúcico e lignocérico, foi determinada experimentalmente por Pratas et al. (2010) e Pratas et al. (2011a) em temperaturas entre 278,15 K e 363,15 K. Os dados obtidos mostraram que a densidade dos ésteres metílicos e etílicos diminui com o aumento no comprimento da cadeia carbônica do grupo alquila e aumenta com o grau de insaturação. Foi observado que as densidades dos ésteres etílicos, em relação às dos ésteres metílicos, foram muito abaixo do esperado pela adição de um grupo metileno (CH_2) à molécula. Esse comportamento foi relacionado à possíveis mudanças no ordenamento das molécula.

O efeito da influência do grau de insaturação e do número de carbonos na cadeia alquílica sobre a densidade dos ésteres metílicos foi quantificado por Ramirez-Verduzco (2013). Foi verificado que o aumento, em pares de átomos carbono, na cadeia do ácido graxo constituinte dos ésteres metílicos saturados, em até seis átmos, levou a decrementos de 0,12%, 0,22% e 0,31% na densidadade desses componentes, enquanto um aumento gradual de uma dupla ligação, em até três ligações, levou a incrementos de 1,33%, 2,66% e 3,99% nessa propriedade.

A equação proposta por Rackett (1970), para o cálculo de volume molar de líquidos saturados, foi primeiramente alterada por Spencer e Danner (1973), com a inclusão do parâmetro de Rackett (Z_{RA}). Apartir dessas lterações, Halvorsen, Mammel Jr e Clements (1993), formularam uma metodologia (equações 17-20) para o cálculo da densidade de óleos vegetais, a partir das propriedades dos ácidos graxos constituintes de

seus triacilgliceróis, dependente de uma densidade experimental de referência para o cálculo do parâmetro de Rackett.

$$\rho_{óleo} = \frac{(\sum x_i MW_i)}{R\left(\sum \frac{x_i T_{ci}}{P_{ci}}\right)(\sum x_i Z_{RAi})^{\left[1+(1-T_r)^{2/7}\right]}} + F_C \quad (17)$$

$$Z_{RA,i} = \left[\frac{M_{w,i} P_{c,i}}{\rho_i R T_{c,i}}\right]^{\left[1+(1-T_r)^{2/7}\right]^{-1}} \quad (18)$$

$$MW_{óleo} = 3\sum x_i MW_i + 38{,}0488 \quad (19)$$

$$F_C = 0{,}0236 + a|875 - MW_{óleo}| \quad (20)$$

onde x_i é a fração molar do ácido graxo no óleo; T_{ci} é a temperatura crítica do ácido graxo; P_{ci} é a pressão crítica do ácido graxo; T_r é a temperatura reduzida em relação à temperatura crítica da mistura; MW_i é a massa molar do ácido graxo; a é uma constante igual a 0,000082 e 0,000098 para triacilgliceróis com massas molares, respectivamente, maiores e menores que 875 $g\ mol^{-1}$; i denota o ácido graxo em consideração.

O uso da temperatura normal de ebulição, obtida a partir de uma metodologia preditiva, no cálculo do parâmetro Z_{RA}, na estimativa das densidades de ésteres metílicos proposta por Anand, Ranjan e Mehta (2010b), resultou em desvios de 0,1% a 2,3%, em relação aos valores experimentais.

As densidades, de 15 a 90 °C, de biodieseis etílicos de óleo de soja, canola, palma, milho e arroz foi determinada experimentalmente por Baroutian et al. (2008). O cálculo das densidades desses biodieseis a partir da metodologia proposta por Halvorsen, Mammel e Clements. (1993), utilizando valores experimentais como densidade de referência e calculando o parâmetro de Rackett para a mistura de ésteres dos biodieseis, resultou em desvios médios menores que 0,2%.

Um modelo de contribuição de grupos nomeado de GCVOL (equações 21-22) foi desenvolvido por Elbro, Fredenslund, Rasmussen (1991) para o cálculo dos volumes molares de solventes, oligômeros e polímeros, incluindo compostos fortemente polares. A partir de uma nova estimativa dos parâmetros relativos ao grupo CH=, Freitas et al. (2011)

calcularam as densidades de dezoito biodieseis por meio dessa metodologia, obtendo desvios relativos de 0,04 a 0,79%, em relação aos valores experimentais .

$$V = \sum_i n_i \Delta v_i \tag{21}$$

$$\Delta v_i = A_i + B_i T + C_i T^2 \tag{22}$$

onde n_i, é o número de grupos i na molécula; Δv_i é a dependência molar de temperatura do grupo; A_i, B_i e C_i são os parâmetros de cada grupo; T é a temperatura na qual a viscosidade é calculda.

2.4. Comportamento Térmico dos Ésteres de Ácidos Graxos e de Biodieseis

Um dos principais problemas associados ao uso de biodiesel é a alteração de suas propriedades físicas devido a baixas temperaturas. O ponto de névoa é a temperatura na qual um material líquido graxo torna-se turvo devido à formação de cristais originados da solidificação de moléculas de maior ponto de fusão. Devido a diminuição da temperatura, maior quantidade de material sólido é formada, dificultando seu escoamento. Moléculas saturadas têm ponto de fusão significativamente maior e em uma mistura cristalizam-se a temperaturas maiores do que as insaturadas (KNOTHE; VAN-GERPEN; KRAHL, 2005).

A calorimetria exploratória diferencial (DSC) é uma poderosa técnica de investigação do ponto de fusão de ésteres, saturados e insaturados, de ácidos graxos. Apartir do uso dessa técnica analítica foi observado que ésteres insaturados com números ímpares de átomos de carbono na molécula têm ponto de fusão maior do que os ésteres pares, com uma unidade de carbono a mais. A presença de mais de um pico de fusão, que ocorre frequentemente nesse tipo de composto, evidencia um comportamento metaestável. Propriedades como ponto de névoa, ponto de escoamento, ponto de entupimento de filtro e teste de escoamento a frio podem ser correlacionadas aos resultados obtidos por DSC (KNOTHE; DUNN, 2009; DUNN ,1999).

A partir do estudo do comportamento térmico de biodieseis metílicos e etílicos de óleo de babaçu por DSC, a taxas de 1 ℃/min, foi relatada a indução da solidificação de ésteres insaturados promovida pela cristalização dos ésteres saturados, tendo sido observadas duas diferentes transições, para os ésteres saturados e insaturados, no perfil térmico de cristalização (SANTOS et al., 2011).

2.5. Equilíbrio Líquido-Líquido

No ELL, moléculas ou íons de soluto interagem com as moléculas de solvente e, quando em concentrações suficientemente elevadas de soluto, com outras moléculas de soluto. Essas interações exercem importante função na distribuição do soluto entre as duas fases líquidas (MARCUS, 2004).

Quando uma partícula de soluto é introduzida em um líquido, interage com as partículas de solvente em sua vizinhança. A totalidade dessas interações é conhecida como solvatação. Esse processo pode ocorrer em diversos estágios, embora apenas a soma dos efeitos das contribuições totais dos estágios possa ser medida. Em um primeiro momento, um espaço deve ser criado de modo que o solvente possa acomodar o soluto. O soluto se encaixa nesse espaço e interage com as moléculas em sua vizinhança, eventualmente formando ligações coordenadas com as mesmas, dando origem a um intermediário, o soluto-solvatado. Finalmente, esse intermediário formado pode interagir com as moléculas vizinhas, ordenando as moléculas de solvente através de forças de atração (MARCUS, 2004).

A regra das fases de Gibbs (equação 23) demonstra que, em um sistema constituído por duas fases e dois componentes, existem dois graus de liberdade.

$$F = C + 2 - P \tag{23}$$

onde F é o número de graus de liberdade; C é o número de componentes; P é o número de fases do sistema.

Nessa situação, duas condições externas como pressão e temperatura, determinam completamente a composição de um sistema em equilíbrio. Desse modo, a composição do sistema é única ao se especificar a pressão e temperatura do mesmo. Cada componente adicional permite um grau de liberdade a mais, representado pela concentração do mesmo em uma das fases. À temperatura e pressão constantes, quando a concentração em uma das fases é especificada, sua concentração na outra fase não pode ser alterada livremente (MARCUS, 2004).

À pressão e temperatura constantes, as condições de ELL são dadas pela igualdade:

$$x_i^I \gamma_i^{xI} = x_i^{II} \gamma_i^{xII} \quad (24)$$

onde x_i é a fração molar de cada componente i; I e II representam as duas fases líquidas do sistema; γ_i o coeficiente de atividade de cada componente.

A equação (24) assume que, para cada componente, a fugacidade no estado de referência é a mesma em ambas as fases (ABBOTT; PRAUSNITZ,1994).

De acordo com Treybal (1963), o efeito da pressão sobre o ELL pode ser considerado relativamente insignificante. Esta constatação limita a discussão a sistemas condensados e considera como variáveis a serem analisadas apenas a temperatura e a concentração dos componentes nas fases líquidas.

A partir da definição de uma solução ideal, na determinação de fugacidades em misturas líquidas deve-se calcular os desvios em termos das funções em excesso, que são os termos que relacionam as propriedades da solução real à ideal. Essas funções levam a expressões para o cálculo de fugacidades através dos coeficientes de atividade, que são definidos em função da energia de Gibbs em excesso parcial molar.

Através do cálculo das funções de excesso a partir de um modelo termodinâmico determinado pode-se obter o coeficiente de atividade por:

$$RTln\gamma_i = g_i^E = \left(\frac{\partial g^E}{\partial n_i}\right)_{T,P,n_j} \quad (25)$$

onde R é a constante dos gases ideais; T é a temperatura do sistema; n_i é o número de moles de cada componente i; g_e é a energia de Gibbs em excesso; γ_i é o coeficiente de atividade de cada componente i (SMITH; VAN-NESS; ABBOTT, 2000).

Após a obtenção do coeficiente de atividade pode ser aplicado o critério de isoatividade (equação 24), para o equilíbrio líquido-líquido, em um sistema com N componentes à pressão e temperatura uniformes.

Quando as massas molares dos componentes na mistura são muito diferentes, torna-se preferível usar a abordagem descrita por Oishi e Prauznitz (1978), na qual a fração mássica (w_i) é adotada como unidade de composição. As equações (26 - 28) apresentam a relação entre o coeficiente de atividade expresso em unidade molar e expresso em unidade mássica:

$$x_i = \frac{w_i/M_i}{\sum w_j/M_j} \tag{26}$$

$$\gamma_i^w w_i = \gamma_i^x x_i \tag{27}$$

$$\gamma_i^w = \frac{\gamma_i^x}{M_i \sum w_j/M_j} \tag{28}$$

onde γ_i^x é o coeficiente de atividade expresso segundo a fração molar do componente i; γ_i^w é o coeficiente de atividade expresso segundo a fração mássica do componente; w_i é a fração mássica do componente; M_i é a massa molar média do componente.

Segundo Tedder (2009), o coeficiente de distribuição k é a base para o uso de modelos termodinâmicos, permitindo estimar o comportamento do equilíbrio de cada componente nas distintas fases. Esse coeficiente, em relação à fração mássica dos componentes, é dado por:

$$k_i = \frac{w_i^{II}}{w_i^{I}} \tag{29}$$

onde w_i é a fração mássica de cada componente $i$em cada fase líquida I e II.

2.5.1. Modelagem Termodinâmica do ELL

A consideração de um comportamento molecular aleatório em misturas de diferentes componentes, nas quais as moléculas de uma espécie química não mostram preferência na interação com as de outras espécies em sua vizinhança, não é válida quando as forças moleculares entre duas moléculas da espécie 1 são muito diferentes das forças moleculares entre duas moléculas da espécie 2. Neste caso, com o objetivo de levar essas interações em conta, foram introduzidas correções para esse comportamento não aleatório. Essas correções são aplicadas em duas das principais equações para o cálculo do coeficiente de atividade; NRTL (*non random two-liquid*) e UNIQUAC (*universal quasi-chemical*), desenvolvidas por Renon e Prausnitz (1968) e Abrams e Prausnitz (1975), respectivamente (ABBOTT; PRAUSNITZ, 1994).

As duas equações normalmente representam de maneira adequada, para misturas de não eletrólitos, propriedades de misturas fortemente não ideais. A principal vantagem dessas equações é o fato de poderem ser facilmente aplicadas para misturas ternárias (e multicomponentes) usando apenas parâmetros de componentes puros e binários (ABBOTT; PRAUSNITZ, 1994).

A equação NRTL possui um parâmetro α_{ij} (= α_{ji}), característico dos componentes em cada binário, que está relacionado com a não aleatoriedade da mistura. Adicionalmente a este parâmetro, a equação NRTL possui dois parâmetros ($A(0)_{ij}$ e $A(0)_{ji}$) relacionados à interação molecular de cada binário. Ainda podem ser adicionados dois parâmetros ($A(1)_{ij}$ e $A(1)_{ji}$) para cada interação binária para representar o efeito da temperatura sobre as propriedades do sistema. Através dos parâmetros binários, podem ser estimados os coeficientes de atividade relativos a cada componente. Estes coeficientes são usados para estimar o coeficiente de atividades para cada ternário, e assim sucessivamente para as misturas multicomponentes (SANDLER, 1999; KHOURY, 2005).

Segundo Rodrigues, Pessoa-Filho e Meirelles (2004), o modelo NRTL para misturas multicomponentes utilizando fração mássica como unidade de concentração se apresenta como (equações 30-34):

$$ln\gamma_i = \frac{\sum_{j=1}^{K} \tau_{ji} G_{ji} w_j / \bar{M}_j}{\sum_{j=1}^{K} G_{ji} w_j / \bar{M}_j} + \sum_{j=1}^{K} \left[\frac{w_j G_{ij}}{\bar{M}_j \sum_{l=1}^{n} G_{lj} w_l / \bar{M}_l} \times \left(\tau_{ij} - \frac{\sum_{l=1}^{K} \tau_{lj} G_{lj} w_l / \bar{M}_l}{\sum_{l=1}^{K} G_{lj} w_l / \bar{M}_l} \right) \right] \quad (30)$$

$$G_{ji} = exp\,(-\alpha_{ij}\tau_{ij}) \quad (31)$$

$$\tau_{ij} = \frac{g_{ij} - g_{jj}}{RT} \quad (32)$$

$$\frac{g_{ij} - g_{jj}}{R} = A(0)_{ij} + A(1)_{ij}T \quad (33)$$

$$\alpha_{ij} = \alpha_{ji} \quad (34)$$

onde g_{ij} e τ_{ij} representam a energia de interação molecular entre os componentes *i* e *j*; α_{ij} é o parâmetro de não aleatoriedade referente a cada binário da mistura; T é a

temperatura absoluta; $A(0)_{ij}$ *e* $A(1)_{ij}$ são os parâmetros de energia, característico das interações entre os componentes *i* e *j*.

A equação UNIQUAC é baseada no modelo "two-liquid" no qual a energia livre de Gibbs em excesso é considerada como sendo o resultado de diferenças nos tamanhos e estruturas moleculares (contribuição entrópica), dada pela parte combinatorial do modelo e da energia de interação entre as moléculas (contribuição entálpica), dada pela parte residual do modelo. A equação requer dados de componentes puros, obtidos de informações da estrutura molecular, para os parâmetros de área e volume, respectivamente q_i e r_i. O modelo contém apenas dois parâmetros ajustáveis, τ_{ij} e τ_{ji} para cada par de binário, podendo ser adicionados dois parâmetros adicionais na representação da dependência de temperatura. Os parâmetros de volume (r) e área (q) são obtidos por métodos de contribuição de grupo. Este conceito baseia-se no fato de que uma molécula pode ser considerada uma coleção de grupos funcionais, e que o volume R_i e a área superficial Q_i do grupo i serão aproximadamente os mesmos em todas as moléculas (Sandler, 1999; Khoury, 2005).

De acordo com Rodrigues, Pessoa-Filho e Meirelles (2004), o modelo UNIQUAC, aplicado a misturas multicomponentes utilizando fração mássica como unidade é representado por (equações 35-41):

$$ln\gamma_i = ln\gamma_i^{Comb} + ln\gamma_i^{Res} \tag{35}$$

$$ln\gamma_i^{Comb} = \frac{ln\emptyset_i}{ln\,(w_i/\zeta M_i)} + 1 - \frac{\zeta M_i \emptyset_i}{w_i} + \frac{z}{2} M_i q_i' ln\frac{\phi_i'}{\theta_i'} - \frac{z}{2} M_i q_i' \left(1 - \frac{\phi_i'}{\theta_i'}\right) \tag{36}$$

$$\zeta = \sum_{j=1}^{K=1} \frac{w_j}{M_j} \tag{37}$$

$$\theta_i' = \frac{q_i' w_i}{\sum_{j=1}^{K} q_j' w_j}; \quad \phi_i' \frac{r_i' w_i}{\sum_{j=1}^{K} r_j' w_j} \tag{38}$$

$$r_i = \sum_K v_K^{(i)} R_k; q_i = \sum_K v_K^{(i)} Q_K \tag{39}$$

$$ln\gamma_i^{Res} = M_i q_i' \left[1 - ln\left(\sum_{j=1}^{K} \theta_j' \tau_{ji}\right) - \sum_{j=1}^{K} \left(\frac{\theta_i' \tau_{ij}}{\sum_{k=1}^{K} \theta_k' \tau_{kj}}\right)\right] \quad (40)$$

$$\tau_{ij} = exp\left(-\frac{A_{ij}}{T}\right) \quad (41)$$

onde *w* é a fração mássica do componente; M é a massa molecular do componente; $v_k^{(i)}$ é o número de grupos funcionais do tipo k na molécula i; R_k e Q_K são, respectivamente, parâmetros de área superficial e volume; τ_{ij} é o parâmetro de interação.

UNIFAC (*uniquac functional group activity coefficient)* é um método de contribuição de grupos que combina o conceito de solução por grupos funcionais com modelos para cálculo de coeficiente de atividades, contendo dois parâmetros ajustáveis por par de grupos funcionais, para a predição de coeficiente de atividade em misturas de líquidos não eletrólitos, apresentado por Fredenslund, Jones e Prauznitz (1975). Uma revisão dos parâmetros do modelo UNIFAC para a predição do comportamento de misturas em equilíbrio líquido-líquido foi apresentada por Magnussen, Rasmussen e Fredenslund (1981).

$$ln\gamma_i = ln\gamma_i^{comb} + ln\gamma_i^{res} \quad (42)$$

$$ln\gamma_i^{comb} = ln\frac{\Phi}{x_i} + 1 - \frac{\Phi}{x_i} - \frac{z}{2} q_i \left(ln\frac{\Phi}{\vartheta_i} + 1 - \frac{\Phi}{\vartheta_i}\right) \quad (43)$$

$$\Phi_i = \frac{r_i x_i}{\sum r_j x_j}; \vartheta_i = \frac{q_i x_i}{\sum q_j x_j} \quad (44)$$

$$ln\gamma_i^{res} = \sum_k v_k^{(i)} \left(ln\Gamma_k - ln\Gamma_k^{(i)}\right) \quad (45)$$

$$ln\Gamma_k = Q_k \left[1 - ln\left(\sum_m \Theta_m \Psi_{mk}\right) - \sum_m \frac{\Theta_m \Psi_{km}}{\sum_n \Theta_n \Psi_{nm}}\right] \quad (46)$$

$$\Theta_m = \frac{X_m Q_m}{\sum_n X_n Q_n} \quad (47)$$

$$X_m = \frac{\sum_j v_m^{(i)} x_j}{\sum_j \sum_n \left(v_n^{(j)} x_j\right)} \quad (48)$$

$$\Psi_{mn} = exp\left(-\frac{a_{mn}}{T}\right) \tag{49}$$

$$a_{mn} = U_{mn} - U_{nn} \tag{50}$$

onde X_m é a fração molar do grupo m na mistura; Γ_k é o coeficiente de atividade residual do grupo k; $\Gamma_k^{(i)}$ é o coeficiente de atividade residual do grupo k em uma solução apenas com moléculas do tipo i; a_{mn}é o parâmetro de interação dos grupos m e n.

Modificações no modelo UNIFAC foram apresentadas por Weidlich e Gmehling (1987), resultando no modelo UNIFAC-DORTMUND. As alterações propostas foram referentes ao cálculo da parte combinatorial e a introdução de parâmetros de interação de grupos com dependência da temperatura, para ser utilizado na predição do comportamento de misturas em equilíbrio. Segundo Gmehling et al. (2002), os parâmetros desse modelo têm sido revisados de acordo com o surgimento de novos dados de equilíbrio, o que possibilita seu uso na predição de diferentes propriedades termodinâmicas de misturas, entre elas o equilíbrio líquido-vapor, líquido-líquido e sólido-líquido, entalpia em excesso e coeficiente de atividade a diluição infinita.

Uma metodologia para o ajuste de parâmetros dos modelos NRTL e UNIQUAC, usando um algorítimo desenvolvido em linguagem de programação FORTRAN, foi formulada por Stragevitch e d'Ávila (1997). Esse algorítimo usa o método simplex modificado aplicado na minimização da função objetivo da composição (equação 51) para estimar os parâmetros termodinâmicos. O procedimento para o cálculo dos parâmetros envolve cálculos *flash* para o ponto médio de composições das linhas de amarrações experimentais.

$$OF_w = \sum_m^D \sum_n^N \sum_i^{K-1} \left[\left(\frac{w_{i,n,m}^{I,exp} - w_{i,n,m}^{I,calc}}{\rho_{w_{i,n,m}^I}} \right)^2 + \left(\frac{w_{i,n,m}^{II,exp} - w_{i,n,m}^{II,calc}}{\rho_{w_{i,n,m}^{II}}} \right)^2 \right] \tag{51}$$

onde D é o número total de conjuntos de dados; N é o número total de linhas de amarração; K é o número total de componentes (ou pseudocomponentes) no conjunto de dados m; w é a fração mássica dos componentes; i, n e m referem-se a cada componente (ou pseudocomponente), a cada linha de amarração e a cada conjunto de dados, respectivamente; I e II são as fases em equilíbrio; exp e $calc$ referem-se a valores

experimentais e calculados, respectivamente; $\rho_{w_{i,n,m}^{I}}$ e $\rho_{w_{i,n,m}^{II}}$ são os desvios padrões da composição nas duas fases em equilíbrio.

2.5.2. Comportamento no ELL de Sistemas Contendo Ésteres Alquílicos de Ácidos Graxos

Com base na análise do ELL em sistemas constituídos por etanol + óleo de soja + ésteres etílicos de óleo soja a 300,2 K, Liu et al. (2008) concluíram que os ésteres etílicos apresentaram considerável solubilidade em ambas as fase formadas, na fase rica em etanol e na fase rica em óleo de soja, com os coeficientes de distribuição, para os ésteres etílicos, variando de 1,46 a 2,92. Nos sistemas constituídos por glicerol + etanol + ésteres etílicos, ocorreu acentuada miscibilidade dos ésteres etílicos e do glicerol no etanol, enquanto a miscibilidade entre glicerol e ésteres etílicos foi bastante reduzida.

A partir do estudo do ELL em misturas ternárias constituídas por metanol + glicerol + oleato de metila, Andreatta et al. (2008) observaram imiscibilidade quase completa entre o glicerol e os ésteres metilíco. À temperatura de 60 °C (333 K), a maior fração mássica de oleato metila na fase rica em glicerol foi de 0,011, enquanto a maior fração mássica de glicerol na fase rica em éster foi de 0,021.

Pesquisando a distribuição do metanol e de catalisador (KOH) entre as fases ricas em ésteres metílicos e em glicerina, Chiu, Goff e Suppes (2005) destacaram que a solubilidade do catalisador alcalino na fase rica em ésteres é muito menor do que na fase rica em glicerol. Os coeficientes de distribuição do KOH situaram-se entre 34,7 e 97,6 da fase rica em glicerol em relação à fase rica em ésteres metílicos, nas duas diferentes temperaturas analisadas.

A investigação do ELL de sistemas compostos por metanol + glicerol + ésteres metílicos de pinhão manso (*Jatropha curcas*) por Zhou, Lu e Liang (2006), demostrou haver uma baixa solubilidade mútua entre os éteres metílicos e o glicerol. O efeito da temperatura sobre o comportamento do equilíbrio líquido-líqui desses sistemas foi pouco pronunciado.

Análises do ELL de sistemas compostos por metanol ou etanol + glicerol + ésteres metílicos de óleo de mamona feitas por França et al. (2009) constataram um

pequeno aumento na região de separação de fases quando da utilização do metanol, ao invés de o etanol, como o álcool constituinte do sistema.

2.5.3. Modelagem do Equilibrio Liquido Liquido em Sistemas Contendo Esteres de Ácidos Graxos

Os modelos NRTL e UNIFAC, quando usados por Lee, Lo e Lin. (2010) na descrição do ELL de sistemas contendo glicerol + metanol + oleato de metil ou linoleato de metila resultaram em desvios médios, respectivamente, de 0,0075 até 0,0196 e de 0,0049 até 0,0071. A predição do ELL de sistemas compostos por água + metanol + ésteres metílicos por meio dos modelos UNIFAC e UNIFAC-Dortmund implicou em desvios cerca de cinco vezes maiores para os sistemas contendo oleato de metila em comparação com os sistemas contendo linoleato de metila.

GC-PPC-SAFT é um método de contribuição de grupos combinado com uma equação de estado baseada em teoria estatística associativa de fluido. A equação apresenta dois parâmetros que consideram interações dispersivas, um parâmetro que considera a formação das cadeias moleculares dos componentes, um parâmetro que contabiliza interações associativas e um parâmetro que considera a polaridade da molécula. Esse método foi utilizado por Barreau et al. (2010). na predição do ELL de um sistema modelo composto por metanol + glicerol + oleato de metila. Esses autores utilizaram nove parâmetros para cada componente puro, obtendo uma descrição satisfatória do comportamento do sistema, embora a mesma tenha subestimado a solubilidade do éster na fase rica em glicerol, principalmente em regiões próximas ao ponto crítico.

A modelagem do ELL de sistemas contendo glicerol + oleato de metila + metanol ou etanol, realizada por Andreatta et al. (2008) e Andreatta (2012) resultou em desvios médios e máximos, por componente, respectivamente, de 0,004 a 0,006 e de 0,012 a 0,047 (sistemas com metanol) e de 0,001 a 0,004 e de 0,009 a 0,012 (sistemas com etanol) usando um método de contribuição de grupos associativo com equação de estado (GCA-EOS). Nestes dois trabalhos, o ELL dos mesmos sistemas foi predito usando um modelo UNIFAC associativo (A-UNIFAC), implicando em desvios médios e máximos, por componentes, respectivamente de 0,005 a 0,007 e de 0,011 a 0,065 (sistema com metanol) e de 0,002 a 0,0013 e de 0,002 a 0,036 (sistema com etanol).

O modelo NRTL, quando usado na descrição do ELL de sistemas constituídos por etanol + glicerol + biodiesel etílico de óleo de soja e de óleo de girassol nas temperaturas de 298,15 e 313,15 K, resultou desvios médios de 1,8 a 2,5% para o sistema contendo biodiesel de soja e de 1,4 a 1,6% para os sistemas contendo biodiesel de girassol.

Utilizando a equação de estado cúbica associativa (CPA-EOS), na modelagem de sistemas contendo glicerol, etanol, biodiesel etílico de óleo de canola ou diferentes ésteres etílicos por, respectivamente, Oliveira et al. (2011) e Follegatti-Romero et al. (2012), os desvios médios foram de 2,6%, para o primeiro sistema, e de 2,7 a 12,5% para os demais.

O modelo UNIQUAC quando utilizado por Mazutti et al. (2013) e por Silva et al. (2012) na descrição do ELL de sistemas binários, ternários e quaternário contendo componentes envolvidos na produção de biodieseis metílicos e etílicos, respectivamente de óleo de soja e de pinhão manso a diferentes temperaturas, implicou em desvio médios globais entre 1,17% e 2,28%.

Os desvios entre os valores experimentais e calculados, nessa seção, estão apresentados conforme citados na literatura. Como diversas formas para esse cálculo foram utilizadas, não foi possível a comparação direta entre os vários valores reportados.

2.5.4. Análise de Sensibilidade na Simulação de Processos

A análise de sensibilidade pode ser definida como o estudo da maneira como a incerteza (ou variabilidade) de uma variável de entrada se propaga por meio de um modelo computacional até a variável de saída (KING; PERERA, 2013).

Em um estudo do efeito das incertezas em propriedades físicas estimadas para simulação de um processo de destilação extrativa, Hukkerikar et al. (2012) destacaram a análise de sensibilidade como uma importante ferramenta na correlação entre as propriedades calculadas e as variáveis de processo e na avaliação do impacto da incerteza das propriedades estimadas sob a operação em análise e na determinação da propriedade de maior impacto no dimensionamento da mesma.

A análise de sensibilidade foi utilizada por Zhang et al. (2003) em um estudo das etapas de catálise ácida e alcalina, na produção de biodiesel a partir de óleo de fritura, de

maneira a descrever a relação entre as variáveis de entrada do processo, preço de matérias primas e produtos, capacidade de produção, pureza do produto, entre outras, e as variáveis de saída.

2.5.5. Aspen Plus na Modelagem de Dados Experimentais e Simulação de Processos

Apesar de algumas diferenças esperadas entre os resultados obtidos por simulação e os econtrados em situações reais, os programas de simulação, dentre os quais o Aspen Plus (Aspen Technology), são comumente usados na obtenção de informações referentes a diferentes processos em operações industriais, uma vez que contam com um vasto banco de dados de substâncias químicas, um conjunto abrangente de modelos termodinâmicos e avançados métodos computacionais de cálculo (WEST; POSARAC; ELLIS, 2008).

O uso do simulador Aspen Plus na análise de processos de produção de biodiesel requer a definição dos componentes químicos em estudo, a seleção de modelos termodinâmicos, a escolha correta das operações unitárias bem como de seus parâmetros de processo e características das correntes de alimentação (VARANDA; PINTO; MARTINS, 2011).

Nem todos os componentes dos sistemas em análise estão presentes nos bancos de dados dos simuladores. Nesta situação, o simulador Aspen Plus pode ser empregado na predição de uma série de propriedades de componentes puros, ou de misturas, a partir da estrutura molecular dos mesmos. Dentre essas propriedades estão a densidade, a viscosidade, a temperatura normal de ebulição, as propriedades críticas, o calor específico e as referentes ao equilíbrio líquido-líquido e líquido-vapor (GARCIA et al., 2010).

O ajuste de parâmetros de modelos termodinâmicos para a representação do ELL usando o simulador Aspen Plus pode ser realizado por meio de diferentes funções objetivo. Podem ser minimizadas as funções objetivo formadas pelos coeficientes de atividade, pelos coeficientes de distribuição e pelas principais variáveis mensuráveis, sendo essa última a função objetivo da verossimilhança (SCHEFFLAN, 2011).

Na regressão de dados de ELL de sistems ternários no simulador Aspen Plus, duas principais possibilidades são recomendadas. Uma delas consiste em primeiramente

ajustar parâmetros referentes a uma mistura binária, na qual o solvente esteja presente, a partir de dados experimentais de solubilidade mútua, e, em seguida, mantendo os valores desses parâmetros constantes, a partir de dados experimentais do sistema ternário, ajustar os demais parâmetros. A outra possibilidade seria realizar o ajuste de todos os parâmetros simultaneamente, a partir dos dados experimentais ternários (SCHEFFLAN, 2011).

Referências Bibliográficas

Abbott, M. M.; Prausnitz, J. M. Modeling the excess Gibbs energy. In: Sandler, S. I. **Models for Thermodynamic and Phase Equilibria Calculations.** New York (New York): Marcel Dekker, Inc, 1994. Cap 1, p. 1-86.

Abrams, D. S., Prausnitz, J. M. Statistical thermodynamics of liquid-mixtures – New expression for excess Gibbs energy of partly or completely miscible systems. **AIChE Journal**, v. 21, p. 116-128, 1975.

Allen, C. A. W.; Watts, K. C.; Ackman, R. G.; Pegg, M. J. Predicting the viscosity of biodiesel fuels from their fatty acid ester composition. **Fuel***,* v. 78, p. 1319-1326, 1999.

Anand, K.; Ranjan, A.; Mehta, P. S. Estimating the viscosity of vegetable oils and biodiesel fuels. **Energy & Fuels***,* v. *24*, p. 664-672, 2010a.

Anand, K.; Ranjan, A.; Mehta, P. S. Predicting the density of straight and processed vegetable oils from fatty acid composition. **Energy & Fuels**, v. 24, p. 3262-3266, 2010b.

Andreatta, A. E.; Casás, L. M.; Hegel, P.; Bottini, S. B.; Brignole, E. A. Phase equilibria in ternary mixtures of methyl oleate, glycerol and methanol. **Industrial & Engineering Chemistry Research**, v. 47, p. 5157-5164, 2008.

Andreatta, E. A. Liquid-liquid equilibria in ternary mixtures of methyl oleate + ethanol + glycerol at atmospheric pressure. **Industrial & Engineering Chemistry Research**, v. 51, p. 9642-9651, 2012.

Atadashi, I. M.; Aroua, M. K.; Abdul-Aziz, A. R.; Sulaiman, N. M. N. Refinning technologies for the purification of crude biodiesel. **Applied Energy**, v. 88, p. 4239-4251, 2011.

Baroutian, S.; Aroua, M. K.; Raman, A. A. A.; Sulaiman, N. M. N. Densities of ethyl esters produced from different vegetable oils. **Journal of Chemical and Engineering Data**, v. *53*, p. 2222-2225, 2008.

Barreau, A.; Brunella, I.; de Hemptinne, J. C.; Coupard, V.; Canet, X.; Rivollet, F. Measurements of liquid-liquid equilibria for a methanol + glycerol + methyl oleate system and prediction using group contribution statistical associating fluid theory. **Industrial & Engineering Chemistry Research**, v. 49, p. 5800-5807, 2010.

Bay, K.; Wanko, H.; Ulrich, J. Biodiesel: high-boiling absorbent for gas purification (Biodiesel: hoch siedendes absorbens fur die gasreinigung), **Chemie Ingenieur Technik**, v. 76, p. 328-333, 2004.

Berrios, M.; Skelton, R. L. Comparison of purification methods for biodiesel. **Chemical and Engineering Journal**, v. 144, p. 459-465, 2008.

Boudy, F.; Seers, P. Impact of Physical Properties of Biodiesel on the Injection Process in a Common-Rail Direct Injection System. **Energy Conversion and Management**, v. *50*, p. 2905-2912, 2009.

Ceriani, R.; Gonçalves, C. B.; Coutinho, J. A. P. Prediction of viscosities of fatty compounds and biodiesel by group contribution. **Energy &. Fuels***,* v. *25*, p. 3712-3717, 2011.

Ceriani, R.; Gonçalves, C. B.; Rabelo, J.; Caruso, M.; Cunha, A. C. C.; Cavaleri, F. W.; Batista, E. A. C.; Meirelles, A. J. A. Group contribution model for predicting viscosity of fatty compounds. **Journal of Chemical and Engineering Data**, v. 52, p. 965-972, 2007.

Chiu, C.; Goff, M. J.; Suppes, G. J. Distribution of methanol and catalysts between biodiesel and glycerin phases. **AIChE Journal**, v. 51, p. 1274-1278, 2005.

Coimbra, M. C.; Jorge, N. Fatty Acids and Bioactive Compounds of The Pulps and Kernels of Brazilian Palm Species, guariroba (*Syagrus oleraces*), jerivá (*Syagrus romanzoffiana*) and macaúba (*Acrocomia aculeata*). **Journal of the Science of Food and Agriculture,** v. 92, p. 679-684, 2012.

Crusciol, C. A. C.; Lima R. L.; Lima E. V.; Andreotti, M.; Moro, E.; Marcon, E. Persistência de Palhada e Liberação de Nutrientes do Nabo-Forrageiro no Plantio Direto. **Pesquisa Agropecuária Brasileira,** v. 40, 161-168, 2005.

do Carmo, F. R.; Sousa-Jr, P. M.; Santiago-Aguiar, R. S.; Sant'Ana, H. B. Development of a new model for biodiesel viscosity prediction based on the principle of corresponding state. **Fuel**, v. 92, p. 250-257, 2012.

Domingos, A. K.; Saad, E. B.; Wilhelm, H. M.; Ramos, L. P. Optimization of the ethanolysis of *Raphanus sativus* (L. Var.) crude oil applying the response surface methodology. **Bioresource Technolology,** v. 99, p.1837-1845, 2008.

Dunn, R. O. Thermal analysis of alternative diesel fuel from vegetable oils. **Journal of the American Oil Chemists' Society,** v. 76, p. 109-115, 1999.

Dunn, R. O. Cold weather properties and performance of biodiesel. In: Knothe, G.; Krahl, J.; Van-Gerpen, J. **The Biodiesel Handbook.** AOCS Press, Champaign, Illinois, 2005, Cap. 6.3, p. 83 – 121.

Dunn, R. O. Crystallization behavior of fatty acid methyl esters. **Journal of the American Oil Chemists' Society,** v. 85, p. 961-972, 2008.

Elbro, H. S.; Fredenslund, A.; Rasmussen, P. Group Contribution method for the prediction of liquid densities as a function of temperature for solvents, oligomers, and polymers. **Industrial & Engineering Chemistry Research**, v. 30, p. 2576-2582, 1991.

Encinar, J. M.; Gonzalez, J. F.; Rodrigez, J. J.; Tejedor, A. Biodiesel fuels from vegetable oils: transesterification of *Cynara cardunculus L.* oils with ethanol. **Energy & Fuels**, v. 16, p. 443-450, 2002.

Falasca, S. L.; Flores, N.; Lamas M. C.; Carballo, S. M.; Aschau, A. *Crambe abyssinica*: An almost unknown crop with a promissory future to produce biodiesel in Argentina. **International Journal of Hydrogen Energy,** v. 35 p. 5808-5812, 2010.

Follegatti-Romero, L. A.; Oliveira, M. B.; Batista, F. R. M.; Batista, E. A. C.; Coutinho, J. A. P.; Meirelles, A. J. A. Liquid-liquid equilibria for ternary systems containing ethyl esters, ethanol and glycerol at 323.15 and 353.15 K. **Fuel**, 94, 386-394, 2012.

França, B. B.; Pinto, F. M.; Pessoa, F. L. P.; Uller, A. M. C. Liquid-liquid equilibria for castor oil biodiesel + glycerol + alcohol. **Journal of Chemical & Engineering**, v. 54, p. 2359-2364, 2009.

Fredenslund A.; Jones R. L.; Prausnitz J. M. Group-contribution estimation of activity coefficients in nonideal liquid mixtures. **AIChE Journal**, v. 21, p. 1086-1099, 1975.

Freitas, S. V. D.; Pratas, M. J.; Ceriani, R.; Lima, A. S.; Coutinho, J. A. P. Evaluation of predictive models for the viscosity of the biodiesel. **Energy & Fuels***,* v. 25, p. 352-358, 2011.

Garcia, M.; Gonzalo, A.; Sánches, J. L.; Arauzo, J.; Peña, J. A. Prediction of normalized biodiesel properties by simulation of multiple feedstock blends. **Bioresource Technology**, v. 101, p. 4431-4439, 2010.

Gmehling, J.; Witting, R.; Lohman, J.; Joh, R. A modified UNIFAC (Dortmund) model. 4. Revision and extension. **Industrial & Engineering Chemistry Research,** v**.** 41, p. 1678-1688, 2002.

Grunberg, L.; Nissan, A. H. Mixture law for viscosity. **Nature**, v.164, p. 799-800, 1949.

Guthrie, J. P.; Rate-equilibrium correlations for the aldol condensation. An analysis in terms of Marcus theory. **Journal of American Chemists Society**, v. 113, p. 7249-7255, 1991.

Halvorsen, J. D.; Mammel Jr., W. C.; Clements, L. D. Density estimation for fatty acid and vegetable oils based on their fatty acid composition. **Journal of the American Oil Chemists' Society**, v. *10*, p. 875-880, 1993.

Hukkerickar, A.; Jones, M.; Sarup, B.; Abildskov, J.; Sin, G.; Gani, R. Sensitivity of process design due to uncertainties in property estimates. **Proceedings of the 11 th International Symposium on Process Systems Engineering**, 15 -19 July, 2012.

Khoury, F. M. Thermodynamics and phase equilibria. In: Khoury, F. M. **Multistage Separation Process.** 3ª ed. Boca Raton (Florida). CRC Press. 2005. Cap. 1.

King, D. M.; Perera, B. J. C. Morris method of sensitivity analysis applied to assess the importance of input variables on urban water supply yield – A case study. **Journal of Hydrology**, v. 477, p. 17-32, 2013.

Knothe, G. Depenence of biodiesel fuel properties on the structure of fatty acid alkyl ester. **Fuel Processing Technology**, v. 86; p. 1059-1070, 2005.

Knothe, G.; Dunn, R. O. A comprehensive evaluation of the melting points of fatty acids and esters determined by differenial scanning calorimetry. **Journal of the American Chemists' Society**, v. 86, p. 843-856, 2009.

Knothe, G.; Steidley, K. R. Kinematic Viscosity of Biofuel Components and Related Compounds: Influence of Compound Structure and Comparison to Petrodiesel Fuel Components. **Fuel,** v. 84, p. 1059-1065, 2005.

Knothe, G.; Van Gerpen, J. Krahl, J. **The Biodiesel Handbook.** AOCS Press: Champaign, Illimois, 2005.

Korus, R. A.; Hoffman, D. S.; Bam, H.; Peterson, C. L.; Brown, D. C. Transesterification process to manufacture ethyl ester of rape oil. **First Biomass Conference of the Americas**, Burlington, VT, v. 2, p. 815-822, 1993.

Krisnangkura, K.; Yimsuwan, T.; Pairintra, R. An empirical approach in predicting biodiesel viscosity at various temperatures. **Fuel***,* v. *85*, p. 107-113, 2006.

Lee, M. J.; Lo Y. C.; Lin H. M. Liquid-liquid equilibria for mixtures containing water, methanol, fatty acid methyl esters, and glycerol. **Fluid Phase Equilibria**, v. 299, p. 180-190, 2010.

Liu, X.; Piao, X.; Wang, Y.; Zhu, S. Liquid-liquid equilibrium for systems of (fatty acid ethyl esters + ethanol + soybean oil and fatty acid ethyl esters + ethanol + glycerol). **Journal of Chemical and Engineering Data**, v. 53, p. 359-362, 2008.

Magnussen, T.; Rasmussen, P.; Fredenslund, A. UNIFAC parameter table for prediction of liquid-liquid equilibrium. **Industrial Engineering Chemistry Process Design and Development**, v. 20, p. 331-339, 1981.

Mandal, S.; Sangita, Y.; Singh, R.; Begun, G.; Suneja, P.; Singh, M. Correlation studies on oil content and fatty acid profile of some Cruciferous species. **Genetic Resources and Crop Evolution,** v. 49, p. 551-556, 2002.

Marchetti, J. M.; Miguel, V. U.; Errazu, A. F. Possible methods for biodiesel production. **Renewable & Sustainable Energy Reviews**, v. 11, p. 1300-1311, 2007.

Marcus, Y. Principles of solubility and solutions. In: Rydberg, J.; Cox, M.; Musikas, C.; Choppin, G. R. **Solvent Extraction Principles and Practice**. 2ª ed. New York: Marcel Dekker, Inc, 2004. cap. 2.

Mazutti, M. A.; Voll, F. A. P.; Cardozo-Filho L.; Corazza, M. L.; Lanza, M.; Priamo, W. L.; Oliveira, J. V. Thermophysical properties of biodiesel and related systems: (Liquid + liquid) equilibrium data for soybean biodiesel. **Journal of Chemical Thermodynamics**, v. 58, p. 83-94, 2013.

Meher, L. C.; Sagar, D. V.; Naik, S. N. Technical aspects of biodiesel production by transterification – A review. **Energy Reviews**, v. 10, p. 248-268, 2006.

Mesquita, F. M. R.; Feitosa, F. X.; Sombra, N. E.; Santiago-Aguiar, R. S.; de Sant'Ana, H. B. Liquid-liquid equilibrium for ternary mixtures of biodiesel (soybean or sunflower) + glycerol + ethanol at different temperatures. **Journal of Chemical and Engineering Data**, v. 56, p. 4061-4067, 2011.

Moser, B. R. Biodiesel production, properties and feedstocks. **In Vitro Cellular & Developmental Biology**, v. 45, p. 229-266, 2009.

Oishi, T.; Prausnitz, J. M. Estimation of solvent activities in polymer solutions using a group-contribution methodology. **Industrial and Engineering Chemistry Process Design and Development,** v. 17, p. 333-339, 1978.

Oliveira, M. B., Barbedo, S., Solleti, J. L., Carvalho, S. H. V., Queimada, A. J., Coutinho, J. A. P. Liquid-liquid equilibria for the canola oil biodiesel + ethanol + glycerol system. **Fuel**, 90, 2738-2745, 2011.

Peters, R. A. Fatty alcohol production and use. **Inform**, v. 7. p. 502-505, 1999.

Pratas, M. J.; Freitas, S.; Oliveira, M. B.; Monteiro, S. C.; Lima, A. S.; Coutinho, J. A. P. Densities and viscosities of fatty acid methyl and ethyl esters. **Journal of Chemical and Engineering Data**, v. 55, p. 3983-3990, 2010.

Pratas, M. J.; Freitas, S.; Oliveira, M. O.; Monteiro, S. C.; Lima, A. S.; Coutinho, J. A. C. Densities and viscosities of minority fatty acid methyl and ethyl esters present in biodiesel. **Journal of Chemical and Engineering Data***, v. 56*, p. 2175-2180, 2011a.

Pratas, M. J.; Freitas, S. V. D.; Oliveira, M. B.; Monteiro, S. C.; Lima, S. L.; Coutinho, J. A. C. Biodiesel density: experimental measurements and prediction models. **Energy & Fuels**, v. 25, p. 2333-2340, 2011b.

Rackett, H. G. Equation of state of saturated liquids. **Journal of Chemical and Engineering Data**, v. *15*, p. 514-517, 1970.

Rahayu, S. S.; Mindaryani, A. Optimization of biodiesel washing by water extraction. **Proceeding of the World Congress on Engineering and Computer Science**, 2007, WCECS, October 24 – 26, San Francisco, USA, p.103-107.

Ramirez-Verduzco, L. F. Density and viscosity of bidiesel as a function of temperature: Empirical models. **Renewable and Sustainable Energy Reviews**, v. 19, p. 652-665, 2013.

Refaat, A. A. Correlation Between the Chemical Structure of Biodiesel and its Physical Properties. **International Journal of Environmental Science and Technology**, v.6, p. 677-694, 2009.

Reid R. C.; Prausnitz J. M.; Poling B. E. **The properties of gases and liquids**, 4th ed. Boston: McGraw-Hill; 1987**.**

Renon, H., Prausnitz, M. Local compositions in thermodynamic excess functions for liquid mixtures. **AIchE Journal**, v. 14, p. 135-144, 1968.

Rodrigues C. E. C., Pessoa Filho, P. A., Meirelles, A. J. A. Phase equilibrium for the system rice bran oil+fatty acids + ethanol + water + γ-orizanol + tocols **Fluid Phase Equilibrium**, v.216, p. 271-283, 2004.

Sandler, S. I. In Sandler, S. I. **Chemical and Engineering Thermodynamics.** 3ª ed. New York (New York): John Willey & Sons, Inc, 1999. Cap 7, p. 388-477.

Santos N. A.; Rosenhaim, R.; Dantas, M. B.; Bicudo, T. C.; Cavalcanti, E. H. S.; Barro, A. K.; Santos, I. M. G.; Souza, A. G. Rheology and MT-DSC studies of the flow properties of ethyl and methyl babassu biodiesel blends. **Journal of Thermal Analysis Calorimetry**, v. 106, p. 501-506, 2011.

Sastri, S. R. S.; Rao, K. K. A new group contribution method for predicting the viscosity of organic liquids. **Chemical Engineering Journal**, v**.** *50*, p. 9-25, 1992.

Shcefflan, R. **Teach Yourself the Basic of Aspen Plus.** John Wiley & Sons Inc. Hoboken, New Jersey, 2011.

Schuchardt, U.; Sercheli, R.; Vargas, R. M. Transesterification of vegetable oils: A review. **Journal of Brazilian Chemists' Societry**, v. 9, n.1, p. 199-210, 1998.

Silva, J. R. F.; Mazutti, M. A.; Voll F. A. P.; Cardozo-Filho L.; Corazza M. L.; Lanza, M.; Priamo W. L.; Oliveira, J. V. Thermophysical properties of biodiesel and related systems: (Liquid + liquid) equilibrium data for *Jatropha curcas* biodiesel. **Journal of Chemical Thermodynamics**, v. 58, p. 468-475, 2012.

Smith, J. M.; Van Ness, H. C.; Abbott, M. M. **Introdução à Termodinâmica da Engenharia Química.** 5ª ed., Rio de Janeiro, Livros Técnicos e Científicos, 2000.

Spencer, C. F.; Danner, R. P. Prediction of bubble point density of mixtures. **Journal of Chemical and Engineering Data**, v. *18*, p. 230-234, 1973.

Sridharan R.; Mathai I. M. Transesterification reactions. **Journal of Scientific & Industrial Research**, v. 22, p. 178-187, 1974.

Stamenkovic, O. S.; Velickovic, A. V.; Veljkovic V. B. The Production of biodiesel from vegetable oils by ethanolysis: Current state and perspectives. **Fuel**, v. 90, p. 3141-3155, 2011.

Stragevitch, L.; d'Avila, S. G. Application of a generalized maximum likelihood method in the reduction of multicomponent liquid liquid equilibrium data**. Brazilian Journal of Chemical Engineering**, v. 14, p. 41–52, 1997.

Taft Jr., R. W.; Newman, M. S.; Verhoek, F. H. The kinetics of the base catalyzed methanolysis of ortho meta and para substituted l-methyl benzoates. **Journal of the American Chemists' Society**, v. 72, p. 4511-4519, 1950.

Tedder, D. W. Liquid-liquid extraction. In: Albright L. F. **Albrights Chemical Engineering Handbook**. Boca Raton, CRC Press, 2009, Cap. 10, p. 709-735.

Treybal, R. E. Liquid equilibria In: Treybal, R. E. **Liquid Extraction,** 2ª ed., New York (New York): Mc Graw-Hill Book Company, 1963. Cap 2, p. 5-55.

Varanda, M. G.; Pinto, G.; Martins, F. Life cycle analysis of biodiesel production. Fuel **Processing Technology**, v. 92, p. 1087-1094, 2011.

Wehlmann, J. Use of esterified rapeseed oil as plasticizer in plastics processing. **Fett/ Lipid**, v.101, p. 249-2561, 1999.

Weidlich U.; Gmehling J. A modified UNIFAC model. 1. Prediction of VLE, h^E, and γ^{∞}. **Industrial & Engineering Chemistry Research**, v. 26, p. 1372-1381, 1987.

West, A. H.; Posarac, D.; Ellis, N. Assessment of four biodiesel production processes using HYSYS.Plant, **Bioresource Technology**, v.99, p. 6587-6601, 2008.

Willing, A. Oleochemical esters-enviromentally compatible raw materials for oils and lubricants from renewable resources. **Fett/Lipid**, v.101, p.192-198, 1999.

Yuan, W.; Hansen, A. C.; Zhang, Q. Predicting the temperature dependent of biodiesel fuels. **Fuel***,* p. 88, v. 1120-1126, 2009.

Zhang, Y; Dubé, M. A.; McLean, D. D.; Kates, M. Biodiesel production from waste cooking oil: 2 Economic assessment and sensitivity analysis. **Bioresource Technology**, v. 90, p. 229-240, 2003.

Zhou, H.; Lu, H.; Liang, B. Solubility of multicomponent systems in the biodiesel production by transesterification of *Jatropha curcas L.* oil with methanol.**Journal of Chemical & Engineering**, v. 51, p. 1130-1135, 2006.

Zhou, W.; Boocock, D. G. B. Phase behavior of the based-catalyzed transesterification of soybean oil. **Journal of the American Oil Chemists' Society,** v. 83, p. 1041-1045, 2006.

Zhou, W.; Konar, S. K.; Boocock, D. G. B. Ethyl esters from single-phase base catalyzed ethanolysis of vegetable oils. **Journal of the American Oil Chemists' Society**. v.80, p.367-371, 2003.

Capítulo 3. Liquid-Liquid Equilibrium Data and Thermodynamic Modeling, at T/K = 298.2, in the Washing Step of Ethyl Biodiesel Production from Crambe, Fodder Radish and Macauba Pulp Oil

Rodrigo Corrêa Basso, Fabio Hideki Miyake, Antonio José de Almeida Meirelles, Eduardo Augusto Caldas Batista

Trabalho submetido ao periódico **Fuel** em 23 de abril de 2013.

Abstract

In this work, pseudo-ternary liquid-liquid equilibrium data were obtained for three systems composed for water + ethanol + ethyl biodiesel from crambe, fodder radish and macauba pulp oil, at T/K = 298.2. Ethanol, which distributes in both phases, had greater affinity for the water phase. Biodiesels and water showed almost complete immiscibility. Modeling with the NRTL and UNIQUAC thermodynamic models was performed, resulting in average deviations ranging from 0.49% to 1.29%. UNIFAC-LLE and UNIFAC-Dortmund were used in prediction of the liquid-liquid equilibrium of these systems, resulting in average deviations ranging from 1.91% to 2.27% for the systems containing biodiesel from crambe and fodder radish oil, and ranging from 3.17% to 3.28% for biodiesel from macauba oil.

Keywords

Biodiesel; Liquid-liquid equilibrium; Thermodynamic model; UNIFAC; NRTL; UNIQUAC

1. Introduction

Biodiesel, defined as mono-alkyl esters of fatty acid from vegetable oil or animal fats, is an environmentally attractive alternative to conventional petroleum diesel fuel. In transesterification, the reaction by which biodiesel is produced, the stoichiometric relationship between alcohol and oil is 3:1, however an excess of alcohol is typically employed to improve conversion towards the desired product. Biodiesel presents many important technical advantages over petroleum diesel including low toxicity, derivation from renewable feedstocks, superior biodegradability, negligible sulfur content, higher flash point and fewer exhaust emissions [1].

The crambe (*Crambe abyssinica*) seed presents high oil content (23-38%), rich in mono-unsaturated fatty acids with an erucic acid content of 57.8% on average, which makes it inadequate for human consumption. This specie presents a very short cycle of 83 to 105 days from sowing to maturation, and it can be sowed between two soy cultivations [2,3]. Macauba (*Acrocomia aculeata*) pulp oil is composed mainly of triacylglycerols with intermediate fatty acid chains (16-18 carbon atoms), with more than fifty percent monounsaturated fatty acids and about twenty five percent palmitic acid esters [4]. Fodder radish (*Raphanus sativus*) has excellent ability to recycle soil micronutrients, rapid plant growth (150 – 200 days), low needs of agronomic nutrients and low cultivation cost per hectare. Its oil has an heterogeneous fatty acid profile, containing about 60% of

monounsaturated fatty acid, (mainly oleic acid, gadoleic acid and, erucic acid), 18% of linoleic acid and 12.5% of linolenic acid as its main fatty acid components [5,6]. The chemical composition of these oils, their agricultural characteristics and physical properties of their esters make them interesting alternatives for biodiesel production [2,6,7,8].

Despite of its elevated price in relation to methanol, the advantages of using ethanol in biodiesel production include higher miscibility with vegetable oils that allows better contact in the reaction step. Although commercial processes use vegetable oils and methanol in the transesterification reaction, the use of ethanol in biodiesel synthesis is appealing because it is produced from biorenewable sources, resulting in a completely agricultural-based fuel obtained by ethanolysis [9,10]. In the reaction of vegetable oils and ethanol in the presence of a catalyst, completely agricultural-based fuels consisted of fatty acid ethyl esters (FAEE) are obtained with physico-chemical properties similar to those of the appropriate methyl esters and diesel fuel [10].

After the transesterification reaction, glycerol is separated by settling or centrifuging to form two distinct phases, an ester-rich phase and a glycerol-rich phase. Considering a typical alkaline catalysis where 3 moles in excess of ethanol are used in the reaction, and an ideal settling, the ester-rich phase has a very low glycerol content, about 0.7 % [8,11], due to the low solubility between glycerol and ethyl esters. Following this separation step, the ester-rich phase is purified before being used as a biofuel [12,13].

Water washing is very effective in removing contaminants from biodiesel in purification steps due to the high solubility of a set of compounds in this solvent. This process can reduce methanol and residual free glycerol levels down to biodiesel standard quality requirements and can be efficiently carried out at ambient temperature, because this is the most economical condition for biodiesel purification [12,13]. In this step of the biodiesel production process, two immiscible phases are formed, one rich in esters and one rich in water, where ethanol distributes in both phases.

The study of liquid-liquid equilibrium (LLE) for washing water in ethyl biodiesel production is important because this step determine the final biodiesel purity according to the biodiesel standard quality requirements and allows for evaluating possible ester losses to the water-rich phase. In addition, knowledge on the LLE of systems containing biodiesel + water + ethanol is crucial for optimization of this purification step, which can allow reduce the large amount of water used in this process.

Despite of the relevance of this knowledge, there is little experimental data related to the LLE behavior of systems composed of water + alcohol + pure methyl esters [14], pure ethyl esters [15] and methyl and ethyl biodiesels [16,17]. Additionally, only one of these works [14] compared different g^E and activity coefficient thermodynamic models when describing the LLE of these systems with similar components. None of these studies compared LLE behavior of these systems as a function of different fatty ester profiles of the biodiesels.

The objectives of this work are to present LLE data, at 298.2 K, for three systems containing water + ethanol + ethyl biodiesel from crambe, macauba pulp and fodder radish oil, whose ester profiles are significantly different; adjust parameters of the NRTL and UNIQUAC models and compare these molecular models with two group contribution activity coefficient models, UNIFAC-LLE and UNIFAC-Dortmund (UNIFAC-DRTM), in relation to prediction of LLE in these systems.

2. Experimental Procedure

2.1. Material

Crude crambe oil and crude macauba pulp oil were respectively supplied by the Foundation MS (Maracaju, MS, Brazil) and Paradigma Óleos Vegetais Ltda (Jaboticatubas, MG, Brazil).

Fodder radish seeds were supplied by Sementes Pirai (Piracicaba, SP, Brazil). Crude fodder radish oil was extracted, using a pilot expeller, and filtered for removal of the fibers from the seeds.

Crude oils were neutralized with a sodium hydroxide solution prior to biodiesel production.

Anhydrous ethanol (Merck, > 0.9999), anhydrous sodium hydroxide (Carlo Erba, > 0.9700), glacial acetic acid (Ecibra, > 0.9970) Hydranal Composite 5 (Fluka Analytical), Hydranal Coulumat CG (Fluka Analytical) and deionized water were used in several steps of this work, without further purification.

Crambe, fodder radish and macauba pulp oil were used for ethyl biodiesel production. The biodiesel ethyl ester profiles were obtained as described in Basso et al. [11]. Ethyl ester biodiesel compositions are presented in mass percentage in Table 1.

2.2. Production of Distilled Biodiesels

Ethyl biodiesels were obtained by alkaline catalysis for 1 h at room temperature (approximately T/K = 298), with sodium hydroxide and reagent molar ratio of 1:6 oil:ethanol. After the washing step, biodiesels were dried under agitation, heating (approximately T/K = 333.15) and vacuum (P/mmHg < 5). Distilled biodiesels were obtained by distillation under vacuum (approximately P/mmHg = 2.25) and heating (approximately T/K = 533.15). All steps in the biodiesel production were described in detail by Basso et al. [11].

2.3. LLE Experiments

LLE data of the systems were determined using sealed headspace glass tubes (20 mL) (Perkin Elmer). Each component was weighted on an analytical balance Adam Equipment, model AAA160L (+/- 0.0001 g). The headspace tubes were vigorously stirred using a vortex Phoenix, model AP56 and then centrifuged in a Centrifuge Jouan, model BR4i for 300 s at 4000 rpm. All systems were left at rest for a minimum of 36 h at constant temperature in a thermostatic bath Paar Physica, model Physica VT2 (T/K +/- 0.2). Two clear layers and a well defined interface were formed when the systems reached the equilibrium state, where the upper layer is the ester-rich phase (EP), and the lower layer the water-rich phase (WP).

2.4. Analytical Methodology

The fatty acid ethyl ester content of each biodiesel was determined in triplicate by a Perkin Elmer gas chromatography system, Clarus 600, FID detector, with a Perkin Elmer Elite-225 capillary column (crossbond, 50% cyanopropylmethyl – 50% phenylmethyl polysiloxane), length of 30 m, internal diameter of 0.25 mm and film thickness of 0.25 μm, according to the methodology presented by Basso et al. [11].

Weighing of the analysis was performed on an analytical balance Precisa, model XT 220 A (+/- 0.0001 g).

Water content in WP was determined using a Karl Fisher Titration system (701 KF Titrino, Metrohm) at least triplicate. Since the Karl Fisher Coulometer has high precision

for low water content, the water in EP was quantified using a Karl Fisher Coulometer (831 KF Coulometer, Metrohm).

Samples of each phase were weighted and transferred, in triplicate, to previously weighed Petri plates. The plates were then taken to an oven with forced air circulation where they were maintained for at least 20 h, at T/K = 353.2 and atmospheric pressure, until complete evaporation of ethanol and water from the samples. The biodiesel mass fraction was determined by plate weighing after complete evaporation of water and ethanol. A similar procedure was performed by Ansolin et al. [18] when studying the LLE of fatty systems with an emphasis on the distribution of tocopherols and tocotrienols in vegetable oils.

With the intention of testing the experimental methodology used for these systems, three synthetic systems containing known contents of water, ethanol and biodiesel were analyzed. Three different levels of water and FAEE from fodder radish were tested. The system containing low water content (0.66 /71.33/ 28.01; water/ ethanol /FAEE in mass percentage) was analyzed using the Karl Fisher coulometer; the system containing high water content (17.33 /81.72/ 0.95; water/ ethanol /FAEE in mass percentage) was analyzed using the Karl Fisher titration and, the system with intermediate water content (5.43 /89.33/ 5.24; water/ ethanol /FAEE in mass percentage) was analyzed using both equipment. The biodiesel from fodder radish oil was used to represent the three biodiesels because it has significant contents of the main ethyl esters (ethyl ester from palmitic acid, oleic acid, linoleic acid, linolenic acid, eicosenoic acid and erucic acid) present in the studied biodiesels.

3. Calculation Approach

3.1. Combined Uncertainty in Experimental Methodology

The combined absolute uncertainty of the analytical methodology was obtained from the difference between true values, by weighting of components used for synthetic systems and analyzed values obtained from analytical methodology, calculated according to equation (1).

$$u_c(\%) = \left(\sum_i (m_i^a - m_i^t)^2 \right)^{1/2} \quad (1)$$

where m is the mass of the component, a is the analyzed value using the described methodology, t is the true value obtained by weighting and i is the component of the systems.

3.2. Calculation of Deviations in Mass Balance of the Phases

Validity of the LLE experimental data was evaluated according to the procedure developed by Marcilla et al.[19] and applied by Rodrigues et al. [20]. In this procedure, the sum of the calculated mass in both phases is compared with the actual value for total mass used in the experiment. According to Marcilla et al. [19], overall mass balance deviations less than 0.5% ensure good quality of experimental data. The mass balance of each component can be calculated according to equation (2).

$$M^{OC} w_i^{OC} = M^{WP} w_i^{WP} + M^{EP} w_i^{EP} \quad (2)$$

where i represents each component of the system; M^{OC} is the mass of the overall composition; M^{WP} and $\mathrm{M}^{\mathrm{EP}}$are the total masses of the WP and EP phases, respectively; $\mathrm{w}_{\mathrm{i}}^{\mathrm{OC}}$ is the mass fraction of component i in the initial mixture; and, $\mathrm{w}_{\mathrm{i}}^{\mathrm{WP}}$ and $\mathrm{w}_{\mathrm{i}}^{\mathrm{EP}}$ are the mass fractions of component i, respectively, in the WP and EP.

When applying K equations related to K balances, the values of M^{WP} and M^{EP} can be calculated from the experimental mass fraction of component i in both phases $\mathrm{w}_{\mathrm{i}}^{\mathrm{WP}}$ and $\mathrm{w}_{\mathrm{i}}^{\mathrm{EP}}$ by least square fitting. Considering M as the matrix formed by the values of $\mathrm{w}_{\mathrm{i}}^{\mathrm{OC}}$, B as the transformation matrix formed by $\mathrm{w}_{\mathrm{i}}^{\mathrm{WP}}$ and $\mathrm{w}_{\mathrm{i}}^{\mathrm{EP}}$, and P as the matrix formed by the masses of the phases M^{WP} and M^{EP}, the system can be mathematically described as:

$$M = B \cdot P \quad (3)$$

Equation (3) can be transformed into the expression below:

$$P = (B^T B)^{-1} B^T M \quad (4)$$

where B^T is the transposed matrix of B and $(B^TB)^{-1}$is the inverse matrix of (B^TB).

Thus, values of M^{WP} and M^{EP} for the systems can be obtained, and the sum of M^{WP} and M^{EP} can be compared to M^{OC} to calculate the overall mass balance deviation by:

$$\delta(\%) = 100 \cdot \frac{|(M^{WP} + M^{EP}) - M^{OC}|}{M^{OC}} \quad (5)$$

The relative average deviation for mass balance of each component i in each system is given by:

$$\delta_i(\%) = \frac{1}{N}\sum_{n}^{N}\left[100 * \frac{\left|\left(w_{i,n}^{GP}M^{GP} + w_{i,n}^{EP}M^{EP}\right) - w_{i,n}^{OC}M^{OC}\right|}{w_{i,n}^{OC}M^{OC}}\right] \quad (6)$$

where n is the tie line number and N is the total number of tie lines for each system.

The maximum combined uncertainty of experimental data for each system was calculated considering the maximum deviation in mass balance among all tie lines of each system using equation (7):

$$u_{ced}(\%) = \left(\sum_{i} {\delta_i}^2\right)^{1/2} \quad (7)$$

3.3. NRTL and UNIQUAC thermodynamic modeling

The experimental data measured for the systems were used to adjust the binary interaction parameters for the NRTL and UNIQUAC models. Mixtures of fatty acid ethyl esters which comprise the three biodiesels were treated as a single ethyl ester with the average molar mass of the ester mixture, denoted as FAEE. This approach assumes that the mixture of different fatty acid ethyl esters behaves similarly in the systems under study. Therefore, the mixture of ethyl esters was replaced by a pseudo-component with the corresponding average physical-chemical properties. Basso et al. [11] validated this approach when studying the LLE of systems containing glycerol + ethanol + ethyl biodiesel from crambe oil at different temperatures. Thus, adjustments to the NRTL and UNIQUAC parameters were made, considering the systems as pseudo-ternary. All parameters were adjusted to the experimental data.

The mass fraction was used as composition unit due the difference in molar masses of the components in the systems; this same approach was presented by Oishi and Prausnitz [21] and used by other authors studying the LLE of systems containing vegetable oils + ethanol + water [22], and studying the LLE of systems containing glycerol + ethanol + ethyl biodiesel [11]. Thus, the isoactivity criterion of LLE developed on a molar fraction basis can be expressed on a mass fraction basis as:

$$(\gamma_i x_i)^{WP} = (\gamma_i x_i)^{EP} \tag{8}$$

$$(\gamma_i^w w_i)^{WP} = (\gamma_i^w w_i)^{EP} \tag{9}$$

where:

$$\gamma_i^w = \frac{\gamma_i}{M_i \sum_j^K \left({}^{w_j}/_{M_j} \right)} \tag{10}$$

Estimation of the NRTL and UNIQUAC parameters was obtained using an algorithm developed in the FORTRAN programming language. This algorithm uses the modified simplex method to estimate thermodynamic parameters by minimizing the objective function of the composition (equation 11). The procedure for calculation of the parameters involves flash calculations for the midpoint composition of the experimental tie lines, according to the procedure developed by Stragevitch and d'Avila [23].

$$OF_w = \sum_m^D \sum_n^N \sum_i^{K-1} \left[\left(\frac{w_{i,n,m}^{WP,exp} - w_{i,n,m}^{WP,calc}}{\sigma_{w_{i,n,m}^{WP}}} \right)^2 + \left(\frac{w_{i,n,m}^{BP,exp} - w_{i,n,m}^{BP,calc}}{\sigma_{w_{i,n,m}^{BP}}} \right)^2 \right] \tag{11}$$

where D is the is the total number of data groups; N is the total number of tie lines; K is the total number of components in the data group; w is the mass fraction; subscripts i, n and m are the component, tie line and group number, respectively; expt and calc represent, respectively, the experimental and calculated compositions; and σ is the standard deviation observed for the composition of each phase.

3.4. UNIFAC-LLE and UNIFAC-DRTM

UNIFAC-LLE and UNIFAC-DRTM were used to test the LLE prediction capability for the systems. The model denoted as UNIFAC-LLE was presented by Fredenslund et al. [24], and its binary interaction parameters for LLE were updated by Magnussen et al. [25]. The model denoted as UNIFAC-DRTM was presented by Weidlich and Gmehling [26], and its LLE binary interaction parameters were updated by Gmehling et al. [27]. Structural molecular groups selected to represent the studied systems were "CH_3", "CH_2", "CH", "CH=CH", "CH_2COO", "OH" and "H_2O".

All individual fatty acid ethyl esters (FAEE) were considered for UNIFAC-LLE and UNIFAC-DRTM modeling. Thus, the systems were represented by water, ethanol and all fatty acid ethyl esters of each biodiesel. However, in ternary diagram representations the esters were grouped by the addition of each individual ester mass fraction, and the systems were graphically represented as pseudo-ternary systems containing water (1) + ethanol (2) + FAEE (3).

The predictive capability of the UNIFAC-LLE and UNIFAC-DRTM models was tested using the commercial simulator software Aspen Plus (Aspen Technology). A thermodynamic flash was performed for the overall composition of all tie lines of each system. Thus, compositions of the WP and EP were obtained and compared to the experimental data.

3.5. Deviations in Description of LLE

Average deviations between the experimental and calculated compositions, for all models and in both phases, were determined according to equation (12), similar to that used by other researchers [28].

$$\Delta w = 100 \cdot \left\{ \frac{\left[\sum_n^N \sum_i^K \left(w_{i,n}^{WP,exp} - w_{i,n}^{WP,calc} \right)^2 + \left(w_{i,n}^{EP,exp} - w_{i,n}^{EP,calc} \right)^2 \right]}{2NK} \right\}^{1/2} \qquad (12)$$

4. Results and Discussions

The fatty acid ethyl ester compositions of the three biodiesels were very different according to Table 1. The FAEE from crambe oil presents ethyl erucate, a long chain ethyl

ester with 24 carbon atoms in the molecule, and ethyl oleate as the main esters, totalizing more than 75% of its composition. The FAEE from macauba pulp oil presents ethyl oleate and ethyl palmitate as the major ethyl esters, representing more than 80% of the biodiesel composition, where saturated ethyl esters (ethyl palmitate and ethyl stearate) make up more than 25% of its components. On the other hand, FAEE from fodder radish oil presents ethyl oleate as the mainly ester and large amounts of four other esters, ethyl linoleate, ethyl linolenate, eicosenoic acid ethyl ester and ethyl erucate. The molar mass of the pseudo-component, calculated from these ethyl ester profiles, were 342.26, 317.80 and 303.03 g·mol^{-1}, respectively, for FAEE from crambe oil, fodder radish oil and macauba pulp oil.

Table 1. Ethyl ester composition of FAEE from crambe, fodder radish and macauba pulp oil in mass percentage.

fatty acid group in ethyl ester	molecular formula	common name	$\frac{M}{(g \cdot mol^{-1})}$	FAEE crambe (100w)	FAEE fodder radish (100w)	FAEE macauba (100w)
c16:0	$C_{18}H_{36}O_2$	ethyl palmitate	284.48	2.07	5.11	21.8
c16:1	$C_{18}H_{34}O_2$	ethyl palmitoleate	282.46	-	-	4.08
c18:0	$C_{20}H_{40}O_2$	ethyl stearate	312.53	1.03	2.36	2.76
c18:1	$C_{20}H_{38}O_2$	ethyl oleate	310.51	19.38	39.47	58.97
c18:2	$C_{20}H_{36}O_2$	ethyl linoleate	308.50	8.33	16.69	11.64
c18:3	$C_{20}H_{34}O_2$	ethyl linolenate	306.48	4.53	12.19	0.75
c20:0	$C_{22}H_{44}O_2$	ethyl arachidate	340.58	1.22	0.87	-
c20:1	$C_{22}H_{42}O_2$	eicosenoic acid ethyl ester	338.57	4.04	10.04	-
c22:0	$C_{24}H_{48}O_2$	ethyl behenate	368.64	1.99	0.36	-
c22:1	$C_{24}H_{46}O_2$	ethyl erucate	366.62	56.39	11.71	-
c22:2	$C_{24}H_{44}O_2$	docosadienoic acid ethyl ester	364.60	0.49	-	-
c24:0	$C_{26}H_{52}O_2$	ethyl lignocerate	394.67	0.53	0.30	-
c24:1	$C_{26}H_{50}O_2$	ethyl nervonate	394.67	-	0.90	-

[a] mass fraction of ethyl ester

The combined absolute uncertainty of the experimental methodology for the system containing low water content, high water content and intermediate water content

were, respectively 1.2 %, 0.8 %, and 1.2 % (using both Karl Fisher devices). Thus, the maximum uncertainty indicates the proper representation of the analyzed systems.

Table 2 shows that the deviations per tie line for overall mass balance, calculated according to the equation 5, were less than 0.32%, considering the three systems. This maximum deviation indicates good quality of the experimental data. The relative deviations in mass balance of each component, calculated according to equation 6, ranged from 0.0024% to 3.4863%, 0.0065% to 4.6183% and 0.0024 to 2.27 %, respectively, for the system containing FAEE from macauba pulp oil, fodder radish oil and crambe oil.

Table 2. Experimental liquid-liquid equilibrium data for the pseudo-ternary systems water (1) + ethanol (2) + FAEE (3/4/5) at T/K = 298.2.

	overall composition			water-rich phase			ester-rich phase			δ (%)
	$100w_1$	$100w_2$	$100w_x$	$100w_1$	$100w_2$	$100w_x$	$100w_1$	$100w_2$	$100w_x$	
FAEE from crambe oil (x=3)[a]	50.09	0.00	49.91	99.99	0.00	0.01	0.19	0.00	99.81	0.00
	32.92	19.59	47.49	63.69	36.22	0.09	0.45	2.74	96.81	0.11
	29.80	30.31	39.89	50.05	49.94	0.01	0.43	3.99	95.58	0.03
	26.19	36.05	37.76	43.06	56.81	0.13	0.48	6.26	93.26	0.11
	16.11	42.10	41.79	28.28	70.31	1.41	0.70	7.21	92.09	0.10
	10.76	49.76	39.48	17.91	79.00	3.09	1.05	12.52	86.43	0.20
FAEE from fodder radish oil (x=4)[b]	49.86	0.00	50.14	99.99	0.00	0.01	0.22	0.00	99.78	0.00
	39.07	10.54	50.39	78.97	21.03	0.00	0.29	0.91	98.80	0.20
	36.30	20.36	43.34	66.66	33.32	0.02	0.48	3.24	96.28	0.32
	34.85	30.02	35.13	57.53	42.46	0.01	0.50	6.10	93.40	0.28
	30.19	39.94	29.87	44.83	55.05	0.12	0.62	6.48	92.90	0.10
	17.18	48.06	34.76	26.94	71.18	1.88	1.01	9.57	89.42	0.00
FAEE from macauba pulp oil (x=5)[c]	46.78	0.00	53.22	99.97	0.00	0.03	0.29	0.00	99.71	0.00
	45.56	8.93	45.51	87.80	12.19	0.01	0.29	4.81	94.90	0.25
	37.94	19.35	42.71	69.70	30.29	0.01	0.47	5.34	94.19	0.23
	34.55	32.74	32.71	52.24	47.68	0.08	0.64	8.38	90.98	0.00
	18.23	39.85	41.92	33.63	65.51	0.86	1.06	13.00	85.94	0.21

[a,b,c] the maximum combined uncertainty, calculated according to equation (7) for the systems containing components (3), (4) and (5) are, respectively, 2.28 %, 5.48 % and 3.49 %.

According to Figure 1 and Table 2, FAEE and water are almost mutually immiscible. The bottoms of the diagrams show that for low ethanol content in overall compositions, the mass fractions of FAEE and water are very low in the WP and EP, respectively. Ethanol distributes between the both phases, and according to the slopes of tie lines, it has greater affinity for the WP. Increase of the ethanol mass fraction in the

overall composition causes a greater increase in FAEE mass fraction in the WP than elevation of the water mass fraction in the EP.

There was phase inversion when the WP made up the upper phase and the EP is in the lower phase, with the tie lines containing mass fractions of 41.79% and 39.48% of FAEE from crambe oil and 34.76% of FAEE from fodder radish oil in overall composition. This behavior occurs at high ethanol content in the overall composition, because ethanol has lower density in relation to all components in the systems and due to the high affinity of ethanol to the WP, this behavior causes the decrease in density of the WP.

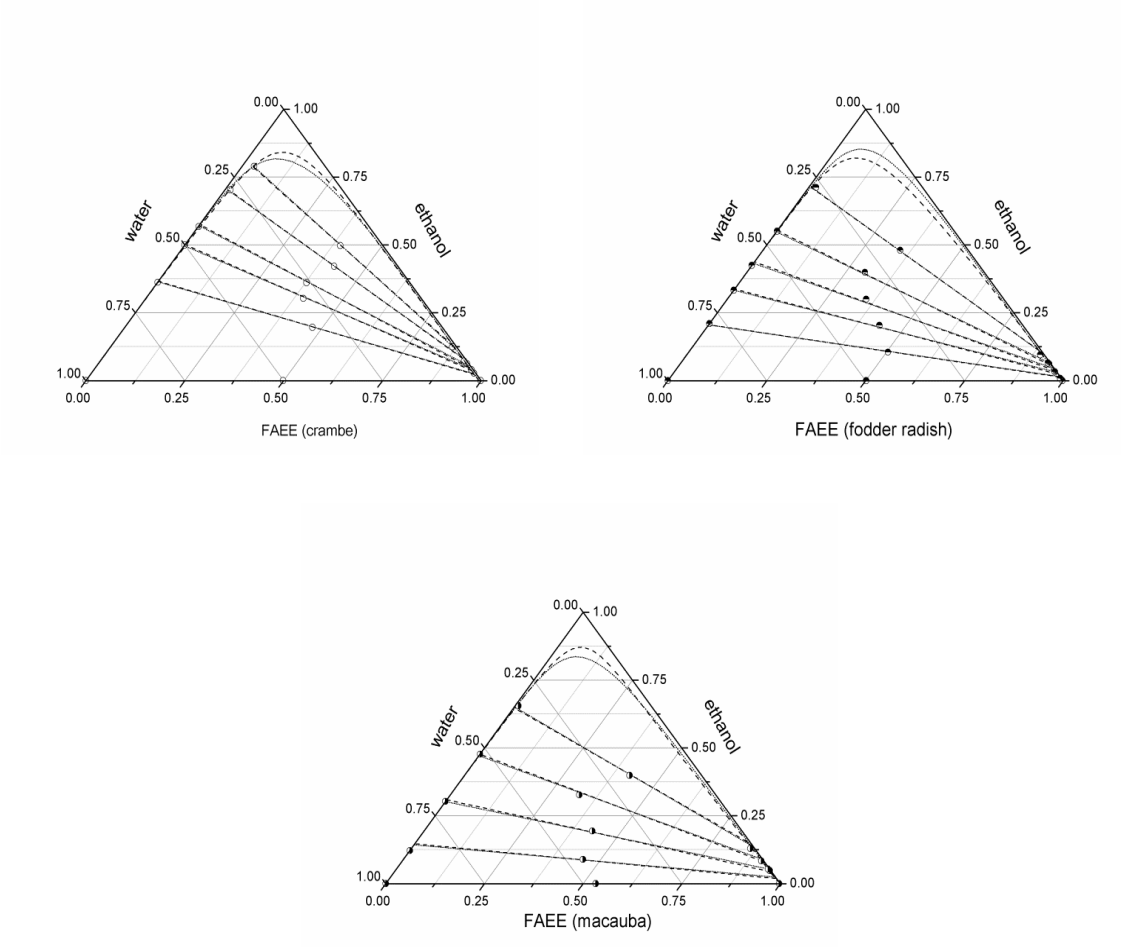

Figure 1. Liquid-liquid equilibrium diagram of systems composed of water (1) + ethanol (2) + FAEE from crambe oil (3)/ FAEE from fodder radish oil (4)/ FAEE from macauba oil (5) at T/K = 298.2: (○), (◓), (◑) experimental data; (···) NRTL model; (---) UNIQUAC model.

Table 3 presents the adjusted parameters for the NRTL and UNIQUAC models of the three systems under study. Both molecular models were able to properly describe the LLE of the systems, where average deviations between experimental data and calculated values (equation 12) were on average lower when using the NRTL model than the UNIQUAC model, according to Table 4.

Table 3. UNIQUAC and NRTL model binary parameters.

	UNIQUAC		NRTL		
pair ij[a]	$A(0)_{ij}$/K	$A(0)_{ji}$/K	$A(0)_{ij}$/K	$A(0)_{ji}$/K	α (0)ij=α (0)ji
12	-251.9600	297.7500	54.4570	279.6700	0.1010
13	-39.0850	768.8600	4057.1000	297.4500	0.1443
23	31.8680	75.0600	812.7000	2224.7000	0.4732
14	60.9410	755.6100	3914.7000	9442.4000	0.1462
24	7.9797	65.41500	812.6800	1340.8000	0.5700
15	-3.9697	874.5500	3076.9000	615.9800	0.1618
25	370.4300	-217.1800	782.0400	-144.4800	0.5700

[a] components: water (1), ethanol (2), FAEE from crambe oil (3), FAEE from fodder radish oil (4), FAEE from macauba pulp oil (5).

Table 4. Average global deviations (Δw) between experimental data and calculated mass fractions.

model	$\Delta w(\%)$ (system 1+2+3)[a]	$\Delta w(\%)$ (system 1+2+4)[a]	$\Delta w(\%)$ (system 1+2+5)[a]
NRTL	0.51	0.66	0.97
UNIQUAC	0.49	0.86	1.29
UNIFAC-LLE	2.27	2.10	3.28
UNIFAC-DRTM	2.25	1.91	3.17

[a] water (1), ethanol (2), FAEE from: crambe oil (3), fodder radish (4), macauba pulp oil (5).

In the system containing FAEE from crambe oil, all tie lines calculated by both models almost overlap the experimental data, indicating a good representation of the LLE by the molecular models of the system for the full studied composition range. The tie line with high ethanol content in the system containing FAEE from fodder radish oil, had its ethanol content slightly underestimated in the WP and overestimated in the EP by the two models. In the system containing FAEE from macauba pulp oil, the tie line with 45.51% of this component presented an overestimated ethanol mass fraction in the WP and underestimated fraction in the EP, the tie line with 41.92% of FAEE had its ethanol content underestimated in the WP and overestimated in the EP.

The binodal curves calculate by the NRTL and UNIQUAC models showed significant differences in description of the LLE behavior in the region with high ethanol mass fraction, at the top of diagrams, for all the three systems. In the WP region the binodal curves overlap each other, indicating the same description of the LLE by both models for all studied systems. The LLE behavior of the systems containing FAEE from crambe and macauba pulp oil were represented similarly by the different binodal in the EP region, but on the other hand, the NRTL model showed a slightly broader region of phase separation than the UNIQUAC model in this region for the system containing FAEE from fodder radish oil.

The differences between deviations obtained by the UNIFAC-LLE and UNIFAC-DRTM models for description of the LLE of each system were lower than 0.25%, indicating a similar prediction capability for LLE behavior for these systems by both models. The LLE of the systems containing FAEE from crambe oil and FAEE from fodder radish oil had similar average deviations between experimental data and predicted values, as observed in Table 4. On the other hand, these deviations were substantially higher for the system containing FAEE from macauba pulp oil. All deviations were higher than 1.9%, indicating that these models were generally not able to properly predict the LLE of these systems.

Both UNIFAC models underestimated the ethanol mass fraction in the EP, and this behavior was more significant in the systems containing biodiesel from macauba pulp oil and fodder radish oil, as showed in Figure 2. The predictive models also underestimated the FAEE mass fraction in the WP. Except for the system containing FAEE from crambe oil, the predictive models also overestimated ethanol content in the WP. The group contribution model could not describe properly the region of phase separation, overestimating it for the three systems.

Different capabilities for predicting the LLE of systems related to biodiesel production, by UNIFAC derived models, considering different alkyl ester compositions, were obtained by other authors. Lee et al. [14], using the UNIFAC-LLE and UNIFAC-DRTM models for predicting the LLE of systems composed of water + methanol + methyl esters, obtained average deviations of about five times higher for system containing methyl oleate in comparison to the systems containing methyl linoleate. Basso et al. [11] and Basso et al. [8] tested the prediction of LLE for systems containing glycerol + ethanol + ethyl biodiesel by UNIFAC-LLE models, and obtained average deviations of 2.72% and

3.52%, respectively, for biodiesel from crambe oil and from macauba pulp oil at T/K = 298.2.

Despite of the great availability of group interaction parameters and their constant updates, the generation of derived models and the practicality in the use, because they are previously programmed in many simulation softwares, the utilization of UNIFAC models in design analysis and process simulation in the biodiesel production process must be done judiciously due to the deviations in prediction of LLE for this type of system.

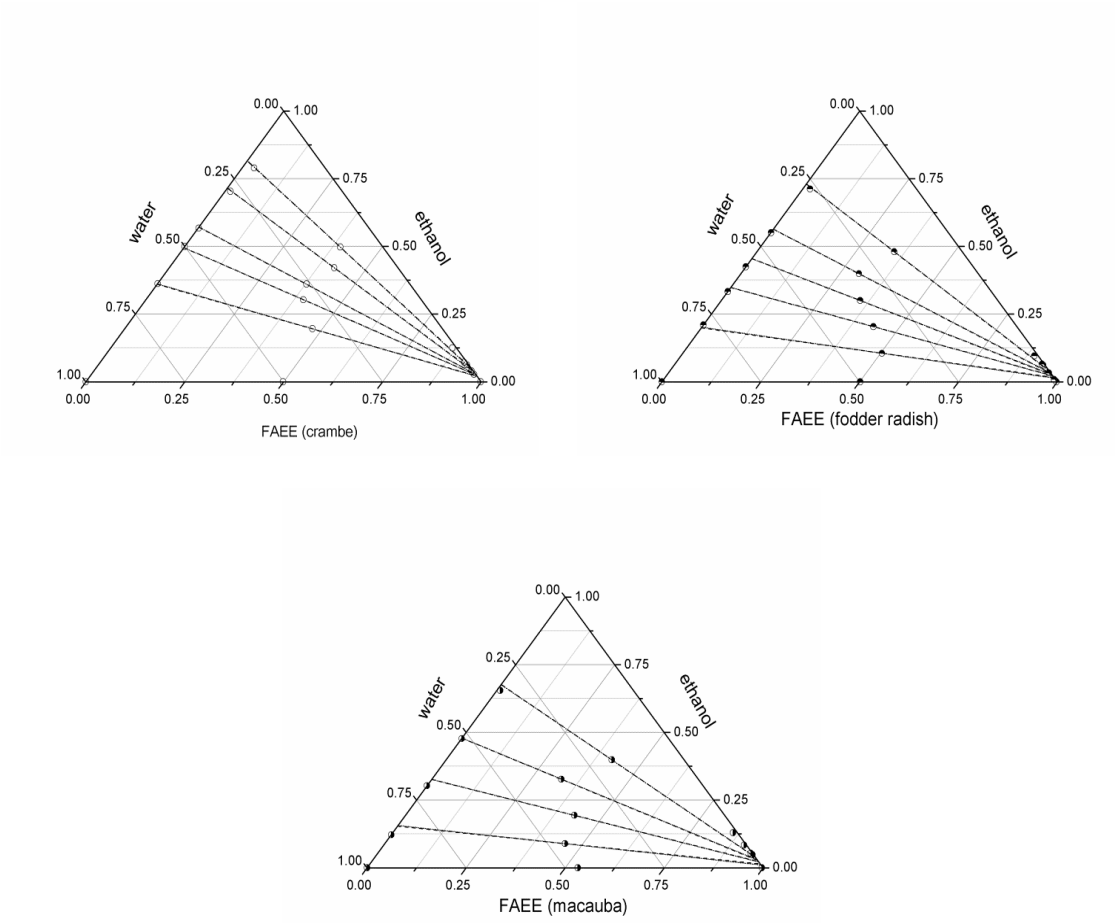

Figure 2. Liquid-liquid equilibrium diagram of systems composed of water (1) + ethanol (2) + FAEE from crambe oil (3)/ FAEE from fodder radish oil (4)/ FAEE from macauba oil (5) /K = 298.2: (○), (◓), (◑) experimental data; (···) UNIFAC-DRTM model; (---) UNIFAC-LLE model.

Thus, the LLE prediction capability for systems containing alkyl esters by UNIFAC derived models is probably directly related to the ester composition of these systems. The number and/or presence of specific structural molecular groups in ester molecules that comprise the biodiesel may have different effects on the LLE prediction capability of this type of system.

5. Conclusions

The results of the present study show that FAEE and water were almost immiscible and ethanol was distributed in both phases, but presented greater affinity for the WP. The NRTL and UNIQUAC thermodynamic models properly described the LLE of these systems with average deviation ranging from 0.49% to 1.29%. Although the UNIFAC-LLE and UNIFAC-DRTM models similarly predicted the LLE of these systems, these models could not properly describe it, with average deviations ranging from 1.91% to 3.28%.

Acknowledgement

The authors would like to acknowledge the Fundação de Amparo a Pesquisa do Estado de São Paulo (FAPESP – process 8/56258-8) for its financial support, and the Conselho Nacional de Desenvolvimento Científico e Tecnológico (CNP_q – process 140362/2009-6) for scholarship.

Appendix A

Activity coefficient γ_i^w of the NRTL model using the mass fraction as concentration unity.

$$ln\gamma_i = \frac{\sum_{j=1}^{K} \tau_{ji} G_{ji} w_j / \overline{M}_j}{\sum_{j=1}^{K} G_{ji} w_j / \overline{M}_j} + \sum_{j=1}^{K} \left[\frac{w_j G_{ij}}{\overline{M}_j \sum_{l=1}^{n} G_{lj} w_l / \overline{M}_l} \times \left(\tau_{ij} - \frac{\sum_{l=1}^{K} \tau_{lj} G_{lj} w_l / \overline{M}_l}{\sum_{l=1}^{K} G_{lj} w_l / \overline{M}_l} \right) \right] \quad \text{(A1)}$$

$$G_{ji} = exp\,(-\alpha_{ij}\tau_{ij}) \quad \text{(A2)}$$

$$\tau_{ij} = \frac{A_{ij}}{T} \quad \text{(A3)}$$

$$\alpha_{ij} = \alpha_{ji} \quad \text{(A4)}$$

$$\tau_{ii} = 0; G_{ii} = 0 \quad \text{(A5)}$$

Activity coefficient γ_i^w of the UNIQUAC model using the mass fraction as concentration unity.

$$ln\gamma_i = ln\gamma_i^{Comb} + ln\gamma_i^{Res} \quad \text{(A6)}$$

$$ln\gamma_i^{Comb} = \frac{ln\emptyset_i}{ln\,(w_i/\zeta\bar{M}_i)} + 1 - \frac{\zeta\bar{M}_i\emptyset_i}{w_i} + \frac{z}{2}\bar{M}_i q_i' ln\frac{\phi_i'}{\theta_i'} - \frac{z}{2}\bar{M}_i q_i'\left(1 - \frac{\phi_i'}{\theta_i'}\right) \quad \text{(A7)}$$

$$\zeta = \sum_{j=1}^{K=1} \frac{w_j}{\bar{M}_j} \quad \text{(A8)}$$

$$\theta_i' = \frac{q_i' w_i}{\sum_{j=1}^{K} q_j' w_j}; \quad \phi_i' \frac{r_i' w_i}{\sum_{j=1}^{K} r_j' w_j} \quad \text{(A9)}$$

$$ln\gamma_i^{Res} = \bar{M}_i q_i'\left[1 - ln\left(\sum_{j=1}^{K}\theta_j'\tau_{ji}\right) - \sum_{j=1}^{K}\left(\frac{\theta_i'\tau_{ij}}{\sum_{k=1}^{K}\theta_k'\tau_{kj}}\right)\right] \quad \text{(A10)}$$

$$\tau_{ij} = exp\left(-\frac{A_{ij}}{T}\right) \quad \text{(A11)}$$

Literature Cited

[1] Moser BR. Biodiesel production, properties, and feedstocks. In Vitro Cell. Dev. Biol. – Plant. 45 (2009) 229-266.

[2] Falasca SL, Flores N, Lamas MC, Carballo SM, Aschau, A. Crambe abyssinica: An almost unknown crop with a promissory future to produce biodiesel in Argentina. Int. J. Hydrogen Energy. 35 (2010) 5808-5812.

[3] Mandal S, Sangita Y, Singh R, Begun G, Suneja P, Singh M. Correlation studies on oil content and fatty acid profile of some Cruciferous species. Genet. Resour. Crop Evol. 49 **(**2002) 551-556.

[4] Coimbra MC, Jorge N. Fatty Acids and Bioactive Compounds of The Pulps and Kernels of Brazilian Palm Species, guariroba (Syagrus oleraces), jerivá (Syagrus romanzoffiana) and macaúba (Acrocomia aculeata). J. Sci. Food Agric., 92 (2012) 679-684.

[5] Crusciol CAC, Lima RL, Lima EV, Andreotti M, Moro E, Marcon E. Persistencia de Palhada e Liberação de Nutrientes do Nabo-Forrageiro no Plantio Direto. Pesq. Agropec. Bras., 40, (2005) 161-168.

[6] Domingos AK, Saad EB, Wilhelm HM, Ramos LP. Optimization of the ethanolysis of Raphanus sativus (L. Var.) crude oil applying the response surface methodology. Bioresource Technol., 99 (2008) 1837-1845.

[7] Valle P, Velez A, Hegel P, Mabe G, Brignole EA. Biodiesel production using supercritical alcohols with a non-edible vegetable oil in a batch reactor. J. of Supercritical Fluids, 54 (2010) 61-70.

[8] Basso RC, Silva CAS, Sousa CO, Meirelles AJA, Batista EAC. LLE Experimental Data, Thermodynamic Modeling and Sensitivity Analysis in the Ethyl Biodiesel from Macauba Pulp Oil Settling Step. Bioresource Technol., 131 (2013) 468-475.

[9] Encinar JM, Gonzalez JF, Rodrigez JJ, Tejedor A. Biodiesel Fuels from Vegetable Oils: Transesterification of Cynara Cardunculus L. Oils with Ethanol. Energ. Fuel 16, (2002). 443-450.

[10] Stamenkovic OS, Velickovic AV, Veljkovic V B. The Production of biodiesel from vegetable oils by ethanolysis: Current state and perspectives. Fuel, 90 (2011) 3141-3155.

[11] Basso RC, Meirelles AJA, Batista EAC. Liquid-liquid equilibrium of pseudoternary systems containing glycerol + ethanol + ethylic biodiesel from crambe oil (*Crambe abyssinica*) at T/K = (298.2, 318.2, 338.2) and thermodynamic modeling. Fluid Phase Equilib., 333, (2012) 55-62.

[12] Atadashi IM, Aroua MK, Abdul-Aziz AR, Sulaiman NMN, Refinning technologies for the purification of crude biodiesel. Appl. Energ. 88 (2011) 4239-4251.

[13] Berrios M, Skelton R L, Comparison of Purification Methods for Biodiesel. Chem. Eng. J., (2008), 144, 459-465.

[14] Lee MJ, Lo YC, Lin HM. Liquid-liquid equilibria for mixtures containing water, methanol, fatty acid methyl esters, and glycerol. Fluid Phase Equilib., 299 (2010) 180-190.

[15] Follegatti-Romero LA, , Oliveira MB, Batista EAC, Coutinho JAP, Meirelles AJA. Liquid-liquid equilibrium for ethyl esters + ethanol + water systems: Exerimental measurents and CPA EoS modeling. Fuel, 96, (2012), 327-334.

[16] Silva JRF, Mazutti MA, Voll FAP, Cardozo-Filho L, Corazza ML, Lanza M, et al. Thermophysical properties of biodiesel and related systems: (Liquid + liquid) equilibrium data for Jatropha curcas biodiesel. J. Chem. Thermodyn. (2012), 58, 468-475.

[17] Mazutti MA, Voll FAP, Cardozo-Filho L, Corazza M L, Lanza M, Priamo WL, et al. Thermophysical properties of biodiesel and related systems: (Liquid + liquid) equilibrium data for soybean biodiesel. J. Chem. Thermodyn. 58 (2013) 83-94.

[18] Ansolin M, Basso RC, Meirelles AJA, Batista EAC. Experimental Data for liquid-liquid equilibrium of fatty systems with emphasis on the distribution of tocopherols and tocotrienols. Fluid Phase Equilib., 338, (2013) 78-86.

[19] Marcilla A, Ruiz F, Garcia AN. Liquid-liquid-solid equilibria of the quaternary system water – ethanol – acetone – sodium chloride at 25 ºC. Fluid Phase Equilib., 112, (1995) 273-289.

[20]Rodrigues CEC, Silva FA, Marsaioli Jr A, Meirelles AJA. Deacidification of Brazil nut and macadamia nut oils by solvent extraction: liquid-liquid equilibrium data at 298.2 K. J. Chem. Eng. Data. 50 (2005) 517-523.

[21] Oishi T, Prausnitz J M, Estimation of solvent activities in polymer solutions using a group-contribution method. Ind. Eng. Chem. Process Des. Dev. 17 (1978) 333-339.

[22] Batista E, Monnerat S, Kato K, Stragevitch L, Meirelles AJA, Liquid-Liquid Equilibrium for Systems of Canola Oil, Oleic Acid and Short-Chain Alcohols J. Chem. Eng. Data. 44 (1999) 1360-1364.

[23] Stragevitch L, d'Ávila SG. Application of a Generalized Maximum Likelihood Method in the Reduction of Multicomponent Phase Equilibrium Data Braz. J. Chem. Eng. 14 (1997) 41-52.

[24] Fredenslund A, Jones RL, Prausnitz JM. Group-contribution estimation of activity coefficients in nonideal liquid mixtures. AIChE J., 21, (1975) 1086-1099.

[25] Magnussen T, Rasmussen P, Fredenslund A UNIFAC parameter table for prediction of liquid-liquid equilibrium. Ind. Eng. Chem. Process Des. Dev., 20, (1981) 331-339.

[26] Weidlich U, Gmehling J. A modified UNIFAC Model. 1. Prediction of VLE, h^E, and γ^∞. Ind. Eng. Chem. Res., 26, (1987) 1372-1381.

[27] Gmehling J, Witting J, Lohmann J, Joh R. A modified UNIFAC (Dortmund) Model. 4. Revision and Extension. Ind. Eng. Chem. Res., 41, (2002) 1678-1688.

[28] Oliveira, M. B.; Barbedo, S.; Soletti, J. I.; Carvalho, S. H. V.; Queimada, A. J.; Coutinho, J. A. P. Liquid-liquid equilibria for the canola oil biodiesel + ethanol + glycerol system. Fuel, 90, (2011), 2738-2745.

Capítulo 4. Liquid-Liquid Equilibrium of Pseudoternary Systems Containing Glycerol + Ethanol + Ethylic Biodiesel from Crambe Oil (*Crambe abyssinica*) at *T/K* = (298.2, 318.2 338.2) and Thermodynamic Modeling

Rodrigo Corrêa Basso, Antonio José de Almeida Meirelles, Eduardo Augusto Caldas Batista

Trabalho publicado no periódico: **Fluid Phase Equilibria**, v. 333, p. 55 - 62, 2012.

dx.doi.org/10.1016/j.fluid.2012.07.018

Abstract

In the present work Liquid-Liquid Equilibrium (LLE) data were obtained for systems composed of glycerol + ethanol + distilled fatty acid ethyl esters from crambe oil at T/K = 298.2, 318.2 and 338.2. The experimental data measured for these systems were used to adjust the binary interaction parameters between their components for NRTL model treating the mixture of ester as a single ethyl ester, with the average molar mass of the mixture of esters. Two sets of UNIFAC binary interaction parameters were also tested to predict the LLE of the systems. Ethanol, wich distributed in the glycerol-rich and ester-rich phases, showed a greater affinity to the glycerol rich phase. Glycerol and FAEE presented very low miscibility. The average deviations related to mass fraction composition between experimental and calculated values by the NRTL model were less than 0.82 % and by the UNIFAC model were between 2.27 and 3.97 %, considering the two different sets of binary interaction parameters.

Keywords

Biodiesel; Crambe; Liquid-Liquid Equilibrium; NRTL model; UNIFAC model

1. Introduction

Biodiesel is an alternative fuel for diesel engines. Its primary advantages are that it is one of the most renewable fuels currently available, non toxic and biodegradable. It can also be used directly in most diesel engines without requiring extensive engine modification. To obtain biodiesel, vegetable oil or animal fat is subjected to a chemical reaction termed transesterification. In the reaction, the vegetable oil (or animal fat) is reacted, in the presence of a catalyst, with an alcohol to give the corresponding fatty acid alkyl esters[1,2].

In addition to serving as a fuel, ester from vegetable oil can be utilized for numerous other purposes. They can serve as intermediates in the production of fatty alcohols to be used in surfactants and cleaning supplies. Branched fatty acid alkyl esters are used as lubricants and are attractive options due to their improved biodegradability, given environmental considerations. Esters from vegetable oils also possess good solvent properties. Esters from rapeseed oil (rich in erucic acid) were suggested to be used as plasticizers in the production of plastics and as high boiling absorbents for scrubbing of gaseous industrial emissions [1,3,4,5,6].

Crambe seed presents high oil content (23-38 %) and a particular characteristic in its fatty acid profile, being rich in mono-unsaturated fatty acids (about 75 %) with a high content of erucic acid (57.8 % on average) which makes it inadequate for human consumption. Thus, crambe oil is an interesting potential raw material for biodiesel production [7,8].

In some countries where ethanol is readily available at low cost, the transesterification reaction with this alcohol is of great interest. In this process two immiscible phases are formed, one rich in glycerol and the other one rich in biodiesel, where the ethanol used in excess distributes in both phases; therefore LLE data are important and useful in the kinetic study of the transesterification reaction, as well as in studies of the purification steps in which the separation of glycerol, ethanol and ethyl esters is desired.

Despite of the importance of this type of information, few research groups have determined LLE data for systems composed of glycerol, fatty acid alkyl esters and ethanol [9,10] or methanol [11,12,13,14]. The objective of the present study was to determine LLE data for the system constituted of glycerol + ethanol + fatty acid ethyl ester from crambe oil mixture at T/K = 298.2, 318.2 and 338.2, adjust parameters of NRTL model and test the prediction of the LLE of the systems by two different sets of binary interaction parameters of the UNIFAC model.

2. Experimental Procedure

2.1. Materials

Crude crambe oil was supplied by the Foundation MS (Maracaju, MS, Brazil). The oil was homogenized and neutralized prior to biodiesel production.

Glycerol (Sigma, > 0.9900), ethanol (Merk, > 0.9990), methanol (Honeywell, > 0.9999), anhydrous sodium hydroxide (Carlo Erba, > 0.9700), glacial acetic acid (Ecibra, > 0.9970), ethyl myristate (Tecnosyn, > 0.9900) were used in several steps of this work, with no further purification.

2.2. Production of Distilled Crambe Oil Ethyl Esters

Fatty acid ethyl esters mixture from crambe oil was obtained by alkaline catalysis. Sodium hydroxide (1 % in relation to vegetable oil weight) was dissolved, prior to the reaction, in ethanol under vigorously agitation in a magnetic stirrer. The reagent molar ratio was 1:6 oil:ethanol, considering the average molar mass of triacylglycerols in crambe oil. The reaction was maintained for one hour under agitation at room temperature (approximately T/K = 298), before being stopped by the addition of glacial acetic acid. This mixture was then transfer to a separatory funnel for glycerol decanting. Deionized water was used to wash the system at least five times to removal of residual soaps, glycerol and ethanol. The pH of the washing water was monitored with pH test paper (Machery-Nagel). This product was dried under agitation, heating (about T/K = 333.15) and vacuum ($P/mmHg$ < 5).

Distilled fatty acid ethyl esters mixture from crambe oil were obtained by distillation under approximately $P/mmHg$ = 2.25 and T/K = 508.15. Additional washing with hot water and drying were performed after the distillation process to remove any possible residual impurities.

2.3. LLE Experiments

LLE data of the systems were determined using sealed headspace glass tubes (20 mL) (Perkin Elmer). Components were weighted on an analytical balance Adam Equipment, model AAA160L ($\pm$ 0.0001 g). The tubes were vigorously stirred using a vortex (Phoenix, model AP56) and then centrifuged (Centrifuge Jouan, model BR4i, equipped with a temperature controller) for 300 s at 4000 rpm and at room temperature. All systems were left to rest for at least 12 h with temperature controlled in a thermostatic bath Paar Physica, model Physica VT2 (T/K $\pm$ 0.2). Two clear layers and a well defined interface were formed when the systems reached the equilibrium state, the upper layer being the ester-rich phase (EP), and the lower layer the glycerol-rich phase (GP).

2.4. Analytical Methodology

The ethyl biodiesel from crambe oil was previously characterized, in relation to fatty acid ethyl ester composition, in triplicate by a Perkin Elmer gas chromatographic system, Clarus 600, FID detector, with a Perkin Elmer Elite-225 capillary column

(crossbond, 50 % cyanopropylmethyl – 50 % phenylmethyl polysiloxane), length of 30 m, internal diameter of 0.25 mm and film thickness of 0.25 µm, with the following conditions: injector and detector *T/K* = 523; oven temperature: initial *T/K* = 373 for 5 min, between *T/K* = 373 and *T/K* = 503 (temperature rate 5 K/min), *T/K* = 503 for 20 min; helium carrier gas: 1 mL/min; 1:40 split; and injected volume of 0.4 µL. The ethyl ester profile of biodiesel was quantified based on relative peak areas.

Glycerol, fatty acid ethyl esters (FAEE) and ethanol quantitation in each equilibrium phase were determined at least in triplicate by a Perkin Elmer gas chromatographic system, Clarus 600, FID detector, with an Agilent capillary column (crossbond, 50 % cyanopropylphenyl – 50 % dimethylpolysiloxane), length of 30 m, internal diameter of 0.25 mm and film thickness of 0.25 µm), with the following conditions: injector and detector *T/K* = 523; oven temperature: initial *T/K* 313 for 1 min, between *T/K* = 313 and *T/K* = 333 K (temperature rate 5 K/min), *T/K* = 333 for 1 min, between *T/K* = 333 and *T/K* = 473 (temperaturerate rate 25 K/min), *T/K* = 473 for 1 min, between *T/K* = 473 and *T/K* = 508 (temperature rate 7 K/min), *T/K* = 508 for 8 min; helium carrier gas: 1 mL/min for 5 min, 2.5 mL/min for 6 min, 1.5 mL/min until the end; 1:40 split; and injected volume of 0.4 µL. Each component in liquid-liquid equilibrium phases was quantified by a different calibration curve, using nine concentration levels of pure ethanol and ethyl myristate (as standard of ethyl ester class) and eight concentration levels of pure glycerol.

3. Theoretical Calculations

3.1. Calculations of Deviations in the Mass Balance of the Phases

Validity of the equilibrium experiments was evaluated according to the procedure developed by Marcilla et al. [15] and applied by Rodrigues et al. [16]. The procedure is based on comparing the sum of the calculated mass in both liquid phases with the actual value for total mass used in the experiment, thus obtaining a relative deviation for each point of the overall mixture. In this approach, independent component balances, totalizing K balances, can be done as given by equation 1:

$$M^{OC} w_i^{OC} = M^{GP} w_i^{GP} + M^{EP} w_i^{EP} \quad (1)$$

where i represents each component of the system; M^{OC} is the mass of the overall composition (initial mixture); M^{GP} and M^{EP} are the total masses of the glycerol-rich and ester-rich phases, respectively; w_i^{OC} is the mass fraction of the component i in the initial mixture; and w_i^{GP} and w_i^{EP} are the mass fractions of the component i, respectively, in the glycerol-rich and ester-rich phases.

Applying these K equations, the values of M^{GP} and M^{EP} can be calculated from the experimental mass fraction of component in both phases (w_i^{EP} and w_i^{EP})by least squares fitting. If M is the matrix formed by the values of w_i^{oc}, B is the transformation matrix formed by w_i^{GP} and w_i^{EP}, and P is the matrix formed by the masses of the phases, M^{GP} and M^{EP}, the system can be mathematically described as:

$$M = B \cdot P \tag{2}$$

Calculations allow the transformation of equation 2 into the expression below:

$$P = (B^T B)^{-1} B^T M \tag{3}$$

where B^T is the transposed matrix of B and $(B^T B)^{-1}$ is the inverse matrix of $(B^T B)$. Thus, the values for M^{GP} and M^{EP}, which minimize the deviations of the system can be found. The sum of M^{GP} and M^{EP} can be compared to M^{OC} to calculate the overall mass balance deviation by:

$$\delta(\%) = 100 \cdot \frac{|(M^{GP} + M^{EP}) - M^{OC}|}{M^{OC}} \tag{4}$$

The relative average deviation for mass balance of each component i at each temperature is given by:

$$\delta_i(\%) = \sum_n^N \left[100 \cdot \frac{\left|\left(w_{i,n}^{GP} M^{GP} + w_{i,n}^{EP} M^{EP}\right) - w_{i,n}^{OC} M^{OC}\right|}{w_{i,n}^{OC} M^{OC}} \right] \tag{5}$$

where n is the tie line number and N is the total number of tie lines at each temperature.

3.2. NRTL Thermodynamic Modeling

The experimental data measured for the systems were used to adjust the binary interaction parameters for the NRTL model. The mixture of fatty acid ethyl esters was treated as a single ethyl ester with the average molar mass of the mixture of esters, denoted as FAEE. This approach assumes that the mixture of different fatty acid ethyl esters behaves similarly in the systems under study. Therefore, the mixture of ethyl esters has been replaced by a pseudocomponent with the corresponding average physical-chemical properties. This approach has been used by several other authors in relation to vegetable oils, considering it as a pseudocomponent with an average molar mass of the mixture of triacylglicerols [16,17,18]. Thus, adjustments were made considering the systems as pseudoternary. All binary interaction parameters were adjusted to the experimental data.

The mass fraction was used as a composition unit due the difference in the molar masses of the components in the systems; this same approach has been applied by other researchers [16,19,20]. In this way, the isoactivity criterion of LLE developed on a molar fraction basis can be expressed in mass fraction basis as:

$$(\gamma_i x_i)^{GP} = (\gamma_i x_i)^{EP} \tag{6}$$

$$(\gamma_i^w w_i)^{GP} = (\gamma_i^w w_i)^{EP} \tag{7}$$

where:

$$\gamma_i^w = \frac{\gamma_i}{M_i \sum_j^K {w_j}/{M_j}} \tag{8}$$

where x_i is the molar fraction of component i; γ_i is the activity coefficient of component i; γ_i^w is the corresponding activity coefficient expressed on the mass fraction scale; and w_i and M_i are the mass fraction and molar mass, respectively, of component i.

Estimation of the NRTL parameters was obtained by an algorithm developed in FORTRAN programming language. This algorithm uses the modified simplex method to estimate thermodynamic parameters by minimization of objective function of composition

(equation 9). The procedure for calculation of parameters involves flash calculations for the midpoint composition of the experimental tie lines, according to the procedure developed by Stragevitch and d'Avila [21].

$$OF_w = \sum_{m}^{D}\sum_{n}^{N}\sum_{i}^{K-1}\left[\left(\frac{w_{i,n,m}^{GP,exp} - w_{i,n,m}^{GP,calc}}{\rho_{w_{i,n,m}^{GP}}}\right)^2 + \left(\frac{w_{i,n,m}^{EP,exp} - w_{i,n,m}^{EP,calc}}{\rho_{w_{i,n,m}^{EP}}}\right)^2\right] \quad (9)$$

where D is the is the total number of data groups; N is the total number of tie lines; K is the total number of components in the data group; w is the mass fraction; subscripts i, n and m are the component, tie line and group number, respectively; expt and calc represent, respectively, the experimental and calculated composition; and σ is the standard deviation observed for the composition of each phase.

The average deviations between the experimental and calculated compositions in both phases were calculated according to equation 10. Similar approach, using molar fraction, was applied by other researchers [22,23].

$$\Delta w = 100 \cdot \left[\frac{\sum_{n}^{N}\sum_{i}^{K}\left(w_{i,n}^{GP,exp} - w_{i,n}^{GP,calc}\right)^2 + \left(w_{i,n}^{EP,exp} - w_{i,n}^{EP,calc}\right)^2}{2NK}\right]^{1/2} \quad (10)$$

3.3. UNIFAC Thermodynamic Modeling

The UNIFAC thermodinamic model was used to predict the LLE of the experimental data. The group volume and area parameter used in modeling, respectively R_k and Q_k, were the same presented by Magnussem et al. [24]. The structural molecular groups selected to represent the studied systems were "CH_3", "CH_2", "CH", "C=C", "COOC" and "OH". Two different sets of UNIFAC binary interaction parameters were used to test the prediction capability of LLE data. The set denoted as UNIFAC-LLE was presented by Magnussen et al. [24]. The set denoted as UNIFAC-ADJ was adjusted by Batista et al. [25], studying systems containing triacylglycerols, free fatty acids and ethanol. The values of structural molecular groups and of the binary interaction parameters are presented in Table 1.

Table 1. UNIFAC binary interaction parameters and structural molecular groups.

	binary interaction parameters					structural molecular groups[d]		
	groups	CH2	C=C	COOC	OH	sub-groups	Volume (R_k)	Surface Area (Q_k)
UNIFAC-LLE[a]	CH2	0	292.30	-320.10	328.20	CH	0.4469	0.2280
	C=C	74.54	0	485.60	470.70	CH2	0.6744	0.5400
	COOC	972.40	-577.50	0	195.60	CH3	0.9011	0.8480
	OH	644.60	724.40	180.60	0	CH=CH	1.1167	0.8670
UNIFAC-ADJ[b]	CH2	-[c]	-[c]	-[c]	-[c]	CH2COO	1.6764	1.4200
	C=C	-[c]	0	-2692.20	-2457.90	OH	1.0000	1.2000
	COOC	-[c]	-149.18	0	247.52			
	OH	-[c]	1172.40	511.90	0			

[a] binary interaction parameters from Magnussen et al.[24]; [b] binary interaction parameters from Batista et al.[25]; [c] value of binary interaction parameters equal to original parameter of UNIFAC-LLE; [d] structural molecular groups values presented by Magnussen et al.[24].

All individual fatty acid ethyl esters were considered to UNIFAC modeling calculations. In this way, the systems were represented for glycerol, ethanol and ten fatty acid ethyl esters. However, in ternary diagram representation, the esters were grouped by the addition of each individual ester mass fraction, and the systems were graphically represented as glycerol (1) + ethanol (2) + FAEE (3).

The average deviations between the experimental and calculated compositions were also calculated according to equation 10. The ternary diagrams were represented using the mass fractions values obtained by the sets of interaction parameters, UNIFAC-LLE and UNIFAC-ADJ, to compare the different behavior of the represented LLE in relation to parameters applied.

4. Results and Discussions

Fatty acid ethyl ester mixture from crambe oil showed less than 7 % of saturated ethyl esters in its composition, as can be observed in Table 2. The main ester that composes the FAEE is the cis-13docosenoic acid ethyl ester (erucic acid ethyl ester), an ester containing twenty four carbons atoms and one double bound in the alkyl group. The average molar mass of the FAEE, considering it as a pseudo-component in NRTL modeling, was calculated according to its ester profile.

Table 2. Experimental ethyl ester composition of FAEE in mass percentage.[a]

fatty acid group in ethyl ester	ethyl ester	molecular formula	$\frac{M}{(g \cdot mol^{-1})}$	100 w[b]
C16:0	hexadecanoic acid ethyl ester	C18H36O2	284.48	2.18
C18:0	octadecanoic acid ethyl ester	C20H40O2	312.53	1.06
C18:1	cis-9 octadecenoic acid ethyl ester	C20H38O2	310.51	20.03
C18:2	cis-9 cis-12 octadecadienoic acid ethyl ester	C20H36O2	308.50	8.87
C18:3	cis-9 cis-12 cis-15 octadecatrienoic acid ethyl ester	C20H34O2	306.48	4.76
C20:0	icosanoate acid ethyl ester	C22H44O2	340.58	1.18
C20:1	cis-11 icosenoic acid ethyl ester	C22H42O2	338.57	3.87
C22:0	docosanoic acid ethyl ester	C24H48O2	368.64	1.83
C22:1	cis-13docosenoic acid ethyl ester	C24H46O2	366.62	55.62
C22:2	cis-13 cis-16 docosadienoic acid ethyl ester	C24H44O2	364.61	0.60
	FAEE (pseudocomponent)		341.22	

[a] standard uncertainty composition u(x) = 0.00025; [b] mass fraction of ethyl ester.

Each ethyl ester in GP and EP were quantified in relation to all tie lines of all the systems. The average molar mass of esters mixtures was calculated in each phase in order to verify the assumption that the FAEE behaves as a pseudo-component. The individual fatty acid ethyl ester composition in each phase of each system and deviations between the average molar mass of FAEE in each phase and average molar mass of FAEE in overall composition were low and are showed in Table 3. The greater deviation in relation to EP was 0.80% and in relation to GP was 5.22 %. Lanza et al. [18], considering soybean oil as a pseudocomponent, compared the average molar mass of triacylglycerols between the alcoholic-rich and triacylglicerol-rich phases. These authors obtained low deviations, approximately 0.6 %. However, in relation to individual fatty acid distribution, specifically considering oleic and linoleic acids which are the major components in soybean oil (about 75 % of total fatty acid content), the deviations obtained were higher than those obtained in the present work in relation to FAEE from crambe oil that has predominace of oleic and erucic acid in alkyl group (about 75 %). Thus, the assumption of pseudo-component behavior could be used.

The behavior of the four main fatty acid ethyl esters from crambe oil in relation to its distribution in GP and in EP can be observed in Figure 1. The distribution coefficient of ethyl esters presents a little increase with the increase of number of unsaturation and a decrease with the increase of the number of carbon in the molecule. This behavior occurs

due the differences in polarity among these components. FAEE (pseudo-component) presents a distribution coefficient intermediate in relation to the main ethyl esters of the mixture. The distribution coefficient was similar to same esters at the three different temperatures, indicating that the distribution of the individual esters is almost not affected in this range of temperature.

Table 3. Individual fatty acid ethyl ester composition in mass percentage in relation to FAEE for the systems in (liquid- liquid) equilibrium, at T/K = (298.2, 318.2, 338.2).[a]

	ester phase											
	$C_{18}H_{36}O_2$	$C_{20}H_{40}O_2$	$C_{20}H_{38}O_2$	$C_{20}H_{36}O_2$	$C_{20}H_{34}O_2$	$C_{22}H_{44}O_2$	$C_{22}H_{42}O_2$	$C_{24}H_{48}O_2$	$C_{24}H_{46}O_2$	$C_{24}H_{44}O_2$		δ[b]
T/K	$100w_k^c$	$100w_k^c$	$100w_k^c$	$100w_k^c$	$100w_k^c$	$100w_k^c$	$100w_k^c$	$100w_k^c$	$100w_k^c$	$100w_k^c$	$\frac{M}{(g \cdot mol^{-1})}$	
298.2	2.23	1.09	21.32	9.13	5.33	1.32	3.93	1.70	53.53	0.42	339.87	0.39
	2.22	1.07	21.33	9.17	5.36	1.30	3.89	1.69	53.54	0.43	339.86	0.40
	2.30	1.10	21.99	9.53	5.64	1.29	3.95	1.62	52.17	0.41	339.00	0.65
	2.32	1.10	22.11	9.62	5.71	1.29	3.93	1.61	51.90	0.41	338.82	0.70
	2.31	1.08	21.99	9.58	5.69	1.27	3.90	1.61	52.16	0.41	338.96	0.66
	2.36	1.10	22.35	9.78	5.83	1.29	3.95	1.57	51.35	0.42	338.48	0.80
318.2	2.14	1.05	20.59	8.87	5.20	1.29	3.88	1.74	54.82	0.42	340.65	0.17
	2.15	1.04	20.66	8.86	5.19	1.27	3.86	1.73	54.78	0.47	340.63	0.17
	2.22	1.06	21.34	9.28	5.49	1.26	3.90	1.63	53.42	0.41	339.73	0.44
	2.27	1.08	21.54	9.38	5.57	1.29	3.93	1.67	52.84	0.43	339.42	0.53
	2.25	1.07	21.48	9.37	5.56	1.29	3.90	1.66	53.00	0.42	339.49	0.51
	2.29	1.08	21.78	9.52	5.67	1.29	3.95	1.63	52.38	0.41	339.12	0.62
338.2	2.20	1.07	21.12	8.94	5.12	1.29	3.93	1.71	54.22	0.40	340.27	0.28
	2.20	1.06	21.13	9.00	5.19	1.28	3.89	1.68	54.16	0.41	340.21	0.30
	2.20	1.05	21.13	8.99	5.17	1.27	3.87	1.69	54.23	0.40	340.24	0.29
	2.24	1.07	21.47	9.19	5.35	1.28	3.91	1.67	53.40	0.42	339.75	0.43
	2.24	1.06	21.45	9.20	5.36	1.27	3.88	1.67	53.46	0.41	339.76	0.43
	2.28	1.08	21.77	7.05	5.33	1.28	5.09	1.69	54.02	0.41	340.52	0.20

	glycerol phase											
	$C_{18}H_{36}O_2$	$C_{20}H_{40}O_2$	$C_{20}H_{38}O_2$	$C_{20}H_{36}O_2$	$C_{20}H_{34}O_2$	$C_{22}H_{44}O_2$	$C_{22}H_{42}O_2$	$C_{24}H_{48}O_2$	$C_{24}H_{46}O_2$	$C_{24}H_{44}O_2$		δ[b]
T/K	$100w_k^c$	$100w_k^c$	$100w_k^c$	$100w_k^c$	$100w_k^c$	$100w_k^c$	$100w_k^c$	$100w_k^c$	$100w_k^c$	$100w_k^c$	$\frac{M}{(g \cdot mol^{-1})}$	
298.2	2.76	1.06	25.16	12.02	7.69	1.07	3.74	1.31	44.81	0.38	334.24	2.05
	3.07	1.02	27.26	13.76	9.14	0.91	3.57	1.06	39.82	0.39	331.07	2.97
	3.23	1.06	28.78	15.01	10.68	1.06	3.22	1.13	35.46	0.37	328.57	3.71
	3.43	1.06	30.03	16.04	12.48	1.10	3.16	0.92	31.41	0.37	326.13	4.42
	3.85	1.16	31.46	17.85	13.51	1.60	2.85	0.72	27.00	0.00	323.40	5.22
	2.89	1.09	26.36	12.83	10.25	2.02	3.16	2.33	39.07	0.00	331.42	2.87
318.2	2.69	1.06	24.58	11.73	7.45	1.02	3.81	1.21	46.07	0.38	334.93	1.84
	2.97	1.04	26.46	13.04	8.49	0.89	3.75	0.99	41.96	0.41	332.34	2.60
	3.22	0.94	28.53	14.86	10.29	0.61	3.66	0.92	36.97	0.00	329.07	3.56
	3.11	0.99	27.27	14.70	10.68	0.99	3.06	1.25	37.95	0.00	329.74	3.36
	2.96	1.05	28.20	15.19	11.80	1.30	3.08	1.24	35.18	0.00	328.34	3.77
	2.71	1.03	24.32	11.19	8.43	1.76	3.70	2.20	44.66	0.00	334.68	1.92
338.2	2.64	1.08	24.26	11.16	6.85	1.12	3.84	1.32	47.39	0.34	335.80	1.59
	2.86	1.05	25.93	12.44	8.00	0.97	3.78	1.03	43.54	0.40	333.32	2.32
	3.22	0.95	28.42	14.38	9.65	0.84	3.61	0.94	37.99	0.00	329.73	3.37
	3.75	1.14	29.51	15.60	10.79	0.91	3.30	0.96	34.04	0.00	327.32	4.07
	3.79	1.05	30.51	16.77	12.32	1.06	3.65	1.06	29.79	0.00	325.18	4.70
	4.28	1.14	32.39	17.91	11.81	0.00	4.24	0.00	28.23	0.00	323.50	5.19

[a] uncertainties u are u(T/K) = 0.1, combined u(w) = 0.0097; [b] deviation in percentage between average molar mass of FAEE per tie line; [c] mass fraction of each ester in FAEE.

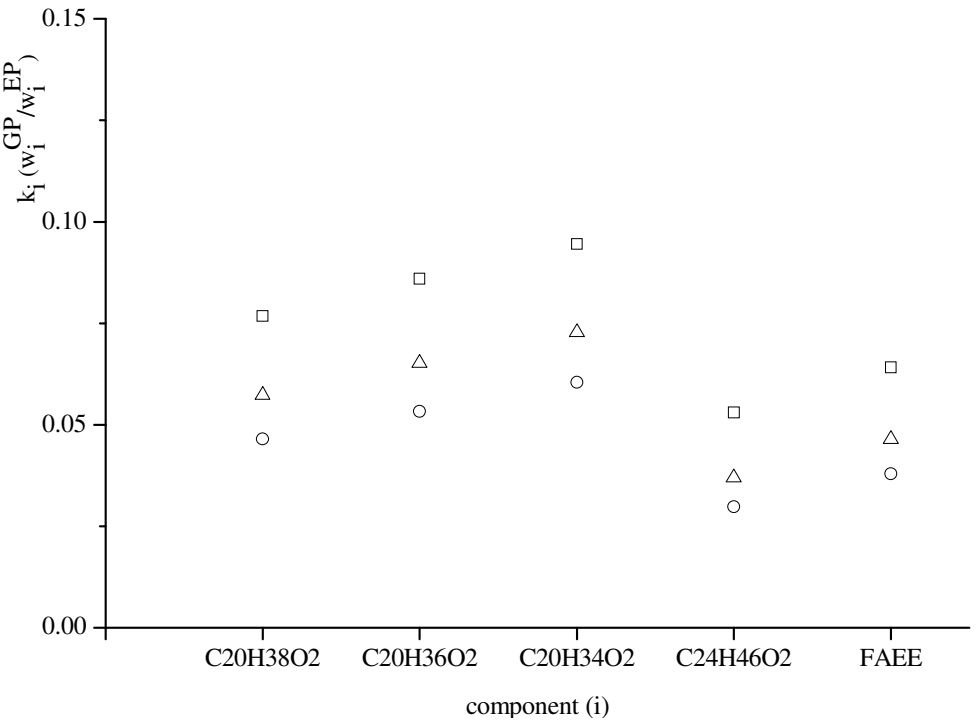

Figure 1. Individual fatty acid ethyl ester distribution coefficient (k_i): (○) 298.2 K; (Δ) 318.2 K; (□) 338.2 K.

Table 4 presents the overall experimental compositions (OC) and the correspondent tie line compositions, in mass fraction of each component for the pseudo-ternary systems composed of glycerol (1) + ethanol (2) + FAEE (3). The overall mass balance deviations calculated according to equation 4 were always lower than 0.45 %, indicating good quality of the experimental data. The relative average deviations for mass balance of each component, according to equation 5, were between 0.04 and 1.83.

Table 5 presents the adjusted binary interaction parameters for the NRTL model of the systems under study. The average deviations between experimental and calculated compositions in both phases (equation 10) were 0.8317 %, 0.5490 % and 0.9927 %, respectively, for the systems at *T/K* = (298.2, 318.2 and 338.2). These results indicate good description of LLE by the NRTL model for these systems.

Tabela 4. Experimental (liquid-liquid) equilibrium data for the pseudoternary systems glycerol (1) + ethanol (2) + FAEE (3), for mass percentage (100w) at T/K = (298.2, 318.2, 338.2).[a]

T/K	oc[b]			gp[c]			ep[d]			δ[e]
	$100w_1$	$100w_2$	$100w_3$	$100w_1$	$100w_2$	$100w_3$	$100w_1$	$100w_2$	$100w_3$	
298.2	14.65	44.66	40.69	25.99	64.01	10.00	2.72	24.91	72.37	0.09
	20.37	39.54	40.09	37.14	58.67	4.19	1.74	18.48	79.78	0.02
	24.72	34.92	40.36	45.62	52.46	1.92	1.25	14.97	83.78	0.02
	30.00	29.90	40.10	54.52	44.70	0.78	0.92	11.99	87.09	0.01
	36.08	24.61	39.31	63.11	36.64	0.25	0.72	9.43	89.85	0.06
	39.69	19.83	40.48	69.95	29.84	0.21	0.54	7.71	91.75	0.16
318.2	15.71	44.04	40.25	27.27	62.14	10.59	4.08	28.01	67.91	0.35
	20.02	40.28	39.70	35.55	59.06	5.39	2.64	22.38	74.98	0.43
	24.41	35.09	40.50	45.37	52.33	2.30	1.87	17.88	80.25	0.11
	29.58	30.04	40.38	54.31	44.62	1.07	1.68	13.77	84.55	0.00
	35.00	24.58	40.42	62.28	37.26	0.46	1.02	11.18	87.80	0.25
	39.76	20.06	40.18	69.90	29.70	0.40	0.68	8.67	90.65	0.21
338.2	15.79	44.57	39.64	26.66	59.9	13.44	7.67	34.79	57.54	0.33
	19.94	39.93	40.13	36.42	56.76	6.82	4.18	26.39	69.43	0.40
	25.45	33.74	40.81	47.69	49.86	2.45	2.51	19.33	78.16	0.15
	30.03	30.34	39.63	55.35	43.44	1.21	1.86	16.20	81.94	0.01
	34.69	25.14	40.17	63.25	36.29	0.46	1.34	12.21	86.45	0.01
	39.69	20.10	40.21	70.84	29.03	0.13	1.03	10.00	88.97	0.20

[a] uncertainties u are u(T/K) = 0.1, u(w) = 0.0097; [b] overall composition; [c] glycerol rich-phase; [d] ester rich-phase; [e] overall mass balance deviation according to equation 4.

Table 5. Binary interaction parameters for NRTL model.

pair ij[a]	$A(0)_{ij}$/K	$A(0)_{ji}$/K	$A(1)_{ij}$	$A(1)_{ji}$	α_{ij}
12	-1015.8000	-705.2800	4.4437	0.8836	0.1100
13	-4196.7000	-3165.3000	24.7510	15.4370	0.1515
23	-191.1500	1000.0000	3.0832	-3.7261	0.5700

[a] components of binary interaction.

According to Figure 2, miscibility between glycerol and FAEE is very low. The bottom of the LLE diagram shows that for small mass fractions of ethanol, the presence of glycerol and FAEE respectively in EP and GP are small. On the other hand, ethanol is distributed in both phase and has greater affinity to the glycerol-rich phase as can be observed from slope of the tie lines.

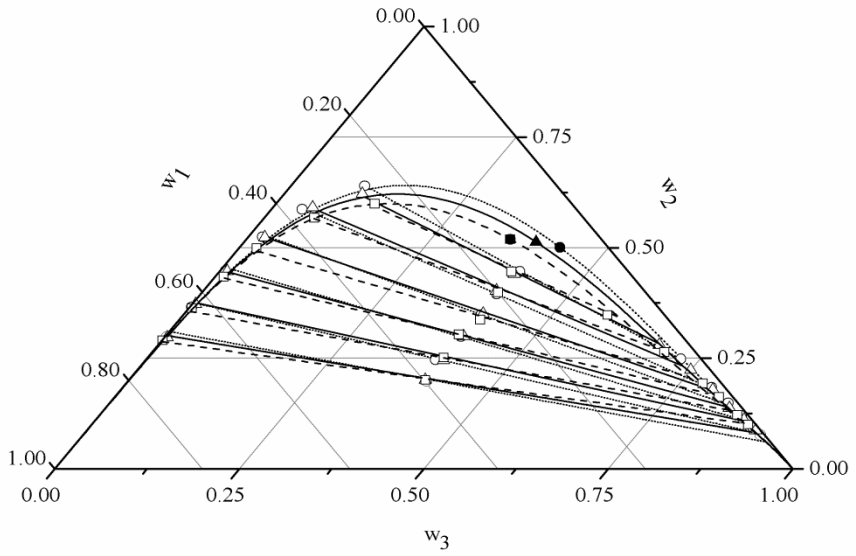

Figure 2. Liquid-Liquid Equilibrium Diagram of the systems glycerol (1) + ethanol (2) + FAEE (3) at 298.2, 318.2 and 338.2 K: (*w*) mass fraction of the component; (···) NRTL at 298.2 K; (—) NRTL at 318.2 K; (---) NRTL at 338.2 K; (●) NRTL plait point at 298.2 K; (▲) NRTL plait point at 318.2 K; (■) NRTL plait point at 338.2 K; (○) experimental data at 298.2 K; (∆) experimental data at 318.2 K; (□)experimental data at 338.2 K.

The systems showed low dependence of the temperature in relation to the solubility between the components mainly in the region near the baseline. The plait points indicate that values suffer small modifications with temperature and binodal curves were almost overlapping in the remote region from the plait point.

The glycerol distribution is highly dependent of the ethanol mass fraction in the overall composition as can be observed by the increase of glycerol mass fraction in glycerol-rich phase in opposition to its decrease in ester-rich phase as function of ethanol mass fraction decrease in overall composition (Figure 2). This distribution increases with the decrease of the ethanol mass fraction in the overall composition. This behavior affects the separation and purification steps in the production of ethyl esters. Whereas a high excess of ethanol is advantageous to the transesterification reaction, the purification and settling steps are hampered by the presence of this reagent in excess due the improved miscibility between glycerol and ethyl esters.

Consequently, it is advantageous to perform the settling process in ethylic biodiesel from crambe oil production in region remote from plait point, were the ethanol composition is lower than next this point.

Considering the complete transesterification reaction, with 3 moles of ethanol in excess, the final stoichiometric molar ratio would be equal to 1 (glycerol) : 3 (ethanol) : 3 (FAEE). In this case, the final mass fraction of each component would be 0.073, 0.1102, 0.8168, respectively, for glycerol, ethanol and FAEE. Using this overall composition and the NRTL model, the liquid-liquid flash could be performed and the phase compositions encountered. The glycerol mass fraction in the ester-rich phase is higher than 0.7 %, indicating the necessity of additional purification of this phase for application as biodiesel fuel.

Figure 3 presents the LLE predicted by UNIFAC-LLE. The model could not represent the experimental data satisfactorily. It is not possible to observe a diminishing in the phase separation region near to the plait point, as occurs with the experimental data. At lower concentrations of glycerol in GP, the UNIFAC-LLE model predicted a lower composition of ethyl esters and a higher composition in ethanol than observed to experimental data. The slopes of the calculated tie lines were considerably more accentuated than the tie lines draw from experimental data, representing a lower presence of ethanol in EP than experimental data.

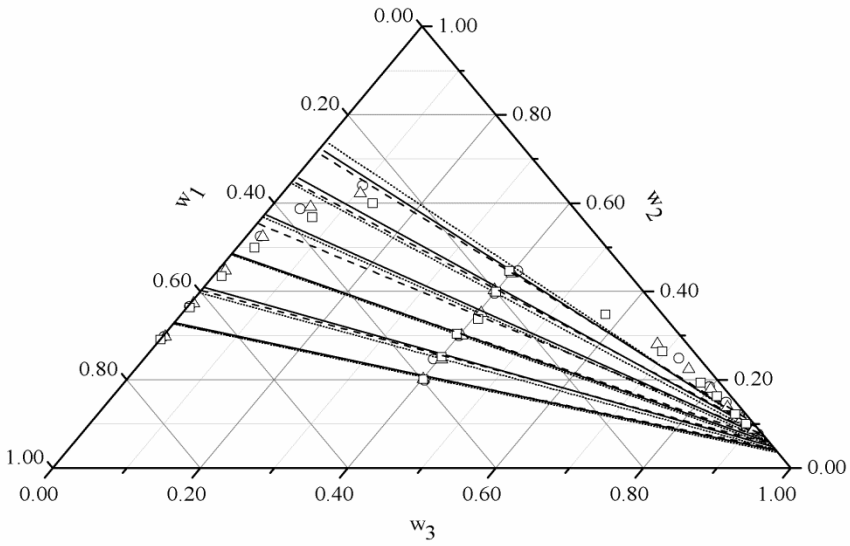

Figure 3. Liquid-Liquid Equilibrium Diagram of the systems glycerol (1) + ethanol (2) + FAEE (3) at 298.2, 318.2 and 338.2 K: (*w*) mass fraction of the component; (···) UNIFAC-LLE at 298.2 K; (—) UNIFAC-LLE at 318.2 K; (---) UNIFAC-LLE at 338.2 K; (○) experimental data at 298.2 K; (Δ) experimental data at 318.2 K; (□)experimental data at 338.2 K.

Figure 4 shows the calculated data using UNIFAC-ADJ. The description of the LLE of the studied systems was improved by the adjustment of the parameter done by Batista et al. [25]. There is a visible diminishing in the phase separation region of the diagram with the increase of the ethanol in the systems near the plait point. The calculated tie lines showed a behavior relatively better than using the UNIFAC-LLE.

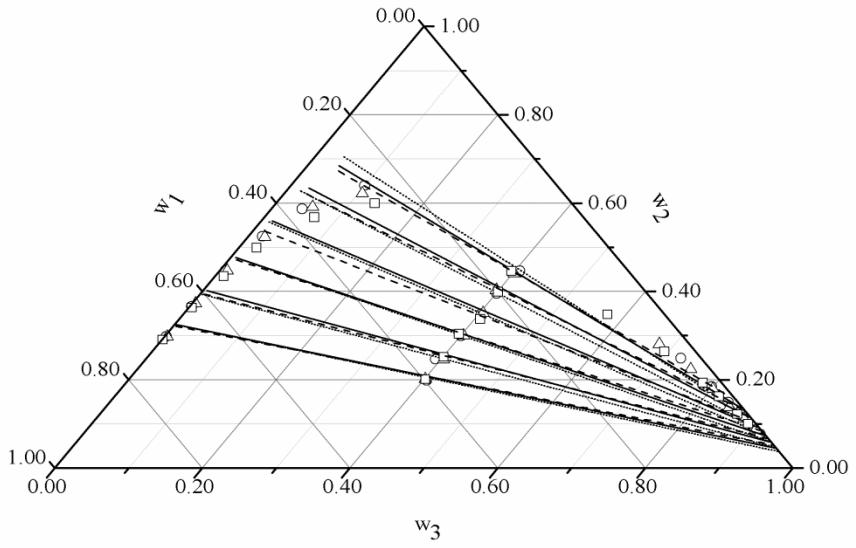

Figure 4. Liquid-Liquid Equilibrium Diagram of the systems glycerol (1) + ethanol (2) + FAEE (3) at 298.2, 318.2 and 338.2 K: (*w*) mass fraction of the component; (···) UNIFAC-ADJ at 298.2 K; (—) UNIFAC-ADJ at 318.2 K; (---) UNIFAC-ADJ at 338.2 K; (○) experimental data at 298.2 K; (Δ) experimental data at 318.2 K; (□)experimental data at 338.2 K.

Despite of the improvement in the representation of the experimental data by UNIFAC-ADJ, both sets of binary parameters could not predict the LLE of the systems with the needed accuracy required for the optimization of the industrial processes design, as can observed by deviations between experimental and calculated data in Table 6.

Table 6. Deviations (δ) between experimental and UNIFAC calculated mass fraction.

T/K	δ (%) UNIFAC-LLE	δ (%) UNIFAC-ADJ
298.2	2.72	2.27
318.2	3.18	2.54
338.2	3.97	3.17

5. Conclusions

The results of the present study show that ethanol is distributed in both phases (EP and GP). Miscibility between FAEE and glycerol is extremely low. High quantities of ethanol in the systems hamper the purification step during FAEE production. The miscibility among the components in the systems is little dependent on temperature. Despite the high complexity of the systems, the estimated parameters of the NRTL model are representative. The applied parameters in UNIFAC calculations need to be readjusted to adequate prediction of LLE of these systems. Application of these LLE data in the study of similar systems contributes to improve the production and purification steps of ethyl esters.

List of symbols

$A(0)_{ij}, A(1)_{ij}$	NRTL characteristic energy interaction parameters
g_{ij}, g_{ji}	NRTL binary molecular energy interaction parameters
G_{ij}	NRTL parameter
T	absolute temperature
α_{ij}, α_{ji}	NRTL non-ramdomness binary interaction parameters
τ_{ij}, τ_{ji}	NRTL binary molecular energy interaction parameters
γ_i^w	mass fraction-scale activity coefficient of component *i*
M	molar mass
w_i	mass fraction of component *i*
R	residual part of equation
C	combinatorial part of equation
v_k^i	number of times that group *k* is in molecule *i*
Γ_k	residual activity coefficient of group *k*

$\Gamma_k^{(i)}$	residual activity coefficient of group k in a solution only with molecules of type *i*
Q	group area parameter
q'	van der Waals molecular area
R_k	group volume parameter
r'	van der Waals molecular volume
U	interaction energy
θ'	area fraction
ϕ'	volume fraction
G	group numbers
i,j,k	component
m,n,k	components in NRTL model/ groups in UNIFAC model

Acknowledgement

The authors would like to acknowledge the Fundação de Amparo a Pesquisa do Estado de São Paulo (FAPESP – process number 8/56258-8) for its financial support, and the Conselho Nacional de Desenvolvimento Científico e Tecnológico (CNP_q – process number 140362/2009-6) for scholarship.

Appendix A

Activity coefficient γ_i^w of NRTL model using mass fraction as concentration unity:

$$ln\gamma_i^w = \frac{\sum_{j=1}^{K} \tau_{ji} G_{ji} w_j / M_j}{\sum_{j=1}^{K} G_{ji} w_j / M_j} + \sum_{j=1}^{K} \left[\frac{w_j G_{ij}}{M_j \sum_{l=1}^{n} G_{lj} w_l / M_l} \times \left(\tau_{ij} - \frac{\sum_{l=1}^{K} \tau_{lj} G_{lj} w_l / M_l}{\sum_{l=1}^{K} G_{lj} w_l / M_l} \right) \right] \quad \text{(A.1)}$$

$$G_{ij} = exp\,(-\alpha_{ij}\tau_{ij}) \quad \text{(A.2)}$$

$$\tau_{ij} = \frac{g_{ii} - g_{jj}}{RT} \quad \text{(A.3)}$$

$$\tau_{ij} = A(0)_{ij} + A(1)_{ij}T \quad \text{(A.4)}$$

$$\alpha_{ij} = \alpha_{ji} \quad \text{(A.5)}$$

Activity coefficient γ_i^w of UNIFAC model using mass fraction as concentration unity:

$$ln\gamma_i = ln\gamma_i^C + ln\gamma_i^R \quad \text{(A.6)}$$

$$ln\gamma_i^R = \sum_k^G v_k^i \left[ln\Gamma_k - ln\Gamma_k^i\right] \quad \text{(A.7)}$$

$$ln\Gamma_k = M_k Q_k \left[1 - ln\left(\sum_m^G \Theta'_m \Psi_{mk}\right) - \sum_m^G \left(\frac{\Theta'_m \Psi_{km}}{\sum_n^G \Theta'_n \Psi_{nm}}\right)\right] \quad \text{(A.8)}$$

$$\Theta'_m = \frac{Q_m W_m}{\sum_n^G Q_n W_n};\ W_m = \frac{\sum_m^C v_m^{(j)} w_j}{\sum_j^C \sum_n^G v_n^{(j)} w_j} \quad \text{(A.9)}$$

$$r'_i = \frac{1}{M_i}\sum_k^G v_k^i R_k;\ q'_i = \frac{1}{M_i}\sum_k^G v_k^{(i)}\, Q_k \quad \text{(A.9)}$$

$$\theta'_i = \frac{q'_i w_i}{\sum_j^C q'_j w_j};\ \phi'_i = \frac{r'_i w_i}{\sum_j^C r'_j w_j} \quad \text{(A.10)}$$

$$\Psi_{mn} = exp - \left(\frac{U_{mn} - U_{nn}}{RT}\right) = exp - \frac{a_{mn}}{T} \quad \text{(A.11)}$$

Literature Cited

[1] G. Knothe, in: G. Knothe, J. Van Gerpen, J. Khrahl, The Biodiesel Handbook, AOCS Press, Champaign, Illimois, 2005.

[2] J. Van Gerpen, B. Shanks, R. Pruszko, D. Clements, G. Knothe, Biodiesel Production Technology, NREL, Golden, Colorado, 2004.

[3] R. A. Peters, Inform 7. (1999) 502-505.

[4] A. Willing, Fett/Lipid. 101 (1999) 192-198.

[5] J. Wehlmann, Fett/ Lipid. 101 (1999) 249-256.

[6] K. Bay, H. Wanko, J. Ulrich, Chem. Ing. Tech. 76 (2004) 328-333.

[7] S. L. Falasca, N. Flores, M. C. Lamas, S. M. Carballo, A. Aschau, Int. J. Hydrogen Energy. 35 (2010) 5808-5812.

[8] S. Mandal, Y. Sangita, R. Singh, G. Begun, P. Suneja, M. Singh, Genet. Resour. Crop Evol. 49 (2002) 551-556.

[9] X. Liu, X. Piao, Y. Wang, S. Zhu, J. Chem. Eng. Data. 53 (2008) 359-362.

[10] B. B. França, F. M. Pinto, F. L. P. Pessoa, A. M. C. Uller, J. Chem. Eng. Data. 54 (2009) 2359-2364.

[11] S. N. Csernica, J. T. Hsu, Ind. Eng. Chem. Res. 50 (2011) 1012-1016.

[12] A. Barreau, I. Brunella, J. C. de Hemptinne, V. Coupard, X. Canet, F. Rivollet, Ind. Eng. Chem. Res. 49 (2010) 5800-5807.

[13] H. Zhou, H. Lu, B. Liang, J. Chem. Eng. Data. 51 (2006) 1130-1135.

[14] M. Lee, Y. Lo, H. Lin. Fluid Phase Equilib. 299 (2010) 180-190.

[15] A. Marcilla, F. Ruiz, A. N. Garcia, Fluid Phase Equilib. 112 (1995) 273-289.

[16] C. E. C. Rodrigues, F. A. Silva, A Marsaioli . Jr., A. J. A. Meirelles, J. Chem. Eng. Data. 50 (2005) 517-523.

[17] E. Batista, S. Monnerat, , K. Kato, L. Stragevitch, A. J. A. Meirelles, J. Chem. Eng. Data. 44 (1999) 1360-1364.

[18] M. Lanza, W. Borges Neto, E. Batista, R. J. Poppi, A. J. A. Meirelles, J. Chem. Eng. Data. 53 (2008) 5-15.

[19] T. Oishi, J. M. Prausnitz, Ind. Eng. Chem. Process Des. Dev. 17 (1978) 333-339.

[20] C. E. C. Rodrigues, E. C. D. Reipert, A. F. Souza, P. A. Pessôa Filho, A. J. A. Meirelles, Fluid Phase Equilib. 238 (2005) 193-203.

[21] L. Stragevitch, S. G. d'Ávila, Braz. J. Chem. Eng. 14 (1997) 41-52.

[22] L. H. de Oliveira, M. Aznar, J. Chem. Thermodynamics. 42 (2010) 1379-1385.

[23] M. C. Batistell, T. C. Alves, T. R. Guadagnini, L. H. de Oliveira, M. Aznar, J. Chem. Thermodynamics. 43 (2011) 1381-1388.

[24] T. Magnussen, P. Rasmussen, A. Fredenslund. Ind. Eng. Chem. Process Des. Dev. 20, (1981) 331-339.

[25] E. Batista, S. Monnerat, L. Stragevitch, C. G. Pina, C. B. Gonçalves, A. J. A. Meirelles. J. Chem. Eng. Data. 44 (1999) 1365-1369.

Capítulo 5. LLE Experimental Data, Thermodynamic Modeling and Sensitivity Analysis in the Ethyl Biodiesel from Macauba Pulp Oil Settling Step

Rodrigo Corrêa Basso, César Augusto Sodré da Silva, Camila de Oliveira Sousa, Antonio José de Almeida Meirelles, Eduardo Augusto Caldas Batista

Trabalho publicado no periódico: **Bioresource Technology**, v. 131, p. 468 - 475, 2013.

dx.doi.org/10.1016/j.biortech.2012.12.190

Abstract

The aims of this study were to obtain experimental data related to Liquid-Liquid Equilibrium (LLE) of systems containing glycerol + ethanol + ethyl biodiesel from macauba pulp oil, perform thermodynamic modeling and simulate the settling step of this biodiesel using simulation software. Binary interaction parameters were adjusted for NRTL and UNIQUAC models. The UNIFAC-LLE and UNIFAC-Dortmund models were used to predict the LLE of the systems. A sensitivity analysis was applied to the settling step to describe the composition of the output streams as a function of ethanol in the feed stream. Ethanol had greater affinity for the glycerol-rich phase. The deviations between experimental data and calculated values were 0.44%, 1.07%, 3.52% and 2.82%, respectively, using the NRTL, UNIQUAC, UNIFAC-LLE and UNIFAC-Dortmund models. Excess ethanol in the feed stream causes losses of ethyl ester in the glycerol-rich stream and high concentration of glycerol in the ester-rich stream.

Keywords

Biodiesel; Macauba Oil; Liquid-Liquid Equilibrium; Themodynamic Modeling; Sensitivity Analysis

1. Introduction

Biodiesel, defined as mono-alkyl esters of fatty acid from vegetable oil or animal fats, is an environmentally attractive alternative to conventional petroleum diesel fuel. Produced by transesterification with a mono-hydric alcohol, biodiesel presents many important technical advantages over petroleum diesel including low toxicity, derivation from renewable feedstocks, superior biodegradability, negligible sulfur content, higher flash point and lower exhaust emissions (Moser, 2009). In transesterification, the reaction by which biodiesel is produced, the stoichiometric relationship between alcohol and oil is 3:1, however an excess of alcohol is typically employed to improve the reaction towards the desired product. In transesterification using supercritical alcohols or in acid catalysis transesterification/esterification, the initial molar ratio alcohol:oil used is about 39:1 and 29:1, respectivelly (Valle et al., 2010; Zhang et al., 2012). Typically, in alkali catalysis, either sodium or potassium hydroxide is used as catalyst along with methanol or ethanol and any type of oil or fat (Marchetti et al., 2007).

Despite its elevated price in relation to methanol, the advantages of using ethanol in biodiesel production include higher miscibility with vegetable oils that allows better contact in the reaction step and lower toxicity. Although commercial processes use vegetable oils and methanol in the transesterification reaction, the use of ethanol in biodiesel synthesis is appealing because it is produced from biorenewable sources, resulting in a completely agricultural-based fuel obtained by ethanolysis (Encinar et al., 2002; Stamenkovic et al., 2011). Based on this point of view, in recent years, several different technologies have been considered to optimize ethyl biodiesel production (Sawangkeaw et al., 2011; Kanitkar et al., 2011; Zhang et al., 2012).

The melting point, oxidative stability and viscosity are important physical properties of biodiesel. Melting point, the property related to biodiesel cold flow, is affected by molecular weight, number and configuration of double carbon bonds and branching of the carbon chain (Knothe and Dunn, 2009). Oxidative stability is associated to tendency of biodiesel to suffer autoxidation and, indirectly, polymerization. This property is inversely related to the degree of unsaturation of alkyl esters (Knothe et al., 2005). Viscosity is one of the most important factors affecting the in-cylinder atomization process in direct-injection diesel engines (Yuan et al., 2009). Viscosity is reduced by shorter chain length and the presence of cis-double bonds. The trans-double bonds have less effect on viscosity compared to saturated compounds with an equal number of carbons. An OH group in the chain considerably increases viscosity (Knothe and Steidley, 2007).

Biodiesel from macauba pulp oil is composed mainly of intermediate alkyl esters (16 and 18 carbons in the fatty acid chain), with more than fifty percent monounsaturated alkyl esters and about twenty five percent esters from palmitic acid (Coimbra and Jorge, 2012). Therefore, when considering the melting point, oxidative stability and viscosity related to chemical composition, esters from macauba pulp oil make up an interesting raw material for biodiesel production.

Ethyl biodiesel is produced in countries were ethanol is readily available. Two immiscible phases are formed in the settling step of ethyl biodiesel purification, an upper phase composed mainly of biodiesel and ethanol, and a lower phase composed mainly of glycerol and ethanol; therefore, design of this step in the biodiesel production process is directly related to the study of Liquid-Liquid Equilibrium (LLE) in systems containing these components.

Different thermodynamic models, using association parameters, have been used in LLE modeling of systems containing glycerol + short chain alcohol + fatty acid alkyl esters. Barreau et al. (2010), using a group contribution method combined with a statistical associating fluid theory equation of state (GC-PPC-SAFT) in modeling of systems containing methanol + glycerol + methyl oleate, reported an overestimated region of phase separation and an underestimated solubility of methyl ester in glycerol rich-phase by this model. Oliveira et al. (2011) and Follegatti-Romero (2012), using cubic plus association equation of state (CPA-EOS) in modeling of systems containing glycerol + ethanol + ethyl biodiesel from canola oil or different pure ethyl esters obtained average deviationsof 2.6 %, for the firstand ranging from 2.7 to 12.5 %, for the last. Andreatta et al. (2008) and Andreatta et al. (2012), modeling systems containing glycerol + methyl oleate + methanol or ethanol, obtained average and maximum deviations, respectively, ranging from 0.004 to 0.006 and from 0.012 to 0.047 (system with methanol), and ranging from 0.001 to 0.004 and from 0.009 to 0.012 (system with ethanol) using a group contribution model with association equation of state (GCA-EOS). In these two last works, the same systems were modeled using a UNIFAC with association (A-UNIFAC) activity coefficient model, resulting on average and maximum deviations ranging from 0.005 to 0.007 and from 0.011 to 0.065 (system with methanol), and ranging from 0.001 to 0.0013 and from 0.002 to 0.036 (system with ethanol).

The use of NRTL and UNIQUAC has resulted in low deviations between experimental and calculated data. Lee et al. (2010), using NRTL and UNIQUAC in the modeling of systems containing glycerol + methanol + methyl oleate or methyl linoleate, obtained average deviations, respectively, ranging from 0.0075 to 0.0196 and from 0.0049 to 0.0071. Basso et al. (2012), in the modeling of system containing glycerol + ethanol + ethyl biodiesel from crambe oil, obtained average absolute deviations ranging from 0.53 to 0.99 %. Mesquita et al. (2011) used NRTL in modeling of systems containing glycerol + ethanol + ethyl biodiesel from soybean or from sunflower oil, resulting on deviations, respectively, ranging from 1.8 to 2.5 % and from 1.4 to 1.6 %.

The use of the NRTL and UNIQUAC models have resulted in properly description of these systems. At same time, UNIFAC (LLE or DRTM) are the most used models in design analysis and process simulation due their predictive capability, wide range of applicability and large amount of group interaction parameters. Moreover, these four

models are previously programmed in simulation software Aspen Plus which allow their ready use in a great variety of process analysis.

Despite of the previously studies, there are little data about LLE of real systems containing ethyl biodiesel + ethanol + glycerol. At same time, only one among the published studies in scientific literature (Basso et al, 2012) quantifies each individual fatty acid alkyl ester in both phases, which really proves the pseudo-component concept in relation to behavior of LLE of biodiesel and allows a deeply analysis of these multi-component systems by group contribution models without additional assumptions. Furthermore, despite of the importance of the settling step in biodiesel production due to the losses of biodiesel in the glycerol rich-phase and the contamination of biodiesel rich-phase with glycerol, comparisons between thermodynamic g^E models in the sensitivity analysis of this step in ethyl biodiesel production by simulation software are not found in scientific literature.

At this way, the objective of the present study was obtain LLE data for systems composed of glycerol (1) + ethanol (2) + fatty acid ethyl esters from macauba pulp oil (3) at 298.2 K, adjust parameters of the NRTL and UNIQUAC models and test the predictions for the LLE of the system based on UNIFAC-LLE and UNIFAC-Dortmund (UNIFAC-DRTM) models. Additionally, a sensitivity analysis was performed by varying the mass fraction of ethanol at the beginning of a hypothetical settling for a system containing glycerol and ethyl biodiesel from macauba pulp oil to test the influence of ethanol in excess in the biodiesel settling and how the LLE behavior of this system is affected according to the thermodynamic model used in simulation.

2. Methods

2.1. Experimental procedure

2.1.1. Material

Crude macauba pulp oil was graciously supplied by Paradigma Óleos Vegetais Ltda (Jaboticatubas/MG, Brazil). Prior to biodiesel production, the oil was homogenized and neutralized in the laboratory.

Glycerol (Sigma, > 0.99; water < 0.003), ethanol (Merk, > 0.999), methanol (Honeywell, 0.9999), anhydrous sodium hydroxide (Carlo Erba, > 0.97), ethyl myristate

(Tecnosyn, > 0.99) and glacial acetic acid (Ecibra> 0.997) were used in the diverse stages of this work with no further purification.

2.1.2. Biodiesel production

Biodiesel from macauba pulp oil was obtained by alkaline catalysis. Sodium hydroxide (1% in relation to vegetable oil weight) was dissolved, prior to reaction, in ethanol under vigorous agitation in a magnetic stirrer. The reagent molar ratio was 1:6 (oil:ethanol), considering the average molar mass of triacylglycerols in macauba pulp oil. The reaction was maintained for one hour under agitation at room temperature (approximately T/K = 298) before being stopped by the addition of glacial acetic acid.

This mixture was then transfer to a separatory funnel for glycerol decanting. Deionized water was used to wash the system at least five times for removal of residual soaps, glycerol and ethanol. The pH of the washing water was monitored with a phenylalanine alcoholic solution, and residual water was removed by filtration of the ester in sodium sulphate.

A distilled fatty acid ethyl ester mixture from macauba pulp oil (FAEE) was obtained by distillation under approximately P/mmHg = 2.25 and T/K = 508.15.

2.1.3. Liquid-liquid equilibrium experiments

LLE jacketed glass cells (about 50 cm^3), with one lower and one upper canal for sample removal, were used for determination of LLE data. Each component was weighted on a Precisa analytical balance, model XT 220A (Sweden), accurate to m/g = 0.0001. The mixtures were vigorously agitated for 20 min with a Cole Parmer magnetic stirrer, model n° 4817. All systems were left to rest for at least 12 h with temperature maintained at T/K = 298.2 using a Cole Parmer thermostatic bath, model 12101-55, (Chicago, USA) accurate to T/K = 0.1. Two clear layers and a well defined interface were formed when the systems reached the equilibrium state, where the upper layer was the ester-rich phase (EP) and the lower layer the glycerol-rich phase (GP).

2.1.4. Analytical methodology

Composition of the fatty acid ethyl esters mixture was determined using a Perkin Elmer gas chromatographic system, Clarus 600, FID detector, with an Agilent capillary column (crossbond, 50% cyanopropylphenyl – 50% dimethylpolysiloxane), length of 30 m,

internal diameter of 0.25 mm and film thickness of 0.25 μm, according to the methodology described by Basso et al. (2012).

Glycerol, fatty acid ethyl esters and ethanol where quantified by a minimum of three repetitions in each equilibrium phase by a Perkin Elmer gas chromatographic system, Clarus 600, FID detector, with an Agilent capillary column (crossbond, 50% cyanopropylphenyl – 50% dimethylpolysiloxane), length of 30 m, internal diameter of 0.25 mm and film thickness of 0.25 μm according to the methodology developed by Basso et al. (2012). Each component in the liquid-liquid equilibrium phases was quantified by a different calibration curve, using nine concentration levels of pure ethanol, eight concentration levels of ethyl myristate (as standard of ethyl ester class) and eleven concentration levels of pure glycerol. The higher combined uncertainty in relation to the three calibration curves was 0.0037.

2.2. Calculation approach

2.2.1. Calculation of deviations in mass balance

Validity of the LLE data was evaluated according to the procedure developed by Marcilla et al. (1995) and applied by Rodrigues et al. (2005). In this procedure, the sum of the calculated mass in both liquid phases is compared with the actual value for total mass used in the experiment. The mass balance of each component can be calculated according to equation (1).

$$M^{OC} w_i^{OC} = M^{GP} w_i^{GP} + M^{EP} w_i^{EP} \quad (1)$$

where i represents each component of the system; M^{OC} is the mass of the overall composition (initial mixture); M^{GP} and M^{EP} are the total masses of the glycerol-rich and ester-rich phases, respectively; w_i^{OC} is the mass fraction of component i in the initial mixture; and, w_i^{GP} and w_i^{EP} are the mass fractions of the component i, respectively, in the glycerol-rich and ester-rich phases.

When applying K equations related to K balances, the values of M^{GP} and M^{EP} can be calculated from the experimental mass fraction of component in both phases (w_i^{GP} and w_i^{EP}) by least square fitting. Considering M as the matrix formed by the values of $\mathrm{w_i^{oc}}$,

B as the transformation matrix formed by w_i^{GP} and w_i^{EP} and P as the matrix formed by the masses of the phases M^{GP} and M^{EP}, the system can be mathematically described as:

$$M = B \cdot P \tag{2}$$

Equation 2 can be transformed into the expression below:

$$P = (B^T B)^{-1} B^T M \tag{3}$$

where B^T is the transposed matrix of B and $(B^T B)^{-1}$ is the inverse matrix of $(B^T B)$.

Thus, the values of M^{GP} and M^{EP} which minimize the deviations of the system can be obtained, and the sum of M^{GP} and M^{EP} can be compared to M^{OC} to calculate the overall mass balance deviation by:

$$\delta(\%) = 100 \cdot \frac{|(M^{GP} + M^{EP}) - M^{OC}|}{M^{OC}} \tag{4}$$

The relative average deviation for the mass balance of each component is given by:

$$\delta_i(\%) = \sum_n^N \left[100 \cdot \frac{\left|\left(w_{i,n}^{GP} M^{GP} + w_{i,n}^{EP} M^{EP}\right) - w_{i,n}^{OC} M^{OC}\right|}{w_{i,n}^{OC} M^{OC}} \right] \tag{5}$$

where n is the tie line number and N is the total number of tie lines at each temperature.

Relative deviations in average molar mass of FAEE in the glycerol-rich and ester-rich phases in relation to average molar mass of the original biodiesel from macauba pulp oil was calculated according to equation 6:

$$d = 100 \cdot \frac{\left|\bar{M}^p - \bar{M}^{bm}\right|}{\bar{M}^{bm}} \tag{6}$$

where $\bar{M}^p$ is the average molar mass of the FAEE pseudo-component in the glycerol-rich or ester-rich phase and $\bar{M}^{bm}$is the average molar mass of the original biodiesel from macauba pulp oil.

2.2.2. Othmer - Tobias equation

In addition to the mass balance, the LLE of the systems was tested according to Othmer and Tobias (1942), equation 7.

$$log\frac{(1-w_1^{EP})}{w_1^{EP}} = a + b \cdot log\frac{(1-w_3^{GP})}{w_3^{GP}} \quad (7)$$

where w_1^{EP} is the glycerol mass fraction in the ester phase, w_3^{GP} is the FAEE mass fraction in the glycerol phase, a is the linear coefficient and b is the angular coefficient.

2.2.3. Modeling procedure

Modeling was performed using the simulation software AspenPlus (Aspen Technology). Average deviations between the experimental and calculated compositions in both phases were determined according to equation 8.

$$\Delta w = 100 \cdot \left\{ \frac{\left[\sum_n^N \sum_i^K \left(w_{i,n}^{GP,exp} - w_{i,n}^{GP,calc}\right)^2 + \left(w_{i,n}^{EP,exp} - w_{i,n}^{EP,calc}\right)^2\right]^{1/2}}{2NK} \right\} \quad (8)$$

2.2.3.1. NRTL and UNIQUAC modeling approaches

The experimental data measured were used to adjust all binary interaction parameters of the NRTL and UNIQUAC models. In relation to these thermodynamic models, the mixture of fatty acid ethyl esters was treated as a single ethyl ester with a molecular structure that presents the average molar mass of the ethyl ester mixture. In the pseudo-molecule structure assembling, the quantity of each group, taken according to UNIFAC groups, presents in each ethyl ester molecule, was weighted by its molar fraction and rounded to the closest integer number. This approach assumes that the mixture of different fatty acid ethyl esters behaves similarly in the systems. The validity of this approach, considering a mixture of ethyl esters from crambe oil as a pseudo-component, was proved by Basso et al. (2012) who obtained maximum deviation between the average molar mass of esters in both phases and the molar mass of the pseudo-component equal to 5.22%. Other authors used the pseudo-component approach in relation to vegetable oils, considering them as pseudo-components with an average molar mass of the triacylglycerol mixture (Rodrigues et al., 2005; Batista et al. 1999; Lanza et al., 2008).

The NRTL model, developed by Renon and Prausnitz (1968), is described as:

$$ln\gamma_i = \frac{\sum_j x_j \tau_{ji} G_{ji}}{\sum_k x_k G_{ki}} + \sum_j \frac{x_j G_{ij}}{\sum_k x_k G_{kj}} \tau_{ij} - \frac{\sum_m x_m \tau_{mj} G_{mj}}{\sum_k x_k G_{kj}} \quad (9)$$

$$G_{ij} = exp\,(-\alpha_{ij}\tau_{ij}) \quad (10)$$

$$\tau_{ij} = \frac{b_{ij}}{T} \quad (11)$$

$$\tau_{ii} = 0; G_{ii} = 0 \quad (12)$$

where γ_i is the activity coefficient of component i; x_i is the molar fraction of the component i in the mixture; G_{ij} is the NRTL parameter; τ_{ij} is the NRTL binary molecular energy interaction parameter; α_{ij} is the NRTL non-randomness binary interaction parameter; T is the absolute temperature; b_{ij} is the NRTL adjustable parameter; and i, j, k, m are components of the systems.

The UNIQUAC model, presented by Abrams and Prausnitz (1975), is represented by:

$$ln\gamma_i = ln\frac{\phi_i}{x_i} + \frac{z}{2} q_i ln\frac{\theta_i}{\phi_i} - q_i ln \sum_k \theta_k \tau_{ki} - \frac{q_i \sum_j \theta_j \tau_{ij}}{\sum_k \theta_k \tau_{kj}} + l_i + q_i - \frac{\phi_i}{x_i} \sum_j x_j l_j \quad (13)$$

$$\theta_i = \frac{q_i x}{\sum_k q_k x_k} \quad (14)$$

$$\phi_i = \frac{r_i x_i}{\sum_k r_k x_k} \quad (15)$$

$$l_i = \frac{z}{2}(r_i - q_i) + 1 - r_i \quad (16)$$

$$\tau_{ij} = exp\left(\frac{b_{ij}}{T}\right) \quad (17)$$

$$r_i = \sum_k v_k^i R_k; \;\; q_i = \sum_k v_k^i Q_k \quad (18)$$

where ϕ_i is the volume fraction of the component i; z is the coordination number (equal to 10); θ_i is the area fraction of component i; r_i is the volume parameter for component i; q_i is the surface area parameter for component i; $\tau_{ij}$is the UNIQUAC parameter; $b_{ij}$is the UNIQUAC adjustable parameter; R_k and Q_k are, respectively, the group volume parameter and the group area parameter calculated according to Bondi (1968).

2.2.3.2. UNIFAC modeling approach

The UNIFAC thermodynamic model was used to predict the LLE of the system. Structural molecular groups selected to represent the studied systems were "CH_3", "CH_2", "CH", "CH=CH", "CH_2COO" and "OH".

UNIFAC-LLE and UNIFAC-DRTM were used to test the prediction capability of LLE data. The model denoted as UNIFAC-LLE was presented by Fredenslund et al. (1975), and its binary interaction parameters for LLE were updated by Magnussen et al. (1981). The model denoted as UNIFAC-DRTM was presented by Weidlich and Gmehling (1987), and the binary interaction parameters for LLE used were updated by Gmehling et al. (2002).

All individual fatty acid ethyl esters were considered for UNIFAC modeling calculations. Thus, the systems were represented by glycerol, ethanol and six fatty acid ethyl esters. However, in ternary diagram representations the esters were grouped by the addition of each individual ester mass fraction, and the systems were graphically represented as a pseudo-ternary system containing glycerol (1) + ethanol (2) + FAEE (3).

The ternary diagrams were represented using the mass fractions obtained by the UNIFAC-LLE and UNIFAC-DRTM models to compare the different behavior of the LLE in relation to the parameters applied.

2.3. Sensitivity analysis

The sensitivity analysis was performed using the simulation software AspenPlus (Aspen Technology). Two molecular models, NRTL and UNIQUAC, with the respectively sets of regressed parameters, as well as two different predictive models, UNIFAC-LLE and UNIFAC-DRTM, were used in the process analysis. A fixed molar ratio of 1 (glycerol) to 3 (FAEE) in the feed stream (FS) was considered as the result for completely conversion of 1 mol of triacylglycerols from macauba oil into 1 mol of glycerol and 3 moles of fatty acid

ethyl esters. Thus, the effect of different excessive ethanol quantities at the end of the transesterification reaction in the biodiesel settling step was analyzed. At this way, the mass flow of ethanol in the FS was gradually increased up to the point that the system did not split in two different phases.

3. Results and discussions

Table 1 shows that the fatty acid ethyl ester mixture from macauba pulp oil contained more than 20% ethyl palmitate and 61% monounsaturated fatty acid ethyl esters, of which about 4% are ethyl ester from palmitoleic acid. The average molar mass of the FAEE as pseudo-component, calculated from this ethyl ester profile, was 303.29 M/(g·mol^{-1}) which was rounded to the pseudo-molecule with molar mass equal to 310.52 M/(g·mol^{-1}).

Table 1. Ethyl ester composition of FAEE.

fatty acid group in ethyl ester	Component	Molecular Formula	$\frac{M}{(g \cdot mol^{-1})}$	100w[a]
C16:0	Hexadecanoic acid, ethyl ester	$C_{18}H_{36}O_2$	284.48	20.78
C16:1	(Z)-9-Hexadecenoic acid, ethyl ester	$C_{18}H_{34}O_2$	282.46	3.97
C18:0	Octadecanoic acid, ethyl ester	$C_{20}H_{40}O_2$	312.53	2.79
C18:1	(Z)-9-Octadecenoic acid, ethyl ester	$C_{20}H_{38}O_2$	310.51	57.37
C18:2	(Z,Z)-9,12-Octadecadienoic acid, ethyl ester	$C_{20}H_{36}O_2$	308.50	14.13
C18:3	(Z,Z,Z)-9,12,15-Octadecatrienoic acid, ethyl ester	$C_{20}H_{34}O_2$	306.48	0.96
FAEE (pseudo-component)			303.29	

[a] ethyl ester mass fraction in FAEE

Each of the individual fatty acid ethyl ester compositions per tie line is shown in Table 2. The average molar mass of the ester mixtures in each phase of all systems was calculated. The deviation between each average molar mass and the molar mass of the pseudo-molecule were compared to verify the validity of representing the ester mixture for the entire system by this assumption. All deviations were similar, in the range from 1.60% to 2.85%, indicating that ethyl esters behave similarly in each phase of all systems. The low deviation in average molar mass of both phases indicates that representing FAEE as a pseudo-molecule can be applied to the systems in this study.

The linear, angular and linear correlation coefficients, a, b and R^2, obtained from Othmer and Tobias equation (equation 7) were 1.251, 0.334 and 0.9893, respectively. Approximation of R^2 to one indicates the good consistency of LLE experimental data.

Combined uncertainties from chromatographic analysis of the GP and EP were lower than 0.0146, indicating good accuracy of the analytical procedure. The maximum deviation in the mass balance per tie line, calculated according to equation 4, was 0.1452% (Table 3), demonstrating the good quality of the LLE experimental data. This result confirm the good linear correlation coefficient (R^2) obtained in equation 7.

Table 2. Individual fatty acid ethyl ester composition per tie line in each phase at T/K = 298.2[a].

Glycerol-rich phase							
$C_{18}H_{36}O_2$	$C_{18}H_{34}O_2$	$C_{20}H_{40}O_2$	$C_{20}H_{38}O_2$	$C_{20}H_{36}O_2$	$C_{20}H_{34}O_2$		δ[c]
$100w_k$	$100w_k$	$100w_k$	$100w_k$	$100w_k$	$100w_k$	$\mathrm{M}/(g \cdot mol^{-1})^b$	(%)
25.86	4.72	2.32	51.38	14.68	1.04	301.6727	2.85
22.91	5.37	1.81	52.74	15.98	1.19	302.2393	2.67
23.83	5.50	1.87	51.65	15.90	1.25	301.9518	2.76
17.57	6.78	1.40	53.97	18.80	1.48	303.1920	2.36
7.05	8.26	0.99	59.47	22.32	1.91	305.5332	1.60
16.53	7.42	1.34	55.24	17.16	2.31	303.2855	2.33

Ester-rich phase							
$C_{18}H_{36}O_2$	$C_{18}H_{34}O_2$	$C_{20}H_{40}O_2$	$C_{20}H_{38}O_2$	$C_{20}H_{36}O_2$	$C_{20}H_{34}O_2$		δ[c]
$100w_k$	$100w_k$	$100w_k$	$100w_k$	$100w_k$	$100w_k$	$\mathrm{M}/(g \cdot mol^{-1})^b$	(%)
20.97	3.80	2.68	57.79	13.90	0.86	303.2922	2.33
21.13	3.82	2.65	57.65	13.89	0.86	303.2392	2.34
21.42	3.85	2.62	57.36	13.90	0.85	303.2392	2.34
21.18	3.85	2.63	57.62	13.85	0.87	303.2195	2.35
21.44	3.85	2.64	57.22	13.98	0.87	303.1445	2.37
20.95	3.90	2.59	57.62	14.07	0.87	303.2625	2.34

[a] relative uncertainties u are u(T/K) = 0.1, combined u(w) = 0.0146; [b] average molar mass of pseudo-component biodiesel in each phase per tie line; [c] deviation between average molar mass of FAEE in phase and molar mass of pseudo-molecule.

Table 3. Liquid-liquid equilibrium data for pseudo-ternary system ethanol (1) + glycerol (2) + FAEE (3) at T/K = 298.[a]

Overal composition			Ester-rich phase			Glycerol-rich phase			
$100w_1$	$100w_2$	$100w_3$	$100w_1$	$100w_2$	$100w_3$	$100w_1$	$100w_2$	$100w_3$	δ (%)[b]
20.00	39.99	40.01	2.02	20.62	77.36	37.29	57.68	5.03	0.1320
25.00	35.00	40.00	1.71	16.55	81.74	47.30	50.49	2.21	0.1452
30.17	30.19	39.64	1.15	13.14	85.71	55.50	43.41	1.09	0.0483
35.14	24.95	39.91	0.77	10.38	88.85	63.57	36.12	0.31	0.1290
39.99	19.99	40.02	0.59	7.89	91.52	70.15	29.75	0.10	0.1246
45.21	14.94	39.85	0.41	5.58	94.01	78.07	21.89	0.04	0.0309

[a]relative uncertainties u are u(T/K) = 0.1, combined u(w) = 0.0146; [b]overall mass balance deviation according to equation 4.

The overall, ester-rich phase and glycerol-rich phase compositions of each tie line, considering the systems as pseudo-ternary, were presented in Table 3.The NRTL and UNIQUAC binary interaction parameters are showed in Table 4. Average deviations between experimental and calculated composition, obtained from equation 8, were 0.44% and 1.07% respectively to the NRTL and the UNIQUAC models. The NRTL model accurately described the LLE behavior of the systems. On the other hand, the UNIQUAC model does not show the same precision, although it can be used for description of the system in an appropriate way. This relative high deviation is mainly due to poor description of the tie line containing higher mass fraction of ethanol in the overall composition, close to the plait point, resulting in a relative high deviation of 2.32%.

Table 4. UNIQUAC and NRTL model binary interaction parameters of the systems containing glycerol + ethanol + FAEE.

	UNIQUAC		NRTL		
pair ij[a]	bij	bji	bij	bji	α (0)ij=α (0)ji
glycerol-ethanol	-765.6455	283.9823	-121.1653	410.6344	0.3529
glycerol-FAEE	-219.7569	-449.7753	5670.2749	1476.0039	0.1564
ethanol-FAEE	63.9871	-246.9285	660.7830	134.0654	0.7037

[a] component of binary interaction

LLE data calculated by the NRTL and the UNIQUAC models are similar in the glycerol-rich phase side for the region containing more than about 40% of glycerol, and in the region close to the bottom of the ternary diagram, where the calculated binodal curves almost overlap, as can be observed in Figure 1. At the region of binodal curves around the plait points, between about 40% of glycerol in the GP to 65% of ester in the EP, the

binodal curve calculated by the NRTL model showed a larger region of phase separation. The plait point calculated by the UNIQUAC model in relation to the plait point calculated by the NRTL model is slightly displaced to the region near the top of diagram, where the mass fraction of ethanol is high. Tie lines calculated by the NRTL model and the experimental data almost overlap, indicating an accurate description of the LLE for the system by the model and confirming the low deviations between experimental data and calculated compositions. The UNIQUAC model does not properly describe the two tie lines in region containing greater ethanol concentrations, although the other four calculated tie lines almost overlap the experimental data.

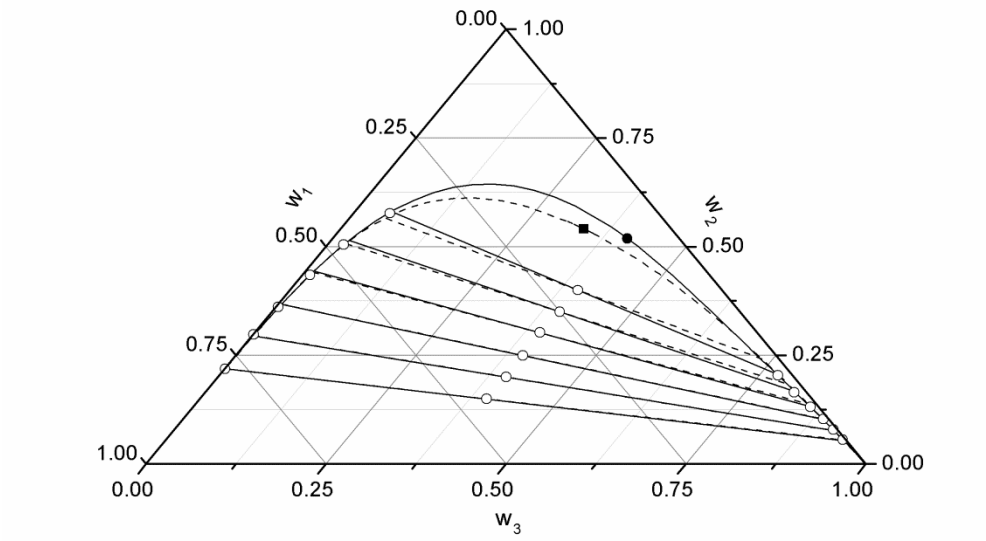

Figure 1. Liquid-Liquid equilibrium diagram of the system containing glycerol (1) + ethanol (2) + FAEE (3) at T/K = 298.2: (w) mass fraction of the component; (—) NRTL; (---) UNIQUAC; (●) NRTL plait point; (■) UNIQUAC plait point; (○) experimental data.

The UNIFAC-LLE and UNIFAC-DRTM models underestimated the ethanol mass fraction in the EP, however this effect was greater when using the first model. Similarly, the predictive models overestimated the ethanol mass fraction in the GP, especially in the region near the plait point. Thus the slope of the calculated tie lines was more accentuated than the slope of the experimental tie lines, according to Figure 2. These two models

underestimated the decrease in phase separation as a function of the increase in the ethanol mass fraction. At same time, UNIFAC models underestimated the glycerol content in ester rich-phase and underestimated the ester content in glycerol rich-phase at high ethanol mass fraction. Both models result in higher deviations between calculated and experimental tie lines in regions with increased ethanol concentrations. These deviations decreased gradually until the region near the bottom of the diagram where minor deviations values were observed. Average deviations between experimental and calculated mass fractions according to equation 8 were 3.52% and 2.82%, respectively, using the UNIFAC-LLE and UNIFAC-DRTM.

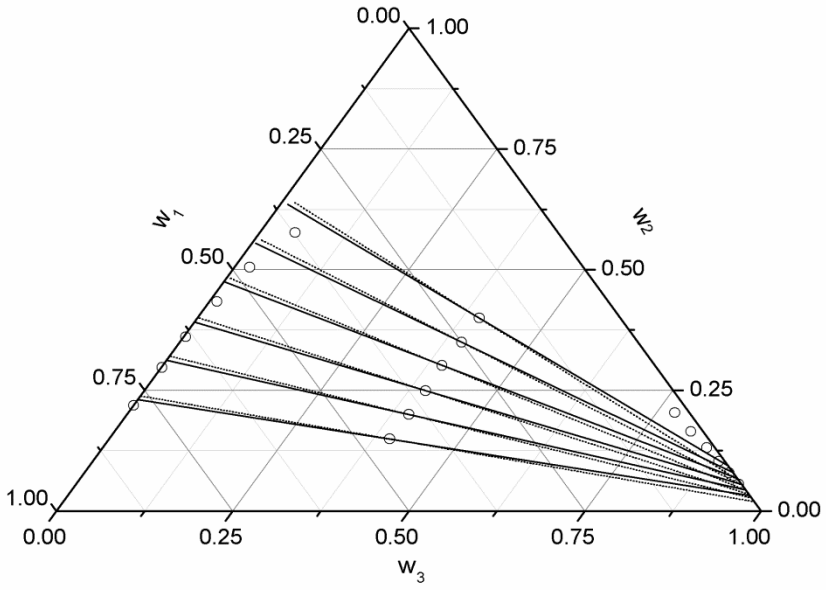

Figure 2. Liquid-Liquid equilibrium diagram of the system containing glycerol (1) + ethanol (2) + FAEE (3) at T/K = 298.2: (w) mass fraction of the component; (—) UNIFAC-DRTM; (···) UNIFAC-LLE; (○) experimental data.

Similar improperly description in LLE modeling of systems containing metanol, glicerol and methyl oleate was obtained by Barreau et al. (2010) using group contribution method combined with a statistical associating fluid theory equation of state (GC-PPC-SAFT). They reported an overestimated region of phase separation and an underestimated solubility of methyl ester in glycerol rich-phase.

In a hypothetical complete transesterification reaction initiated with 3 moles of excess ethanol, which is typical in alkaline catalyzed reactions the final stoichiometric molar ratio would be equal to 1 (glycerol) : 3 (ethanol) : 3 (FAEE), resulting in mass fractions respectively equal to 0.08 : 0.12 : 0.80. This composition may be considered as the FS of an ideal decanter during biodiesel settling. By simulating this biodiesel purification step using the simulator AspenPlus (Aspen Technology), the compositions of the glycerol-rich stream (GRS) and of the ester-rich stream (ERS), according to the thermodynamic model used, are presented in Table 5. The compositions obtained by the NRTL model, which resulted in minor deviations in relation to the experimental data, and the UNIQUAC model were similar for both streams. From these results, glycerol concentrations in the ERS are about 0.7%, greater than 0.02% which is the maximum level accepted according to biodiesel quality standards, indicating the need for additional purification of this phase for application as biodiesel fuel. On the other hand, based on the results obtained by the predictive models, the glycerol concentration in the ERS would be much lower, and according to the results of the UNIFAC-LLE, the ERS would exempt further purification with respect to glycerol removal for use as biodiesel fuel. In contrast, the UNIFAC-LLE model overestimates FAEE losses in the GRS.

Table 5. Stream compositions in the settling simulation, considering the feed stream molar composition 1 (glycerol) : 3 (ethanol) : 3 (FAEE), according to each thermodynamic model used.

Models	Glycerol-rich stream			Ester-rich stream		
	$100w_1$[a]	$100w_2$[a]	$100w_3$[a]	$100w_1$[a]	$100w_2$[a]	$100w_3$[a]
NRTL	65.53	34.13	0.34	0.74	9.31	89.95
UNIQUAC	65.48	34.18	0.34	0.71	9.29	90.00
UNIFAC-LLE	49.06	50.26	0.68	0.02	4.62	95.36
UNIFAC-DRTM	54.80	45.04	0.16	0.03	6.44	93.53

[a] w_1, w_2, w_3 are, respectively, mass fractions of glycerol, ethanol and FAEE.

In the sensitivity analyses, while the NRTL and UNIQUAC models determined a phase split up to, respectively, 43.4% and 39.6% of ethanol in the FS, the UNIFAC-LLE and UNIFAC-DRTM models determined phase separation up to, respectively, 77.1% and 74.0%. Figure 3 shows the two predictive models, compared to molecular models, underestimate FAEE losses in the GRS above 25% of ethanol in FS. The increasing of ethanol, from this level, results in higher differences between FAEE in GRS calculated by molecular and predictive models. The NRTL model indicated a greater FAEE mass

fraction in the GRS compared with the UNIQUAC model, where this difference increased as a function of the mass fraction of ethanol in the FS. As can be observed at Figure 4, considering the ERS composition, both NRTL and UNIQUAC models presented similar results up to about 30% of ethanol in the FS, where after this point the UNIQUAC model overestimates the glycerol mass fraction in the ERS. The UNIFAC-LLE and UNIFAC-DRTM models did not present accurate description of the composition of the ERS.

Behavior of the sensitivity analysis is in accordance with what was indicated by the ternary diagram. Considering that the NRTL model properly described the LLE behavior of the systems, this analysis indicated that use of the UNIFAC-LLE and UNIFAC-DRTM models in design analysis involving LLE for systems containing glycerol + ethanol + FAEE can cause severe errors in predicting stream compositions, and consequently in stream flows of biodiesel settling. It can be observed that during biodiesel purification, biodiesel settling should occur with a low mass fraction of ethanol to avoid FAEE losses in the GRS and diminish the glycerol content in the ERS. In processes that utilize large amounts of excess ethanol, such as acid catalysis or transesterification/esterification at high pressures, it is recommended that ethanol is partially or completely removed prior to the settling step.

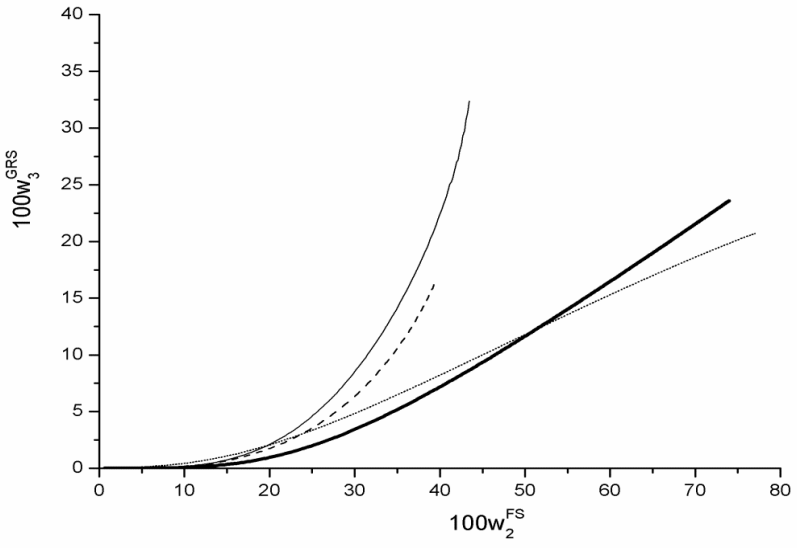

Figure 3. FAEE (3) concentration in the glycerol-rich stream (GRS) as a function of ethanol (2) in the feed stream (FS): (—) NRTL, (---) UNIQUAC, (···) UNIFAC-LLE, (━) UNIFAC-DRTM.

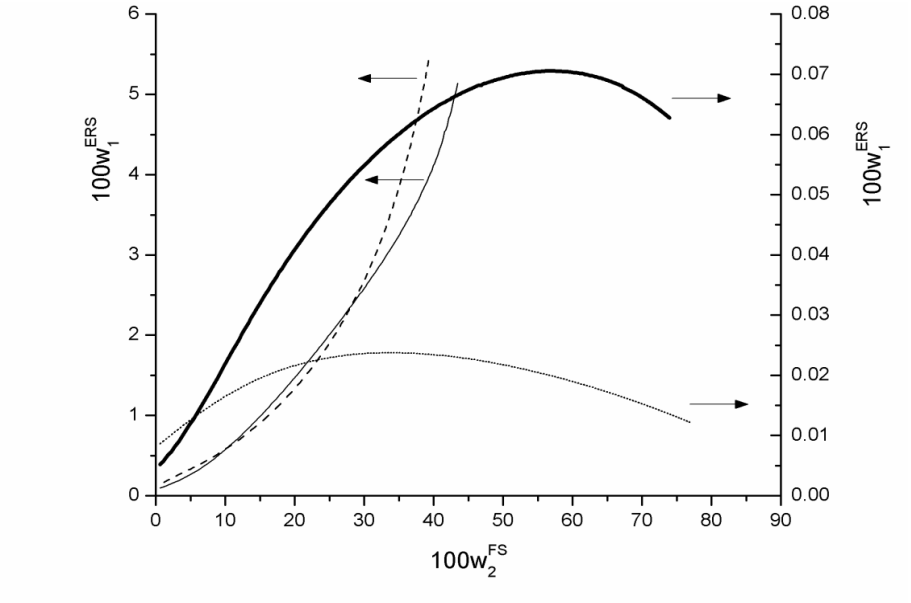

Figure 4. Glycerol (1) concentration in the ester-rich stream (ERS) as a function of ethanol (2) in the feed stream (FS): (—) NRTL, (---) UNIQUAC; (···) UNIFAC-LLE, (**━**) UNIFAC-DRTM.

4. Conclusions

Ethanol has greater affinity for the GP than the EP in LLE of systems containing glycerol + ethanol + FAEE from macauba pulp oil. Large quantities of ethanol in the systems hamper biodiesel purification by settling. The NRTL model represented more accurately the LLE of the system than the UNIQUAC model. The UNIFAC-LLE and UNIFAC-DRTM models, using the sets of parameters from literature, are not recommended to represent the LLE behavior of the system in study without further adjustment. LLE data and molecular thermodynamic models can be used to improve the biodiesel production process design.

Acknowledgement

The authors would like to acknowledge the Fundação de Amparo a Pesquisa do Estado de São Paulo (FAPESP – process number 08/56258-8) for its financial support, and the Conselho Nacional de Desenvolvimento Científico e Tecnológico (CNP_q – process number 140362/2009-6) for scholarship.

References

1. Abrams, D. S. Prausnitz, J. M., 1975. Statistical thermodynamics of liquid mixtures: a new expression for the excess gibbs energy of partly or completely miscible systems. AIChE J., 21, 116-128.

2. Andreatta, E. A., 2012. Liquid-liquid equilibria in ternary mixtures of methyl oleate + ethanol + glycerol at atmospheric pressure. Ind. Eng. Chem. Res., 51, 9642-9651.

3. Andreatta, E. A., Casás, L. M., Hegel, P., Bottini, S. B., Brignole, E. A., 2008. Phase equilibria in ternary mixtures of methyl oleate, glycerol, and methanol. Ind. Eng. Chem. Res., 47, 5157-5164.

4. Barreau, A., Brunella, I., de Hemptinne, J. C., Coupard, V., Canet, X., Rivollet, F., 2010. Measurements of liquid-liquid equilibria for a methanol + glycerol + methyl oleate system and prediction using group contribution statistical associating fluid theory. Ind. Eng. Chem. Res., 49, 5800-5807.

5. Basso, R.C., Meirelles, A.J.A., Batista, E.A.C. Liquid-liquid equilibrium of pseudoternary systems containing glycerol + ethanol + ethylic biodiesel from crambe oil (*Crambe abyssinica*) at T/K = (298.2, 318.2, 338.2) and thermodynamic modeling. Fluid Phase Equilib., 333, 55-62.

6. Batista, E., Monnerat, S., Kato, K., Stragevitch, L., Meirelles, A.J.A., 1999. Liquid-liquid equilibrium for systems of canola oil, oleic acid, and short-chain alcohols. J. Chem. Eng. Data, 44, 1360-1364.

7. Bondi, A., 1968. Physical Properties of Molecular Crystals, Liquids and Gases**,** Willey, New York.

8. Coimbra, M.C., Jorge, N., 2012. Fatty acids and bioactive compounds of the pulps and kernels of brazilian palm species, guariroba (Syagrus oleraces), jerivá (Syagrus romanzoffiana) and macaúba (Acrocomia aculeata). J. Sci. Food Agric., 92, 679-684.

9. Encinar, J.M., Gonzalez, J.F, Rodrigez, J.J., Tejedor, A., 2002. Biodiesel Fuels from Vegetable Oils: Transesterification of Cynara Cardunculus L. Oils with Ethanol. Energ. Fuel 16, 443-450.

10. Follegatti-Romero, L. A., Oliveira, M. B., Batista, F. R. M., Batista, E. A. C., Coutinho, J. A. P., 2012. Liquid-liquid equilibria for ternary systems containing ethyl esters, ethanol and glycerol at 323.15 and 353.15 K. Fuel, 94, 386-394.

11. Fredenslund, A., Jones, R. L., Prausnitz, J. M., 1975. Group-contribution estimation of activity coefficients in nonideal liquid mixtures. AIChE J., 21, 1086-1099.

12. Gmehling, J., Witting, R., Lohmann, J., Joh, R., 2002. A modified UNIFAC (Dortmund) Model. 4. Revision and Extension. Ind. Eng. Chem. Res., 41, 1678-1688.

13. Kanitkar, A., Balasubramanian, S., Lima, M., Boldor, D., 2011. A critical comparison of methyl and ethyl esters production from soybean and rice bran oil in the presence of microwaves. Bioresource Technol., 102, 7896-7902.

14. Knothe, G., Dunn, R.O., 2009. A comprehensive Evaluation of the Melting Points of Fatty Acids and Esters Determined by Differential Scanning Calorimetry. J. Am. Oil Chem. Soc., 86, 843-856.

15. Knothe, G., Steidley, K.R., 2007. Kinematic Viscosity of Biodiesel Components (fatty acid alkyl esters) and Related Compounds at Low Temperatures. Fuel, 86, 2560-2567.

16. Knothe, G., VanGerpen, J., Khrahl, J., 2005. The Biodiesel Handbook, AOCS Press, Champaign, Illimois.

17. Lanza, M., Borges-Neto, W., Batista, E.A.C., Poppi, R. J., Meirelles, A. J. A., 2008. Liquid-liquid equilibrium data for reactional systems of ethanolysis at 298.2 K. J. Chem. Eng. Data, 53, 5-15.

18. Lee, M. J., Lo, Y. C., Lin, H. M., 2010. Liquid-liquid equilibria for mixtures containing water, methanol, fatty acid methyl esters, and glycerol. Fluid Phase Equilib., 299, 180-190.

19. Magnussen, T., Rasmussen, P., Fredenslund, A., 1981. UNIFAC parameter table for prediction of liquid-liquid equilibrium. Ind. Eng. Chem. Process Des. Dev., 20, 331-339.

20. Marchetti, J.M., Miguel, V.U., Errazu, A.F., 2007. Possible Methods for Biodiesel Production. Renew. Sust. Energ. Rev. 11, 1300-1311.

21. Marcilla, A., Ruiz, F., Garcia, A.N., 1995. Liquid-liquid-solid equilibria of the quaternary system water – ethanol – acetone – sodium chloride at 25 °C. Fluid Phase Equilib., 112, 273-289.

22. Mesquita, F. M. R., Feitosa, F. X., Sombra, N. E., Santiago-Aguiar, R. S., de Sant'Ana, H. B., 2011. Liquid-liquid equilibrium for ternary mixtures of biodiesel (Soybean or Sunflower) + Glycerol + Ethanol at different temperatures. J. Chem. Eng. Data, 56, 4061-4067.

23. Moser, B.R., 2009. Biodiesel production, properties, and feedstocks. In Vitro Cell. Dev. Biol. – Plant. 45, 229-266.

24. Oliveira, M. B., Barbedo, S., Solleti, J. L., Carvalho, S. H. V., Queimada, A. J., Coutinho, J. A. P., 2011. Liquid-liquid equilibria for the canola oil biodiesel + ethanol + glycerol system. Fuel, 90, 2738-2745.

25. Othmer, D.F., Tobias, P.E., 1942. Tie Line Correlation. Ind. Eng. Chem., 34, 693 – 696.

26. Renon, H., Prausnitz, J. M., 1968. Local compositions in thermodynamic excess functions for liquid mixtures. AIChE J., 14, 135-144.

27. Rodrigues, C. E. C.; Silva, F. A.; Marsaioli, A., Jr.; Meirelle, A. J. A., 2005. Deacidification of Brazil Nut and Macadamia Nuts Oil by Solvent Extraction: Liquid-Liquid Data at 298.2 K. J. Chem. Eng. Data., 50, 517-523.

28. Sawangkeaw, R., Teeravitud, S., Bunyakiat, K., Ngamprasertsith, S., 2011. Biofuel production from palm oil with supercritical alcohols: Effects of the alcohol to oil molar ratios on the biofuel chemical composition and properties. Bioresource Technol., 102, 10704 – 10710.

29. Stamenkovic, O.S., Velickovic, A.V., Veljkovic V. B., 2011. The Production of biodiesel from vegetable oils by ethanolysis: Current state and perspectives. Fuel, 90, 3141-3155.

30. Valle, P., Velez, A., Hegel, P., Mabe, G., Brignole, E. A., 2010. Biodiesel production using supercritical alcohos with a non-edible vegetable oil in a batch reactor. J. Supercrit. Fluids, 54, 61-70.

31. Weidlich, U., Gmehling, J., 1987. A modified UNIFAC Model. 1. Prediction of VLE, h^E, and γ^{∞}. Ind. Eng. Chem. Res., 26, 1372-1381.

32. Yuan, W., Hansen, A.C., Zhang, Q., 2009. Predicting the Temperature Dependent Viscosity of Biodiesel Fuels. Fuel, 88, 1120-1126.

33. Zhang, H., Ding, J., Qiu; Yanli, Q., Zhao, Z., 2012. Kinectics of esterification of acidified oil with different alcohols by a cation ion-exchange resin/polyethersulfone hybrid catalytic membrane. Bioresource Technol., 112, 28-33.

Capítulo 6. Experimental Data, NRTL Thermodynamic Modeling and Sensitivity Analysis in the Purification Steps of Ethyl Biodiesel Production from Fodder Radish Oil

Rodrigo Corrêa Basso, Antonio José de Almeida Meirelles, Eduardo Augusto Caldas Batista

Trabalho a ser submetido ao periódico **Bioresource Technology**.

Abstract

The goals of this work were to present liquid-liquid equilibrium data of the system containing glycerol + ethanol + ethyl biodiesel from fodder radish oil; adjust binary parameters of the NRTL model based on thermodynamic modeling of this system and simulate different mixer/settler flowsheets in the biodiesel purification steps. In thermodynamic modeling, the deviation between experimental data and calculated values was 0.97%. After the transesterification reaction, with 3 mols of excess ethanol, the glycerol mass fraction in the ester-rich phase is 0.06% after the separation of the glycerol-rich phase. Removal of ethanol and glycerol from biodiesel to the level required for the biodiesel standard requirement can be performed using two sets of countercurrent mixer/settler, using 0.27% of water in relation to ester content in the feed stream.

Keywords

Biodiesel; Liquid-Liquid Equilibrium; NRTL; Themodynamic Model; Biodiesel Purification; Fodder Radish Oil

1. Introduction

The chemical transformation of lipid feedstock to biodiesel involves the transesterification of glyceride species with alcohol to alkyl esters (Lotero et al., 2005). This is an equilibrium reaction in which the presence of a catalyst, typically a strong acid or base, considerably accelerates adjustment of the equilibrium, and in order to achieve a high either yield, the alcohol is used in excess (Schuchardt et al., 1998). Even though transesterification is feasible using homogeneous base-catalysts, this process has some limitations that translate into high biodiesel production costs. Some technical requirements in this type of process include the demand for lipid feedstocks with low free fatty acids, since these compounds react with metal hydroxides forming soaps, and low water content in the system, because this substance causes hydrolysis of alkyl ester into free fatty acids (Lotero et al., 2005). Alternatives to this process are acid catalysis and alcohols in supercritical conditions, that use high molar alcohol:oil ratios ranging from 12:1 to 50:1 (Sawangkeaw et al., 2011; Zhang et al., 2003), instead of 6:1 used in the traditional alkaline reaction.

Ethyl biodiesel is produced in countries were ethanol is readily available. Despite its elevated price in relation to methanol, the advantages of using ethanol in biodiesel

production include higher miscibility with vegetable oils that allows better contact in the reaction step and lower toxicity. In addition, the use of ethanol in biodiesel synthesis is appealing because it is produced from biorenewable sources, resulting in a completely agricultural-based fuel obtained by ethanolysis (Encinar et al., 2002; Stamenkovic et al., 2011). Based on this point of view, in recent years several different technologies have been considered to optimize ethyl biodiesel production (Valle et al., 2010; Kanitkar et al., 2011; Zhang et al., 2012).

Fodder radish (*Raphanus sativus*) has excellent ability to recycle soil micronutrients, has rapid plant growth (150 – 200 days), low agronomic nutrient demands and low cultivation cost per hectare. Its oil has a heterogeneous fatty acid profile, containing about 60% monounsaturated acid, (mainly oleic acid, gadoleic acid and erucic acid), 18% linoleic acid and 12.5% linolenic acid as its main fatty acid components. The chemical composition, its agricultural characteristics and its ester physical properties make this oil an interesting alternative to biodiesel production (Valle et al., 2010; Domingos et al., 2008; Crusciol et al., 2005).

After the transesterification reaction, glycerol is separated by settling or centrifuging, forming two different phases, an ester-rich phase (EP) and a glycerol-rich phase (GP). Considering a typical alkaline catalysis, using 3 moles of excess ethanol in the reaction and an ideal settling, the EP has a very low glycerol content, about 0.7 % (Basso et al., 2012; Basso et al. 2013a), due to the low solubility between glycerol and ethyl esters. Similarly, studying catalyst distribution between the GP and EP with methanol in the system, Chiu et al. (2005) measured a very low mass fraction of potassium hydroxide in the EP, lower than 0.00061 when in equilibrium with the GP. In the sequence of this separation step, EP is purified before being used as a biofuel (Atadashi et al., 2011; Berrios and Skelton, 2008). The biodiesel standard requirement for the final content of the three major compounds related to the biodiesel synthesis and purification, glycerol, alcohol and water, are 0.02%, 0.2% and 0.05%, respectively.

Water washing is very effective in removing contaminants from biodiesel in purification steps due to the high solubility of a set of compounds in this solvent. This process can reduce alcohol and residual free glycerol levels down to biodiesel standard quality requirements and can be efficiently carried out at ambient temperature, because this is the most economical condition for biodiesel purification (Atadashi et al., 2011;

Berrios and Skelton, 2008). Glisic and Skala (2009), studying design and optimization of the purification procedure for biodiesel washing, it was observed that for complete removal of NaOH from the EP, a multistep water washing must be used. In this step of the biodiesel production process, two immiscible phases are formed, one EP and one water-rich phase (WP), where the alcohol distributes in both phases. The design analysis of this step must be judiciously performed since based on the observations of Basso et al. (2013b) there is a phase inversion in which WP is found in the upper phase and EP in the lower phase, depending on the amount of ethanol in the system.

The knowledge of liquid-liquid equilibrium in systems containing the major compounds involved in the purification steps of biodiesel synthesis (glycerol, ethanol, biodiesel and water) is essential for proper design analysis and simulation of these steps. Thus, some research groups have evaluated the LLE of systems containing alcohol, biodiesel or alkyl esters, glycerol or water (Liu et al., 2008), modeled them using thermodynamic models with associating parameters (Barreau et al., 2010; Oliveira et al., 2011; Andreatta et al., 2008) or using classical thermodynamic molecular models like NRTL (Mesquita et al., 2011) and UNIQUAC (Mazzutti et al., 2013). In addition, some works compare molecular models with predictive models in relation to description of the LLE for this type of system (Lee et al., 2010).

Despite the convenience in use and wide range of applicability, description of equilibrium behavior for systems containing the major compounds present in the biodiesel purification step by predictive models (UNIFAC-LLE and UNIFAC-Dortmund) must be judiciously evaluated due the high deviations obtained when compared to the molecular models with adjusted parameters (Basso et al., 2012; Basso et al., 2013a).

Notwithstanding the rise in this type of LLE experimental data, there is little data on systems containing ethyl biodiesels with long chain esters, and only two works in scientific literature have quantified each individual fatty acid alkyl ester in both phases (Basso et al., 2012; Basso et al., 2013a), which really proves the pseudo-component concept in relation to behavior of the LLE for biodiesel and allows for a deeply analysis of these multi-component systems by group contribution models without additional assumptions. Furthermore, there is a lack of studies simulating the biodiesel purification steps using only adjusted parameters, which allows for much more reliable results. The sensitivity analysis is an adequate method for exploring the impact of different feed

streams which occurs in biodiesel production since many different feedstock and catalysis type can be used in the same plant, but it has not been used in the settling and washing steps of ethyl biodiesel production in previously works.

Therefore, this work presents original LLE data of a system composed of glycerol + ethanol + fatty acid ethyl esters (FAEE) from fodder radish oil at 298.2 K, including the individual distribution of each ethyl ester, adjust and/or readjust parameters of the NRTL model related to major compounds present in this biodiesel purification, and results from a set of sensitivity analyses, considering three different flowsheets the sets of mixer/settlers, in the simulation of settling and water washing steps for production of this biodiesel using only NRTL adjusted parameters.

2. Methods

2.1. Experimental procedure

2.1.1. Material

Seeds of fodder radish were supplied by Sementes Pirai (Piracicaba, SP, Brazil). The crude fodder radish oil was extracted, using a pilot expeller, and filtered for the removing of fibers from the seeds.

Crude oil was neutralized with a sodium hydroxide solution prior to biodiesel production.

Glycerol (Sigma, > 0.99; water < 0.003), ethanol (Merk, > 0.999), methanol (J. T. Baker, 0.999), anhydrous sodium hydroxide (Carlo Erba, > 0.97), ethyl myristate (Tecnosyn, > 0.99) and glacial acetic acid (Ecibra, > 0.997) were used in the diverse stages of this work with no further purification.

2.1.2. Biodiesel production

The biodiesel was produced as described in detail by Basso et al (2012).

Biodiesel from fodder radish oil was obtained by alkaline catalysis with sodium hydroxide dissolved, prior to reaction, in ethanol. The reagent molar ratio was 1:6 (oil:ethanol), and the reaction was maintained for one hour under agitation at room temperature (approximately T/K = 298).

Deionized water was used to wash the system at least five times for removal of residual soaps, glycerol and ethanol. A distilled fatty acid ethyl ester mixture from fodder radish oil (FAEE) was obtained by distillation under approximately P/mmHg = 2.25 and T/K = 508.15.

2.1.3. LLE Experiments

LLE data of the systems were determined using sealed headspace glass tubes (20 mL) (Perkin Elmer). Components were weighted on an analytical balance Adam Equipment, model AAA160L (+/- 0.0001 g). The tubes were vigorously stirred using a vortex (Phoenix, model AP56) and then centrifuged (Centrifuge Jouan, model BR4i) for 300 s at 4000 rpm and room temperature. All systems were left to rest for at least 12 h with temperature controlled in a thermostatic bath Paar Physica, model Physica VT2 (*T/K* +/- 0.2). Two clear layers and a well defined interface were formed when the systems reached the equilibrium state, the upper layer being the EP, and the lower layer the GP.

2.1.4. Analytical Methodology

Ethyl biodiesel from fodder radish oil was previously characterize in triplicate with respect to the fatty acid ethyl ester profile by a Perkin Elmer gas chromatographic system, Clarus 600, FID detector, with a Agilent capillary column (crossbond, 50 % cyanopropylphenyl – 50 % dimethylpolysiloxane), length of 30 m, internal diameter of 0.25 mm and film thickness of 0.25 µm, using the analytical conditions described by Basso et al. (2012).

Quantification of glycerol, individual fatty acid ethyl esters and ethanol in each equilibrium phase were determined in at least triplicate by a Perkin Elmer gas chromatographic system, Clarus 600, FID detector, with an Agilent capillary column (crossbond, 50 % cyanopropylphenyl – 50 % dimethylpolysiloxane), length of 30 m, internal diameter of 0.25 mm and film thickness of 0.25 µm), based on the methodology described by Basso et al. (2012). Each component in the liquid - liquid equilibrium phases was quantified by a different calibration curve, using nine concentration levels of pure ethanol and eight concentration levels of ethyl myristate (as standard of ethyl ester class) and pure glycerol.

2.2. Calculation Approach

2.2.1. Calculations of Deviations in the Mass Balance of the Phases

Validity of the equilibrium experiments was evaluated according to the procedure developed by Marcilla et al. (1995) and applied by Rodrigues et al. (2005). In this procedure the sum of the calculated masses of both liquid phases is compared with the actual value for total mass used in the experiment. In this approach, independent component balances, totaling K balances, can be performed according to equation 1:

$$M^{OC} w_i^{OC} = M^{EP} w_i^{EP} + M^{GP} w_i^{GP} \quad (1)$$

where *i* represents each component of the system; M^{OC} is the mass of the overall composition; M^{GP} and M^{EP} are the total masses of the GP and EP, respectively; w_i^{OC} is the mass fraction of component i in the overall composition; and w_i^{GP} and w_i^{EP} are the mass fractions of component i, respectively, in the GP and EP. Applying these K equations, the values of M^{GP} and M^{EP} can be calculated from the experimental mass fraction of each component in both phases by least squares fitting. If *M* is the matrix formed by the values of w_i^{oc}, *B* is the transformation matrix formed by w_i^{GP} and w_i^{EP}, and *P* is the matrix composed of the masses of the phases, $M^{GP}$and M^{EP}; the system can be mathematically described as:

$$M = B \cdot P \quad (2)$$

Calculations allow for transformation of equation 2 into the expression below:

$$P = (B^T B)^{-1} B^T M \quad (3)$$

where B^T is the transposed matrix of *B* and $(B^T B)^{-1}$ is the inverse matrix of ($B^T B$). Thus, the values for $M^{GP}$and M^{EP} which minimize the deviations of the system can be found. The sum of $M^{GP}$and M^{EP} can be compared to M^{OC} and the overall mass balance deviation calculated by:

$$\delta(\%) = 100 \cdot \frac{|(M^{GP} + M^{EP}) - M^{OC}|}{M^{OC}} \quad (4)$$

2.2.2. NRTL Thermodynamic Modeling

The experimental data measured for the system glycerol (1) + ethanol (2) + FAEE from fodder radish oil (3) presented in this work and the experimental data presented by Basso et al. (2013b) for the system water (4) + ethanol (2) + FAEE from fodder radish oil (3), were used to adjust/readjust binary interaction parameters for the NRTL model. The mixture of fatty acid ethyl esters was treated as a single ethyl ester with a molecular structure that presents the average molar mass of the ethyl ester mixture. In the hypothetical molecule structure assembling, the quantity of each group, obtained according to UNIFAC groups present in each ethyl ester molecule, was weighted by its molar fraction and rounded to the closest integer number. This approach assumes that the mixture of different fatty acid ethyl esters behaves similarly in the systems under study. Therefore, the mixture of ethyl esters has been replaced by a pseudo-component with the corresponding average physical-chemical properties. The validity of this approach, considering a mixture of ethyl esters as a pseudo-component, was proved by Basso et al. (2012) and by Basso et al. (2013a) who evaluated other similar systems with different ethyl biodiesels; they obtained maximum deviation between the average molar mass of esters in both phases and the molar mass of the pseudo-component equal to 5.22% and 2.85%, respectively. Thus, adjustments were made considering the systems as pseudo-ternary. All binary interaction parameters were adjusted to the experimental data.

The mass fraction (w) was used as a composition unit due to the difference in molar masses of the system components, according to Oishi and Prausnitz (1978). In this way, the isoactivity criterion of the LLE developed on a molar fraction basis can be expressed in a mass fraction basis as:

$$(\gamma_i x_i)^I = (\gamma_i x_i)^{II} \tag{5}$$

$$(\gamma_i^w w_i)^I = (\gamma_i^w w_i)^{II} \tag{6}$$

where:

$$\gamma_i^w = \frac{\gamma_i}{M_i \sum_j^K {w_j}/{M_j}} \tag{7}$$

where x_i is the molar fraction of component i; γ_i is the activity coefficient of component i; γ_i^w is the corresponding activity coefficient expressed on the mass fraction scale; and w_i and M_i are the mass fraction and molar mass, respectively, of component *i*.

Estimation of the NRTL parameters was obtained by an algorithm developed in the FORTRAN programming language. This algorithm uses the modified simplex method applied to the objective function of composition (equation 8) to estimate thermodynamic parameters. The procedure for calculation of parameters involves flash calculations for the midpoint composition of the experimental tie lines, according to the procedure developed by Stragevitch and d'Avila (1997).

$$OF_w = \sum_m^D \sum_n^N \sum_i^{K-1} \left[\left(\frac{w_{i,n,m}^{I,exp} - w_{i,n,m}^{I,calc}}{\sigma_{w_{i,n,m}^I}} \right)^2 + \left(\frac{w_{i,n,m}^{II,exp} - w_{i,n,m}^{II,calc}}{\sigma_{w_{i,n,m}^{II}}} \right)^2 \right] \tag{8}$$

where *D* is the is the total number of data systems; *N* is the total number of tie lines; *K* is the total number of components in the data system; *w* is the mass fraction; subscripts *i*, *n* and *m* are the component, tie line and system number, respectively; exp and calc represent, respectively, the experimental and calculated composition; and σ is the standard deviation observed for the composition of each phase.

The average deviations between the experimental and calculated compositions in both phases were calculated according to equation 9.

$$\Delta = 100 \cdot \left\{ \frac{\sum_n^N \sum_i^K \left[\left(w_{i,n}^{I,exp} - w_{i,n}^{I,calc} \right)^2 + \left(w_{i,n}^{II,exp} - w_{i,n}^{II,calc} \right)^2 \right]}{2NK} \right\}^{1/2} \tag{9}$$

2.2.3. Simulation and Sensitivity analysis

In the simulation of sensitivity analysis only NRTL binary interaction parameters obtained from experimental data were used. Considering the components glycerol (1),

ethanol (2), FAEE from fodder radish oil (3) and water (4), the NRTL binary parameters for component pairs (12), (13) and (23) were obtained from experimental data presented in this work; the NRTL binary parameters for component pairs (24) and (34) were readjusted in this work from data presented by Basso et al. (2013b); the NRTL binary parameters for component pair (14) were obtained by Krishna et al. (1989).

The sensitivity analysis was performed using the simulation software AspenPlus (Aspen Technology), always considering a final stoichiometric ratio between glycerol:FAEE of 1:3. In that analysis three different flowsheets for biodiesel water washing were simulated, as showed in Figure 1. In all simulations, the first settler (SET-A) was dedicated to glycerol-rich stream separation, a common step to the three propositions. In the first proposition, the biodiesel washing step is composed only by one mixer/settler unity, MIX-B and SET-B in Flowsheet I. In the second proposition, one more mixer/settler unity (MIX-C and SET-C) was added to the biodiesel washing step, resulting in a purification system with two pure water streams in crosscurrent flow (Flowsheet II). In the last, two mixer/settler unities are utilized in a countercurrent arrangement with the pure water stream (WTR-C) fed in mixer C (MIX-C).

Components i = 1, 2, 3 and 4 correspond, in this order, to glycerol, ethanol, FAEE and water. In the acronyms representation, M_i^{stx} and w_i^{stx} are, respectively, the mass flow and mass fraction of component i in stream x, with the streams named according to Figure 1. The water requirements for biodiesel purification were always presented as a ratio to FAEE in the feed stream (M_{water}/M_3^{FEED}) since this stream was never changed in the different simulations performed, which allows for a constant reference value.

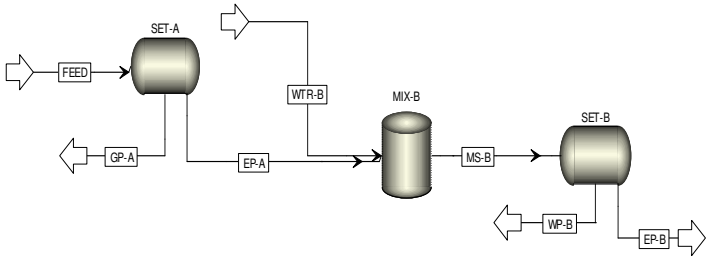

Flowsheet I

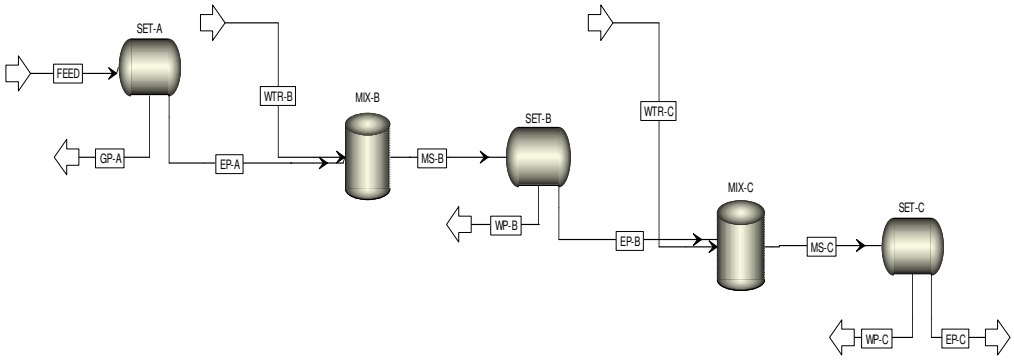

Flowsheet II

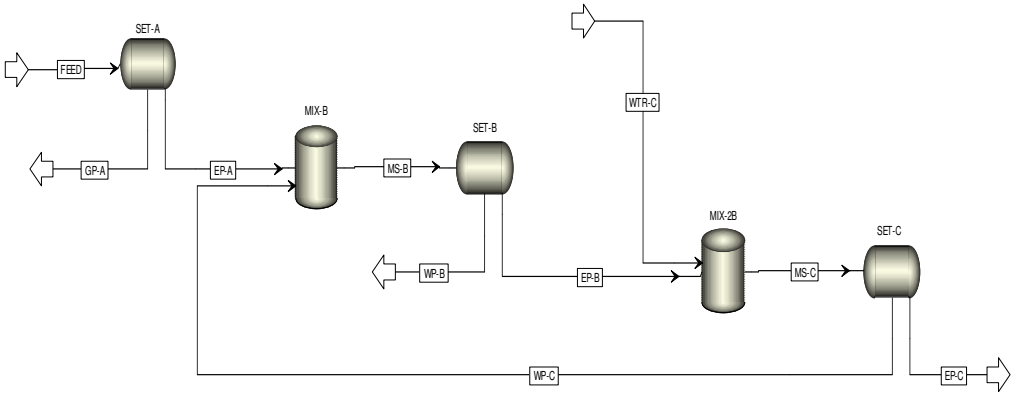

Flowsheet III

Figure 1. Flowsheets of Biodiesel Purification Steps: (FEED) products from transesterification reaction; (SET-A) settler for the glycerol-rich phase separation; (SET/MIX – B or C) settler/ mixer unity for biodiesel water washing; (EP) ester-rich phase; (GP) glycerol-rich phase; (WTR) pure water streams.

In flowsheet (I), two different processes were simulated. In the glycerol separation step, performed in the SET-A unity, the composition of ethanol and glycerol in the ester-rich stream, respectively, w_2^{EP-A} and w_1^{EP-A} were evaluated as a function of different mass fractions of excess ethanol in the feed stream (w_2^{FEED}). In addition, using only one water washing stage, the water mass flow requirement in the stream WTR-B (M_{WTR-B}/M_3^{FEED}) to obtain an ethanol mass fraction in the stream EP-B (w_2^{EP-B}) lower than 0.002 (biodiesel standard requirements) was evaluated until w_2^{FEED} was equal to 0.12, a value correspondent to 3 mols of excess ethanol from a previous hypothetical transesterification reaction.

In flowsheet (II), taking in to account a two step crosscurrent water washing process and 3 mols of excess ethanol from the transesterification reaction, the water mass flow requirement in stream WTR-C was evaluated as a function of the water mass flow requirement in stream WTR-B to obtain w_2^{EP-C} lower than 0.002. Similarly, the total water mass flow, given by the sum of water mass flows in streams WTR-B and WTR-C, was evaluated as a function of M_{WTR-B}/M_3^{FEED} to achieve w_2^{EP-C} lower than 0.002, so as to determine the minimum water requirement for biodiesel purification.

In flowsheet (III), considering a countecurrent biodiesel water washing process, the water requirement in stream WTR-C to obtain w_2^{EP-C} lower than 0.002 was evaluated as a function of different ethanol contents in the FEED stream until w_2^{FEED} was equal to 0.12, so as to quantify the water required for removing different quantities of ethanol until reaching the biodiesel standard requirement. Additionally, decreases to the ethanol mass fraction in stream EP-C (w_2^{EP-C}) as a function of $M_{WTR}/M_3^{(FEED)}$ was evaluated to estimate how different water contents added to the process affect ethanol removal from the system under study.

3. Results and discussions

Biodiesel from fodder radish oil is characterized by ethyl oleate as the mainly ester and large quantities of, ethyl linoleate, ethyl linolenate, eicosenoic acid ethyl ester and ethyl erucate, as shown in Table1. Its composition is very heterogeneous, containing ethyl esters with up to eight carbon atoms of difference and presenting more than 70% of saturated or monounsaturated esters, which permits for a biodiesel with proper oxidative stability. From this composition, the average molar mass of FAEE from fodder radish oil

was 316.63 $M/(g \cdot mol^{-1})$ and rounded to the hypothetical molecule with molar mass of 310.52 $M/(g \cdot mol^{-1})$.

Table 2 shows the individual ethyl ester composition in each phase per tie line. The maximum deviation between the average molar mass of FAEE per tie line and the hypothetical molecule molar mass was 1.46%, lower than that obtained by Basso et al. (2012) and Basso et al. (2013a) who studied similar systems containing FAEE from macauba pulp and crambe oil, respectively. This lower deviation indicates adequacy of the pseudo-component for this system, since there was not a considerable difference in the individual distribution of ethyl esters between GP and EP.

Table 1. Ethyl ester composition of biodiesel from fodder radish oil in mass percentage.

fatty acid in ethyl ester	molecular formula	common name	$M/(g \cdot mol^{-1})$	100w [a]
C16:0	$C_{18}H_{36}O_2$	ethyl palmitate	284.48	5.47
C18:0	$C_{20}H_{40}O_2$	ethyl stearate	312.53	2.48
C18:1	$C_{20}H_{38}O_2$	ethyl oleate	310.51	40.89
C18:2	$C_{20}H_{36}O_2$	ethyl linoleate	308.50	16.89
C18:3	$C_{20}H_{34}O_2$	ethyl linolenate	306.48	11.99
C20:0	$C_{22}H_{44}O_2$	ethyl arachidate	340.58	0.87
C20:1	$C_{22}H_{42}O_2$	eicosenoic acid ethyl ester	338.57	10.13
C22:1	$C_{24}H_{46}O_2$	ethyl erucate	366.62	10.59
C24:1	$C_{26}H_{50}O_2$	ethyl nervonate	394.67	0.69

[a] mass fraction of ethyl ester

The liquid-liquid equilibrium data for the pseudo-ternary system glycerol (1) + ethanol (2) + FAEE from fodder radish oil (3) is shown in Table 3. The maximum deviation in mass balance per tie line is 0.45%, with average deviation equal to 0.19%, indicating the good quality of experimental data.

The adjusted/readjusted NRTL parameters used in all simulations are presented in Table 4. NRTL interaction parameters for the components water and glycerol were obtained directly from literature (Krishna et al., 1989).

The Average deviation between experimental and calculated values for readjustment of the NRTL binary parameters from data presented by Basso et al. (2013b)

in the system ethanol (2) + FAEE from fodder radish oil (3) + water (4), calculated according to equation (9) was 1.22%, and the maximum deviation per tie line was 2.35%.

The average deviation between experimental and calculated values for the system glycerol (1) + ethanol (2) + FAEE from fodder radish oil (3), calculated according to equation (9) was 0.97%, and the maximum deviation per tie line was 1.48%. Both tie lines with high ethanol composition presented higher deviation with the NRTL model underestimating FAEE composition in GP, while the deviations for other tie lines were less than 0.91%. It can be observed from Figure 2 that modeling underestimated ethanol composition in the GP close to the plait point, describing a slight smaller phase separation region than that indicated by the experimental data. Despite the heterogeneous composition of FAEE from fodder radish oil, there is no considerable difference between the LLE behavior of this and other similar systems from literature (Basso et al., 2012; Basso et al., 2013a), including the individual ethyl ester distribution.

Table 2. Individual fatty acid ethyl ester composition of FAEE from fodder radish oil per tie line in each phase at 298.2 K.

$C_{18}H_{36}O_2$ 100w	$C_{20}H_{40}O_2$ 100w	$C_{20}H_{38}O_2$ 100w	$C_{20}H_{36}O_2$ 100w	$C_{20}H_{34}O_2$ 100w	$C_{22}H_{44}O_2$ 100w	$C_{22}H_{42}O_2$ 100w	$C_{24}H_{46}O_2$ 100w	$C_{26}H_{50}O_2$ 100w	$M/(g \cdot mol^{-1})$[a]	Δ (%)[b]
glycerol-rich phase										
5.61	2.21	41.29	18.38	13.80	0.70	9.19	8.37	0.45	314.92	0.54
5.88	1.96	41.27	20.10	16.52	0.45	7.75	5.73	0.33	312.88	1.19
5.96	1.81	40.81	20.80	17.62	0.34	7.17	5.22	0.26	312.32	1.36
5.86	1.69	38.72	21.00	20.69	0.28	6.12	3.98	1.66	312.26	1.38
6.33	1.48	38.33	22.08	19.06	0.61	5.84	5.77	0.49	312.26	1.38
5.50	1.26	37.83	21.43	21.55	0.08	7.29	4.89	0.18	312.01	1.46
ester-rich phase										
5.36	2.45	40.85	16.77	11.74	0.89	10.34	10.92	0.67	316.89	0.08
5.28	2.42	40.65	16.79	12.03	0.88	10.25	10.77	0.91	316.96	0.11
5.31	2.41	40.63	16.81	12.04	0.89	10.25	10.85	0.81	316.92	0.09
5.31	2.40	40.71	16.91	12.15	0.86	10.20	10.72	0.75	316.79	0.05
5.34	2.39	40.71	16.90	12.07	0.87	10.31	10.75	0.65	316.76	0.04
5.40	2.40	40.69	17.04	12.29	0.85	10.13	10.54	0.65	316.58	0.02

[a] average molar mass of FAEE per tie line in each phase.

[b] deviation, per tie line, between FAEE average molar mass and pseudo-molecule molar mass.

Table 3. Liquid-liquid equilibrium data, in mass percentage, for the pseudo-ternary system glycerol (1) + ethanol (2) + FAEE from fodder radish oil (3), at 298.2 K.

overall composition			ester-rich phase			glycerol-rich phase			δ (%)[a]
$100w_1$	$100w_2$	$100w_3$	$100w_1$	$100w_2$	$100w_3$	$100w_1$	$100w_2$	$100w_3$	
15.29	44.86	39.85	3.58	32.31	64.11	26.59	59.33	14.08	0.45
21.14	38.89	39.97	0.93	24.36	74.71	41.21	54.06	4.73	0.11
23.39	34.68	41.93	1.10	18.54	80.36	47.14	50.17	2.69	0.13
29.49	29.53	40.98	0.44	15.82	83.74	55.86	43.03	1.11	0.02
35.09	24.42	40.49	0.74	10.31	88.95	64.74	34.77	0.49	0.30
39.67	19.65	40.68	0.68	8.28	91.04	71.46	28.34	0.20	0.15

[a] mass balance deviation per tie line calculated according to equation 4.

Table 4. Liquid-liquid equilibrium binary interaction parameters for NRTL model.

NRTL			
pair	$A(0)_{ij}$/K	$A(0)_{ji}$/K	α (0)ij=α (0)ji
12	412.1500	0.5564	0.1000
13	3799.4000	2912.9000	0.1000
14[a]	-385.5100[a]	-453.1800[a]	0.2000[a]
23	291.1200	225.6800	0.5552
24	440.7000	-104.6800	0.1000
34	778.4000	4969.7000	0.1000

[a] binary parameters obtained from literature (Krishna et al. 1989)

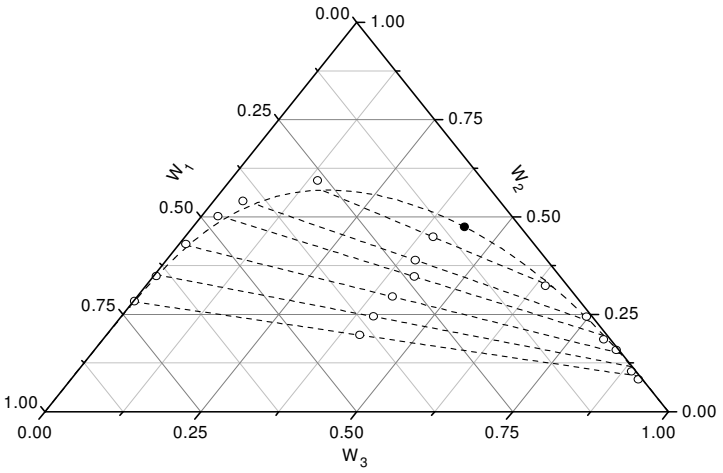

Figure 2. Liquid-liquid equilibrium diagram for the system glycerol (1) + ethanol (2) + FAEE from fodder radish oil (3) at T/K = 298,2: w is the mass fraction of the component; (○) experimental data; (●) NRTL calculated plait point; (---) NRTL calculated binodal curve.

In the first settling step of biodiesel purification, when glycerol is separated from the system, the relation between ethanol mass fraction in the FEED stream (w_2^{FEED}) and in the EP-A stream (w_2^{EP-A}) showed a approximately linear behavior, with the ratio between the first and the second values varying from about 0.84 to 1.00, respectively, as shown in Figure 3a. On the other hand, the glycerol mass fraction in the EP-A stream (w_1^{EP-A}) showed an exponential reduction with the decrease in w_2^{FEED}. When 3 mols of excess ethanol from a previous hypothetical reaction are present in the FEED stream, the w_1^{EP-A} is about 0.0007, higher than the high limit allowed by the biodiesel standard requirement (0.02%). The partial removal of ethanol, by evaporating for example, from the system until w_2^{FEED} is equal to 0.08, before an ideal settling step, permits for a glycerol content in the ester-rich stream lower than 0.02%, without an additional purification step to remove this component.

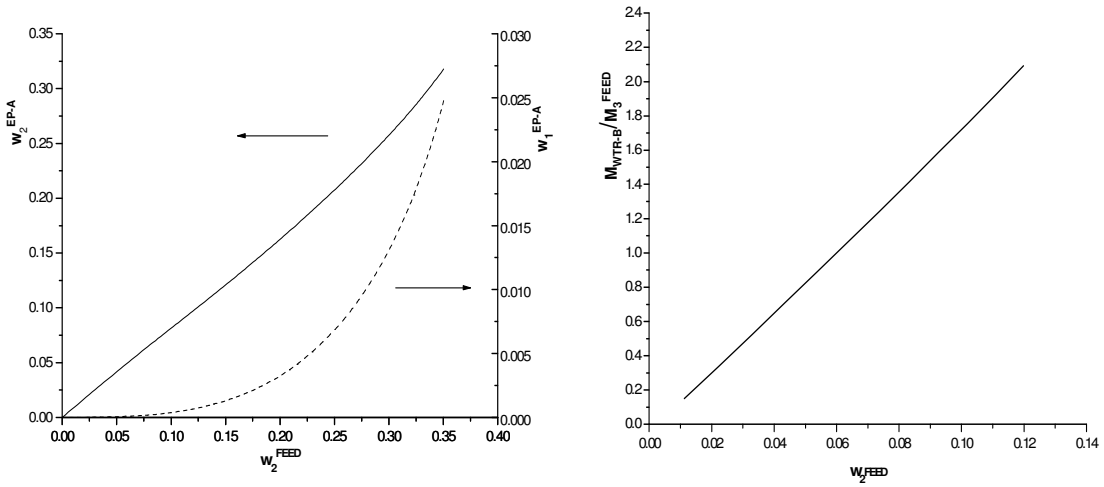

(a) (b)

Figure 3. Flowsheet I - (a): (—) w_2 and (---) w_1 in stream EP-A as function of w_2 in FEED stream; (b): (—) water mass flow requirement (M_{WTR-B}/M_3^{FEED}) to achieve (w_2^{EP-B}) lower than 0.002 as function of w_2 in FEED stream.

The requirement of water content, given by M_{WTR-A}/M_3^{FEED}, for removing ethanol from stream EP-B to levels lower than 0.2% (biodiesel standard requirement), has a direct linear relationship with the increase of ethanol in the FEED stream, as observed in Figure 3b. After the separation of GP by settling (SET-A), considering the water washing with one

mixer/settler stage (flowsheet A) and 3 moles of excess ethanol in the FEED stream ($w_2^{FEED} \cong 0.12$), the water requirement for removing ethanol from the EP-B stream to levels lower than 0.2% is about 2.12 times the mass flow of FAEE from fodder radish in the FEED stream.

In the water washing step, taking in to account 3 moles of excess ethanol in the FEED stream, and using two sets of mixer/settler unities in crosscurrent with two water streams (flowsheet II), the decreased water requirement in stream WTR-C, (M_{WTR-C}/M_3^{FEED}) as a function of water used in stream WTR-B (M_{WTR-C}/M_3^{FEED}) to achieve 0.2% of ethanol in EP-C stream, showed a parabolic behavior as described in Figure 4. The minimum total water requirement to achieve 0.2% of ethanol in EP-C occurred using similar ratios of M_{WTR-B}/M_3^{FEED} and M_{WTR-C}/M_3^{FEED}, equal to 0.249 and 0.259, respectively. Thus, the use of two sets of mixer/settler unities in crosscurrent assembly resulted in a water use of about one quarter of than that used in the single stage mixer/settler to achieve similar biodiesel purity.

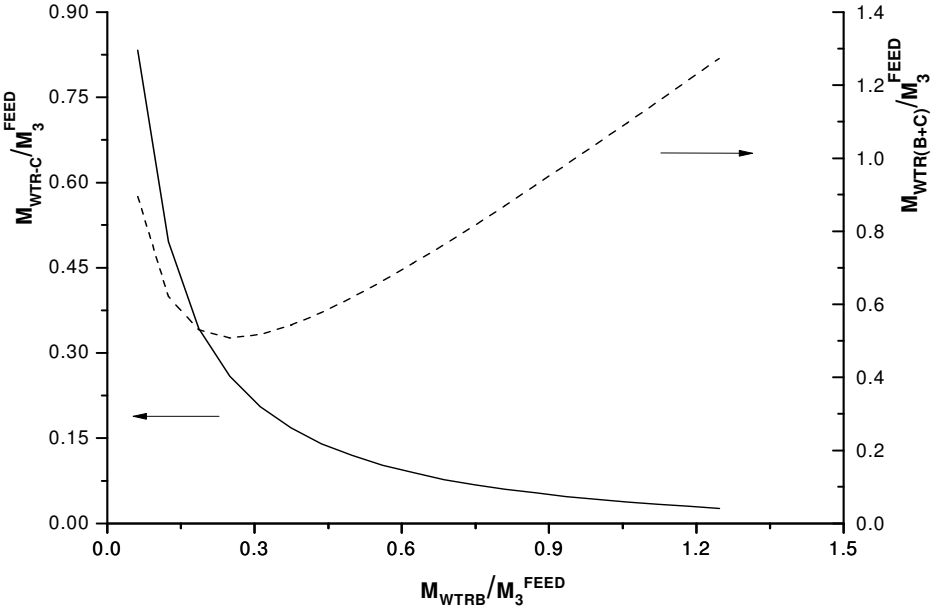

Figure 4. Flowsheet II: (—) M_{WTR-C}/M_3^{FEED} as function of M_{WTR-B}/M_3^{FEED} to w_2 in stream EP-C lower than 0.002; (---) $M_{WTR(B+C)}/M_3^{FEED}$ as function of M_{WTR-B}/M_3^{FEED} to w_2 in stream EP-C lower than 0.002.

Rahayu and Mindaryani (2007), in a study on optimized water washing of biodiesel from castor oil, observed that when using 50% of water in relation to biodiesel volume, it was possible to achieve a reduction in glycerol content from 0.9331% to 0.09%. The same authors reported that to achieve a glycerol content lower than 0.02%, washing should be done in a multiple stage process.

According to Figure 5a, the water requirement (M_{WTR}/M_3^{FEED}) as a function of w_2^{FEED} to remove ethanol from the EP-C stream to levels lower than 0.2% using two mixer/settler unities in countercurrent (flowsheet III), has a logarithmic behavior, different from that of the mixer/settler stage (flowsheet) that has a linear behavior. When 3 moles of excess ethanol are present in the FEED stream, the ratio M_{WTR}/M_3^{FEED} required to remove ethanol from the system to an ethanol content in EP-C to contents lower than that specified in the biodiesel standard requirements was about 0.27, almost half the water mass flow used in the crosscurrent flowsheet. The decreasing of w_2^{EP-C} as a function of M_{WTR}/M_3^{FEED} presented a parabolic behavior, according to that shown in Figure 5b.

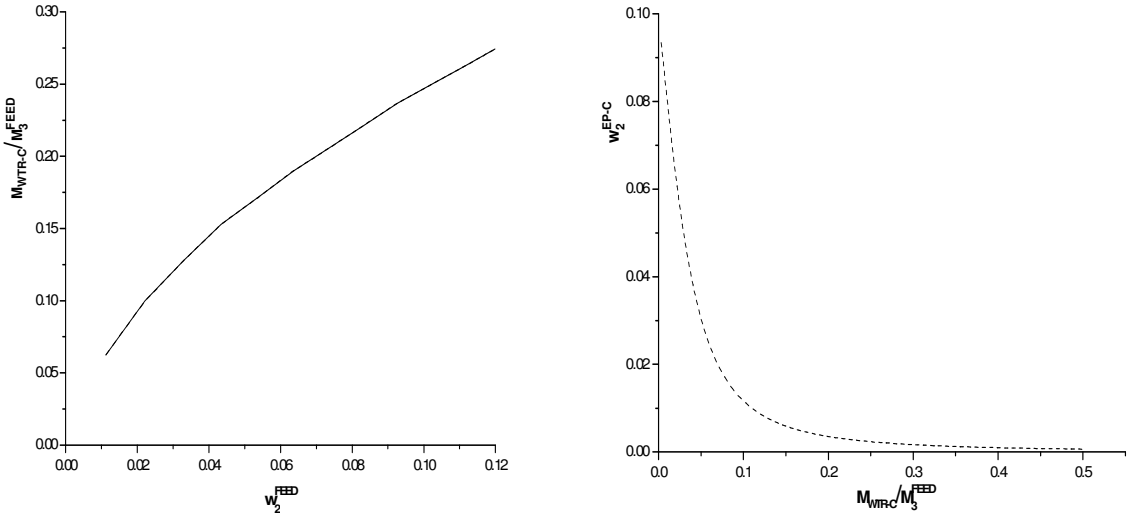

(a) (b)

Figure 5. Flowsheet III – (a) (—) M_{WTR}/M_3^{FEED} as function of w_2 in FEED stream to w_2 in stream EP-C lower than 0.002;(b) (---) w_2 in stream EP-C as a function of M_{WTR}/M_3^{FEED}.

4. Conclusions

The NRTL model properly described the system glycerol + ethanol + FAEE from fodder radish oil, with deviation less than 1.0%. Partial removal of ethanol from the system until w_2 is equal to 0.08 before an ideal settling step, allows for a glycerol content lower than 0.02% in the EP, without additional purification. Two mixer/settler sets in countercurrent, after the glycerol removal step, resulted in the minimum water requirement for ethanol removal, given by $M_{wtr}/M_3^{(st101)}$ of about 0.27. The simulation of biodiesel purification, using adjusted parameters, allows for complete optimization of the steps involved in the biodiesel purification process.

Acknowledgement

The authors would like to acknowledge the Fundação de Amparo a Pesquisa do Estado de São Paulo (FAPESP – process 08/56258-8) for its financial support, and the Conselho Nacional de Desenvolvimento Científico e Tecnológico (CNP_q – process number 140362/2009-6) for scholarship.

References

Andreatta, E.A., Casás, L.M., Hegel, P., Bottini, S.B., Brignole, E.A., 2008. Phase equilibria in ternary mixtures of methyl oleate, glycerol, and methanol. Ind. Eng. Chem. Res. 47, 5157-5164.

Atadashi I.M., Aroua M.K., Abdul-Aziz A.R., Sulaiman N.M.N., 2011. Refinning technologies for the purification of crude biodiesel. Appl. Energ. 88, 4239-4251.

Barreau, A., Brunella, I., de Hemptinne, J.C., Coupard, V., Canet, X., Rivollet, F., 2010. Measurements of liquid-liquid equilibria for a methanol + glycerol + methyl oleate system and prediction using group contribution statistical associating fluid theory. Ind. Eng. Chem. Res., 49, 5800-5807.

Basso R.C., Meirelles A.J.A., Batista E.A.C., 2012. Liquid-liquid equilibrium of pseudoternary systems containing glycerol + ethanol + ethylic biodiesel from crambe oil (*Crambe abyssinica*) at T/K = (298.2, 318.2, 338.2) and thermodynamic modeling. Fluid Phase Equilib. 333, 55-62.

Basso R.C., Silva C.A.S., Sousa C.O., Meirelles A.J.A., Batista E.A.C., 2013a. LLE experimental data, thermodynamic modeling and sensitivity analysis in the ethyl biodiesel from macauba pulp oil settling step. Bioresource Technol. 131, 468-475.

Basso, R.C., Miyake F.H., Meirelles, A.J.A., Batista, E.A.C., 2013b. Liquid-liquid equilibrium data and thermodynamic modeling, at T/K = 298.2, in the production washing step of ethyl biodiesel from crambe, fodder radish and macauba pulp oil (Capítulo 3 - to be sent to FUEL)

Berrios M., Skelton R.L., 2008. Comparison of purification methods for biodiesel. Chem. Eng. J. 144, 459-465.

Chiu, C.W., Goff, M.J., Suppes, G.J., 2005. Distribution of methanol and catalysts between biodiesel and glycerin phases. AIChE J. 51, 1274-1278.

Crusciol, C.A.C., Lima, R.L., Lima, E.V., Andreotti, M., Moro, E., Marcon, E., 2005. Persistencia de palhada e liberação de nutrientes do nabo-forrageiro no plantio direto. Pesq. Agropec. Bras. 40, 161-168.

Domingos. A.K., Saad, E.B., Wilhelm, H.M., Ramos, L.P., 2008. Optimization of the ethanolysis of Raphanus sativus (L. Var.) crude oil applying the response surface methodology. Bioresource Technol. 99, 1837-1845.

Encinar, J.M., Gonzalez, J.F, Rodrigez, J.J., Tejedor, A., 2002. Biodiesel fuels from vegetable oils: transesterification of Cynara Cardunculus L. Oils with Ethanol. Energ. Fuel 16, 443-450.

Glisic, S. B., Skala, D.U., 2009. Design and optimization of purification procedure for biodiesel washing. Chem. Ind. Chem. Eng. Q. 15, 159-168.

Kanitkar, A., Balasubramanian, S., Lima, M., Boldor, D., 2011. A critical comparison of methyl and ethyl esters production from soybean and rice bran oil in the presence of microwaves. Bioresource Technol. 102, 7896-7902.

Krishna, R., Low, C. Y., Newsham, D. M. T., Oliveira-Fontes, C. G., Paybarah, A.,1989. Liquid-liquid equilibrium in the system glycerol-water-acetone at 25 °C. Fluid Phase Equilib. 45, 115-120.

Lee, M.J., Lo, Y.C., Lin, H.M., 2010. Liquid-liquid equilibria for mixtures containing water, methanol, fatty acid methyl esters, and glycerol. Fluid Phase Equilib., 299, 180-190.

Liu X., Piao X., Wang Y., Zhu, S., 2008. Liquid-liquid equilibrium for systems of (fatty acid ethyl esters + ethanol + soybean oil and fatty acid ethyl esters + ethanol + glycerol). J. Chem. Eng. Data 53, 359-362.

Lotero, E., Liu, Y., Lopez, D.E., Swannakarn, K., Bruce, D.A., Goodwin-Jr, J.G., 2005. Synthesis of biodiesel via acid catalysis. Ind. Eng. Chem. Res. 44, 5353-5363.

Marcilla, A., Ruiz, F., Garcia, A.N., 1995. Liquid-liquid-solid equilibria of the quaternary system water – ethanol – acetone – sodium chloride at 25 ºC. Fluid Phase Equilib., 112, 273-289.

Mazutti, M.A., Voll, F.A.P., Cardozo-Filho, L, Corazza, M. L., Lanza, M., Priamo, W.L., Oliveira, J.V., 2013. Thermophysical properties of biodiesel and related systems: (Liquid + liquid) equilibrium data for soybean biodiesel. J. Chem. Thermodyn. 58, 83-94.

Mesquita, F.M.R., Feitosa, F.X., Sombra, N.E., Santiago-Aguiar, R.S., de Sant'Ana, H.B., 2011. Liquid-liquid equilibrium for ternary mixtures of biodiesel (soybean or sunflower) + glycerol + ethanol at different temperatures. J. Chem. Eng. Data, 56, 4061-4067.

Oishi, T., Prausnitz, J.M., 1978. Estimation of solvent activities in polymer solutions using a group-contribution method. Ind. Eng. Chem. Process Des. Dev. 17, 333-339.

Oliveira, M.B., Barbedo, S., Solleti, J.L., Carvalho, S.H.V., Queimada, A.J., Coutinho, J.A.P., 2011. Liquid-liquid equilibria for the canola oil biodiesel + ethanol + glycerol system. Fuel 90, 2738-2745.

Rahayu, S.S., Mindaryani, A., 2007. Optimization of biodiesel washing by water extraction. Proceedings of the World Congress on Engineering and Computer Science, San Franciso, USA.

Rodrigues, C.E.C., Silva, F.A., Marsaioli-Jr, A., Meirelles, A.J.A., 2005. Deacidification of Brazil nut and macadamia nut oils by solvent extraction: liquid-liquid equilibrium data at 298.2 K. J. Chem. Eng. Data. 50, 517-523.

Sawangkeaw, R., Teeravitud, S., Bunyakiat, K., Ngamprasertsith, S., 2011. Biofuel production from palm oil with supercritical alcohols: Effects of the alcohol to oil molar ratios on the biofuel chemical composition and properties. Bioresource Technol. 102, 10704 – 10710.

Schuchardt, U., Sercheli, R., Vargas, R.M., 1998. Transesterification of vegetable oils: a review. J. Braz. Chem. Soc. 9, 199-210.

Stamenkovic, O.S., Velickovic, A.V., Veljkovic V. B., 2011. The Production of biodiesel from vegetable oils by ethanolysis: Current state and perspectives. Fuel 90, 3141-3155.

Stragevitch, L.; d'Avila, S.G., 1997 Application of a generalized maximum likelihood method in the reduction of multicomponent liquid liquid equilibrium data. Braz. J. Chem. Eng. 14, 41–52,

Valle, P., Velez, A., Hegel, P., Mabe, G., Brignole, E.A., 2010. Biodiesel production using supercritical alcohos with a non-edible vegetable oil in a batch reactor. J. Supercrit. Fluids. 54, 61-70.

Zhang, H., Ding, J., Qiu; Yanli, Q., Zhao, Z., 2012. Kinectics of esterification of acidified oil with different alcohols by a cation ion-exchange resin/polyethersulfone hybrid catalytic membrane. Bioresource Technol. 112, 28-33.

Zhang, Y., Dubé, M.A., McLean, D.D., Kates, M., 2003. Biodiesel production from waste cooking oil: 1. Process design and technological assessment. Bioresource Technol. 89, 1-16.

Capítulo 7. Densities and Viscosities of Fatty Acid Ethyl Esters and Biodiesels Produced by Ethanolysis from Palm, Canola and Soybean Oils: Experimental Data and Calculation Methodologies

Rodrigo Corrêa Basso, Antonio José de Almeida Meirelles, Eduardo Augusto Caldas Batista

Trabalho publicado no periódico: **Industrial & Engineering Chemistry Research**, v. 52, p. 2985 - 2994, 2013.

dx.doi.org/10.1021/ie3026899

Abstract

Knowledge of the densities and viscosities of biodiesels is of great importance when designing equipment for synthesis processes and use of this biofuel in engines. Calculation methods for determining density and viscosity of products obtained from natural raw materials are powerful tools because the composition of this fuel varies. Despite of the importance of biodiesel as a completely renewable biofuel, little data is available regarding the determination of its physical properties when produced with ethanol. In the present work, the density and viscosity of three biodiesels produced by ethanolysis were determined at different temperatures. A modified methodology was developed to calculate the viscosity of ethyl esters and a new approach was presented for calculating density of ethyl esters and biodiesels produced by ethanolysis. The experimental data were compared to calculated data, resulting in average relative deviations ranging from 0.81 to 16.31% and from 0.25 to 0.62%, respectively, for biodiesel viscosity and density.

Keywords

Ethyl Ester; Biodiesel; Density; Viscosity, Physical Property Estimation

1. INTRODUCTION

Biodiesel is a mixture of alkyl esters that can be obtained from a reaction between a short chain alcohol and the triacylglycerols present in animal fat or vegetable oil, termed as transesterification. Throughout the world, vegetable oils are typical lipid feedstocks for biodiesel production. Availability of vegetable oils varies with location, and the most abundant lipid is generally the most common feedstock.[1]

Despite of the elevated price in relation to methanol, the advantages of using ethanol in biodiesel production include higher miscibility with vegetable oils that allows better contact in the reaction step and lower toxicity. Although commercial processes use vegetable oils and methanol for biodiesel production, the use of ethanol in biodiesel synthesis is appealing because it is produced from biorenewable sources, resulting in a completely agricultural-based fuel obtained by ethanolysis[2,3].

The kinematic viscosity of fatty compounds is significantly influenced by their chemical structure. Chain length, number, position and chemical group in which the double bond is located, as well as the nature of the oxygenated moieties are all influencing

factors. Viscosity increases with carbon chain length and decreases with the number of double bonds[4].

In relation to engine operation, fuels with high viscosity tend to form larger droplets upon injection, which may result in poor fuel atomization during spray, increases in engine deposits, greater energy demands for the fuel pump and wear of fuel pump elements and injectors. On the other hand, fuels with low viscosity may not provide sufficient lubrication for the precision fit of fuel injection pumps, resulting in leakage or increased wear[4,5]. It has been further shown that fuel density is the main property influencing the amount of mass injected in the engine[6].

In the biodiesel synthesis process, the knowledge of physical properties, including density and viscosity, is of great importance. Design of pipes, reactors, pumps, mixers, settlers and other equipments involved in unit operations related to alkyl esters and/or biodiesel production is highly dependent on these properties.

During process design of biodiesel production, it is possible to test a great number of operational parameters such as temperature or different compositions of raw material or generated products. Changes in these process conditions result in modification of the physical properties of biodiesel during the design analysis. Moreover, biodiesel presents a constantly changing composition because it is produced from an array of different natural raw fatty materials. From this point of view, the experimental measurement of density and viscosity at all possible operational or technical conditions is not practice. Thus, the use of models to describe the densities and viscosities of biodiesel components based only on their composition is of significant technical relevance and has being gaining importance, as indicated by methods recently presented in literature.[7-12]

Ceriani et al.[7] proposed a group contribution method to predict the viscosity of fatty compounds, including esters from fatty acids containing different alcohols (methyl, ethyl or propyl alcohol) as alkyl groups in the molecule. Considering pure fatty alkyl esters, the mainly components of biodiesel, the relative deviations in relation to experimental data ranged from 0.0004 to 16.43%.

Krisnangkura et al.[8] presented a set of equations for determination of kinematic viscosity of pure methyl esters. Compared to other methodologies, these equations were considered advantageous since they were based on thermodynamic parameters and, according to the authors, allow for further refinement and a possible extension to calculate

the viscosity of other homologous series. Regarding biodiesel viscosity calculations, the large relative deviations in relation to experimental published data were 9.2% for biodiesel produced by methanolysis (BPM) from coconut oil and 4.48% for BPM from palm oil.

Anand et al.[9] modified the group contribution method proposed by Sastri and Rao[13] to improve prediction of methyl ester viscosities. These modifications resulted in lower deviations compared to other methods, and considering the measured viscosities of fourteen BPMs, the average deviations were between 4.2% and 10.0%, considered reasonable in relation to this physical property.

Halvorsen et al.[14] proposed the use of the Rackett equation[15] modified by Spencer and Danner[16], using at least one density of reference obtained experimentally to determine the density of vegetable oils, obtaining relative deviations less than 0.7%. Sales-Cruz et al.[17] and Baroutian et al.[18] proposed the use of the modified Rackett equation using at least one experimental density of reference to calculate, respectively, the densities of methyl esters and biodiesels produced by ethanolysis (BPEs), obtaining deviations lower than 0.2%.

Despite of the importance of density and viscosity in design analysis and engine operation, there is a lack of models capable of describing the behavior of density and viscosity of ethyl esters and BPEs compared to those developed to specifically describe these behaviors in methyl esters and BPMs. Some of the existing methodologies which can be applied to calculation of viscosity or density of ethyl esters, or could be extended to these calculations by further adjustment, depend on a great number of parameters and/or equations, as well as the knowledge of specific group division methodology, the existence of reference experimental data or previous determination of other physical properties. Similarly, little experimental data is available on the determination of these physical properties in BPEs from different vegetable oils[18-20], highlighting the fact that BPE is an interesting alternative as a completely renewable biofuel.

The goals of the present study were to measure densities and viscosities of BPEs from canola oil, soybean oil and palm oil in temperatures up to 363.2 K; present and evaluate a simple model, based on that presented by Krisnangkura et al.[8], developed to describe the viscosity of ethyl esters using an unique equation with previously adjusted parameters and dependent only on the knowledge of the number of carbon atoms and double bonds present in ethyl ester molecule; compare the experimental data to that

calculated by the model proposed by Ceriani et al.[7] and by Anand et al.[9] (modified Sastri & Rao method[13]); and, present and evaluate a new approach, independent of previous experimental reference density, of the methodology proposed by Halvorsen et al.[14] to calculate the densities of fatty acid ethyl esters and BPEs.

2. EXPERIMENTAL METHODOLOGY

2.1. Material

Commercial refined soybean and canola oils, and deacidified crude palm oil were used for BPE production.

Ethanol (Merck, > 0.999/Synth, > 0.994), anhydrous sodium hydroxide (Carlo Erba, > 0.97), glacial acetic acid (Ecibra, > 0.997) and sodium sulfate (Ecibra, > 0.989) were used in the biodiesel production with no further purification.

2.2. BPE production

BPEs were produced using alkaline catalysis. Anhydrous sodium hydroxide (1% in relation to vegetable oil weight) was dissolved in ethanol prior to the transesterification reaction, under heating and vigorous agitation with a magnetic stirrer. The reagent molar ratio was 1:6 oil:ethanol when considering the average molar mass of triacylglycerols in each vegetable oil, and the reaction temperatures were about 298.2 K. At the end of the production of the three BPEs, the ester rich phase was washed with distilled hot water (about 363.2 K) at least five times. In this step, the excess ethanol, salt and residuals soaps produced by the reaction between fatty acids and the alkaline catalyst were removed.

Two different procedures were used in the reaction and purification steps of BPE production according to the refining process of the vegetable oil (completely refined or deacidified). Biodiesel production using refined canola and soybean oils was performed in two reaction steps, with a glycerol settling stage between them, with no further purification steps. Since deacidified crude palm oil is rich in compounds that are not esterified and may hamper complete transesterification, distillation was included as the last purification step of BPE from this oil.

2.3. Chromatographic Analysis

Compositions of biodiesel ethyl esters were determined in triplicate using a Perkin Elmer gas chromatographic system, Clarus 600 with a FID detector and Perkin Elmer Elite-225 capillary column (crossbond, 50% cyanopropylmethyl – 50% phenylmethyl polysiloxane) with dimensions of 30 m in length, internal diameter of 0.25 mm and film thickness of 0.25 μm, according to methodology presented by Basso et al.[21]. Identification of ethyl esters was done by comparing the retention times with those of previously identified ethyl esters from vegetable oils. Composition was based on relative peaks areas, considering the ethyl ester with molar fraction greater than 0.6%.

2.4. Viscosity Analysis

The soybean and canola oil BPE viscosities were determined for the temperature range of 283.2 to 363.2 K, and the palm oil BPE viscosity was determined from 293.2 to 363.2 K. Temperature repeatability was 0.05 K. All measurements were taken at T = 10 K intervals by a capillary microviscosimeter, Anton Paar (Austria), model AMVn. Calibration was previously verified from 293.2 to 363.2 K using a standard viscosity fluid, IPT-77 OP-6, certified by the Technological Research Institute (Instituto de Pesquisas Tecnológicas (IPT) – Brazil). The higher expanded uncertainty of fluid specified by the certifier was 0.04 mm^2/s (at 293.2 K). All relative uncertainties in the temperature range analyzed were less than 1.85%.

2.5. Density Analysis

Soybean and canola oil BPE densities were determined in triplicate for temperatures ranging from 283.2 to 363.2 K and for palm oil BPE in the range from 293.2 to 363.2 K. Temperature repeatability was 0.01 K. The measurements were taken at T = 10 K intervals, in triplicate, by a digital densimeter Anton Paar (Austria), model DMA 4500. Calibration was previously verified from 283.2 to 363.2 K using a standard viscosity fluid, IPT-77 OP-6, certified by the Technological Research Institute (Instituto de Pesquisas Tecnológicas (IPT) – Brazil). The higher expanded uncertainty of fluid specified by the certifier was 0.0001 g/cm^3. All relative uncertainties in the analyzed temperature range were less than 0.36%.

3. CALCULATION APPROACHES

A new equation based on a model developed by Krisnangkura et al.[8] for calculating the viscosity of methyl esters, presented as a simplified model for ethyl ester viscosity calculations (SMEEV), was proposed to calculate viscosities of pure FAEEs. In this new approach, the parameters of SMEEV were adjusted from pure FAEEs viscosity data obtained from literature[22,23]. The model proposed by Ceriani et al.[7] (Ceriani model) and a modification of the Satri and Rao method[13], proposed by Anand et al.[9] (SRA model), were used in their original forms and were compared to the SMEEV. Viscosities of BPEs were calculated using the simplified Grunberg-Nissan equation [24]. Densities of pure FAEEs and BPEs were calculated using a systematized and fully predictive methodology, based on the method described by Halvorsen et al.[14] which uses that proposed by Constantinou and Gani[25] for the critical properties of pure ethyl esters and that of Constantinou et al.[26] for the reference density calculations, entitled as the Halvorsen-Constantinou-Constantinou (HCC) methodology.

3.1. Viscosities

3.1.1. Ceriani model

The Ceriani model[7] is a group contribution method developed to predict fatty compound viscosities based on six “perturbation terms” obtained from regression of an experimental databank associated to each functional group in the molecules, with temperature dependence and one correction term according to equations 1-5.

$$ln(\eta_i) = \left[\sum_k N_k \cdot A_{1k} + \frac{\sum_k N_k \cdot B_{1k}}{(T + \sum_k N_k \cdot C_{1k})}\right] + M_i \left[\sum_k N_k \cdot A_{2k} + \frac{\sum_k N_k \cdot B_{2k}}{(T + \sum_k N_k \cdot C_{2k})}\right] + Q \quad (1)$$

$$Q = \xi_1 q + \xi_2 \quad (2)$$

$$q = \alpha + \frac{\beta}{T + \gamma} \quad (3)$$

$$\xi_1 = f_0 + N_c f_1 \quad (4)$$

$$\xi_2 = s_0 + N_{cs} s_1 \quad (5)$$

where η_i is the dynamic viscosity (mPa·s), A_{1k}, B_{1k}, C_{1k}, A_{2k}, B_{2k} and C_{2k} are the perturbation terms, M_i is the component molecular weight, N_k is the number of *k* groups in molecule *i*, *T* is the absolute temperature (K), Q is the correction term, q is a function of absolute temperature, α, β, and γ are optimized parameters obtained by regression of the data bank, N_c is the number of carbon atoms in the molecule, f_0 and f_1 are optimized constants, ξ_1 is a function of N_c, N_{cs} is the number of carbon atoms in the alkyl group (ethyl group in this work) of the molecule, s_0 and s_1 are optimized constants and ξ_2 is the term that describes the differences between viscosities of isomer esters at the same temperature.

All perturbation terms (A_{ik}, B_{ik} *and* C_{ik}) and optimized parameters (α, β, and γ) are constant values and were obtained by Ceriani et al.[7] by regression of the databank as a whole. The optimized constants (f_0, f_1, s_0 and s_1) are specific values related to the class of fatty compounds (fatty acids, esters, alcohols or acylglycerols) under study.

3.1.2. SRA model

The SRA model[9] consists of predicting the dynamic viscosity (η_i) of pure fatty acid methyl esters using predicted values of vapor pressure and two parameters for each functional group of the molecule, according to equations 6-8.

$$\eta_i = \sum \Delta\eta_B p_{vp}{}^{-(0.25+\alpha)} \tag{6}$$

$$lnp_{vp} = (4.5398 + 1.0309 lnT_{nb})\left\{1 - \frac{[3 - 2(T/T_{nb})]^{\beta}}{T/T_{nb}}\right. \tag{7}$$

$$\alpha = \sum \Delta N - 0.01 n_d - 0.005 \tag{8}$$

where p_{vp} is the vapor pressure of the component (atm), $\Delta\eta_B$ and ΔN are group contribution parameters, T_{nb} is the normal boiling point temperature (K), T is the studied temperature (K), β = 0.155, α is a function of the number of double bonds and n_d is the number of double bonds in the unsaturated methyl ester.

The normal boiling point temperatures (T_{nb}) of the FAEEs are obtained using the method developed by Constantinou and Gani[25] (equation 9), which is based on two orders of group structural complexity.

$$f(X) = \sum_i N_i C_i + W \cdot \sum_j M_j D_j \tag{9}$$

where *f(X)* is a function of the desired property, *i* indicates the first-order groups, j indicates the second order groups, *N* and *M* denote the number of first and second-order groups, respectively, and *W* is a constant, set to 0 for first-order calculations and 1 for second-order calculations.

3.1.3. SMEEV

The original methodology of Krisnangkura et al.[8] uses two sets of equations based on thermodynamic parameters to calculate viscosity of saturated and unsaturated methyl esters, respectively, equations (10 – 11) and equations (12 – 14). Moreover, this method uses two different sets of parameters for calculating viscosity of saturated short chain fatty acid methyl esters (equation 10), up to twelve carbon atoms, and medium chain (equation 11), up to eighteen carbon atoms, and three different sets of parameters to calculate the viscosity of three unsaturated esters, methyl oleate (equation 12), methyl linoleate (equation 13) and methyl linolenate (equation 14).

$$ln\mu = -2{,}915 - 0{,}158z + \frac{492{,}12}{T} + \frac{108{,}35z}{T} \tag{10}$$

$$ln\mu = -2{,}177 - 0{,}202z + \frac{403{,}66}{T} + \frac{109{,}77z}{T} \tag{11}$$

$$ln\mu = -5{,}03 + \frac{2051{,}5}{T} \tag{12}$$

$$ln\mu = -4{,}51 + \frac{1822{,}5}{T} \tag{13}$$

$$ln\mu = -4{,}18 + \frac{1685{,}5}{T} \tag{14}$$

where μ is the kinematic viscosity ($mm^2 \cdot s^{-1}$), T is the absolute temperature (K), z is the carbon number of the homologous series.

The SMEEV, represented by equation 15, was developed for pure FAEE viscosity calculations and uses a single equation to calculate the viscosities of both types of ethyl esters, saturated and unsaturated. Moreover, the SMEEV uses a unique set of previously adjustable parameters to describe the viscosity behavior of ethyl esters.

In development of the SMEEV, a decrease in kinematic viscosity of ethyl esters caused by addition of one unsaturated bond was considered proportional to that caused by removing 1.5 carbon atoms from the saturated ethyl esters. This assumption was based on the analysis of the average decrease in viscosity, in common temperature range, of each pure FAEE, and the comparison of this effect as a function of the increase in number of double bonds and decrease in number of carbon atoms in the FAEE molecule, as described in Figure 1. Thus, the average decrease in viscosity was calculated for each pair of saturated FAEE in the sequence of carbon numbers and compared to the average decrease in viscosity, in relation to ethyl stearate, due to the presence of one, two and three double bonds, respectively, in ethyl oleate, ethyl linoleate and ethyl linolenate. Therefore, the addition of each double bond has a similar effect to removing 1 to 2 carbon atoms. A similar observation in relation to the decrease in methyl ester viscosity was reported by Yuan et al[27]. In the adjustment of parameters, using the Brown methodology[28], a value equal to 1.5 resulted in low deviations between calculated values and experimental data from literature[22, 23] as a whole.

Thus, the parameter z, present in the general form of the equation showed by Krisnangkura et al.[8], was substituted for $(n_c - 1.5n_d)$ which allowed a general representation of all ethyl esters accordingly to its molecular structure by a single equation. The constant numerical values in the original equation were considered as adjustable parameters, and based on these assumptions the final form of SMEEV is presented in equation 15.

$$ln(\mu) = -2.4738 - 0.1181(n_c - 1.5n_d) + \frac{496.5629}{T} + \frac{79.1093(n_c - 1.5n_d)}{T} \qquad (15)$$

where μ is the kinematic viscosity ($mm^2 \cdot s^{-1}$), T is the absolute temperature (K), n_c is the carbon number of the molecule and n_d is the double bond number in the ethyl ester.

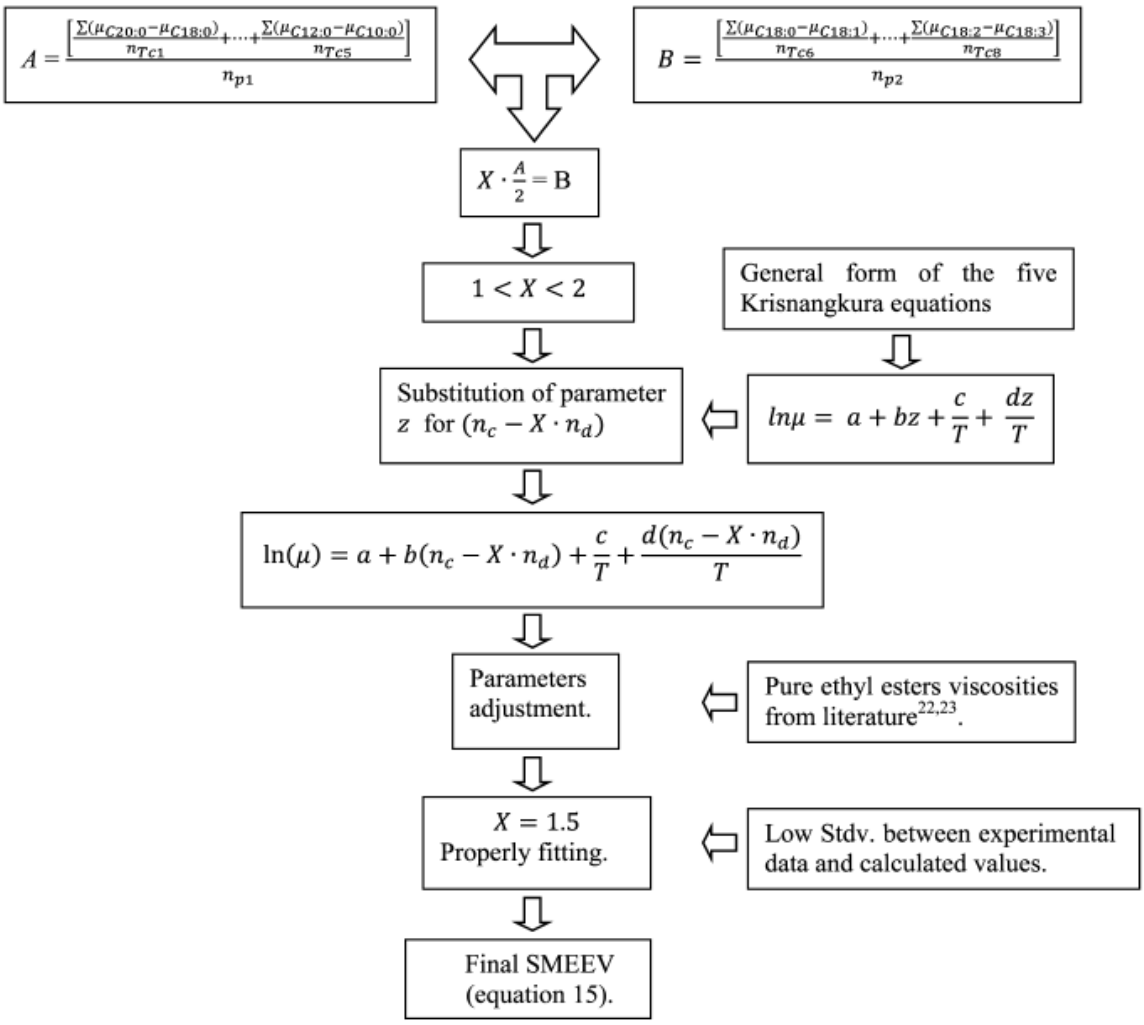

Figure 1. Steps in the SMEEV development diagram: (n_{Tci}; $i = 1,2 \ldots 8$) number of common temperatures for experimental viscosities of each compared pair; (n_{p1}) number of compared pairs of saturated FAEE; (n_{p2}) number of compared pairs of FAEEs of fatty acids with eighteen carbon atoms; (*X*) compensating factor; (n_c) number of carbon atoms in the FAEE molecule; (n_d) number double bonds in the FAEE molecule.

The reference values used in the parameters adjustment to equation 15 were the viscosities of FAEEs of the following fatty acids: capric, lauric, myristic, palmitic, stearic, oleic, linoleic, linolenic and arachidic obtained from literature[22,23], totalizing 136 data points. The temperature range of each pure FAEE viscosity measurement used for parameter adjustments were: 278.2 – 363.2 K for ethyl oleate (C18:1) and ethyl linoleate (C18:2); 278.2 – 373.2 K for ethyl linolenate (C18:3); 283.2 – 353.2 K for ethyl caprate (C10:0),

ethyl laurate (C12:0) and ethyl myristate (C14:0); 303.2 – 363.2 K for ethyl palmitate (C16:0); 313.2 – 363.2 K for ethyl stearate (C18:0) and 323.2 – 373.2 K for ethyl arachidate (C20:0). The obtained kinematic viscosity values (mm^2/s) of FAEEs were converted into units of dynamic viscosities (mPa·s) using density values from published experimental data[22,23] or predicted by the HCC methodology.

Calculations of pure FAEE viscosities were performed by direct substitution of temperature (K), number of carbon atoms (n_c) and double bonds (n_d), present in the FAEE molecule, in the equation 15.

3.1.4. Biodiesel viscosity calculations

Although the Grunberg-Nissan model considers interaction terms when calculating the viscosities of mixtures, many authors[7,29-31] consider these terms equal to zero for biodiesel viscosity calculations. According to Allen et al.[29], these biofuels are non-associated liquids that are comprised of mixtures of fatty acid esters whose chemical structure are similar, and due to this similarity, the components in mixture probably do not interact with each other and thus should behave in a similar manner as individual components. In this way, the simplified Grunberg-Nissan equation[24] without the interactions terms is represented as a function of dynamic viscosity, but can also be used in for kinematic viscosity.

The BPE viscosities are calculated from the pure FAEE viscosities obtained by SMEEV, using the simplified Grunberg-Nissan equation.[24] From this mixing rule, the logarithm of biodiesel viscosities at each temperature is equal to the logarithm of pure FAEE viscosities weighted by its molar fraction (equation 16).

$$ln\,(\eta_{mix}) = \sum_i x_i \cdot ln(\eta_i) \qquad (16)$$

where η_{mix} is the dynamic viscosity of the BPE, x_i is the molar fraction of ethyl ester *i* in BPE and η_i is the viscosity (dynamic or kinematic) of fatty acid ethyl ester *i* present in biodiesel.

In relation to BPE viscosities calculated by the SMEEV, because there are no experimental viscosities and densities measurements for all pure FAEEs are studied in the same temperature range (283.2 to 363.2 K) in literature due to temperature restrictions, the representative capability of the SMEEV was tested in two different ways: extrapolating

and not extrapolating the viscosity calculations in relation to temperature for pure ethyl esters used to adjust parameters of the model.

3.2. Densities

The proposed HCC methodology is based on a method developed by Halvorsen et al.[14] for density calculation, which in turn requires the values of critical temperature and critical pressure, and uses Rackett's equation[15] modified by Spencer and Danner[16], according to equation 17.

$$\rho = \frac{\sum_i x_i M_{w,i}}{R \cdot \left(\sum_i \frac{x_i T_{c,i}}{P_{c,i}}\right) \cdot \left(\sum_i x_i z_{RA,i}\right)^{(1+(1-T_r))^{2/7}}} \quad (17)$$

where ρ is the biodiesel density, x_i is the molar fraction of component *i*, $M_{w,i}$ is the molar weight of component *i*; R is the ideal gas constant, $T_{c,i}$ is the critical temperature of component *i*, $P_{c,i}$ is the critical pressure of component *i*, $Z_{RA,i}$ is the Rackett's parameter of component *i*, and T_r is the reduced temperature in relation to the studied temperature.

The critical temperatures ($T_{c,i}$) and critical pressures ($P_{c,i}$) of FAEE were calculated by the method of Constantinou and Gani[25] (equation 9).

Calculation of the Rackett's parameter uses at least one reference density, as described by equation 18.

$$Z_{RA,i} = \left[\frac{M_{w,i} P_{c,i}}{\rho_i R T_{c,i}}\right]^{\left[1+(1-T_r)^{2/7}\right]^{-1}} \quad (18)$$

where ρ_i is the reference density of component *i*.

Probably due to the lack of systematization in use of the model proposed Halvorsen et al.[14], some authors[17,18,32,33] have used this model always associated with an experimental reference density, and other authors[23] do not consider it a predictive method due to the need of experimental data, which restricts its use. In the HCC methodology presented in this work, the reference density at 298 K was determined using the predictive method proposed by Constantinou et al.[26] (equation 19) for calculating the liquid molar

volume of pure fatty acid alkyl esters. Therefore, the HCC methodology can be used as a predictive method, since experimental data is not needed for density calculation.

$$V_l - d = \sum_i N_i v_{1i} + A \cdot \sum_j M_j v_{2j} \tag{19}$$

where V_l is the liquid molar volume (m^3·kmol), d = 0.01211 m^3·kmol, *i* indicates the first-order groups, *j* indicates the second order groups, N and M denote the number of first-order and second-order groups, respectively, and A is a constant, set as 0 for first-order calculations and 1 for second-order calculation.

The HCC methodology should be used in the calculation of biodiesel densities as well as in the calculation of pure alkyl ester densities according to specifications in molar fraction of the terms of equation 17. Density calculations follow all steps described in Figure 2. Similarly, Table 3 presents the previously calculated Rackett parameters ($Z_{RA,i}$) of a set of methyl and ethyl esters, from which it is possible to calculate the densities of a great variety of biodiesels.

3.3. Deviations in Calculations

The relative deviations (δ_i) and average relative deviations (ARD) were calculated according to equations 20 – 21.

$$\delta_i(\%) = 100 \cdot \left(\frac{p_i^{exp} - p_i^{calc}}{p_i^{exp}} \right) \tag{20}$$

$$ARD(\%) = 100 \cdot {}^1\!/_n \cdot \sum_{i=1}^{n} \left({}^{\left|(p_i^{exp} - p_i^{calc})\right|}\!/_{p_i^{exp}} \right) \tag{21}$$

where $p_i^{exp}$and p_i^{calc} are the experimental and calculated properties under study, respectively, and n is the number of data points.

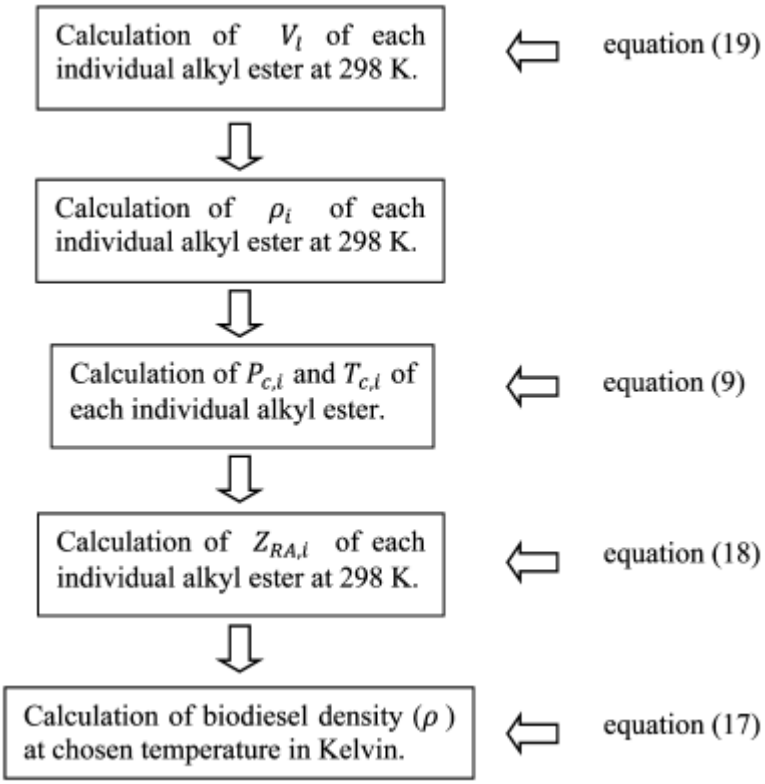

Figure 2. Steps in the HCC methodology calculation diagram: (V_l) molar volume; (ρ_i) reference density; ($P_{c,i}$) critical pressure; ($T_{c,i}$) critical temperature; ($Z_{RA,i}$) Rackett parameter; ($M_{w,i}$) molar mass of each alkyl ester in biodiesel.

4. RESULTS AND DISCUSSIONS

Table 1 shows the fatty acid ethyl ester composition of the three biodiesels studied. Biodiesel from palm oil presents ethyl palmitate and ethyl oleate as the major FAEEs in similar amounts, totalizing more than 83% of total fatty acid ethyl esters. Ethyl linoleate and ethyl oleate are the major fatty acid ethyl esters in biodiesel from soybean and canola oils, where the sum of these two esters, in both biodiesels, totals more than 85% of the ester composition.

Table 1. Fatty acid ethyl ester composition of biodiesels.

component	commom name	Canola	Soybean	Palm
		molar (%)	molar (%)	molar (%)
dodecanoic acid, ethyl ester	ethyl laurate	-	-	0.66
tetradecanoic acid, ethyl ester	ethyl myristate	-	-	0.87
hexadecanoic acid, ethyl ester	ethyl palmitate	8.40	11.62	40.29
octadecanoic acid, ethyl ester	ethyl stearate	3.03	2.90	4.57
(Z)-9-octadecenoic acid, ethyl ester	ethyl oleate	49.33	26.95	43.61
(Z,Z)-9,12-octadecadienoic acid, ethyl ester	ethyl linoleate	33.29	52.74	10.00
(Z,Z,Z)-9,12,15-octadecatrienoic acid, ethyl ester	ethyl linolenate	5.95	5.79	-

[a] standard uncertainty of composition u(x) = 0.0092.

The SMEEV, whose parameters were adjusted from viscosity of pure FAEEs obtained from literature[22,23], has the advantage of using a single equation with only four parameters for the viscosity calculation of both types (saturated and unsaturated) of FAEEs. Adjusted parameters are showed in equation 15. The average relative deviation (ARD) obtained in relation to pure FAEE experimental viscosities available in literature[22,23] was 3.8%. Higher and lower ARDs were obtained, respectively, for ethyl caprate (8.7%) and ethyl palmitate (1.1%). Figure 3 indicates an increase in individual deviations between experimental and calculated viscosities of each ethyl ester as a function of decreasing temperature.

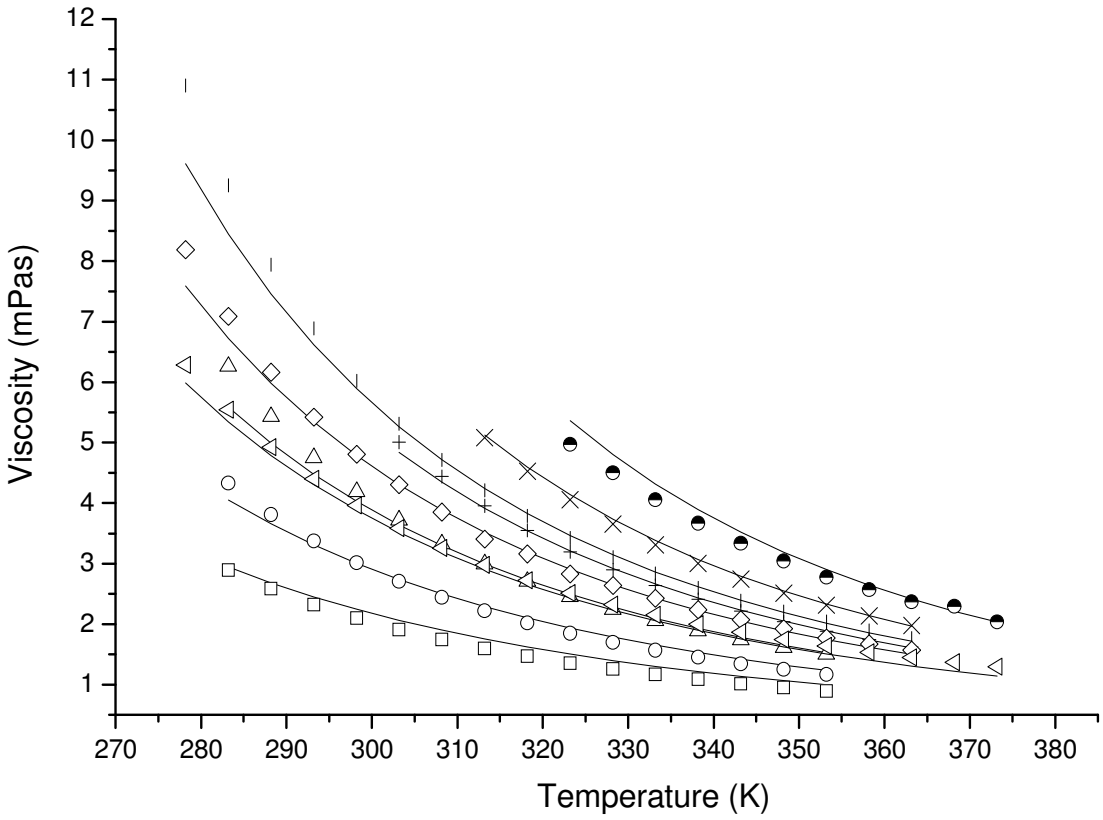

Figure 3. Experimental[22,23] and calculated viscosities of pure ethyl esters: (□) experimental ethyl caprate; (○) experimental ethyl laurate; (Δ)experimental ethyl miristate; (+) experimental ethyl palmitate; (x) experimental ethyl stearate; (|) experimental ethyl oleate; (◇) experimental ethyl linoleate; (◁) experimental ethyl linolenate; (◓) experimental ethyl arachidate; (—) calculated data (SMEEV) of the pure ethyl ester viscosities.

In relation to the measurement of the three BPE viscosities, standard deviations at each temperature were less than 0.0260 mPa·s. The viscosities of BPEs from canola, soybean and palm oil ranged from 9.9760 to 1.8644 mPa·s, 8.4939 to 1.7366 mPa·s and 6.7239 to 1.7217 mPa·s, respectively. Thus, the viscosity of biodiesel from canola oil was on average 0.5520 mPa·s and 0.3560 mPa·s higher than the respective viscosities of biodiesels from soybean and palm oil; and this difference increases as a function of reducing temperature, as can be observed in Figure 3. Since the ester viscosities decrease with the increased number of double bonds and with the decrease in number of carbon atoms in the molecule, these differences in viscosity are due to the larger amount of di-unsaturated ethyl esters in biodiesel from soybean oil and the increased quantity of ethyl palmitate, a saturated ester with 18 carbon atoms in its molecule, in biodiesel from

palm oil. The viscosity of biodiesel from palm oil is, on average, 0.0854 g/cm^3 higher than the viscosity of biodiesel from soybean oil. This similarity in viscosities of these biodiesels can be explained by their FAEE composition. The large amount of ethyl linoleate (ester with 18 carbon atoms and two double bonds) in biodiesel from soybean oil appears to have the same effect on viscosity of the large quantities of ethyl palmitate and ethyl oleate in biodiesel from palm oils. This effect also can be observed in Figure 3 where the viscosities of ethyl palmitate and ethyl oleate are similar and higher to those of ethyl linoleate.

The viscosities of BPEs were compared with those of BPMs from similar oils in the same temperature range as reported in literature[30]. Average BPE viscosities were 0.4101, 0.5273 and 0.0413 mPa·s higher than average BPM viscosities from soybean, canola and palm oil, respectfully. Although the viscosities of biodiesel produced with ethanol were on average higher than the viscosities of biodiesel produced with methanol, because the ethanol molecule has only one more carbon atom, the different ester profile has a greater influence on this property than substitution of the alcohol in the alkyl group.

In the calculations of BPE viscosities with the three models, the Ceriani model, when used for the whole temperature range of measured viscosities, slightly better represented the three biodiesel viscosity behaviors than the SMEEV, as can be observed by the lowers ARDs (Table 2). On the other hand, if restricting the temperature range to where all FAEEs have experimental viscosity data used in the adjustment of the parameters of the SMEEV, this model was more suitable than the Ceriani model for describing the viscosity behaviors of biodiesels from palm and canola oils. These differences probably occur due to the need for extrapolating calculations of densities of pure FAEEs used into transformation from kinematic to dynamic viscosity in temperatures below their melting points. The description of viscosity behaviors by the modified SRA model resulted in higher ARDs than those obtained by the other two methods for the three biodiesel samples, indicating that proper viscosity description of BPMs by this model reported in literature[9] cannot be reproduced for BPEs without further adjustment.

Table 2. Deviations between experimental and calculated biodiesel viscosities.

	Canola		Soybean		Palm	
	ARD (%)	range δ_i (%)	ARD (%)	range δ_i (%)	ARD (%)	range δ_i (%)
Ceriani model	12.9092	(10.8804) (16.6790)	6.0001	(4.5412) (8.4994)	1.3047	(-0.5558) (3.6766)
SRA model	16.3124	(10.3089) (29.3134)	9.1566	(5.5950) (19.7271)	4.4368	(1.0583) (13.3315)
SMEEV	14.7247	(11.0121) (23.6317)	8.1182	(5.4869) (14.4020)	2.1797	(-0.0938) (6.5929)
restricted SMEEV [a]	12.0995	(11.0121) (13.5110)	6.8940	(5.4869) (9.7144)	0.8122	(-0.0938) (2.3382)

[a] restricted temperature range according to that specified in published data.[19,20]

Use of the Constantinou et al.[26] model in reference density calculations was verified with the available experimental densities of FAEEs at 298 K obtained from literature[22,23], resulting in relative deviations (equation 15) of -0.66%, -0.70%, -0.73%, -0.41%, -0.06% and 0.11%, respectively, for ethyl caprate, ethyl laurate, ethyl mirystate, ethyl oleate, ethyl linoleate and ethyl linolenate.

The densities of pure fatty acid methyl and ethyl esters were calculated by the HCC methodology, and when compared to the published values[22,23], the ARDs were equal to 0.30% and 0.46%, respectively, as reported in Table 3. The lowest deviations were obtained for esters of linoleic, linolenic and arachidic acids of the ethyl alkyl groups, and for esters of myristic, oleic and palmitic acids of the methyl alkyl groups. Although ARDs reported in literature[17,32] are lower than 0.2% for density calculation of pure fatty acid methyl ester by the modified Rackett equation, at least one experimental density value was required as the reference density, which represents an unfavorable feature in relation to this HCC methodology. From Figure 4, it is possible to conclude that the behaviors of pure ethyl ester density deviations were not greatly affected by temperature since abrupt changes in this behavior were not observed along the temperature range.

Table 3. Calculated densities, Rackett parameters and deviations between experimental measurements[19,20] and the HCC methodology for pure ester densities.

common name	fatty acid in alkyl group	FAEE[a]				FAME[b]	
		$\frac{\rho_{ref}}{g/cm^3}$	Z_{RA}	ARD (%)	range δ (%)	ARD (%)	range $\boldsymbol{\delta}$ (%)
methyl/ethyl caprilate	C8:0	0.86774	0.25593752			0.7434	(0.3247) - (1.2852)
methyl/ethyl caprate	C10:0	0.86590	0.24786423	0.5629	(-0.6486) - (-0.3962)	0.3930	(0.1106) - (0.8237)
methyl/ethyl laurate	C12:0	0.86452	0.24069735	0.6418	(-0.6826) - (-0.5490)	0.1001	(0.0697) - (0.1543)
methyl/ethyl myristate	C14:0	0.86344	0.23429595	0.6993	(-0.7267) - (-0.6449)	0.0529	(-0.0108) - (0.1682)
methyl/ethyl palmitate	C16:0	0.86258	0.22856060	0.7191	(-0.7473) - (-0.6525)	0.0729	(-0.112) - (0.0219)
methyl/ethyl palmitoleate	C16:1	0.87206	0.22848115	-	-	0.8875	(-0.9194) - (-0.8189)
methyl/ethyl stearate	C18:0	0.86187	0.22341251	0.7563	(-0.7681) - (-0.7312)	0.1417	(-0.1819) - (-0.0699)
methyl/ethyl oleate	C18:1	0.87047	0.22337470	0.4206	(-0.4616) - (-0.3350)	0.0548	(-0.0861) - (0.0246)
methyl/ethyl linoleate	C18:2	0.87936	0.22333089	0.0395	(-0.0691) - (0.0380)	0.2810	(0.2296) - (0.3911)
methyl/ethyl linolenate	C18:3	0.88856	0.22328046	0.1336	(0.0851) - (0.2424)	0.9477	(0.8942) - (1.0839)
methyl/ethyl arachidate	C20:0	0.86128	0.21878567	0.1825	(-0.2155) - (-0.1119)	0.1654	(-0.214) - (-0.0662)
methyl/ethyl gadoleate	C20:1	0.86915	0.21877107	-	-	0.0972	(0.0459) - (0.2387)
methyl/ethyl behenate	C22:0	0.86078	0.21462347	-	-	0.1418	(-0.2066) - (-0.0460)
methyl/ethyl erucate	C22:1	0.86803	0.21462023	-	-	0.1571	(-0.1997) - (-0.0544)
methyl/ethyl lignocerate	C24:0	0.86035	0.21087680	-	-	0.3021	(-0.332) - (-0.2508)
overall				0.4617		0.3026	

[a] fatty acid ethyl ester; [b] fatty acid methyl ester.

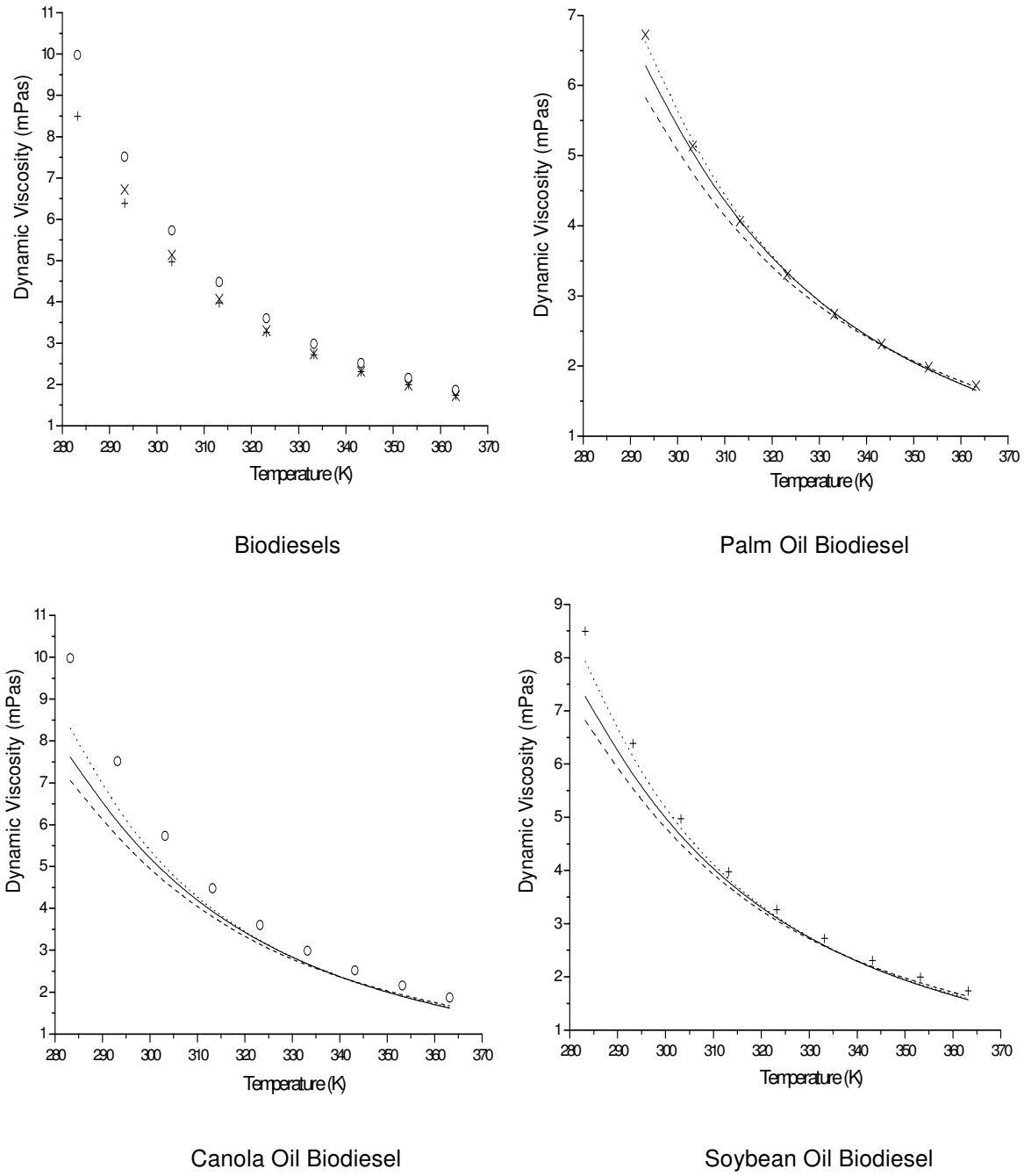

Figure 4. Experimental and calculated biodiesels viscosities: (×) palm; (○) canola; (+) soybean; (—) SMEEV; (···) Ceriani model; (---) SRA model.

Standard deviations in relation to three measurements of BPE densities, at each temperature, were lower than 0.00006 g/cm^3 for all biodiesel densities. The densities of biodiesels from canola, soybean and palm oil ranged from 0.88212 to 0.82337 g/cm^3,

0.88215 to 0.82337 g/cm^3 and 0.86490 to 0.81315 g/cm^3, respectfully. From these results the densities of biodiesel from palm oil were, on average, 0.0100 g/cm^3 lower than those of biodiesels from soybean and canola oil which were similar to each other, as observed in Figure 5. These results are in agreement with those observed by Baroutian et al.[18] in relation to these biodiesels. The higher densities can be explained by the ester composition of biodiesels from canola and soybean oil, which are richer in unsaturated ethyl esters and in esters with more carbon atoms in the molecule when compared to biodiesel from palm oil. According to the observations of Pratas et al.[22], the density of ethyl esters decreases with increasing alkyl chain length and increases with the level of unsaturation.

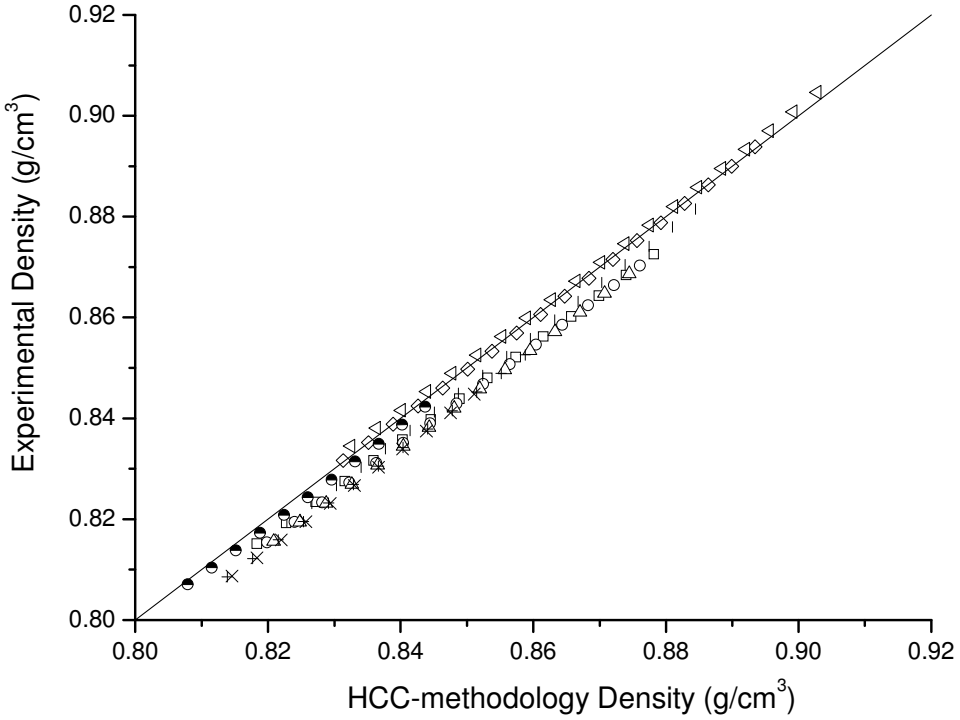

Figure 5. Experimental data[22,23] and calculated densities of pure ethyl esters: (□) ethyl caprate; (○) ethyl laurate; (Δ) ethyl myristate; (+) ethyl palmitate; (x) ethyl stearate; (|) ethyl oleate; (◇) ethyl linoleate; (◁) ethyl linolenate; (◓) ethyl arachidate.

The densities of BPE from canola, soybean and palm oil were 0.0107, 0.0102 and 0.0079 g/cm^3 lower, on average, than densities of BPM from similar oils obtained from literature[34-35]. This behavior is probably related to the higher molar volume of fatty acid ethyl ester molecules in comparison to methyl ester molecules due to the presence of one additional "CH_2" group in the ethanol molecule.

Densities calculated by the HCC methodology resulted in ARDs for biodiesels from canola oil, soybean oil and palm oil equal to 0.2516%, 0.4075% and 0.6228%, respectively. Although Baroutian et al.[18] reported ARDs lower than 0.12% in calculations of three BPE densities using the modified Rackett equation, their methodology is dependent on reference biodiesel density values. Moreover, different from the methodology proposed by Baroutian et al.[18], the HCC methodology is based on density of pure ethyl esters, and therefore it can be used for all BPE density calculations, using the Rackett parameters (Z_{RA}) as shown in Table 3.

Conclusions

The viscosities of BPEs from canola oil were 0.5520 mPa·s and 0.3560 mPa·s higher, on average, than the viscosities of BPEs from soybean and palm oil, respectively. Densities of biodiesel from palm oil were on average 0.0100 g/cm^3 lower than those of biodiesels from soybean and canola oil which were similar to each other. Viscosities of pure FAEEs and BPEs calculated by the SMEEV resulted in maximum ARDs respectively equal to 8.7% and 14.7%. Although the Ceriani model and SMEEV properly described the viscosities of fatty acid ethyl esters and BPEs, the SMEEV method has the advantage of being simpler than the other tested models, which makes its programming more practical in biodiesel viscosity evaluations and design analysis. The HCC methodology showed to be an accurate and useful completely predictive methodology for calculating the densities of alkyl esters and BPE, resulting in maximum ARD lower than 1.0%.

Acknowledgement

The authors would like to acknowledge the Fundação de Amparo a Pesquisa do Estado de São Paulo (FAPESP – process number 08/56258-8) for its financial support, and the Conselho Nacional de Desenvolvimento Científico e Tecnológico (CNPq – process number 140362/2009-6) for the scholarship.

References

[1] Knothe, G.; Van Gerpen, J.; Khrahl, J. *The Biodiesel Handbook*; AOCS Press: Champaign, Illimois, 2005.

[2] Encinar J. M.; Gonzalez J. F., Rodrigez J. J.; Tejedor A. Biodiesel Fuels from Vegetable Oils: Transesterification of Cynara Cardunculus L. Oils with Ethanol. *Energ. Fuel.* 2002, *16*, 443.

[3] Stamenkovic, O. S.; Velickovic, A. V.; Veljkovic V. B. The Production of biodiesel from vegetable oils by ethanolysis: Current state and perspectives. *Fuel.* 2011, *90*, 3141.

[4] Knothe, G.; Steidlei, K. R. Kinematic Viscosity of Biofuel Components and Related Compounds: Influence of Compound Structure and Comparison to Petrodiesel Fuel Components. *Fuel.* 2005, *84*, 1059.

[5] Refaat, A. A. Correlation Between the Chemical Structure of Biodiesel and its Physical Properties. *Int. J. Environ. Sci. Technol.* 2009, *6*, 677.

[6] Boudy, F.; Seers, P. Impact of Physical Properties of Biodiesel on the Injection Process in a Common-Rail Direct Injection System. *Energy Convers. Manage.* 2009, *50*, 2905.

[7] Ceriani, R.; Gonçalves, C. B.; Coutinho, J. A. P. Prediction of Viscosities of Fatty Compounds and Biodiesel by Group Contribution. *Energ. Fuel.* 2011, *25*, 3712.

[8] Krisnangkura, K.; Yimsuwan, T.; Pairintra, R. An Empirical Approach in Predicting Biodiesel Viscosity at Various Temperatures. *Fuel.* 2006, *85*, 107.

[9] Anand, K.; Ranjan, A.; Mehta, P. S. Estimating the Viscosity of Vegetable Oils and Biodiesel Fuels. *Energ. Fuel.* 2010, *24*, 664.

[10] Su, Y. C.; Liu, Y. A.; Tovar, C. A. D.; Gani, R. Selection of Prediction Methods for Thermophysical Properties for Process Modeling and Product Design of Biodiesel Manufacturing. *Ind. Eng. Chem. Res.* 2011, *50*, 6809.

[11] Zong, L.; Ramanathan, S.; Chen, C. C. Fragment-Base Approach for Estimating Thermophysical of Fats and Vegetable Oils for Modeling Biodiesel Production Process. *Ind. Eng. Chem. Res.* 2010, *49*, 876.

[12] Zong, L.; Ramanathan, S.; Chen, C. C. Predicting Thermophysical Properties of Mono- and Diglycerides with the Chemical Constituent Fragment Approach. *Ind. Eng. Chem. Res.* 2010, *49*, 5479.

[13] Sastri, S. R. S.; Rao, K. K. A New Group Contribution Method for Predicting the Viscosity of Organic Liquids. *Chem. Eng. J.* 1992, *50*, 9.

[14] Halvorsen, J. D.; Mammel-Jr, W. C.; Clements, L. D. Density Estimation for Fatty Acid and Vegetable Oils Based on Their Fatty Acid Composition. *J. Am. Oil Chem. Soc.* 1993, *10*, 875.

[15] Rackett, H. G. Equation of State of Saturated liquids. *J. Chem. Eng. Data.* 1970, *15*, 514.

[16] Spencer, C. F.; Danner, R. P. Prediction of Bubble Point Density of Mixtures. *J. Chem. Eng. Data.* 1973, *18*, 230.

[17] Sales-Cruz, M.; Aca-Aca, G.; Sánchez-Daza, O.; López-Arenas, T. Predicting Critical Properties, Density and Viscosity of Fatty Acids, Triacylglycerols and Methyl Esters by Group Contribution Methods. *20th European Symposium on Computer Aided Process Engineering – (ESCAPE20)*, 2010.

[18] Baroutian, S.; Aroua, M. K.; Raman, A. A. A.; Sulaiman, N. M. N. Densities of Ethyl Esters Produced from Different Vegetable Oils. *J. Chem. Eng. Data.* 2008, *53*, 2222.

[19] Santos, N. A.; Rosenhaim, R.; Dantas, M. B.; Bicudo, T. C.; Cavalcanti, E. H. S.; Barro, A. K.; Santos, I. M. G.; Souza, A. G.; Rheology and MT-DSC Studies of Flow Properties of Ethyl and Methyl Babassu Biodiesel and Blends. *J. Therm. Anal. Calorim.* 2011, *106*, 501.

[20] Tate, R. E.; Watts, K. C.; Allen, C. A. W.; Wilkie, K. I. The Viscosities of Three Biodiesel Fuels at Temperatures up to 300 °C. *Fuel.* 2006, *85*, 1010.

[21] Basso, R. C.; Meirelles, A. J. A.; Batista, E. A. C. Liquid-liquid equilibrium of pseudoternary systems containing glycerol + ethanol + ethylic biodiesel from crambe oil (Crambe abyssinica) at T/K = (298,2, 318,2, 338,2) and thermodynamic modeling. *Fluid Phase Equilib.* 2012, *333*, 55.

[22] Pratas, M. J.; Freitas, S.; Oliveira, M. B.; Monteiro, S. C.; Lima, A. S.; Coutinho, J. A. P. Densities and Viscosities of Fatty Acid Methyl and Ethyl Ester. *J. Chem. Eng. Data.* 2010, *55*, 3983.

[23] Pratas, M. J.; Freitas, S.; Oliveira, M. O.; Monteiro, S. C.; Lima, A. S.; Coutinho, J. A. C. Densities and Viscosities of Minority Fatty Acid Methyl and Ethyl Esters Present in Biodiesel. *J. Chem. Eng. Data.* 2011, *56*, 2175.

[24] Grunberg, L.; Nissan, A. H. Mixture law for viscosity. *Nature* 1949, 164, 799.

[25] Constantinou, L.; Gani, R. New Group Contribution Method for Estimating Properties of Pure Components. *AICHE J.* 1994, *70*, 1697.

[26] Constantinou, L.; Gani, R.; O'Connel, J. P. Estimation of the Acentric Factor and Liquid Molar Volume at 298 K Using a New Group Contribution Method. *Fluid Phase Equilib.* 1995, *103*, 11.

[27] Yuan, W.; Hansen, A. C.; Zhang, Q. Predicting the Temperature Dependent of Biodiesel Fuels. *Fuel.* 2009, 88, 1120.

[28] Brown, A. M.; A Step-by-Step Guide to Non-Linear Regression Analysis of Experimental Data Using a Microsoft Excel Spreadsheet. *Comput. Meth Programs Biomed.* 2001, 65, 191.

[29] Allen, C. A. W.; Watts, K. C.; Ackman, R. G.; Pegg, M. J. Predicting the Viscosity of Biodiesel Fuels from their Fatty Acid Ester Composition. *Fuel.* 1999, 78, 1319.

[30] Freitas, S. V. D.; Pratas, M. J.; Ceriani, R.; Lima, A. S.; Coutinho, J. A. P. Evaluation of Predictive Models for the Viscosity of the Biodiesel. *Energ. Fuel.* 2011, 25, 352.

[31] do Carmo, F. R.; Sousa Jr, P. M.; Aguiar, R. S.; Sant'Ana, H. B. Development of a New Model for Biodiesel Viscosity Prediction Based on the Principle of Corresponding State. *Fuel*. 2012, 92, 250.

[32] Veny, H.; Baroutian, S.; Aroua, M. K.; Hasan, M.; Raman, A. A.; Sulaiman, N. M. N. Density of Jatropha curcas Seed Oil and its Methyl Esters: Measurement and Estimations. *Int. J. Thermophys*. 2009, 30, 529.

[33] Blangino, E.; Riveros, A. F.; Romano, S. D. Numerical Expressions for Viscosity, Surface Tension and Density of Biodiesel: Analysis and Experimental Validation. *Phys. Chem. Liq.* 2008, *46*, 527.

[34] Feitosa, F. X.; Rodrigues, M. L.; Veloso, C. B.; Cavalcante Jr, C. L.; Albuquerque M. C. G.; Sant'Ana, H. B. Viscosities and Densities of Binary Mixtures of Coconut + Colza and Coconut + Soybean Biodiesel at Various Temperatures. *J. Chem. Eng. Data.* 2010, 55, 3909.

[35] Baroutian, S. Aroua, M. K.; Raman, A. A. A.; Sulaiman, N. M. Density of Palm Oil-Based Methyl Ester. *J. Chem. Eng. Data.* 2008, 53, 877.

Capítulo 8. Biodiesels Produced by Ethanolysis: Melting Profile, Densities and Viscosities Correlated to Ester Composition and Calculation Methodologies

Rodrigo Corrêa Basso, Antonio José de Almeida Meirelles, Eduardo Augusto Caldas Batista

Trabalho submetido ao periódico **Energy & Fuels** em 12 de junho de 2013.

Abstract

Little information on the density, viscosity and melting profile are available regarding biodiesel produced by ethanolysis, although it presents the appeal of being a completely biorenewable biofuel. In the present work, the densities, viscosities and melting profiles of four biodiesels produced by ethanolysis were presented. The ethyl ester compositions of the biodiesels were associated with the behavior of these physical properties. Two methodologies for calculating density and viscosity were tested. Biodiesel from macauba pulp oil presented the highest melting point while biodiesel from crambe and fodder radish oil presented, respectively, the highest viscosities and densities. The average relative deviations between calculated and experimental values were from 5.1% to 14.3% and from 7.1% to 12.6% using, respectively, the Basso model and Ceriani model for viscosity calculation, and less than 1.1% when using the predictive Halvorsen methodology and GCVOL, a group contribution model, for density calculation.

Keywords

Biodiesel; Viscosity; Density; DSC; Physical Properties

1. Introduction

Biodiesel is a mixture of alkyl esters that can be obtained by transesterification, a reaction between a short chain alcohols and triacylglycerols. Throughout the world, vegetable oils are typical lipid feedstocks for biodiesel production.[1] In addition to the agricultural availability of the oil plants, the selection of vegetable oil depends on its fatty acid composition because the final product must meet a set of physical and chemical quality standard requirements in order for its use as a biofuel. Low poly-unsaturated fatty acid content is one of the desired characteristics for vegetable oils considered interesting raw materials for biodiesel production.[2]

Despite the high price of ethanol compared to methanol, some of the advantages of using ethanol in biodiesel production are higher miscibility with vegetable oils that allows better contact in the reaction step and lower toxicity. Additionally, although commercial processes use vegetable oils and methanol for biodiesel production, the use of ethanol in biodiesel synthesis is appealing because it is produced from biorenewable sources, resulting in a completely agricultural-based fuel.[3,4]

The viscosity of fatty compounds is significantly influenced by their molecular structure. Carbon chain length, number, position and chemical group in which the double bond is located, as well as the nature of the oxygenated moieties, are the mainly influencing factors. In general, viscosity of the alkyl esters increases with carbon chain length and decreases with the number of double bonds.[5] The melting point of a substance plays a major role in determining the suitability and applicability of a substance. Numerous structural factors influence the melting point of long-chain fatty compounds, including the molecular weight, the position, number and configuration of unsaturated bonds, branching and polar moieties.[6]

In relation to engine operation, fuels with high viscosity tend to form larger droplets upon injection, which may result in poor fuel atomization during spraying, increases in engine deposits, greater energy demands for the fuel pump and wear of fuel pump elements and injectors. On the other hand, fuels with low viscosity may not provide sufficient lubrication for the precision fit of fuel injection pumps, resulting in leakage or increased wear.[5,7] It has been further shown that fuel density is the main property influencing the amount of mass injected in the engine.[8] Biodiesels in their crystallized form can restrict flow through fuel lines and block filters in the engine.[9,10]

In the biodiesel synthesis process, the knowledge of physical properties is of great importance. Design of pipes, reactors, pumps, mixers, settlers and other equipments involved in unit operations related to alkyl esters and/or biodiesel production is highly dependent on these properties.[11]

Some important thermal properties of biodiesel can be assessed with differential scanning calorimetry analyses. Properties related to the melting and cooling behavior of alkyl esters including cloud point, pour point, cold-filter plugging point, and low-temperature flow test were determined from this type of analysis and correlated with results obtained using classical methods.[6,12]

Although the biorenewable and sustainable ethanol is appealing and the fatty acid profiles of crambe, fodder radish, coconut and macauba oil show promise for biodiesel production, there is no data regarding the physical properties of biodiesels produced by ethanolysis from these promising raw materials.

Therefore, the objectives of the present work were to present experimental densities and viscosities for biodiesels produced by ethanolysis from crambe oil (BPECr),

fodder radish oil (BPEFR), coconut oil (BPEC) and macauba pulp oil (BPEMP) at temperatures up to 363.2 K; compare experimental data with calculated viscosities from the models proposed by Ceriani et al.[13] and Basso et al.[11], and with densities calculated using the GCVOL model[14] and a systematized predictive methodology[11] based on the methodology proposed by Halvorsen et al.[15]; and determine, using differential scanning calorimetry, the melting profile of these four promising biofuels and correlate the three studied physical properties to the ethyl ester composition of each biodiesel.

2. Experimental methodology

2.1. Material

Ethanol (Merck, > 0.999 or Synth, > 0.994), anhydrous sodium hydroxide (Carlo Erba, > 0.97), glacial acetic acid (Ecibra, > 0.997) and sodium sulfate (Ecibra, > 0.989) were used in the biodiesel production with no further purification.

Refined coconut oil and deacidified crude crambe, macauba pulp and fodder radish oils were used for ethyl biodiesel production, performed according to the procedure reported by Basso et al.[11]. Ethyl ester biodiesel compositions were obtained according to described in section 2.2, and are presented in molar percentage in Table 1.

2.2. Chromatographic analysis

Biodiesel compositions were determined in triplicate using a Perkin Elmer gas chromatographic system, Clarus 600, with a FID detector and Perkin Elmer Elite-225 capillary column (crossbond, 50% cyanopropylmethyl – 50% phenylmethyl polysiloxane) with dimensions of 30 m in length, internal diameter of 0.25 mm and film thickness of 0.25 μm, according to the methodology presented by Basso et al.[16]. Identification of ethyl esters was done by comparing the retention times with those of previously identified ethyl esters from vegetable oils. Composition was based on relative peak areas, considering ethyl esters with molar percentage greater than 0.5 %.

Table 1. Biodiesel composition in ethyl ester.[a]

			molar (%)			
fatty acid group in the ethyl ester	ethyl ester	M ($g \cdot mol^{-1}$)	BPECr	BPEFR	BPEMP	BPEC
C8:0	octanoic acid ethyl ester	172.27	-	-	-	5.04
C10:0	decanoic acid ethyl ester	200.32	-	-	-	4.05
C12:0	dodecanoic acid ethyl ester	228.37	-	-	-	51.56
C14:0	tetradecanoic acid ethyl ester	256.42	-	-	-	15.24
C16:0	hexadecanoic acid ethyl ester	284.48	2.51	5.74	23.22	7.28
C16:1	hexadecenoic acid ethyl ester	282.46	-	-	4.38	-
C18:0	octadecanoic acid ethyl ester	312.53	1.14	2.41	2.68	1.74
C18:1	octadecenoic acid ethyl ester	310.51	21.56	40.64	57.55	13.04
C18:2	octadienoic acid ethyl ester	308.5	9.33	17.29	11.43	2.05
C18:3	octadecatrienoic ethyl ester	306.48	5.11	12.71	0.74	-
C20:0	eicosanoic acid ethyl ester	340.58	1.24	0.81	-	-
C20:1	eicosenoic acid ethyl ester	338.57	4.12	9.47	-	-
C22:0	docosanoic acid ethyl ester	368.64	1.87	-	-	-
C22:1	docosenoic acid ethyl ester	366.62	53.12	10.21	-	-
C24:1	tetracosenoic acid ethyl ester	394.67	-	0.72	-	-

[a] molar percentage > 0.5%.

2.3. Density analysis

Ethyl biodiesel densities were determined in triplicate for temperatures ranging from 283.2 to 363.2 K. Temperature repeatability was 0.01 K. The measurements were taken at T = 5 K intervals, in triplicate, with the digital densimeter Anton Paar (Austria), model DMA 4500. Calibration was previously verified using a standard fluid, IPT-77 OP-6, certified by the Technological Research Institute (Instituto de Pesquisas Tecnológicas (IPT) – Brazil). The higher expanded uncertainty of the fluid specified by the certifier was 0.0001 g/cm^3. The absolute relative deviation between experimental and measured values, using the standard fluid, was 0.36%, at T/K = 363.2.

2.4. Viscosity analysis

Ethyl biodiesel viscosities were determined for the temperature range of 283.2 to 363.2 K. Temperature repeatability was 0.05 K. All measurements were taken at T = 5 K intervals by a capillary microviscosimeter, Anton Paar (Austria), model AMVn. Calibration was previously verified using a standard viscosity fluid, IPT-77 OP-6, certified by the Technological Research Institute (Instituto de Pesquisas Tecnológicas (IPT) – Brazil). The higher expanded uncertainty of the fluid specified by the certifier was 0.04 mm^2/s (at 293.2 K). The absolute relative deviation between experimental and measured values, using the standard fluid, was 3.23% at T/K = 363.2.

2.5. Melting profile analysis

Biodiesel melting behavior was analyzed using a differential scanning calorimeter (DSC) Perkin Elmer (USA) model DSC 8500.Samples were weighted (about 5 mg) on a microanalytical balance Perkin Elmer (USA), model AD6. An empty sealed aluminum pan was used as a reference. The samples were subjected to the following temperature programs: cooling at 1 K/min down to 193 K and maintained at isothermal conditions for 30 min, heating at 1 K/min up to 353 K. A similar heating rate was used by Santos et al.[17] when studying some physical properties of methyl and ethyl biodiesel from babassu and oil blends using differential scanning calorimetry. Calibration was performed using cyclohexane and indium as references. The initial and final temperatures for each melting peak were considered as the points in which the baseline decoupled from the original trajectory.

3. Calculation approach

3.1. Density methodologies

A completely predictive methodology systematized by Basso et al.[11] and a group contribution model developed by Elbro et al.[13] were used for the calculation of biodiesel densities.

3.1.1. Systematized Halvorsen methodology

Halvorsen et al.[15] proposed the use of the Rackett equation[18] modified by Spencer and Danner[19], including at least one reference density obtained experimentally to

determine the density of vegetable oils. A complete predictive methodology, based on the Halvorsen et al.[15] method was described in detail by Basso et al.[11] for the biodiesel density calculation, according to equation (1).

$$\rho = \frac{\sum_i x_i M_{w,i}}{R \cdot \left(\sum_i \frac{x_i T_{c,i}}{P_{c,i}}\right) \cdot \left(\sum_i x_i z_{RA,i}\right)^{\left(1+(1-T_r)\right)^{2/7}}} \quad (1)$$

where ρ is the biodiesel density, x_i is the molar fraction of component *i*, $M_{w,i}$ is the molar weight of component *i*; R is the ideal gas constant, $T_{c,i}$ is the critical temperature of component *i*, $P_{c,i}$ is the critical pressure of component *i*, $Z_{RA,i}$ is the Rackett's parameter of component *i*, and T_r is the reduced temperature in relation to the studied temperature.

The Rackett's parameter for each ethyl ester was previously calculated by Basso et al.[11].

This methodology uses that proposed by Constantinou et al.[20] (equation 2) for calculating the reference density.

$$V_l - d = \sum_i N_i v_{1i} + A \cdot \sum_j M_j v_{2j} \quad (2)$$

where V_l is the liquid molar volume ($m^3 \cdot kmol^{-1}$), d = 0.01211 $m^3 \cdot kmol^{-1}$, *i* indicates the first-order groups, *j* indicates the second order groups, N and M denote the number of first-order and second-order groups, respectively, and A is a constant, set to 0 for first-order calculations and 1 for second-order calculations.

The critical temperatures ($T_{c,i}$) and critical pressures ($P_{c,i}$) of the ethyl esters used in this methodology were calculated from the method presented by Constantinou and Gani[21] (equation 3).

$$f(X) = \sum_i N_i C_i + W \cdot \sum_j M_j D_j \quad (3)$$

where *f(X)* is a function of the desired property, *i* indicates the first-order groups, *j* indicates the second-order groups, *N* and *M* denote the number of first and second-order groups, respectively, and *W* is a constant, set to 0 for first-order calculations and 1 for second-order calculations.

3.1.2. Elbro methodology

Elbro et al.[14] developed a group contribution model (equations 4 - 5), consisting of 36 different group volume increments for the chemical families of noncyclic alkanes, aromatics, alkenes, ketones, ethers, esters, chlorides and siloxanes. Pratas et al.[22] used this model for calculation of the molar volume of methyl esters in the biodiesel density calculations (equation 6).

$$\Delta v_i = A_i + B_i T + C_i T^2 \tag{4}$$

$$V = \sum n_i \, \Delta v_i \tag{5}$$

$$\rho = \frac{\sum x_j \, MW_j}{\sum x_j V_j} \tag{6}$$

where x is the molar fraction of the component, MW is the molar weight of the component, V is the molar fraction of the component, n is the group number, Δv is the molar volume of the group, A, B and C are the group parameters, and i and j denote, respectively, the group and component in study.

3.2. Viscosity models

The viscosities of the pure ethyl esters comprising the biodiesels produced by ethanolysis were calculated by a group contribution model developed by Ceriani et al.[13] and by a model proposed by Basso et al.[11]

3.2.1. Basso model

A simplified model, using a single equation (equation 7) with only one set of previously calculated parameters and with temperature dependence that requires the number of carbon atoms and double bonds in the molecule, was developed by Basso et al.[11], based on the model presented by Krisnangkura et al.[23] for ethyl ester viscositiy calculations.

$$ln(\mu) = -2.4738 - 0.1181(n_c - 1.5n_d) + \frac{496.5629}{T} + \frac{79.1093(n_c - 1.5n_d)}{T} \tag{7}$$

where μ is the kinematic viscosity ($mm^2 \cdot s^{-1}$), T is the absolute temperature (K), n_c is the carbon number of the molecule and n_d is the double bond number in the ethyl ester.

3.2.2. Ceriani model

A group contribution method was developed by Ceriani et al.[13] in the calculation of the viscosities of fatty compounds with temperature dependence. This methodology is based on six "perturbation terms", obtained from regression of an experimental data bank and associated to each functional group in the molecules, presenting one correction term, according to equations 8 - 12.

$$ln(\eta_i) = \left[\sum_k N_k \cdot A_{1k} + \frac{\sum_k N_k \cdot B_{1k}}{(T + \sum_k N_k \cdot C_{1k})}\right] + M_i \left[\sum_k N_k \cdot A_{2k} + \frac{\sum_k N_k \cdot B_{2k}}{(T + \sum_k N_k \cdot C_{2k})}\right] + Q \quad (8)$$

$$Q = \xi_1 q + \xi_2 \quad (9)$$

$$q = \alpha + \frac{\beta}{T + \gamma} \quad (10)$$

$$\xi_1 = f_0 + N_c f_1 \quad (11)$$

$$\xi_2 = s_0 + N_{cs} s_1 \quad (12)$$

where η_i is the dynamic viscosity (mPa·s), $A_{1k}, B_{1k}, C_{1k}, A_{2k}, B_{2k}$ and C_{2k} are the perturbation terms, M_i is the component molecular weight, N_k is the number of *k* groups in molecule *i*, *T* is the absolute temperature (K), Q is the correction term, q is a function of absolute temperature, α, β, and γ are optimized parameters obtained by regression of the data bank, N_c is the number of carbon atoms in the molecule, f_0 and f_1 are optimized constants, ξ_1 is a function of N_c, N_{cs} is the number of carbon atoms in the alkyl group (ethyl group in this work) of the molecule, s_0 and s_1 are optimized constants and ξ_2 is the term that describes the differences between viscosities of isomer esters at the same temperature.

3.2.3. Biodiesel Viscosity Calculation

Although the original Grunberg-Nissan equation[24] considers interaction terms when calculating the viscosities of mixtures, Allen et al.[25] reported that these biofuels are non-associated liquids that are comprised of mixtures of fatty acid esters whose chemical structure is similar, and due to this similarity the components in the mixture probably do not interact with each other but behave as individual components. In this way, as was proposed for by Basso et al.[11] and Ceriani et al.[13], the biodiesel viscosities were obtained using the simplified Grunberg-Nissan equation (equation 13), without an interaction term.

$$ln\ \eta_{mix} = \sum_{i} x_i \cdot ln\ \eta_i \tag{13}$$

3.3. Average relative deviations

The average relative deviations (ARD) between experimental and calculated viscosities and densities were obtained using equation (14).

$$ARD(\%) = 100 \cdot {}^{1}\!/_{n} \cdot \sum_{i=1}^{n} \left({}^{\left|(p_i^{exp} - p_i^{calc})\right|}\!/_{p_i^{exp}} \right) \tag{14}$$

where $p_i^{exp}$and p_i^{calc} are the experimental and calculated properties under study, respectively, and n is the number of data points.

4. Results and discussions

Table 1 shows that the BPECr has a high content of mono-unsaturated ethyl esters, about 79% of total esters, with more than 50% composed of ethyl erucate, a fatty acid alkyl ester with 24 carbon atoms. BPEFR is composed mainly of five unsaturated ethyl esters, with about 40% ethyl oleate. BPEMP consists of approximately 26% saturated ethyl esters and 57.8% ethyl oleate. BPEC has about 85% saturated ethyl ester, with more than 51% ethyl laurate, a short chain fatty acid alkyl ester. All biodiesels have low contents of polyunsaturated ethyl esters, a favorable characteristic for biodiesel, since the oxidative stability decreases with increase of the unsaturation level. The different ethyl ester profiles allow for analyzing the behavior of the densities, viscosities and melting profiles as a function of the very different biodiesel compositions.

As observed in Table 2, the densities of BPEC were lower than the densities of the other three biodiesels, where this difference increases with temperature. On the other hand, the densities of BPECr and BPEMP were similar at all temperatures. The densities of BPEFR were little high than those of BPECr and BPEMP for all studied temperatures.

Pratas et al.[26] showed that the density of ethyl esters decreases with increasing in alkyl chain length and increases with the number of unsaturated bonds. Ramirez-Verduzco[27], studying fatty acid methyl esters, reported a decrease in density of about 0.11% when increasing the ester chain length by two carbon atoms, and an increase of about 1.3% when adding one double bond in the ester molecule. Therefore, the lower densities of biodiesel from coconut oil in relation to other biodiesels is caused by the low content of unsaturated ethyl esters, despite a higher content of ethyl esters with short carbon chain length.

Table 2. Biodiesel densities.

T/K	ρ/(kg·(m^3)$^{-1}$)			
	BPECr	BPEFR	BPEMP	BPEC
283.2	876.80	879.11	876.76	871.58
288.2	873.01	875.51	874.07	867.73
293.2	869.70	871.79	869.38	863.86
298.2	865.78	868.21	866.71	860.00
303.2	862.60	864.53	862.09	856.15
308.2	858.63	860.93	859.38	852.33
313.2	855.52	857.24	854.73	848.45
318.2	851.43	853.67	852.01	844.57
323.2	848.46	849.97	847.39	840.70
328.2	844.28	846.39	844.68	836.84
333.2	841.41	842.71	840.05	832.97
338.2	837.10	839.13	837.33	829.04
343.2	834.35	835.44	832.71	825.15
348.2	829.97	831.85	829.98	821.26
353.2	827.27	828.18	825.36	817.38
358.2	822.79	824.58	822.62	813.45
363.2	820.20	820.93	818.06	809.63

Viscosities of the BPEC were, on average, about 61 % of the viscosities of BPEFR and BPEMP and about 50% those of BPECr, as presented in Table 3. This difference increases at lower temperatures. The viscosities of BPEMP and BPEFR were similar for the entire studied temperature range, and on average 89% of the BPECr viscosity.

Ramirez-Verduzco[27], when studying methyl ester viscosity, reported an increase greater than 20% with the increase of two carbon atoms in ester chain length and a decrease greater than 10% due to the addition of one double bond in the ester molecule. Yuan et al.[28] presented and Allen et al.[25] observed a curvilinear increasing trend in saturated fatty acid ester viscosities with carbon number, and a decrease from 13 to 21% of methyl ester viscosity with the increase in saturation level. Basso et al.[11] used the consideration of a decrease in ethyl ester viscosity due to the addition of one double bond similar to that caused by the removal of 1.5 carbon atoms from the ethyl ester molecule in the formulation of a simplified methodology for ethyl ester viscosity calculation with temperature dependence. Therefore, despite the high content of saturated esters, BPEC has the lowest viscosity among the four biodiesels due to the short chain length of its ethyl esters. Although BPEMP has a significant content of saturated ester, BPEFR has a greater amount of long chain esters than BPEMP, resulting in a similar viscosity for both biodiesels. BPECr is rich in long chain ethyl esters with only one double bond resulting from the higher viscosity among the four biodiesels.

Table 3. Biodiesel viscosities.

T/K	η/(mPa·s)			
	BPECr	BPEFR	BPEMP	BPEC
283.2	13.6866	9.9151	10.5147	5.7270
288.2	11.8737	8.7677	8.6489	4.9759
293.2	9.9463	7.7111	7.7569	4.3636
298.2	8.5565	6.6231	6.6686	3.8565
303.2	7.2745	5.9488	5.8090	3.4350
308.2	6.5248	5.1637	5.2108	3.0783
313.2	5.6489	4.7394	4.6404	2.7771
318.2	5.1477	4.1700	4.1699	2.5184
323.2	4.5192	3.8520	3.6759	2.2940
328.2	4.1640	3.4267	3.4151	2.1228
333.2	3.6978	3.2057	3.0667	1.9509
338.2	3.4329	2.8702	2.8520	1.8001
343.2	3.0830	2.7091	2.5897	1.6702
348.2	2.8820	2.4407	2.4233	1.5496
353.2	2.6113	2.3210	2.2208	1.4439
358.2	2.4560	2.1033	2.0870	1.3495
363.2	2.2425	2.0191	1.9291	1.2648

As observed in Table 4, although the GCVOL properly described the biodiesel densities, with ARDs lower than 1.1%, the systematized Halvorsen methodology[11] presented a lower overall ARD, indicating a better description of this biodiesel property. Despite the low ARDs, the models presented distinct behavior in relation to BPEC with the systematized Halvorsen methodology[11] and GCVOL[14] model, respectively, underestimating and overestimating the densities of this biodiesel, as showed in Figure 1.

Table 4. Average relative deviations between experimental and calculated values.

	Density - ARD (%)		Viscosity - ARD (%)	
	Systematized Halvorsen model	GCVOL model	Ceriani model	Basso model
BPEC	0.89	1.02	7.02	6.20
BPEMP	0.30	0.45	12.64	14.32
BPEFR	0.53	0.48	9.84	10.92
BPECr	0.11	0.45	7.14	5.06

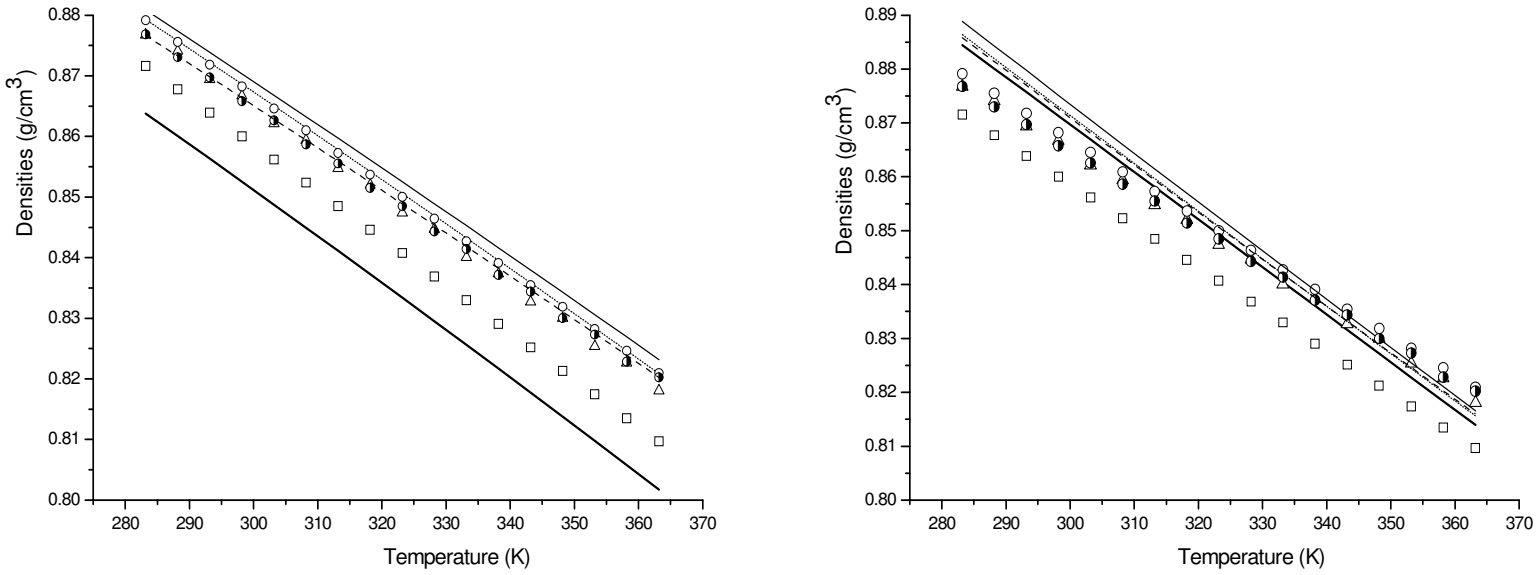

Systematized Halvorsen methodology GCVOL model

Figure 1. Biodiesel Densities; experimental data: (□) coconut, (△) macauba, (○)fodder radish, (◑) crambe; systematized Halvorsen model:(—) coconut, (···) macauba, (—) fodder radish, (---) crambe.

The ARDs were similar to those obtained by Basso et al.[11], from 0.25% to 0.62%, studying the densities of three different ethyl biodiesels. Although Baroutian et al.[29] used the modified Rackett equation in the density calculations of ethyl biodiesels from canola, soybean, and palm oil, obtaining deviations less than 0.12%; at least one experimental density value was required as reference which represents an unfavorable feature of this methodology in comparison with that used in the present study. Pratas et al.[22] obtained ARDs from 0.14% to 1.1% and from 0.04% to 0.79%, using the original and a set of re-estimated GCVOL model parameters in the density calculation of biodiesels produced by methanolysis, respectively. Anand et al.[30] proposed a modification in the Rackett equation for the calculation of vegetable oil and methyl biodiesel densities, obtaining absolute deviations from 0.1% to 2.3% in relation to the experimental values. Ramirez-Verduzco[27] developed an empirical methodology for the calculation of densities of methyl biodiesel, and obtained average absolute deviations ranging from 0.17% to 0.74% for all tested biodiesels.

The ARDs for the viscosities calculated by the model proposed by Basso et al.[11] were lower than those calculated using that proposed by Ceriani et al.[13] for BPEC and BPECr, and higher for BPEMP and BPEFR, as observed in Table 4. Freitas et al.[31], when analyzing three different methodologies and one set of revised parameters to calculate the viscosities of methyl biodiesels and their mixtures, obtained average deviations from 4.7% to 8.1%, considering all biodiesels. Do Carmo et al.[32] when using a methodology based on the principle of corresponding state for the viscosity calculations of methyl biodiesels and their mixtures obtained overall ARDs of 9.4% and 8.3%, respectively, using one and two reference fluids. Ramirez-Verduzco[27] developed an empirical methodology for the calculation of viscosities of methyl biodiesel, and obtained average absolute deviations from 2.4% to 17% among all tested biodiesels.

The models proposed by Basso et al.[11] and Ceriani et al.[13] properly described the viscosities of the biodiesels containing a great variety of saturated and unsaturated ethyl esters. Despite the low ARDs, the precision of the models for the representation of the biodiesel viscosities increased with temperature, as showed in the Figure 2.

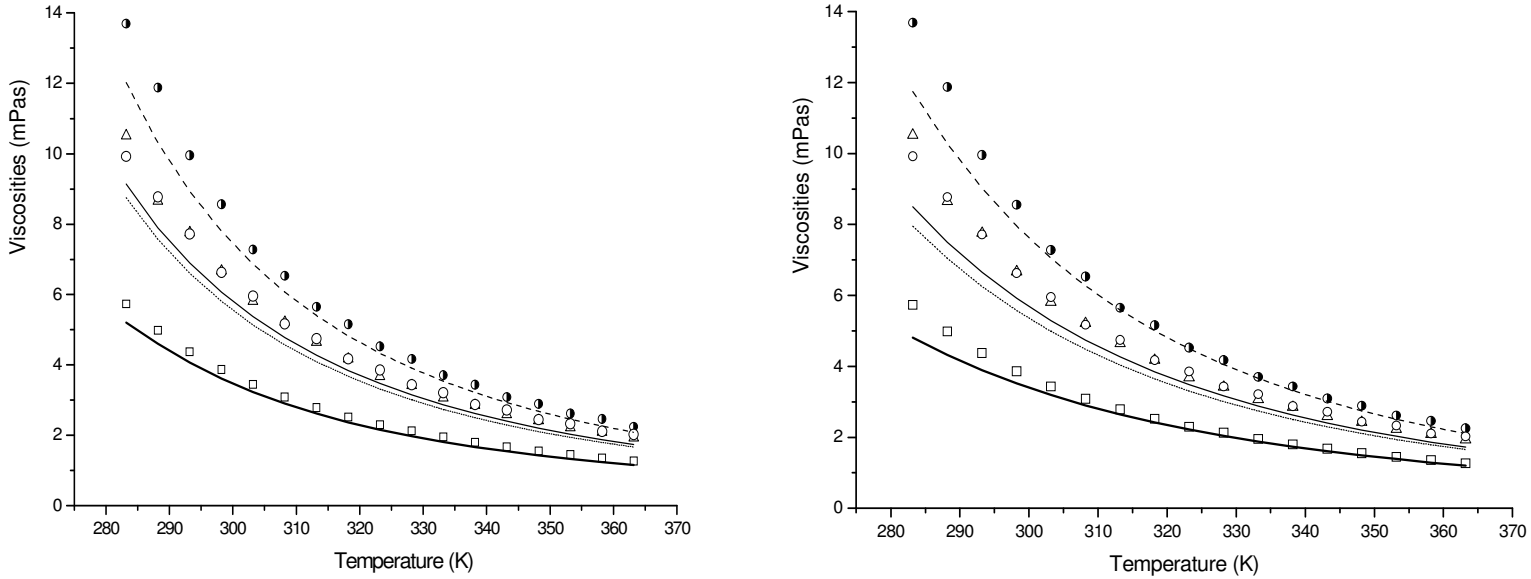

Ceriani model

Basso model

Figure 2. Biodiesel Viscosities; experimental data: (□) coconut, (△) macauba, (○)fodder radish, (◑) crambe; Calculated by models:(—) coconut, (···) macauba, (—) fodder radish, (---) crambe.

According to observations of Tan and Che Man[33], thermal analysis of fats and oils do not exhibit specific melting and crystallization temperatures, but instead melting and crystallization profiles because they are composed of complex mixtures of a great variety of triacylglycerols. The former assertion is valid for biodiesel since these biofuels are composed for a mixture of alkyl esters, showing polymorphic behavior and presenting a broad range of melting points. Moreover, phenomena where the components with low melting points in liquid state tend to solubilize, the components with high melting points in solid state cannot be neglected. On the other hand, esters in solid state induce material in the liquid state to crystallize, according to observations of Santos et al. (2011). Therefore, the melting points of pure ethyl esters obtained from literature[6] were considered only as a reference in the assumptions of what happens to esters when subjected to these phenomena per temperature range, in the biodiesels studied.

The melting profiles of BPECr, BPEC and BPEMP were characterized by two peaks while that of BPEFR was characterized by one peak, as observed in Figure 3. Extension of the melting ranges for each peak is related to the variety of ethyl esters with different melting points and the effect of the inter-solubility among them. The characteristic values, peak temperature (Tp), temperature of initial melting (Ti), final melting temperature (Tf), and heat of fusion of esters mixtures (ΔH) of the melting profiles are shown in Table 5.

The single melting peak in the melting profile of BPEFR is explained by large amount of unsaturated esters with similar or sequential carbon number. Although this biodiesel presents approximately 10% ethyl erucate, the massive presence of other unsaturated esters resulted in the solubilization of ethyl erucate at temperatures less than the temperatures of the second peak observed for BPECr.

In the melting profile of the BPECr, the first peak, under T/K = 248.2, is primary related to melting and inter-solubility of the unsaturated ethyl esters with 18 carbon atoms in the molecule. The second peak, above T/K =248.6, is mainly related to the melting and inter-solubility of the small content of saturated esters present and mono-unsaturated long chain esters, mainly ethyl erucate, present in this biodiesel.

In the melting profile of the BPEMP, the first peak, under T/K = 247.4, mainly shows the melting and inter-solubility of unsaturated ethyl esters while, the second peak, above T/K = 265.4, shows the melting and inter-solubility of primary mono-unsaturated and saturated ethyl esters.

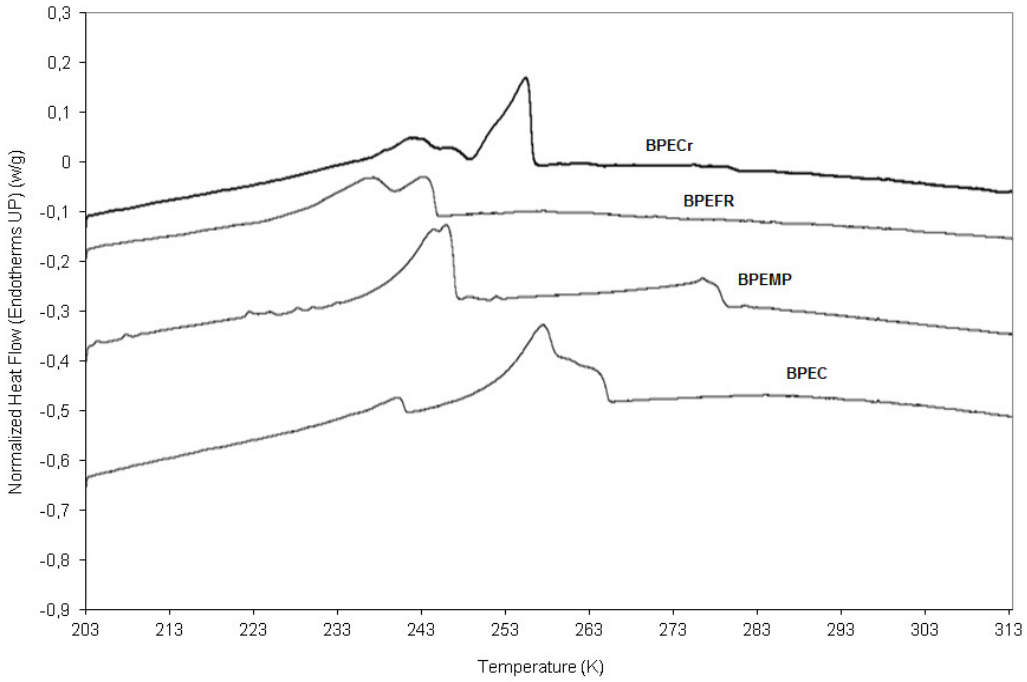

Figure 3. Melting Profiles of the biodiesels.

Table 5. Biodiesels thermal behavior.

properties		biodiesels			
		crambe	fodder radish	macauba	coconut
peak 1	Ti/K	225.94	223.23	231.03	224.99
	Tf/K	248.21	244.88	247.43	241.16
	Tp/K	241.28	236.88	245.60	239.63
	$\Delta H/(J \cdot g^{-1})$	31.7391	60.4583	57.9380	12.6666
peak 2	Ti/K	248.56	-	265.36	241.28
	Tf/K	257.00	-	280.00	265.55
	Tp/K	255.10	-	276.20	257.15
	$\Delta H/(J \cdot g^{-1})$	39.5940	-	18.9731	88.4194

In the melting of BPEC, the first peak, under T/K = 241.2, indicates the melting and inter-solubility mainly of the unsaturated and short chain saturated esters, ethyl esters from octanoic and decanoic acid; while the second peak, above T/K = 241.3, is related to the melting and inter-solubility of primary short and middle chain saturated esters.

The melting temperature of the biodiesels was considered as the final temperature of the peak located in the higher temperature region, since above this temperature there is no material in the solid state. Therefore, the BPEMP presented a higher melting temperature due to its significant ethyl ester composition composed of palmitic and stearic acid, followed by BPEC, whose composition is rich in short and middle chain saturated esters. BPECr, due to its high concentration of ethyl erucate, presented a higher melting temperature than BPEFR.

The ΔH (Table 5), per temperature range, is the result of a set of phenomena which occurs during melting of each biodiesel: the energy used per ethyl ester in its melting process, the energy used or released in a polymorphic transition per ethyl ester, the intersolubilization effect among the esters and the ratio, per temperature range, of material subjected to these phenomena. Despite all these phenomena, it may be assumed that each ΔH per temperature range roughly corresponds to the melting and/or interaction of the mixture of ethyl esters with similar melting point for each temperature range, as it was indicated in the previous description of the melting curves for the biodiesels.

5. Conclusions

The studied physical properties were directly influenced by the biodiesel compositions. BPEC and BPEFR have, respectively, the lowest and the highest densities among the four biodiesels. The viscosities of BPEC were, on average, about 61% of the viscosities of BPEFR and BPEMP which are, on average, about 89% of the BPECr viscosities. BPEMP and BPEFR had the highest (T/K = 280) and lowest (T/K = 245) melting temperatures in relation to the four biodiesels, respectfully. The predictive Halvorsen methodology properly represented the biodiesel densities with ARDs lower than 0.9%. Both the Basso and Ceriani models properly described the biodiesel viscosities resulting in ARDs from 5.1% to 14.3% and from 7.0% to 12.6%, and they can be used in the viscosity description of biodiesel with very different ethyl ester compositions.

References

(1) Knothe, G.; Van Gerpen, J.; Khral, J. The Biodiesel Handbook; AOCS Press: Champaign, IL, 2005.

(2) Hoeckman, S. K.; Broch, A.; Robbins, C.; Ceniceros, E.; Natarajan, M. Review of biodiesel composition, properties, and specifications. Renew. Sust. Energ. Rev. **2012**, 16, 143-169.

(3) Encinar, J. M.; Gonzalez, J. F; Rodrigez, J. J.; Tejedor, A. Biodiesel Fuels from Vegetable Oils: Transesterification of Cynara Cardunculus L. Oils with Ethanol. Energ. Fuel. **2002**, 16, 443-450.

(4) Stamenkovic, O. S.; Velickovic, A. V.; Veljkovic V. B. The Production of biodiesel from vegetable oils by ethanolysis: Current state and perspectives. Fuel, **2011**, 90, 3141-3155.

(5) Knothe, G.; Steidlei, K. R. Kinematic Viscosity of Biofuel Components and Related Compounds: Influence of Compound Structure and Comparison to Petrodiesel Fuel Components. Fuel, **2005**, *84*, 1059-1065.

(6) Knothe, G.; Dunn, R. O. A comprehensive evaluation of the melting points of fatty acids and esters determined by differential scanning calorimetry. J. Am. Oil Chem. Soc. **2009**, 86, 843-856.

(7) Refaat, A. A. Correlation Between the Chemical Structure of Biodiesel and its Physical Properties. *Int. J. Environ. Sci. Technol.* **2009**, *6*, 677.

(8) Boudy, F.; Seers, P. Impact of Physical Properties of Biodiesel on the Injection Process in a Common-Rail Direct Injection System. *Energ. Convers. Manage.* **2009**, *50*, 2905.

(9) Dunn, R. O.; Bagby, M. O. Low temperature properties of triglycerides based diesel fuels: transesterified methyl esters and petroleum middle distillate/ester blends. J. Am. Oil Chem. Soc. **1995**, 72, 895-904.

(10)Srivastava, A.; Prasad, R. Triglycerides-based diesel fuels. Renewable and Sustainable Energy Reviews 2002, 4, 111-133.

(11) Basso, R. C.; Meirelles, A. J. A.; Batista, E. A. C. Densities and Viscosities of Fatty Acid Esters and Biodiesels Produced by Ethanolysis from Palm, Canola, and Soybean Oils: Experimental Data and Calculation Methodologies. *Ind. Eng. Chem. Res. 2013*

(12) Dunn, R. O. Thermal analysis of alternative diesel fuel from vegetable oils. J. Am. Oil Chem. Soc. **1999**, 76, 109-115.

(13) Elbro, H. S.; Fredenslund, A.; Rasmussen, P. Group contribution method for the prediction of liquid densities as a function of temperature for solvents, oligomers, and polymers. Ind. Eng. Chem. Res., **1991**, 30, 2576-2582.

(14) Ceriani, R.; Gonçalves, C. B.; Coutinho, J. A. P. Prediction of Viscosities of Fatty Compounds and Biodiesel by Group Contribution. *Energ. Fuel.* **2011**, *25*, 3712.

(15) Halvorsen, J. D.; Mammel-Jr, W. C.; Clements, L. D. Density Estimation for Fatty Acid and Vegetable Oils Based on Their Fatty Acid Composition. *J. Am. Oil Chem. Soc.* **1993**, *10*, 875.

(16) Basso, R. C.; Meirelles, A. J. A.; Batista, E. A. C. Liquid-liquid equilibrium of pseudoternary systems containing glycerol + ethanol + ethylic biodiesel from crambe oil (Crambe abyssinica) at T/K = (298,2, 318,2, 338,2) and thermodynamic modeling. *Fluid Phase Equilib.* **2012**, *333*, 55-62.

(17) Santos N. A.; Rosenhaim, R.; Dantas, M. B.; Bicudo, T. C.; Cavalcanti, E. H. S.; Barro, A. K.; Santos, I. M. G.; Souza, A. G. Rheology and MT-DSC studies of the flow properties of ethyl and methyl babassu biodiesel blends. J. Therm. Anal. Calorim. **2011**, 106, 501-506.

(18) Rackett, H. G. Equation of State of Saturated liquids. *J. Chem. Eng. Data.* **1970**, *15*, 514.

(19) Spencer, C. F.; Danner, R. P. Improved Equation for Prediction of Saturated Liquid Density. *J. Chem. Eng. Data.* **1972**, *17*, 236-241.

(20) Constantinou, L.; Gani, R.; O'Connel, J. P. Estimation of the Acentric Factor and Liquid Molar Volume at 298 K Using a New Group Contribution Method. *Fluid Phase Equilib.* **1995**, *103*, 11-22.

(21) Constantinou, L.; Gani, R. New Group Contribution Method for Estimating Properties of Pure Components. *AICHE J.* **1994**, *70*, 1697-1710.

(22) Pratas, M. J.; Freitas, S. V. D.; Oliveira, M. B.; Monteiro, S. C.; Lima, A. S.; Coutinho, J. A. P. Biodiesel Density: Experimental Measuremts and Preditction Models. Energ. Fuel., **2011**, 25, 2333-2340.

(23) Krisnangkura, K.; Yimsuwan, T.; Pairintra, R. An Empirical Approach in Predicting Biodiesel Viscosity at Various Temperatures. *Fuel* **2006**, *85*, 107.

(24) Grunberg, L.; Nissan, A. H. Mixture law for viscosity. Nature **1949**, 164, 799.

(25) Allen, C. A. W.; Watts, K. C.; Ackman, R. G.; Pegg, M. J. Predicting the Viscosity of Biodiesel Fuels from their Fatty Acid Ester Composition. *Fuel* **1999**, 78, 1319.

(26) Pratas, M. J.; Freitas, S.; Oliveira, M. B.; Monteiro, S. C.; Lima, A. S.; Coutinho, J. A. P. Densities and Viscosities of Fatty Acid Methyl and Ethyl Ester. *J. Chem. Eng. Data.* **2010**, *55*, 3983.

(27) Ramirez-Verduzco, L. F. Density and viscosity of bidiesel as a function of temperature: Empirical models. Renew. Sust. Energ. Rev. **2013**, 19, 652-665.

(28) Yuan, W.; Hansen, A. C.; Zhang, Q. Predicting the Temperature Dependent of Biodiesel Fuels. *Fuel* **2009**, 88, 1120-1126.

(29) Baroutian, S.; Aroua, M. K.; Raman, A. A. A.; Sulaiman, N. M. N. Densities of Ethyl Esters Produced from Different Vegetable Oils. *J. Chem. Eng. Data* **2008**, *53*, 2222-2225.

(30) Anand, K.; Ranjan, A.; Mehta, P. R. Predicting the Density of Straight and Processed Vegetable Oils from Fatty Acid Composition. Energ. Fuel. **2010**, 24, 3262-3266.

(31) Freitas, S. V. D.; Pratas, M. J.; Ceriani, R.; Lima, A. S.; Coutinho, J. A. P. Evaluation of Predictive Models for the Viscosity of the Biodiesel. *Energ. Fuel*. **2011**, 25, 352.

(32) do Carmo, F. R.; Sousa Jr, P. M.; Aguiar, R. S.; Sant'Ana, H. B. Development of a New Model for Biodiesel Viscosity Prediction Based on the Principle of Corresponding State. *Fuel* **2012**, 92, 250.

(33) Tan, C. P.; Che Man, Y. B., Differential Scanning Calorimetric Analysis of Edible Oils: Comparison of Thermal Properties and Chemical Composition. J. Am. Oil Chem. Soc. **2000**, 77, 143-155.

Capítulo 9. Conclusões Gerais

Os resultados obtidos no presente trabalho permitem estabelecer um conjunto de conclusões relativas ao ELL em etapas de purificação de biodieseis etílicos e ao comportamento da densidade, viscosidade e perfil térmico durante a fusão desses biocombustíveis.

O ELL dos sistemas constituídos por glicerol + etanol + biodieseis etílicos foi caracterizado por uma miscibilidade muito reduzida entre o glicerol e o biodiesel, enquanto o etanol se distribuiu entre as duas fases ricas nesses componentes, com maior afinidade pela fase rica em glicerol. Por sua vez, o ELL dos sistemas constituídos por água + etanol + biodieseis etílicos pode ser descrito por uma imiscibilidade muito elevada entre a água e o biodiesel, ao mesmo tempo em que o etanol se distribuiu entre as duas fases. O etanol apresenta menor afinidade pela fase rica em glicerol nos primeiros sistemas do que pela fase rica em água, nos sistemas contendo esse composto.

A consideração de pseudocomponente, comumente feita na modelagem do ELL das etapas de produção de biodiesel usando modelos moleculares, foi confirmada nos sistemas nos quais o glicerol esteve presente. Nos sistemas compostos por glicerol + etanol + biodiesel de óleo de crambe, alterações da temperatura, na faixa entre 25 °C e 65 °C, demonstraram ter pouco efeito em relação ao ELL dos mesmos.

Os modelos termodinâmicos NRTL e UNIQUAC apresentaram boa capacidade descritiva do ELL dos sistemas constituídos por glicerol + etanol + biodieseis etílicos e daqueles constituídos por água + etanol + biodieseis etílicos, sendo que o uso do primeiro modelo, de modo geral, resultou em menores desvios entre os valores calculados e experimentais. Por sua vez, a representação do ELL dos sistemas contendo glicerol e daqueles contendo água, pelos modelos de contribuição de grupos UNIFAC-LLE e UNIFAC-Dortmund, foi inadequada, embora o segundo modelo tenha implicado em desvios um pouco menores do que o primeiro. Devido à baixa capacidade preditiva, o uso desses modelos na simulação da etapa de decantação do biodiesel de óleo de polpa de macaúba para a separação da fase rica em glicerol subestimou os teores de glicerol e de etanol na fase rica em biodiesel.

No processo de purificação do biodiesel de nabo forrageiro, a remoção parcial do teor de etanol, previamente à etapa de decantação da fase rica em glicerol de sistemas constituídos por glicerol + etanol + biodiesel etílico, possibilita a redução do teor de glicerol na fase rica em biodiesel a teores inferiores ao mínimo requerido pelas normas de

pureza especificadas para esse biocombustível, ao mesmo tempo em que reduz as perdas de ésteres etílicos para a fase rica em glicerol.

Considerando um excesso de três moles de etanol na reação de transesterificação para a produção do biodiesel de nabo forrageiro, o uso de um único conjunto “misturador/ separador” na etapa de lavagem deste biocombustível necessitou de uma quantidade de água duas vezes maior do que a massa de biodiesel alimentada no processo de purificação, para que fosse alcançada uma redução do teor de etanol a concentrações inferiores às especificadas pelas normas internacionais de qualidade. De modo diferente, o emprego de duas configurações distintas com dois conjuntos “misturador/ separador”, uma em correntes cruzadas e a outra em contra corrente, exigiram, respectivamente, um quarto e um oitavo da quantidade de água usada na configuração em único estágio para obter o mesmo teor final de etanol no biodiesel purificado.

O comportamento da viscosidade dos sete biodieseis etílicos teve uma forte correlação com as suas composições em ésteres etílicos. O biodiesel de óleo de coco, composto majoritariamente por ésteres contendo menos de 18 átomos de carbono em suas moléculas, e o biodiesel de óleo de crambe, composto majoritariamente por ésteres com mais de 20 átomos de carbono, apresentaram, respectivamente, as menores e as maiores viscosidades na mesma faixa de temperatura. Demonstrando comportamento distinto, a densidade foi menos sensível à variabilidade dos perfis de ésteres etílicos, uma vez que os valores dessa propriedade, na mesma faixa de temperatura, foram similares entre todos os biodieseis estudados.

A calorimetria exploratória diferencial tornou possível correlacionar a composição em ésteres etílicos dos biodieseis com seu comportamento térmico durante o processo de fusão. O biodiesel de macaúba, por ter aproximadamente 25% de ésteres saturados com mais de 18 carbonos na molécula (ésteres de ácido palmítico e de ácido esteárico) em sua composição, apresentou o maior ponto de fusão, enquanto o biodiesel de nabo forrageiro, por ter mais de 70% de ésteres insaturados com menos de 22 carbonos, demonstrou ter o menor ponto de fusão dentre os biodieseis analisados.

Sugestões para Trabalhos Futuros

i. Obtenção de dados experimentais de equilíbrio líquido-vapor e modelagem termodinâmica de sistemas constituídos por etanol + biodieseis etílicos + glicerol e por etanol + biodieseis etílicos + água;
ii. Aquisição de dados experimentais de equilíbrio líquido-líquido e modelagem termodinâmica de sistemas envolvidos na purificação de biodieseis etílicos contendo catalisadores inativos (na forma de sais, por exemplo);
iii. Simulação das etapas de purificação de biodieseis etílicos considerando a presença de catalisador e as etapas de remoção de etanol e de água;
iv. Estudo experimental de viscosidades de misturas de ésteres (etílicos ou metílicos) que comprovem ou neguem a hipótese de não associatividade entre esses componentes em uma mistura;
v. Análise do efeito de compostos minoritários como inteferentes na viscosidade e no comportamento térmico de biodieseis etílicos.

Apêndice

Metodologia Experimental Utilizada nos Artigos Apresentados

Produção e Purificação dos Biodieseis Etílicos

Previamente a produção dos biodieseis etílicos, os óleos vegetais brutos foram filtrados, neutralizados e tiveram seu teor de fosfolipídios determinados.

Os biodieseis etílicos utilizados nos ensaios de equilíbrio líquido-líquido do presente trabalho foram obtidos por catálise alcalina. Previamente à reação de transesterificação, hidróxido de sódio (1% em relação a massa de óleo vegetal) foi dissolvido em etanol sob intensa agitação, utilizando-se um agitador magnético. A razão molar foi de 1:6 óleo vegetal:etanol, considerando-se a massa molecular média do óleo. A reação foi mantida por uma hora sob agitação em temperatura ambiente (aproximadamente 25 °C) antes de ser interrompida pela adição de ácido acético glacial. A mistura foi transferida para um funil de separação para a decantação do glicerol. A fase superior, rica em ésteres etílicos, foi lavada com água deionizada aquecida (aproximadamente 80 °C) por, no mínimo, cinco vezes para a remoção de sabões, sais, glicerol e etanol residuais. O produto obtido foi secado sob agitação intensa, aquecimento (pelo menos 60 °C) e vácuo, a pressões menores que 5 mmHg. O biodiesel foi destilado sob vácuo, a pressões menores que 2,25 mmHg e temperaturas mínimas de 235 °C. Após a destilação, foram feitas lavagens adicionais com água quente, e secagem sob vácuo, para a remoção de quaisquer impurezas residuais.

Experimentos de Equilíbrio Líquido-Líquido

Na determinação do equilíbrio líquido-líquido, os componentes constituintes dos sistemas foram pesados em uma balança analítica (marca Adam Equipment, modelo AAA160L, com precisão de +/- 0.0001 g), e transferidos para tubos de “headspace”. de 20 mL. Os tubos foram vigorosamente agitados usando um agitador tipo “vortex” (marca Phoenix, modelo AP56) e centrifugados (centrífuga marca Jouan, modelo BR4i) por 5 min a 4000 rpm a temperatura ambiente. Todos os sistemas foram mantidos em repouso por, no mínimo, 12 h com a temperatura controlada por um banho termostático (marca Paar Physica, modelo Physica VT2, com precisão de +/- 0,2 °C). O equilíbrio foi determinado visualmente, pela formação de duas fases límpidas e de uma interface bem definida.

Determinação do perfil de ácidos graxos

A caracterização em ésteres etílicos dos biodieseis foi feita por meio de cromatografia em fase gasosa, com ensaios realizados em triplicata. Foi utilizado um cromatógrafo gasoso Perkin Elmer - Clarus 600, com detector FID; uma coluna capilar Elite-225 (fase estacionária composta por 50% cianopropil metil – 50% fenil metil polisiloxano), marca Perkin Elmer, com comprimento de 30 m, diâmetro interno de 0,25 mm e espessura da fase estacionária de 0,25 µm; com hélio como gás de arraste.

As condições analíticas utilizadas foram: vazão de hélio de 1 mL/min; temperaturas do injetor e do detector de 250 °C; temperatura inicial do forno de 100°C mantida por 5 min, rampa de aquecimento de 5 °C/min até 230 °C, mantida por 20 min; "split" de 1:40 e volume de injeção de 0,4 µL. Os ésteres etílicos foram quantificados pelas áreas relativa dos picos.

Caracterização das Fases em Equilíbrio Líquido-Líquido dos Sistemas Constituídos por Etanol + Biodieseis Etílicos + Gicerol

A quantificação dos teores de glicerol, de ésteres etílicos de ácidos graxos (determinados individualmente) e de etanol em cada fase em equilíbrio foi determinada com ensaios realizados, no mínimo, em triplicata. Foi utilizado um cromatógrafo gasoso Perkin Elmer - Clarus 600, com detector FID; uma coluna capilar DB-225 (fase estacionária composta por 50% cianopropil fenil – 50% dimetil polisiloxano), marca Agilent, com comprimento de 30 m, diâmetro interno de 0,25 mm e espessura da fase estacionária de 0,25 µm; com hélio como gás de arraste.

As condições analíticas utilizadas foram: vazão inicial de hélio de 1 mL/min, mantida por 5 min, vazão de hélio de 2,5 ml/min, mantida por 6 min e, vazão de hélio de 1,5 ml/min até o término da análise; temperaturas do injetor e do detector de 250 °C; temperatura inicial do forno de 40°C mantida por 1 min, rampa de aquecimento de 5 °C/min até 60 °C, mantida por 1 min, rampa de aquecimento de 25 °C/ min até 200 °C, mantida por 1 min e rampa de aquecimento de 7 °C/min até 235 °C, mantida por 8 min; "split" de 1:40 e volume de injeção de 0,4 µL.

Os componentes foram quantificados por meio de curvas de calibrações, sendo que estas foram constituídas por nove concentrações de etanol e miristato de etila (como padrão para os ésteres etílicos) e oito concentrações de glicerol.

Caracterização das Fases em Equilíbrio Líquido - Líquido dos Sistemas Constituídos por Etanol + Biodiesel Etílico + Água

A composição em água na fase rica nesse componente foi determinada usando um titulador Karl Fisher (701 KF Titrino, Metrohm), com ensaios realizados, no mínimo em triplicata.

O teor de água na fase rica em biodiesel foi determinado usando um sistema de análise de Karl Fisher coulométrico (KF Coulometer, Metrohm), mais preciso para baixos teores de água que o equipamento descrito anteriormente, com ensaios realizados, no mínimo, em triplicata.

Para a obtenção do teor de biodiesel, amostras de cada fase em equilíbrio dos sistemas constituídos por etanol + biodiesel etílico + água foram pesadas, em uma balança analítica (marca Precisa, modelo XT 220 A com precisão de +/- 0.0001 g) e transferidas, em triplicata, para placas de Petri previamente pesadas. As placas foram levadas a uma estufa com circulação de ar (marca Marconi, modelo MA 035), onde foram mantidas por, no mínimo, 20 h a 80 °C e a pressão atmosférica, até a completa evaporação da água e do etanol. A massa de biodiesel foi obtida por pesagem das placas após a evaporação do etanol e da água.

O teor de etanol foi determinado partir da diferença entre a massa total pesada na placa de Petri e as massas de água e de biodiesel.

Determinação da viscosidade

A determinação da viscosidade dos biodieseis etílicos foi feita em um microviscosímetro capilar (marca Anton Paar, modelo AMVn), seguindo uma programação que consistiu em quatro medições em inclinação de 70 °, quatro medições em inclinação 60° e seis medições em inclinação de 50°. A viscosidade foi obtida por meio da média das quatorze medições. A calibração foi previamente verificada, na faixa de temperatura de 20 °C até 90 °C, usando um fluido de calibração IPT-77 OP-6, certificado pelo Instituto de Pesquisas Tecnológicas (IPT), Brasil.

Determinação da densidade

A determinação da densidade foi realizada por ensaios em triplicata, em um densímetro capilar (marca Anton Paar, modelo DMA 4500). A calibração foi previamente verificada, na faixa de temperatura de 20 °C até 90 °C, usando um fluido de calibração

IPT-77 OP-6, certificado pelo Instituto de Pesquisas Tecnológicas (IPT), Brasil. Previamente a cada análise, foram feitas verificações da calibração do equipamento com água Mili-Q, sendo aceitos desvios inferiores a 0,0001 g/cm^3.

Determinação do Comportamento Térmico Durante a Fusão

O comportamento térmico dos biodieseis etílicos durante a fusão foi obtido em um calorímetro exploratório diferencial (marca Perkin Elmer, modelo DSC 8500). As amostras foram pesadas (aproximadamente 5 mg) em uma balança microanalítica (marca Perkin Elmer, modelo AD6). Uma panela hermética de alumínio vazia foi usada como referência. As amostras foram submetidas à seguinte programação de temperatura: resfriamento a uma taxa de 1 °C/min até -80 °C, manutenção dessa temperatura por 30 min e, aquecimento a uma taxa de 1 °C/min até 80 °C. A calibração foi feita utilizando índio e ciclohexano como referência. As temperaturas iniciais e finais referentes aos fenômenos térmicos foram consideradas como aquelas nas quais a linha base modifica sua trajetória original.